UNIVERSIDAD AUTONOMA DE MADRID

Programa doctorado Biociencias Moleculares

Exogenous and endogenous factors that modify telomere length in hereditary breast and ovarian cancer patients

Tesis doctoral

Carlos Benítez-Buelga

Madrid, 2017

PROGRAMA DE BIOBIENCIAS MOLECULARES

FACULTAD DE MEDICINA

UNIVERSIDAD AUTÓNOMA DE MADRID

Exogenous and endogenous factors that modify telomere length in hereditary breast and ovarian cancer patients

Tesis doctoral presentada por:

Carlos Benítez-Buelga

Licenciado en Biología por la Universidad de Alcalá de Henares (UAH)

Directores de la Tesis:

Dr. Javier Benítez

Director del Programa de Genética del Cáncer Humano (CNIO)

Jefe del Grupo de Genética Humana (CNIO)

Dra. Ana Osorio Cabrero

Investigadora del Grupo de Genética Humana (CNIO)

GRUPO DE GENÉTICA HUMANA

PROGRAMA DE GENÉTICA DEL CÁNCER HUMANO

CENTRO NACIONAL DE INVESTIGACIONES ONCOLÓGICAS (CNIO)

Dr. Javier Benítez Ortiz, director del Programa de Genética del Cáncer Humano Centro Nacional de Investigaciones Oncológicas (CNIO), como director.

Dra. Ana Osorio Cabrero, Investigadora del grupo de Genética Humana del centro nacional de investigaciones oncológicas como codirectora.

Así como la doctora Gema Moreno Bueno, tutora del doctorando durante todo el proceso de la Tesis.

CERTIFICAN

Que Don Carlos Benítez-Buelga, Licenciado en Biología por la Universidad de Alcalá de Henares, ha realizado bajo nuestra supervisión, la presente Tesis Doctoral "Exogenous and endogenous factors that modify telomere length in Hereditary breast and ovarian cancer patients " y que a su juicio reúne plenamente todos los requisitos necesarios para optar al grado de Doctor, a cuyos efectos será presentada en la Universidad Autónoma de Madrid, autorizando su presentación ante el Tribunal Calificador.

Y para que así conste se extiende el presente certificado,

Madrid, 7 de marzo de 2017

Firma del director/es:

La presente Tesis Doctoral se realizó en el Centro Nacional de Investigaciones Oncológicas (CNIO) de Madrid entre los años 2013 y 2017 bajo la supervisión del Dr. Javier Benítez y la Dra. Ana Osorio Cabrero.

Las siguientes becas, ayudas y proyectos han permitido la realización de esta Tesis Doctoral:

- **Proyecto PI12/00070 Fondo de Investigación Sanitaria (FIS) del Instituto de Salud Carlos III dirigido por el Dr. Javier Benítez. Periodo: 2013-2017**
- **Proyecto HORIZON 2020-BRIDGES (2015-2019)**
- **FEBS Short-term fellowship (2016)**

A mi Madre

RESUMEN/ABSTRACT

RESUMEN

El acortamiento telomérico como un factor causal del riesgo a desarrollar cáncer, es un tema complejo, que parece depender de varios factores. En un trabajo anterior publicado por nuestro grupo, encontramos que los pacientes portadores de mutaciones en los genes *BRCA1* y *BRCA2* presentaban un acortamiento telomérico acelerado que se asociaba con un fenómeno de anticipación trans-generacional en la aparición del cáncer, lo que sugería que en el contexto de cáncer de mama hereditario, las mutaciones en *BRCA1* y *BRCA2* modificaban el riesgo al desarrollo de la enfermedad a través de su efecto modificador en la biología del mantenimiento telomérico. Posteriormente, dos trabajos independientes con un tamaño muestral superior encontraron resultados muy dispares en relación a los publicados inicialmente por nuestro grupo; sin embargo, los tres trabajos eran estudios retrospectivos y no tuvieron en cuenta la existencia de posibles modificadores de la longitud telomérica como factores de confusión.

De esta manera el objetivo principal de esta Tesis ha estado enfocado en la identificación de factores genéticos y exógenos modificadores de la longitud telomérica, principalmente dentro del contexto de cáncer de mama y ovario hereditario. Para ello hemos planteado un estudio prospectivo con familias portadoras o no, de mutación en los genes *BRCA1* y *BRCA2* a los que se ha citado en consulta para la extracción de muestras biológicas y para completar un cuestionario sobre su tratamiento y evolución de la enfermedad.

En relación a los factores exógenos, en un primer estudio pudimos confirmar que la quimioterapia acortaba los telómeros en los pacientes que estaban en siendo tratados; aunque este efecto era de carácter transitorio. Así, al corregir los resultados de longitud telomérica por el estado de tratamiento, tanto los resultados como las conclusiones eran diferentes en relación al efecto modificador de la longitud telomérica de los genes *BRCA1* y *BRCA2* como factor causal en riesgo al desarrollo de cáncer. Lo que nos lleva a pensar que la quimioterapia es un factor de confusión en este tipo de estudios.

Continuamos estudiando factores genéticos como potenciales modificadores de la longitud telomérica. Así pues, se evaluaron 2 polimorfismos modificadores del riesgo a desarrollar cáncer de mama y ovario para portadores de mutaciones en los genes *BRCA1* y *BRCA2*. Estos polimorfismos, se encuentran en regiones reguladoras de la transcripción de las glucosilasas *OGG1* y *NEIL2,* las cuales están involucradas en la vía de reparación del ADN por escisión de base (BER), muy activa en la reparación del daño oxidativo a nivel telomérico. De esta forma, nos planteamos estudiar las bases moleculares responsables de esta asociación y su relación con la biología del mantenimiento de la longitud telomérica. Para ello, se evaluó el papel de estos polimorfismos en relación a la regulación transcripcional de *OGG1 y NEIL2*, su contribución en la inestabilidad genómica y/o telomérica, así como su relación con el estrés oxidativo. De esta manera, identificamos que estos polimorfismos tienen un efecto funcional a nivel transcripcional y pueden afectar a la eficiencia de la reparación del daño oxidativo en el telómero. Además, parecen tener un papel importante en la regulación de la longitud telomérica en portadores de mutaciones en *BRCA1* y *BRCA2*.

Basándonos en la posibilidad de una posible relación de letalidad sintética entre *OGG1* (BER) y *BRCA1* de la vía de reparación del ADN de recombinación homóloga (HR), hemos probado la inhibición farmacológica de la enzima OGG1, utilizando un panel de inhibidores de *OGG1*, en un conjunto de líneas celulares de cáncer deficientes de *BRCA1* y *BRCA2*.Hemos identificado que en las células con el mismo fondo genético, la inactivación de BRCA1 hace células muy sensibles a estos inhibidores, lo que podría abrir un nuevo marco para el tratamiento del cáncer de mama hereditario.

Complementariamente, en la presente Tesis doctoral se muestran dos ejemplos de enfermedades hereditarias, angiosarcoma cardiaco hereditario y anemia aplásica, en las que el factor desencadenante de la enfermedad es la desregulación de la longitud telomérica, causada por mutaciones en los genes asociados a las shelterinas, y a la telomerasa respectivamente. Lo que pone de manifiesto la relación existente entre la biología del telomero en relación al cáncer y/o a otras enfermedades.

ABSTRACT

The role of telomere shortening on cancer risk is a complex issue, and likely depending on several factors. In a previous study published by our group, we showed that patients harboring mutations in the *BRCA1* and/or *BRCA2* genes presented an accelerated telomeric shortening and an anticipation in the onset of cancer across successive generations in families affected. This suggested, that in the context of hereditary breast and ovarian cancer, mutations in *BRCA1* and *BRCA2* modified the risk of developing cancer through an accelerated telomere shortening.

Subsequently, two independent studies using a larger number of families found very different results, compared to those reported by our group; however, the three studies were retrospective, and did not consider the possible existence of telomere length modifiers as confounding factors. In this way, the main objective of this Thesis has been focused on the identification of genetic and environmental factors modifying the telomere length, mainly in the context of hereditary breast and ovary cancer. To this end, we proposed a prospective study involving families affected by hereditary breast and ovarian cancer, with or without mutation in the *BRCA1* and *BRCA2* genes. Participants, have been cited in medical consultancy for the extraction of biological samples and to complete a questionnaire about their treatment and evolution of the disease.

Regarding the exogenous factors, in a first study we could confirm that the chemotherapy shortened the telomeres in the patients who were being treated, although this effect was transitory. After correction for the treatment status, both the results and the conclusions were different in relation to the effect of the *BRCA1* and *BRCA2* mutations on telomere shortening as a causal risk factor for developing of cancer. Suggesting that chemotherapy was indeed a confounding factor for this type of studies.

We continued studying genetic factors as potential telomere length modifiers: In this case, two "cancer risk polymorphisms", which modify breast and ovarian cancer risk susceptibility, for *BRCA1* and *BRCA2* mutation carriers.

These polymorphisms were found in transcriptional regulatory regions of *OGG1* and *NEIL2* genes. Both genes, encoding for DNA glycosylases which are key enzymes, involved in the base excision repair pathway (BER) which has an important role on repairing oxidative DNA damage at telomeres. Hence, we wanted to study molecular bases responsible for this association and its role on the telomere biology.

Hence, we evaluated the role of these SNPs in relation to *OGG1* and *NEIL2* transcriptional regulation, its contribution on genomic and / or telomere instability, as well as its possible relation with systemic oxidative stress. Thus, we identified that these SNPs have a functional effect at the transcriptional level and can affect the enzyme efficiency of repairing oxidative DNA damage at the telomere, as well as telomere length for *BRCA1* and *BRCA2* mutations carriers.

Based on a possible synthetic lethality relationship between OGG1 (BER) and BRCA1 (HR) DNA repair pathways, we tested the antiproliferative properties of inhibiting pharmacologically OGG1 enzyme using a panel of OGG1 inhibitors, in a set of BRCA1 and BRCA2 deficient cancer cell lines. We have identified that in cells with the same genetic background, inactivation of BRCA1 make cells very sensitive to OGG1 inhibitors. This may open a new framework for the treatment of hereditary breast cancer.

In addition, we present two examples of hereditary diseases, hereditary cardiac angiosarcoma and aplastic anemia, in which the molecular mechanism of the disease initiation is telomere dysregulation, caused by mutations in genes associated with the shelterin complex and the telomerase respectively. This examples illustrate the complexity of telomere biology in relation to cancer and / or other diseases.

Abbreviations …… 1
INTRODUCTION …… 5
1. General aspects of telomere biology …… 7
2. Telomere structure …… 8
2.1. Telomere DNA …… 8
2.2. Telomere lengthening: Telomerase …….. 9
2.3. Telomere protection: shelterin complex ……... 10
3. Reactive Oxygen Species affect telomere biology, aging and cancer ……. 12
3.1. Oxidative DNA damage and Base Excision Repair …… 12
3.2. BER in telomere maintenance ……. 15
4. Telomeres in cancer …… 16
5. Leukocytes telomere length and disease …….. 17
6. Telomeropathies ……... 18
6.1. Telomere biology in hereditary breast and ovarian cancer (FBOC) …… 19
7. Telomere length variation in humans …….. 20
7.1. Genetic basis of TL …… 20
7.2. Inflammation, oxidative stress and telomere length …… 21
7.3. Environmental factors that affect telomere length in human ……... 22
7.4. Cancer therapies that affect telomere length …… 22
HYPOTHESIS. OBJECTIVES …… 23
ARTICLES …… 25
ARTICLE 1. Impact of chemotherapy on telomere length in sporadic and familial breast cancer patients …… 27
ARTICLE 2. Molecular insights into the OGG1 gene, a cancer risk modifier in BRCA1 and BRCA2 mutation carriers…… 51
ARTICLE 3. Variation in the NEIL2 DNA glycosylase gene is associated with oxidative DNA damage in BRCA2 mutation carriers …….. 71
ARTICLE 4. Synthetic lethality in BRCA1 deficient breast cancer cell lines after OGG1 drug inhibition …… 107
Examples of telomere length dysregulation as a cause of cancer/disease development ... 125
ARTICLE 5. A mutation in POT1 gene is responsible for cardiac angiosarcoma in TP53-negative-Li-Fraumeni-like families …… 127
ARTICLE 6. Telomerase gene therapy rescues telomere length, bone marrow aplasia, and survival in mice with aplastic anemia ……. 149
DISCUSSION …… 169
- Exogenous factors that modify telomere length: chemotherapy. Article 1…….. 172

- Endogenous factors that modify telomere length: “Cancer risk polymorphisms in DNA glycosylases of the BER pathway” …… 175
  - Article 2 …… 176
  - Article 3 …… 178
- BER DNA glycosylases as potential targets for treating BRCA1/BRCA2-derived tumors. Article 4 …… 180
- TL modifications caused by other genetic events …… 181
  - Article 5 …… 181
  - Article 6 …… 182
- General discussion …….. 182

CONCLUSIONS/CONCLUSIONES …….. 185

BIBLIOGRAPHY …… 191

ABBREVIATIONS

5-aza-CdR: Agent 5-aza-2´-deoxycytidine

AAV-9: Adeno-associated virus 9

BRCAX: Individuals from families without mutations in *BRCA1* or *BRCA2*

hoC: 5-hydroxycytosine

OB: Oligonucleotide/oligosaccharide-binding

AC+T: A (Doxorubicin), C (Cyclophosphamide), T (Paclitaxel)

FEC+T: F (5-fluoracil), E (Epirubicin), C (Cisplatin), T (Taxol)

T+AC: T (Taxol), A (Doxorubicin), C (Cyclophosphamide)

T+FEC: T (Taxol), F (5-fluoracil), E (Epirubicin), C (Cisplatin)

3-meA: N3-methyladenine

4OOH-CPA: 4-hydroperoxycyclophosphamide

5-FU: Fluorouracil

5´-OH: 5´ Dihydroxyle

8-oxoG: 7,8-Dihydro-8-oxoguanine

ACYP2: Acylphosphatase-2

ALT: Alternative lengthening of telomeres

ATM: ATM serine/threonine kinase

ATR: ATR serine/threonine kinase

BER: Base Excision Repair

BRCA1: Breast cancer gene 1

BRCA2: Breast cancer gene 2

c-MYC: Proto-Oncogene C-Myc

CTC1: Telomere Replication Complex Component 1

DNA: Deoxyribonucleic acid

dNTPs: Deoxynucleotide

dRP: Deoxyribose phosphate

DSBs: Double strand breaks

E2F: *E2F* transcription factor 1

eQTL: Expression quantitative trait loci

FapyA: 4,6-diamino-5-formamidopyrimidine

FapyG: 2,6-diamino-4-hydroxy-5-formamidopyrimidine

FBOC: Familial breast and ovarian cancer

FEN1: Flap structure-specific endonuclease 1

fU: Fluorouracil

G4: G-quadruplex

GWAS: Genome-wide association study

hmU: 5-hydroxymethyluracil

hoU: 5-Hydroxyuracil

HR: Homologous recombination

hTR: The component produced from the TERC gene (RNA molecule)

IFN-γ: Interferon gamma

IL-1βa: Interleukine- 1βα

IL-6: Interleukin 6

LCLs: Lymphoblastoid cell lines

LD: Linkage disequilibrium

LTL: Leukocyte Telomere Length

MBD4: Methyl-CpG-binding domain protein 4

MDA: Malondialdehyde

miRNA: MicroRNA

MPG: N-Methylpurine DNA Glycosylase

mRNA: Messenger RNA

MYH: MutY DNA glycosylase

NAF1: Nuclear Assembly Factor 1 Ribonucleoprotein

NEIL1-NEIL3: Endonuclease VIII-like 1, Endonuclease VIII-like 2, Endonuclease VIII-like 3

NFR2: Nuclear factor E2-related factor 2

NHP2: Ribonucleoprotein

NOP10: Member of the H/ACA snoRNPs (small nucleolar ribonucleoproteins) gene family.

NTH1: Bifunctional DNA N-Glycosylase/DNA-(Apurinic Or Apyrimidinic Site) Lyase

OBFC1: Oligonucleotide/oligosaccharide-binding fold-containing protein 1

OGG1: 8-oxoguanine DNA glycosylase

OH: Hydroxyle

POT1: Protection of Telomeres 1 gene

qPCR: Quantitative polymerase chain reaction

RAP1: Ras-related protein 1

ROS: Reactive oxygen species

RTEL1: Regulator of telomere elongation helicase 1

Sin3Ak-20: Transcription Regulator Family Member A

SMUG1: Single-Strand-Selective Monofunctional Uracil-DNA Glycosylase 1

SSBs: Single-strand breaks

TCAB1: Also known as WRAP53 gene (implicated in cancer development)

TDG: Thymine-DNA glycosylase

TERC: Telomerase RNA component

TERT: Telomerase reverse transcriptase

Tg: Thymine glycol

TH5487: OGG1 inhibitor developed at Thomas Helliday's lab

TIN2: Is a component of the shelterin protein complex found at the end of telomeres

TIN2: TERF1-interacting nuclear factor 2

TL: Telomere length

TNF-α: Tumor necrosis factor α

TP53: Tumor protein 53

TPP1: Tripeptidyl peptidase 1

TRF1: Telomeric Repeat Binding Protein 1

TRF2: Telomeric Repeat Binding Protein 2

UNG: Uracil DNA Glycosylase

UTR: Untranslated region

WNT: Refers to the canonical Wnt pathway

XRCC1: X-ray repair cross-complementing protein 1

YY1: Transcription factor Yin Yang 1

ZNF208: Zinc Finger Protein 208

γH2AX: Histone H2AX phosphorylation on serine 139 (Marker for DNA double-strand breaks)

INTRODUCTION

1. GENERAL ASPECTS OF TELOMERE BIOLOGY

DNA replication at the end of the chromosome is a challenging task for eukaryotes (De Lange 2009). There are two main problems that are solved by a unique structure: first, DNA polymerases require a primer because they can only proceed in the 5´ to 3´ direction. Hence, after each round of replication, sequences of DNA would be lost at the end of the chromosome. This is known as the DNA "end-replication problem". In eukaryotes, this sequence length equilibrium is solved by telomeres, which contain an array of tandemly repeated nucleotide sequences localized at the end of the chromosome that act as a "buffer" to withstand the erosion of DNA. Hence, in the absence of special telomere maintenance mechanisms, linear chromosomes shorten progressively with every round of DNA replication, eventually leading to cellular senescence or apoptosis (Lingner *et al*. 1995).

However, a cellular reverse transcriptase called telomerase counteracts telomere shortening in many organisms, including humans (Gilson & Géli 2007). Telomerase is required for unlimited proliferation of immortal human tumor cells, as well as for the extended proliferation in germinal, embryonic and certain stem cells where it contributes to the maintenance of telomere length (TL), but it is absent in most somatic cells (Gilson & Géli 2007).

The other biological problem that was referred to above is called the "end-protection problem". In eukaryotes, the ends of chromosomes could be mistaken for damaged or broken DNA. In this scenario, cells might attempt to "repair" the chromosome ends recognized as double-stranded breaks (DSBs). In mammals, telomeres solve the end-protection problem through a multiprotein structure called the "shelterin complex" that includes *TRF1, TRF2, RAP1, TIN2, POT1***,** and *TPP1* gene products. This multiprotein complex coats the repeating sequences of the telomeres (De Lange 2005). Telomere regions are frequently compromised by DNA damage that accumulates during aging (Cesare *et al*. 2009), likely through oxidation-mediated base modifications and associated strand breaks (Hewitt *et al*. 2012). In addition, compaction of the telomere by the shelterin complex may render telomere DNA damage more resistant to DNA repair (Fumagalli *et al*. 2012). If not repaired efficiently, damaged telomeres will suffer accelerated erosion and restrict the proliferative lifespan of cells. Currently, how the telomeric structure and the shelterin proteins protect telomeres against DNA damage are urgent questions for understanding the role of telomeres during oncogenesis.

2. TELOMERE STRUCTURE

2.1. Telomere DNA

TL is highly variable between species, within species, within an organism, and even between chromosomes. In humans, TL ranges from 10-15 kb of the repetitive G-rich sequence 5′-T_2AG_3-3′, plus 75-600 nucleotides of a 3′ single-stranded overhang (McElligott & Wellinger 1997; Canela *et al*. 2007) (Figure 1A). In humans, DNA shortens by around 30-150 bp per replication cycle in cells without telomere maintenance mechanisms (Harley *et al*. 1990; Takubo *et al*. 2002).

The 3′ single-stranded overhang of a telomere can invade the double-stranded telomeric tracts and thus form two internal loops, the d-loop and the T-loop (Griffith *et al*. 1999; Greider 1999) (Figure 1B). In addition to T-loops, G-strand telomeric DNA from most organisms forms G-quadruplex (G4) structures, stable secondary DNA structures that are held together by multiple guanine–guanine base pairs (Webb *et al*. 2013).

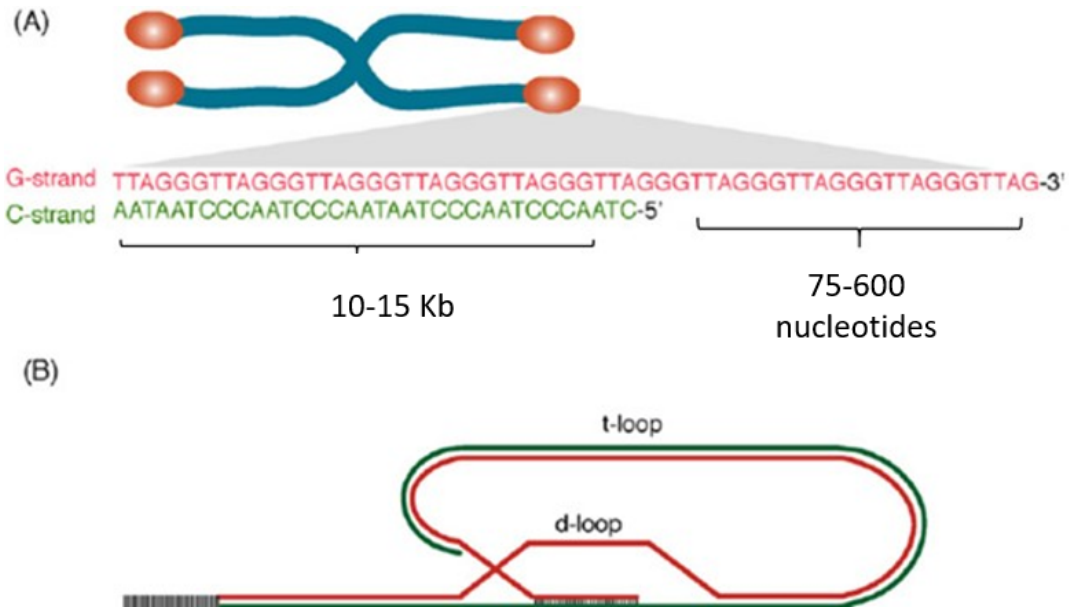

Figure 1. Structure of mammalian telomeres. (A) Chromosomes in mammalian cells end in long arrays of [TTAGGG] repeats. The strand containing the 3′ terminus, termed the G-strand, is rich in guanine and is many nucleotides longer than its complementary C-strand. This G overhang varies in length between different organisms. **(B)** Schematic representation of a telomere in a T-loop configuration. The G-strand is shown in red, the C-strand in green. This figure was modified from (Lazzerini 2009).

Presumably, the T-loop acts like a protective cap at the end of the chromosomes by preventing recognition by the DNA damage repair machinery as DNA double-strand breaks and subsequent inappropriate activation of DNA damage checkpoints (De Lange 2005). However, cell division will inevitably lead to telomere shortening and thus to destabilization of the telomeres, due to the inability to recruit the proteins of the shelterin complex. Consequently, the T-loop will no longer form properly, the chromosome ends will be left uncapped, and the cells will either trigger senescence or apoptosis.

2.2. Telomere lengthening: Telomerase

Telomere shortening can be counteracted by two known lengthening mechanisms. Most cancer cells, as well as germline and stem cells, activate the ribonucleoprotein enzyme telomerase to compensate for telomere loss (Kim *et al*. 1994; Wright *et al*. 1996). In contrast, in approximately 10% to 15% of cancers, telomeres are maintained by homologous recombination (HR) dependent alternative lengthening of telomeres (ALT) rather than by telomerase activation (Dilley *et al*. 2016).

Telomerase reverse transcriptase (TERT) is a unique cellular enzyme that is a component of the ribonucleoprotein telomerase: via reverse transcription of its own RNA template (*TERC*), telomerase synthesizes the tandem 5′-TTAGGG-3′ exonucleotide repeats of telomeric DNA, which prevents chromosome attrition resulting from incomplete semiconservative DNA replication at chromosomal ends (Bryan & Cech 1999). By using *TERC*, TERT can add a six-nucleotide repeating sequence, 5′-TTAGGG (in vertebrates, the sequence differs in other organisms) to the 3′ strand of chromosomes. These TTAGGG repeats (with their various protein binding partners) are called telomeres. The template region of *TERC* is 3′-CAAUCCCAAUC-5′ (Gavory *et al*. 2002) (Figure 2).

Telomerase is not active in most human somatic cells because transcription by TERT, the catalytic subunit, is repressed by several tumor suppressor pathways (Lin & Elledge 2003). For instance, the WNT signaling pathway, which is important for stem cell identity, affects *TERT* gene expression. β-catenin, a central player in WNT signaling, acts directly to activate *TERT* transcription in embryonic and adult stem cells as well as in human cancer cells (Hoffmeyer *et al*. 2012). The *c-MYC* oncogene also positively regulates *TERT* transcription (Wu *et al*. 1999). Hence, activation of oncogenes during carcinogenesis correlates with unlimited telomerase activation.

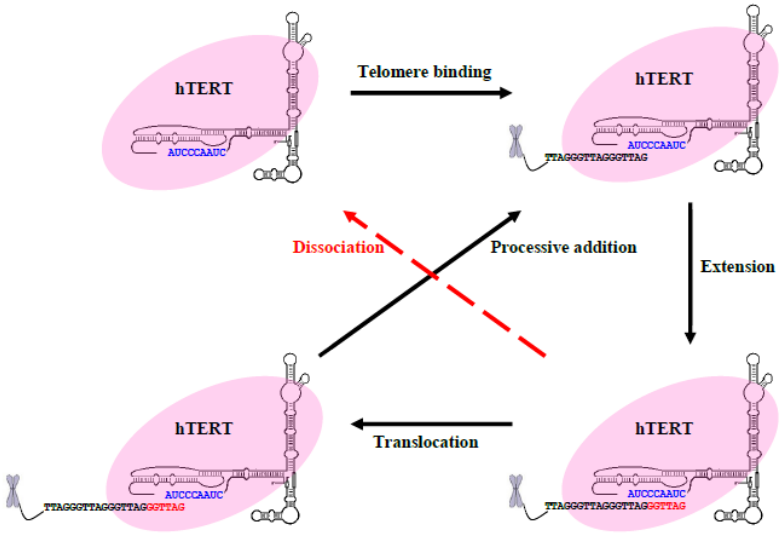

Figure 2. Mechanism of telomere extension by telomerase. Human telomerase ribonucleoprotein consisting of telomerase reverse transcriptase (TERT) and telomerase RNA (TR) is illustrated. The processive cycle of telomere binding to the telomerase RNA template (blue), extension through addition of dNTPs (red), and translocation adds GGTTAG repeats to the 3´ telomeric terminus. The process is interrupted when the extended telomere dissociates from telomerase (dotted red line). This figure was adapted from (Harley 2002).

2.3. Telomere protection: shelterin complex

The tandemly repeated telomere sequence TTAGGG associates with the six-protein shelterin complex, which enables cells to distinguish their natural chromosome ends from DNA breaks, represses DNA repair reactions, and regulates telomerase-based telomere maintenance (Palm & De Lange 2008) (Figure 3). During the non-mitotic phase of the cell cycle, both the double and single-stranded telomeric DNA is protected by the telomeric repeat-binding factor 1 (TRF1), TRF2, RAP1, TERF1-interacting nuclear factor 2 (TIN2), TPP1 and POT1 (De Lange 2005). Deletion of any of these genes leads to disruption of TL regulation and end protection.
The telomeric repeat binding factors TRF1 and TRF2 bind to double-stranded telomeric DNA and have a role in telomere stabilization and TL regulation (Van Steensel & De Lange 1997; Van Steensel *et al*. 1998). Both proteins are extremely abundant and ubiquitously expressed during the cell cycle (Crabbe *et al*. 2004).

RAP1 is an essential but poorly characterized constitutive binding partner of TRF2 (Li *et al*. 2000). RAP1 forms a complex with TRF2 (Matsutani *et al*. 2001) and is dependent on TRF2 for its telomeric localization and stability; most of it is lost upon *TRF2* gene deletion (Celli & De

Lange 2005). Additionally, RAP1 is recruited to telomeres via TRF2 and it is known to negatively regulate TL (De Lange 2005).

Other proteins from the shelterin complex do not directly interact with telomeric DNA. TIN2 associates with TRF1, TRF2 and TPP1, and forms a heterodimer with POT1 (Houghtaling *et al*. 2004; Kim *et al*. 2004; Kim *et al*. 1999; Ye *et al*. 2004). TPP1 connects POT1 with TIN2. These interactions are necessary for proper telomere association of POT1 and are essential for TL regulation (Sexton *et al*. 2014). Finally, POT1 is a protein that in humans is encoded by the *POT1* gene; it contains two N-terminal oligonucleotide/oligosaccharide-binding (OB) folds, which allows its binding to the telomeric G-strand overhang (Lei *et al*. 2004; Baumann & Cech 2001; Loayza & De Lange 2003). POT1 regulates TL by preventing telomerase access to telomeres by sequestering the DNA terminus (Loayza & De Lange 2003; Chen *et al*. 2007).

Shelterin represses two main DNA-damage signaling pathways: the ATR kinase pathway, blocked by POT1, and the ATM kinase pathway, blocked by TRF2 (De Lange 2010).

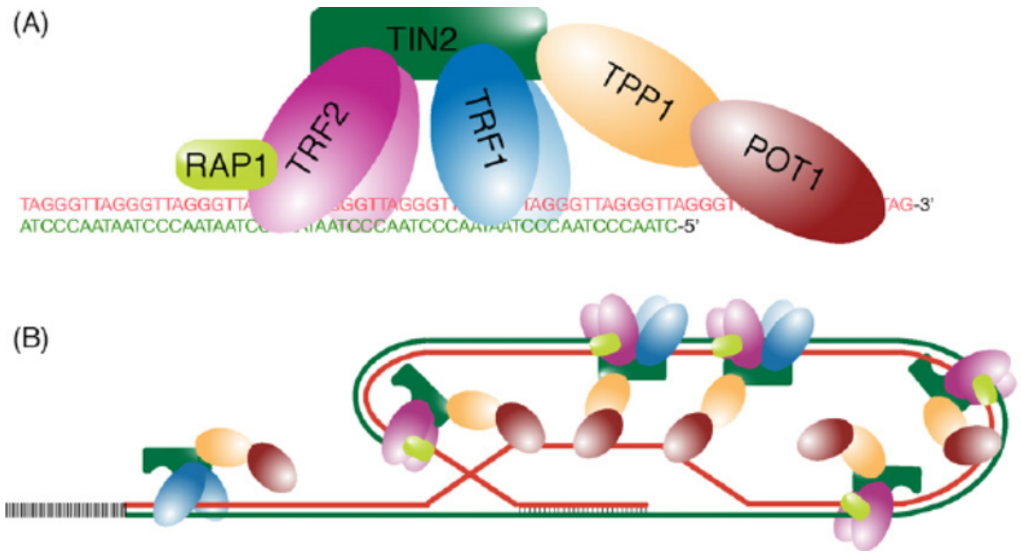

Figure 3. The shelterin complex. (A) The six proteins that constitute the shelterin complex (see text for details). **(B)** Schematic model of shelterin complex bound to a telomere in a T-loop configuration. TRF1 and TRF2 bind double-stranded TTAGGG repeats and TIN2 independently, thus different subcomplexes can exist at telomeres and are depicted in this scheme. This figure was modified from (Lazzerini *et al* 2009).

3. REACTIVE OXYGEN SPECIES AFFECT TELOMERE BIOLOGY, AGING AND CANCER

In normal human somatic cells, telomeres gradually shorten after each cell division. Once telomeres become too short, cells enter senescence. Therefore, telomeres limit the number of cell divisions. Even though progressive shortening of telomeres occurs after each cell division, the speed at which telomeres shorten depends on many factors (Passos *et al*. 2007; Hewitt *et al*. 2012). Cellular environment is crucial for regulating TL and telomerase activity. In particular, oxidative stress is one of the main contributors to the shortening of telomeres. When mitochondrial dysfunction occurs concomitant with increased reactive oxygen species (ROS) generation, the susceptibility of telomeres to oxidative damage leads to accelerated telomere shortening, increased probability of uncapping, activation of a DNA damage response, and irreversible cell cycle arrest (Martens *et al*. 2000; Borodkina *et al*. 2014). In addition, it has been documented that oxidative stress also interferes with telomere maintenance via its effect on telomerase activity (Finkel *et al*. 2000; Fouquerel *et al*. 2016).

Free radicals and other ROS are produced in a wide range of physiological processes. Mitochondrial respiration is a major endogenous source of ROS. The electron transport chain or oxidative phosphorylation system is located in the inner mitochondrial membrane and is responsible for the production of ATP, generation of ROS, and regulation of programmed cell death.

Chronic elevation of the levels of ROS causes damage to the electron transport system, which in turn produces ROS at an even higher rate. Reactive oxygen species can also cause mutations in DNA that lead to cancer (Mena *et al*. 2009; Audeh *et al*. 2010). Thus oxidative stress plays an important role in cell death, which can lead to accelerated aging and various pathologies including neoplastic, cardiovascular, inflammatory, and degenerative diseases (Benz & Yau 2008; Stephens *et al*. 2009).

3.1. Oxidative DNA damage and Base Excision Repair

The chemical instability of the DNA molecule can result in hydrolytic loss of DNA bases, base oxidations, non-enzymatic methylations and other chemical alterations. DNA damage can also occur because of reactions with exogenous (environmental) and endogenous (intracellular) DNA-reactive species (Lindahl 1993; Friedberg 2003).

A nucleic acid can be oxidized by ROS through a Fenton reaction (Wardman & Candeias 1996). To date, around 20 oxidative lesions have been discovered in DNA (Cooke *et al*. 2003).

The most frequently oxidized bases found at the telomere region are oxidation products of guanine, 8-oxoG and FapyG lesions (Figure 4).

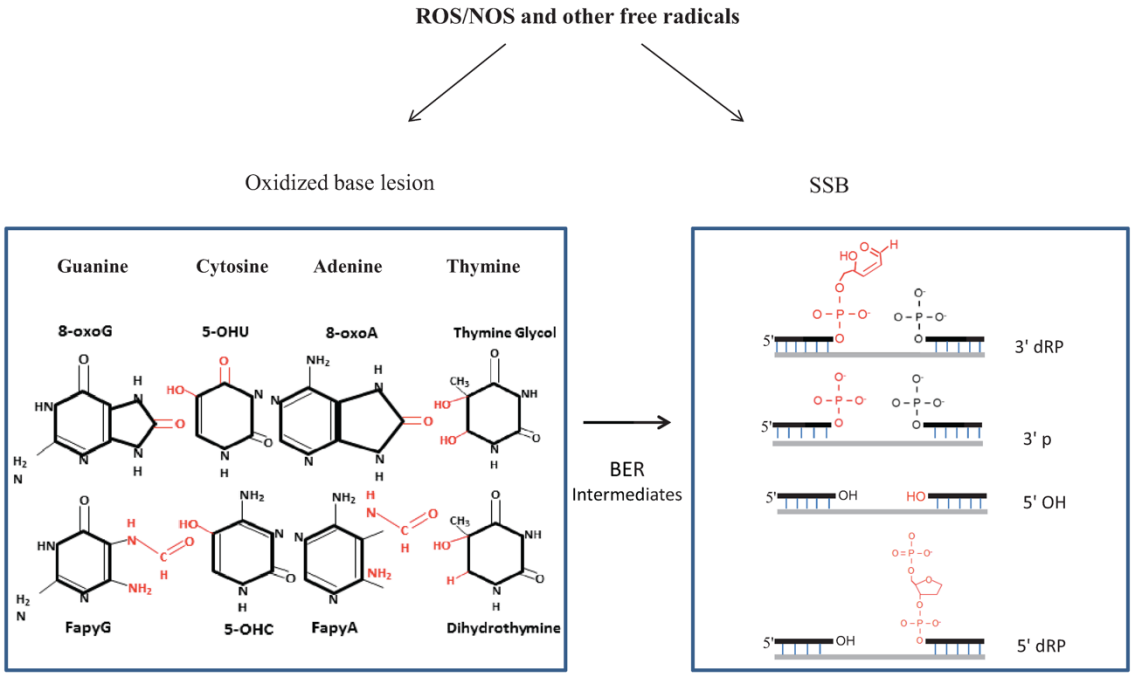

Figure 4. ROS and Reactive Nitrogen Species are constantly produced during aerobic metabolism. ROS generate several dozen oxidized base lesions and single-strand breaks (SSBs) in the genome. SSBs are also generated as intermediates during the processing of oxidized bases via Base Excision Repair (BER). ROS-induced SSBs contain diverse termini, like 3´-phosphoglycolate, 3´-phosphate, 5´-OH and 5´-deoxyribose phosphate (5´dRP) (Mitra *et al*. 2014).

The Base Excision Repair (BER) pathway is an essential repair pathway that corrects multiple DNA alterations that frequently occur in DNA. BER deficiency affects genome stability and it is involved in different pathological conditions, including premature aging (Lombard *et al*. 2005), neurodegeneration (Caldecott 2008) and cancer (Bartkova *et al*. 2006).

The major players involved in BER have been known for a long time (Lindahl 1990), and the entire BER process has been reconstituted with purified enzymes (Kubota *et al*. 1996; Dianov & Lindahl 1994) (Figure 5). BER is initiated by a damage-specific DNA glycosylase (Lindahl 1979). Currently, 11 human DNA glycosylases that recognize and excise a wide range of DNA base damages are described to act at the first step of the pathway (Table 1).

Table 1. Summary of the properties of known glycosylases in humans

GLYCOSYLASE	TYPE*	SUBSTRATES
MPG	monofunctional	3-meA, hypoxanthine
UNG	monofunctional	uracil
OGG1	bifunctional	8-oxoG, FapyG
NTH1	bifunctional	Tg, hoU, hoC, urea, FapyG
NEIL1-NEIL3	bifunctional	Tg, hoU, hoC, urea, FapyG, FapyA
MYH	monofunctional	A:8-oxoG
SMUG1	monofunctional	U, hoU, hmU, fU
TDG	monofunctional	T:G mispair
MBD4	monofunctional	T:G mispair

***monofunctional glycosylases** have only glycosylase activity, whereas **bifunctional glycosylases** also possess AP lyase activity.

Following the removal of the damaged base, APE1 (apurinic/apyrimidinic endonuclease 1) cuts the DNA backbone at abasic sites, leaving a single nucleotide gap and a deoxyribose fragment. The gap is then repaired by short-patch or long-patch repair depending on the cell cycle phase and nature of the deoxyribose fragment (Figure 5). In short-patch repair, the repair gap is only one nucleotide, while in long-patch repair replicative polymerases insert 2-8 nucleotides, displacing the pre-existing bases 3′ to the original lesion. In the long patch pathway, the overhanging single-strand flap is removed by flap endonuclease 1 (FEN1). In short patch repair DNA polymerase β (Polβ) inserts a single nucleotide and removes the dRP-fragment through its associated dRPase activity, and the single-strand break is sealed in a ligation step completed either by the DNA repair enzyme DNA ligase III in association with XRCC1 for the short patch pathway or by the replicative DNA ligase I in the long patch pathway (reviewed in (Wallace 2014)).

Pathogenic defects in BER have only been identified for the initiating DNA glycosylases (UNG-Hyper-IgM syndrome and MUTYH associated polyposis (Kavli *et al*. 2005; Oliver *et al*. 2003) possibly because repair defects at BER intermediate steps are poorly tolerated. Attempts at generation knockout mice for APE1, FEN1, Polβ, XRCC1 or Ligase III results in embryonic lethality at an early stage of embryogenesis (Tebbs *et al*. 1999; Gu *et al.* 1994; Puebla-Osorio *et al*. 2006; Kucherlapati *et al*. 2006; Kucherlapati *et al*. 2002; Xanthoudakis *et al.* 1999).

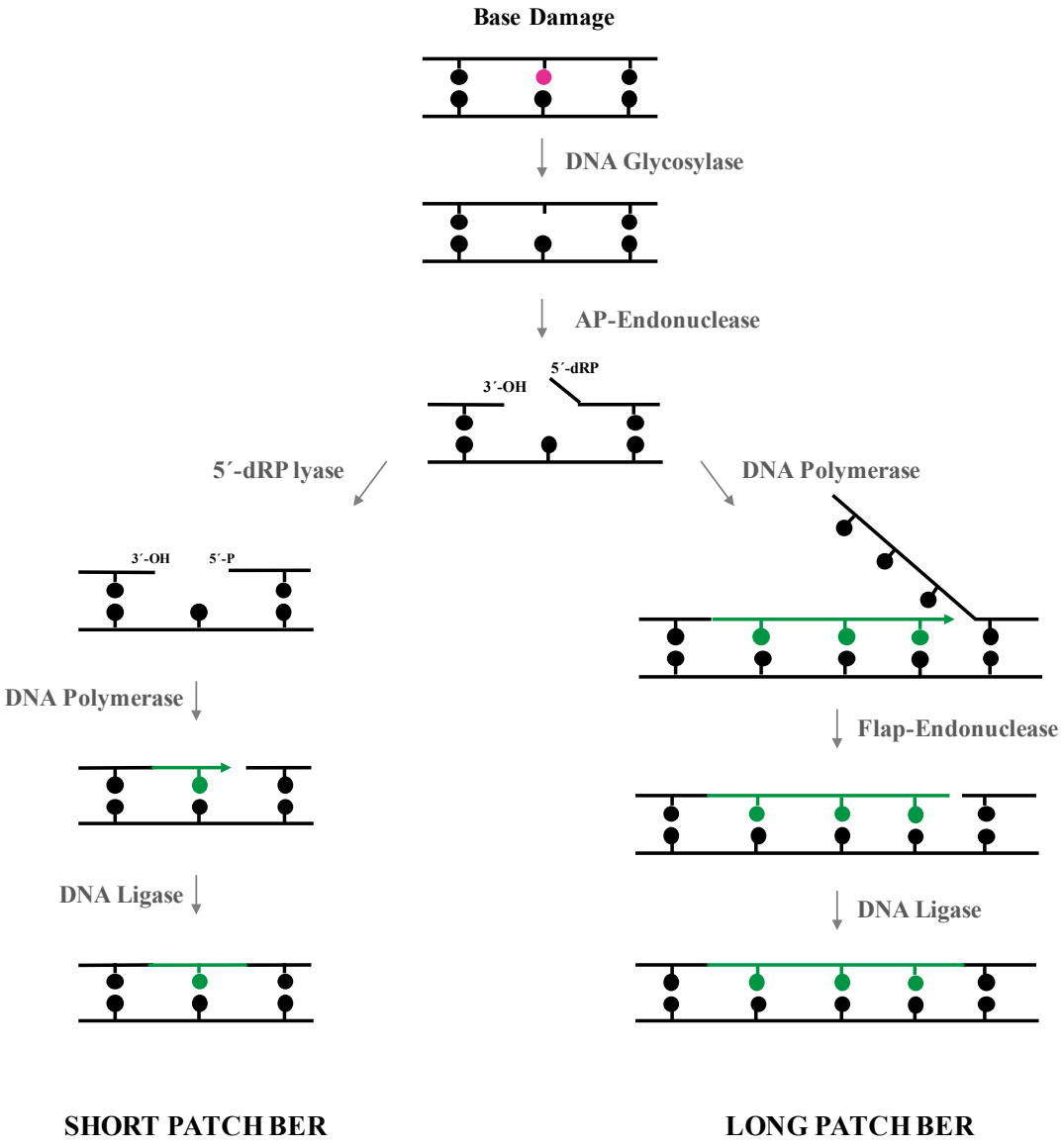

Figure 5. Steps involved in Short Patch and Long Patch Base Excision Repair pathway.

3.2. BER in telomere maintenance

The long arrays of TTAGGG repeats make telomeres particularly susceptible to oxidative lesions. Oxidative damage is thought to be a primary cause of telomere shortening, based on observations that telomere attrition rate is significantly decreased when cells are grown under hypoxic conditions or in the presence of antioxidants (Von Zglinicki 2002; Richter & Zglinicki 2007). In addition, both uracil residues and oxidized guanine derivatives are commonly present at telomeres (Vallabhaneni *et al*. 2015; Oikawa & Kawanishi 1999). Mounting evidence from both *in vivo* and *in vitro* studies suggests that BER is actively promoted at telomeres (Vorlícková

et al. 2012; Rhee *et al*. 2011; Wang *et al*. 2010; Chakraborty *et al*. 2015; Zhou *et al*. 2015), although the exact mechanism of BER at telomeres is still unknown.

In relation with this, DNA glycosylases like OGG1 and NEIL1-3 have an important role in oxidative damage repair at telomeres (Dziaman *et al*. 2014; Wang *et al*. 2010; Zhou *et al*. 2015; Osorio *et al*. 2014). Accumulation of oxidative DNA damage at the telomere region by incorrect functioning of BER can affect TL and cause different abnormalities like telomere sister chromatid exchanges, increased telomere single- and double-strand breaks, and telomere G-strand losses. The accumulation of 8-oxo-G at telomeres can disrupt TRF1 and TRF2 binding to the telomere, leading to uncapped telomeres (Opresko *et al*. 2005) and subsequent telomere instability. In addition, it was recently described that 8-oxoG regulates telomere elongation by telomerase in humans (Fouquerel *et al*. 2016).

4. TELOMERES IN CANCER

Telomere erosion can promote genome instability when combined with other cellular and genomic alterations, potentially leading to tumorigenesis. Conversely, it can also act as a powerful tumor suppressor by activation of the replicative senescence process (Shay & Wright 2002; Counter *et al*. 1992; Ma *et al*. 2011).

In humans, the distribution of TL among different chromosome arms is heterogeneous, with some chromosomes having longer telomeres than others (Zou *et al*. 2004). Importantly, this telomere signature is partially a heritable trait that is determined at fertilization and maintained throughout life (Broer *et al*. 2013; Slagboom *et al*. 1994). The time point at which chromosome arms will become uncapped depends on the specific telomere shortening rate occurring in each cell type or tissue. When TL reaches a very short threshold (perhaps when T-loops cannot be maintained) an uncapping signal is generated, resulting in cellular senescence (Figure 6). However, rare cells (~$1{:}10^6$–10^7), after having acquired sufficient genome / telomere instability, progress to the activation of a telomere maintenance mechanism (telomerase or ALT) that leads to immortalization and malignancy. Emerging evidence indicates that telomerase promoter mutations are highly prevalent in multiple cancer types (Heidenreich *et al*. 2014).

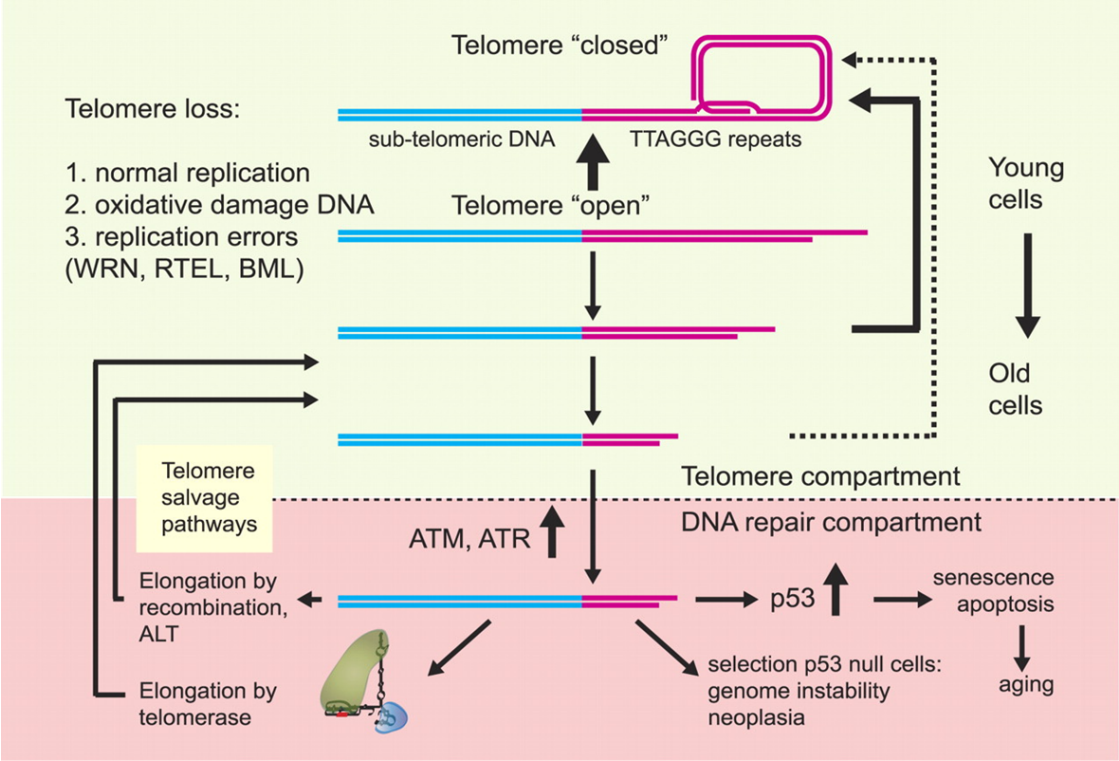

Figure 6. Diagram of factors affecting telomere length in primary somatic cells from human tissues. This figure was obtained from (Aubert & Lansdorp 2008).

5. LEUKOCYTE TELOMERE LENGTH AND DISEASE

Measurement of leukocyte telomere length (LTL) in large epidemiologic studies has become popular since 2002, when a qPCR method to measure LTL was first reported (Cawthon 2002). The qPCR approach is advantageous in such studies, because it is amenable to high-throughput platforms and requires very small amounts of DNA. There is also an adequate correlation between qPCR and terminal restriction fragment length, the previous method used to quantify TL (Cawthon 2009). Its implementation led to early association studies of LTL and cancer, which suggested that shorter LTL was associated with increased risk for certain cancers (Wu *et al*. 2003). Indeed, early meta-analyses were conducted to determine whether "short telomeres are associated with cancer risk" and found an increased overall risk for cancer (Ma *et al*. 2011; Wentzensen *et al*. 2011). Because telomere shortening is observed in the aging process, several studies also addressed a likely connection between LTL and mortality. Initial studies suggested that telomere shortening in human beings contributes to mortality in many age-related

diseases (Cawthon *et al*. 2003). Hence, during the initial period of TL association studies, there was agreement that telomere shortening was associated with cancer risk and mortality.

Further studies revealed a large complexity in TL association studies (Weischer *et al*. 2013; Rode *et al*. 2015). These studies were significantly improved by population-based designs to minimize selection bias, large sample size, long follow-up, and by prospective study designs that conferred them accuracy and minimized reverse causality. The conclusions of these studies suggested that there was no association between cancer risk and short TL, although reduced survival was associated with short LTL after cancer (Weischer *et al*. 2013) and high mortality (Rode *et al*. 2015).

Because genotype-phenotype associations are not vulnerable to biases caused by reverse causation or environmental confounding, the latest TL association studies tried to avoid this problem by implementing Mendelian randomization in TL association studies. This is an epidemiologic technique wherein genetic variants known to be associated with long or short LTL are used as surrogate markers to investigate the effect of those genetic variants on cancer/disease (Smith & Ebrahim 2003). This approach has been established as the technically most consistent method to estimate the relationships between TL and cancer risk in the past few years (Zhang *et al*. 2015; Codd *et al*. 2013; Iles *et al*. 2014). Recently, TL-associated genotype studies conducted in 95,568 individuals from the general population concluded that genetic determinants of long telomeres are associated with increased cancer risk, particularly melanoma and lung cancer (Rode *et al*. 2015). However, this latter study lacked ethnic diversity, since all samples were from the Danish population. This may result to be a limitation if these results are extrapolated.

6. TELOMEROPATHIES

Defects in genes involved in telomere maintenance (shelterin complex or telomerase) result in a wide spectrum of overlapping symptoms (Kirwan & Dokal 2008) which converge in disease manifestation.

The symptoms of these disorders are extensive; the age of onset is highly variable and genetic anticipation is involved. However, these disorders share a similar underlying molecular mechanism, premature telomere shortening, that leads to a spectrum of diseases (Holohan *et al*. 2014) (Table 2).

Table 2. List of genes/complexes that cause telomere disorders when defective (Opresko & Shay 2016)

GENE	DISEASES
TIN2	Dyskeratosis congenita/ Hoyeraal Hreidarsson syndrome/ Revesz syndrome
RTEL 1	Dyskeratosis congenita/ Hoyeraal Hreidarsson syndrome
CTC1	Coats Plus
Apollo *(SNM1B)*	Hoyeraal Hreidarsson syndrome
TERT, TERC, Dyskerin, NHP2, NOP10	Dyskeratosis congenita, idiophatic pulmonary fibrosis, aplastic anemia
TCAB1	Diskeratosis congenita

6.1. Telomere biology in Hereditary Breast and Ovarian Cancer (FBOC)

Inherited predisposition to breast and ovarian cancer accounts for approximately 5% of all breast and ovarian cancer cases and is characterized by an autosomal dominant pattern of inheritance, young age of onset and bilateral breast and ovarian cancer. FBOC is associated with inherited mutations mainly in two genes, *BRCA1* and *BRCA2*, which are tumor suppressor genes responsible for maintaining genome stability through their involvement in homologous recombination (HR) double-stranded break (DSB) DNA repair (Roy *et al*. 2012). Carrying an inherited mutation in the *BRCA1* or *BRCA2* genes increases a woman's lifetime risk of developing breast and ovarian cancer, although there are considerable differences in disease manifestation. At the age of 70, cumulative cancer risk for *BRCA1* and *BRCA2* mutation carriers ranges from 43% to 88% for breast cancer development, and from 11% to 59% for ovarian cancer (Antoniou *et al*. 2003; Milne *et al*. 2008).

This high variability is the consequence of other genetic modifiers and/or environmental factors. For example, we recently described that two single nucleotide polymorphisms (SNPs) located in the *OGG1* and *NEIL2* genes (Table 1), were cancer risk modifiers for *BRCA1* and *BRCA2* mutation carriers, respectively (Osorio *et al*. 2014).

Genetic anticipation, is a phenomenon whereby as a genetic disorder is passed on to the next generation, the symptoms of the genetic disorder become apparent at an earlier age with each generation. Genetic anticipation, has previously been described in several hereditary cancer syndromes (Table 1) and also in FBOC (Dagan & Gershoni-Baruch 2001; Peixoto *et al.* 2006).

Telomere shortening was more recently described as a mechanism of cancer anticipation. Importantly, there is evidence that BRCA1 protein is localized at telomeres and may regulate TL and stability (Blasco 2005; Badie *et al*. 2015; Badie *et al*. 2010; Cabuy *et al*. 2009; Uziel *et al*. 2016). In addition, *BRCA2* gene has been described to be involved in telomere replication (Badie *et al*. 2010).

Based on the above evidence, our group hypothesized that telomere shortening may be associated with age anticipation in hereditary breast cancer. In an initial study, we showed that cancer cases harboring mutations in the *BRCA1* and *BRCA2* genes presented significantly shorter LTL compared to sporadic cancer cases. In addition, progressive telomere shortening in those cases was associated with earlier onset of breast cancer in successive generations of affected families (Martinez-Delgado *et al*. 2011). These results provided evidence that telomere shortening could be the causal explanation for earlier age of cancer onset in successive generations among breast cancer families, and suggested that it might be a mechanism of genetic anticipation in hereditary breast cancer (Martinez-Delgado *et al*. 2011), as observed previously in other genetic disorders such as Dyskeratosis Congenita.

After this initial study, 2 consecutive studies including a larger sample size of *BRCA1* and *BRCA2* mutation carriers found contradictory associations between BRCA mutations and TL. The first study reported that TL was normal in *BRCA1* and *BRCA2* mutation carriers (Killick *et al*. 2014), and the second study showed that LTL was long in *BRCA1 and BRCA2* mutation carriers, although it was not associated with an increased cancer risk (Killick *et al*. 2014). These results led to a contradiction in the literature regarding the association between TL and cancer or other diseases, and point to differences in the strategies used to perform these studies (prospective or retrospective), technical issues, and/or the existence of TL modifiers as the possible source of variability (Aviv *et al*. 2011; Raschenberger *et al*. 2016).

7. TELOMERE LENGTH VARIATION IN HUMANS

7.1. Genetic basis of TL

Intra-uterine variables including genetic and other factors during pregnancy determine TL of individuals at birth (Benetos *et al*. 2014). Genetic determinants of TL have been widely investigated. Twin studies indicate that heritable factors may contribute up to 80% of the inter-individual variation in TL (Graakjaer *et al*. 2004; Slagboom *et al*. 1994). Quantitative trait linkage studies have mapped several loci for TL (Mangino *et al*. 2008; Vasa-Nicotera *et al*. 2005; Andrew et al. 2006). Recently, genetic variants at *ACYP2*, *TERC*, *TERT*, *NAF1*, *OBFC1*, *ZNF208* and

RTEL1 have been identified to be associated with TL in three genome-wide association studies (GWAS) in people of European descent (Codd *et al*. 2010; Codd *et al*. 2013; Levy *et al*. 2010; Bojesen *et al*. 2013) and in a Chinese population (Du *et al*. 2015), although each of the LTL-associated variants explains only a small proportion of the total variance in TL across individuals (Codd *et al*. 2013). It is therefore possible that other as yet undiscovered genetic variants can explain TL variability in the general population or in the context of FBOC.

After birth, internal and external environmental factors accelerate or slow down the attrition of telomeres (Kimura *et al*. 2008). Some of these factors are described below.

7.2. Inflammation, oxidative stress and telomere length

Oxidative stress has been shown to exert a major influence on the rate of telomere shortening (Houben *et al*. 2009) because oxidative damage is repaired less well in telomeric DNA than elsewhere in the chromosome (Von Zglinicki 2002). The inflammatory process induces oxidative stress and reduces cellular antioxidant capacity. Many chronic conditions in humans are associated with chronic inflammation, immune system impairment and accelerated aging. In addition, abnormalities in the telomere/telomerase system of these patients have been reported in many of these disorders.

There is a long list of autoimmune diseases like rheumatoid arthritis, systemic lupus erythematosus, multiple sclerosis, etc. that are characterized by immune system dysfunction, and thus inflammatory cascades seem to play a major part in disease onset and progression (Kordinas *et al*. 2016). Telomere shortening and deregulation of telomerase activity have been reported in association with autoimmune diseases (Dehbi *et al*. 2013; Wu *et al*. 2007; Guan *et al*. 2015).

A common disease like periodontitis, a chronic infection with a prevalence between 10-30% in the general adult population, is associated with chronic inflammation, oxidative stress and telomere shortening (Masi *et al*. 2011). Diabetes is a spectrum of diseases with the most important ones being type 1 diabetes and type 2 diabetes, and it has a prevalence of around 8.5%. Diabetes is associated with inflammation and oxidative stress and some studies have identified a connection between telomere/telomerase dysfunction and diabetes (Liew *et al*. 2009).

Psychiatric disorders such as depression, schizophrenia, anxiety disorder, bipolar disorder and post-traumatic stress disorder pose serious and emerging global health threats and have in recent years been associated with accelerated aging, chronic inflammation and immune system deregulation (Lindqvist *et al*. 2015). For example, depression affects 350 million people worldwide and is associated with higher levels of IL-1β, IL-6, IFN-γ and TNF-α (Hughes *et al*. 2016). In addition, there are studies connecting psychiatric disorders with telomeres and telomerase. Leucocyte telomere length has been studied in many psychiatric disorders. Shorter telomeres have been observed in depressed patients compared to healthy controls, and in addition

shorter telomeres where associated with the severity and duration of the disease (Lindqvist *et al*. 2015).

7.3. Environmental factors that affect telomere length in humans

Some environmental stresses disrupt TL homeostasis (Romano *et al*. 2013). In humans, stresses like alcohol or tobacco intake shorten telomeres (Pavanello *et al*. 2011; Salihu *et al*. 2014). Postnatal exposure to different kinds of environmental stressors such as environmental pollution (Meillère *et al*. 2015)**,** social and psychological stress (Boonekamp *et al*. 2014; Price *et al*. 2013) and nutritional deficiencies (Noguera *et al*. 2015) can accelerate the rate of telomere loss, possibly related to the fact that telomere shortening is greater after increased exposure to stress hormones (Haussmann *et al*. 2012; Herborn *et al*. 2014)**.** Cortisol is a hormone associated with chronic stress, and is related with telomere shortening and lower levels of telomerase activity (Shaffer *et al*. 2012). In addition, other factors related with lifestyle are known to modify TL in the general population: dietary patterns (Rafie *et al*. 2016) and common pathological conditions like obesity or depression have been associated with telomere shortening (Shaffer *et al*. 2012; Chen *et al*. 2014). Interestingly, poor sleep quality and short sleep duration are associated with shorter LTL in men (Jackowska *et al*. 2012).

7.4. Cancer therapies that affect telomere length

In cancer patients, additional factors such as exposure to chemotherapeutic agents or radiotherapy can modify TL (Li *et al*. 2012). Telomere dysfunction induced by chemotherapeutic agents is drug-specific. The alkylating agent cyclophosphomide was shown to induce in spermatogonial cells a significant increase in DNA damage, which was localized preferentially at telomeres. This telomere DNA damage was accompanied by telomere shortening and a significant reduction in both telomerase mRNA levels and telomerase activity (Marcon *et al*. 2011; Liu *et al*. 2015). In addition, it is known that mitotic inhibitors such as Taxol, which are normally included in conventional breast cancer chemotherapy schedules, can cause telomere uncapping and trigger telomere dysfunction in cancer cells (Lu *et al*. 2013). In contrast, telomere elongation has been detected after treatment with the hypomethylating agent 5-aza-2'-deoxycytidine (5-aza-CdR) and/ or the histone deacetylase inhibitors trichostatin A (TSA).

In summary, TL exhibits considerable inter-individual variability, and it is likely that all sources of variability mentioned above should be considered in TL association studies in order to obtain reliable results and clarify the utility of LTL as a biomarker to predict cancer/disease susceptibility.

HYPOTHESIS

Cells from peripheral blood are exposed to internal and external agents that can alter DNA repair capacity, oxidative stress or cell cycle speed. Most of them are related directly or indirectly with TL. Therefore, retrospective studies or studies that do not take these factors into consideration can lead to misleading results regarding TL in association with disease susceptibility.

OBJECTIVES

In the present study, we tried to confirm the above hypothesis by analyzing exogenous (chemotherapy) and endogenous (genetic variants in *OGG1* and *NEIL2*) factors that can act as modifiers of TL. To this end, we worked prospectively with a series of families with a history of breast and ovarian cancer screened for *BRCA1* and *BRCA2* mutations. The families included affected and unaffected *BRCA1* and *BRCA2* mutation carriers, *BRCAX* cancer cases and non-carrier controls. We followed these families for three years and took blood samples every 12 months in order to:

1. Evaluate the effect of chemotherapy as a possible telomere length modifier;
2. Evaluate the role of rs2304277 in *OGG1*, a DNA glycosylase involved in BER pathway, as a modifier of cancer risk;
3. Evaluate the role of rs804271 in *NEIL2*, another DNA glycosylase involved in BER pathway, as a modifiers of cancer risk;
4. Evaluate the possible synthetic lethal/sickness interaction between homologous recombination and BER DNA repair pathways, and its implication for the treatment of *BRCA1* and *BRCA2* cancer cases.

ARTICLES

ARTICLE 1

Impact of chemotherapy on telomere length in sporadic and familial breast cancer patients.

Authors: Benitez-Buelga C, Sanchez-Barroso L, Gallardo M, Apellániz-Ruiz M, Inglada-Pérez L, Yanowski K, Carrillo J, Garcia-Estevez L, Calvo I, Perona R, Urioste M, Osorio A, Blasco MA, Rodriguez-Antona C, Benitez J.

Journal: Breast Cancer Research and Treatment
Publication Date: January 2015
Ref: 149(2):385-94
Personal contribution: Collection, control and preparation of the samples, Telomere length studies, statistical analysis, preparation of the manuscript.

The impact of chemotherapy on telomere length (TL) have been already addressed *in vitro* (cultured cell lines and normal human leucocytes) and *in vivo* (in different tumors). We have tried to evaluate whether chemotherapy could be a confounding factor for TL association studies evaluating telomere shortening as a causal explanation for cancer risk susceptibility in hereditary breast cancer. In relation to this topic, previous finding and conclusions have led to a confusing scenario in the literature

To summarize, our study has focused on the effect of cancer treatment on TL in both familial and sporadic breast cancer cases. We have found that chemotherapy exerts a transient telomere shortening effect on human leukocytes, and that after the treatment a normal TL can be recovered. In the context of familiar breast cancer patients, we cannot rule out that *BRCA*1 and *BRCA2* might be minor modifiers of TL, but it appears that treatment is the true cause of TL modifications. The rates of telomere shortening and recovery may vary depending on the type of treatment.

We performed a cross-sectional study measuring leukocyte TL of 266 sporadic breasts cancer patients treated with first-line chemotherapy, with a median follow up of 240 days. Additionally, we performed both cross-sectional and longitudinal studies in a series of 236 familial breast cancer patients that included affected and non-affected *BRCA1/2* mutation carriers. We have measured in leukocytes from peripheral blood: The telomere-length, percentage of short telomeres (<3Kb), telomerase activity levels and the annual telomere shortening speed.

These results stress the need to perform prospective and retrospective studies, considering the variability found as a consequence of the treatment status (untreated, during treatment and post treatment) of the patients, to obtain conclusive results about the relationship between telomere-length and disease.

Impact factor (IF) = 4.085

Published in final edited form as:
Breast Cancer Res Treat. 2015 January ; 149(2): 385–394. doi:10.1007/s10549-014-3246-6.

Impact of chemotherapy on telomere-length in sporadic and familial breast cancer patients

C. Benitez-Buelga, MS[1], **L. Sanchez-Barroso, MS**[2], **M. Gallardo, PhD**[3], **María Apellániz-Ruiz, MS**[2], **L. Inglada-Pérez, PhD**[2,4], **K. Yanowski, PhD**[1], **J. Carrillo, PhD**[4,5], **L. Garcia-Estevez, MD**[6], **I. Calvo, MD**[7], **R. Perona, PhD**[4,5], **M. Urioste, MD, PhD**[4,8], **A. Osorio, PhD**[1,4], **MA. Blasco, PhD**[3], **C. Rodriguez-Antona, PhD**[2,4], and **J. Benitez, PhD**[1,4]

[1]Human Genetics Group, Spanish National Cancer Research Center (CNIO), Madrid 28029, Spain

[2]Endocrine Cancer Group, Spanish National Cancer Research Center (CNIO), Madrid 28029, Spain

[3]Telomere and Telomerase Group, Spanish National Cancer Research Center (CNIO), Madrid 28029, Spain

[4]Center for Biomedical Network Research on Rare Diseases (CIBERER), CNIO, Madrid 28029, Spain

[5]Biomedical Research Institute Alberto Sols (CSIC-UAM), Madrid 28029, Spain

[6]Medical Oncology Dptm. Centro Integral Oncológico Clara Campal, Madrid, Spain

[7]Medical Oncology Dptm. Hospital Montepríncipe, Madrid, Spain

[8]Familial Cancer Unit, Spanish National Cancer Research Center (CNIO), Madrid 28029, Spain

Abstract

Purpose—Recently, we observed that telomeres of *BRCA1/2* mutation carriers were shorter than those of controls or sporadic breast cancer patients, suggesting that mutations in these genes might be responsible for this event. Given the contradictory results reported in the literature, we tested whether other parameters, such as chemotherapy, could be modifying telomere-length.

Methods—We performed a cross-sectional study measuring leukocyte telomere-length of 266 sporadic breasts cancer patients treated with first-line chemotherapy, with a median follow up of 240 days.

Additionally, we performed both cross-sectional and longitudinal studies in a series of 236 familial breast cancer patients that included affected and non-affected *BRCA1/2* mutation carriers. We

Corresponding author: Javier Benitez, jbenitez@cnio.es, Human Genetics Group Spanish National Cancer Research Center (CNIO), c/ Melchor Fernández Almagro nº 3, 28029 Madrid – SPAIN, Phone: +34917328057, fax: 91 224 69 11.

Ethical standards:
The authors declare that this work complies with current Spanish laws.

Conflict of interest:
The authors declare that they have no conflicts of interest.

Europe PMC Funders Author Manuscripts

have measured in leukocytes from peripheral blood: The telomere-length, percentage of short telomeres (<3Kb), telomerase activity levels and the annual telomere shortening speed.

Results—In sporadic cases we found that chemotherapy exerts a transient telomere shortening effect (around 2 years) that varies depending on the drug combination.

In familial cases, only patients receiving treatment were associated with telomere shortening but they recovered normal telomere-length after a period of two years.

Conclusion—Chemotherapy affects telomere-length and should be considered in the studies that correlate telomere-length with disease susceptibility.

Keywords

Chemotherapy; Sporadic Breast Cancer; Familial Breast and Ovarian Cancer; telomere-length; Telomerase

INTRODUCTION

Telomeres are nucleoprotein structures that cap and protect the ends of chromosomes against chromosomal fusion, recombination and terminal DNA degradation [1]. In humans, the average telomere-length typically ranges from 10 to 15 kb [2], but telomere DNA shortens with each cell replication. This leads to a progressive telomere shortening during life that ranges from 24.7 to 45.5 bp/year [3]. This shortening continues until the telomere reaches a critical length [4], which triggers cell-cycle arrest leading to senescence or apoptotic cell death.

Germ cells and stem cells can counteract telomere shortening through the action of an enzyme called telomerase, which can synthesize telomeric DNA de novo [5]. However, cancer cells present altered DNA damage response mechanisms and are able to divide even when they present critically short telomeres by up regulating telomerase activity or activating the 'alternative lengthening of telomeres' mechanism [5].

There are several retrospective case-control and longitudinal studies suggesting that short telomeres found in DNA from surrogate tissues may predispose to different diseases including cancer [6-11]. However, the largest prospective study in the general population to date (47,102 subjects with a 20-year follow-up) has recently suggested only a weak relationship between short telomeres and breast cancer risk among a large group of cancer types [12].

These results led to a contradiction in the literature regarding the association between telomere-length and cancer or other diseases, and point to differences in the strategies used to perform these studies (prospective or retrospective), technical issues, and/or the existence of telomere-length modifiers as sources of variability [13-16].

In a previous study we found that patients with hereditary breast cancer (*BRCA1/2* and non-*BRCA1/2* carriers) presented shorter telomeres than sporadic breast cancer patients and the control population, suggesting a modifier effect of the *BRCA1* and *BRCA2* genes on telomere-length[17]. Because our study was retrospective, like two other recent studies that

Europe PMC Funders Author Manuscripts

presented contradictory results [18, 19], we decided to investigate the possible cause of these discrepancies.

We have focused our attention on the possible impact of chemotherapeutic cancer treatment, because some publications have already suggested a telomere shortening effect after the administration of chemotherapy in vivo (in different tumors) and in vitro (in normal human leukocytes and a mouse spermatogonial cell line) [20, 21].

We have explored this hypothesis in sporadic and familial breast cancer, and we have found that chemotherapy has a telomere shortening effect that is reversible after a period of time once the treatment is finished.

SAMPLES AND METHODS

Samples

Two different series of patients and two different strategies were used. We took a cross-sectional approach in a set of sporadic breast cancer cases and both a cross-sectional and a longitudinal approach in a series of familial breast cancer cases.

The first series comprised 253 sporadic breast cancer patients (age range: 30-81years) who were undergoing or had already received chemotherapy and 13 patients recently diagnosed that had not received chemotherapy (age range: 28-68y). They were included in a clinical trial that involved chemotherapy based on taxane derivatives and were followed for a median of 240 days (range 5-1855 days). We established two main categories based on their status: “During treatment” and “Post treatment”. In addition, patients were classified according to the taxane combination they received (Table1). Details regarding doses, number of cycles, duration and patient follow-up after treatment are summarized in Table S1.

The second series consisted of 236 familial breast cancer patients belonging to 104 families (23 harboring deleterious mutations in *BRCA1*, 28 in *BRCA2*, and 53 not associated to any of the known genes (*BRCAX*)). Most of the families were selected from the registry of the Familial Cancer Consultation of the CNIO and had been attended between 2011 and 2013. Individuals from these families met high risk criteria and [22] had been previously screened for mutations in *BRCA1* and *BRCA2* by a combination of denaturing high-performance liquid chromatography (DHPLC) and direct sequencing as previously reported [23]. Due to the lack of a complete knowledge concerning the specific chemotherapy treatment regimens and the follow up of the patients after finishing the treatment, we established two general groups of patients. Only patients that were known to have been treated with any kind of chemotherapy were included in this analysis. Those, whose sample was extracted less than two years after diagnosis were considered as “During treatment”; while those whose sample was extracted more than two years after diagnosis were considered as “Post treatment”.

We measured leukocyte telomere-length by quantitative PCR, in the DNA of all individuals from this series, and whenever possible we measured the telomere-length and the percentage of short telomeres by High Throughput QFISH, and the telomerase activity levels in peripheral blood. In the FBOC series, we had the opportunity to compare 2 telomere-length

measurements that corresponded to samples obtained at two different time points, with an average of 6 years between both extraction points. Using the 2 measurements we were able to calculate the telomere shortening rate per year.

A summary of all pertinent information (sample size, median age, age range and the experiments performed) of both cohorts of patients is shown in Table 2.

A set of 330 healthy Spanish women previously described [24], without personal or familial antecedents of cancer (age range 19-77y) was used as a control population (Table2-controls$_1$) in order to adjust the telomere-length of both sporadic and familial breast cancer cases according to age.

The study was performed in accordance with the principles of the Declaration of Helsinki. Written informed consent was obtained from all patients prior to sample collection, and the study was approved by the Ethics Committee of Clinical Investigation from Centro Integral Oncologico Clara Campal, Madrid.

Telomere-length quantification

DNA from peripheral blood was extracted using MagNA Pure LC 2.0 System (Roche Diagnostics, Indianapolis, Indiana). Telomere-length was measured using quantitative PCR-based technique. This technique calculates the telomere-length as a ratio of telomere amount (t) relative to 36B4 reference gene amount (s)[25].The measurement unit used in this technology is the t/s value. Primers used to perform the quantitative PCR have been described previously[17]. DNA samples were amplified in a total reaction volume of 10 µl containing 1× Gotaq quantitative PCR Master Mix (Promega, Madison, Wisconsin), 500 nM of primer Tel1, 1000 nM of primer Tel2, 10-30 ng of DNA and a common thermal cycling profile for both “t” and “s” determination. For *36B4* reactions, the concentrations of primers were 500 nM of 36B4u and 500 nM of 36B4d. All samples were analyzed in triplicate using an ABI 7900HT thermal cycler, in 384-well format. Telomere-length was calculated as previously described [17].

Measurement of telomere-length and short telomere content by High Throughput Q-FISH

For telomere-length by High Throughput Q-FISH measurement, peripheral blood mononuclear cells were hybridized with a PNA-tel Cy3-labeled probe. Telomere-length was determined as previously described [26] .

DAPI and Cy3 signals were acquired simultaneously in separate channels using a Leica TCS-SP5 confocal microscope (Wechsler, Germany). and maximum intensity projections from image stacks were generated for image quantification. In all cases, background noise was subtracted from the image prior to quantification. The “average telomere fluorescence” values represent the average Cy3 pixel intensity for the total nuclear area. Percentage of cells with short telomeres was calculated as those with intensity values within the first quartile.

Telomerase Assay

Protein extracts were obtained from peripheral blood mononuclear cells cultured in RPMI supplemented with 20 % fetal bovine serum and phytohemagglutinin during 4-5 days,

Europe PMC Funders Author Manuscripts

according to the recommendations of the manufacturer of the TRAPeze telomerase detection kit (Merck Millipore, Darmstadt, Germany). The average telomerase activity was determined in each sample using 0.5, 0.25 and 0.125 μg of protein extract and normalized with the internal control included in the assay.

Telomere Shortening Rate

When possible, we calculated the difference in t/s values between blood samples extracted in two different time points (average of six years). The result was divided by the number of years that separated both samples. A positive result indicated shortening, while a negative value indicated elongation of the telomere.

Statistical analysis

Telomere-length measurements were adjusted for age using the line of best fit for controls. Thus, the difference between the actual and the predicted value was calculated for each sample. Following this method we adjusted t/s values obtained by quantitative PCR (y= −0.0174*X+1.96), the Kb obtained by High Throughput Q-FISH (−0.0587*X+12.007) and the percentage of short telomeres (0.1501*X+11.331).

The Kolmogorov-Smirnov test was used to evaluate whether telomere-length measurements obtained from healthy controls, familial breast cancer and sporadic cancer cases followed a normal distribution. As a normal distribution could not be assumed for healthy controls, a Mann-Whitney U test was applied (Table S2, figure 3a and figure 3b) Unpaired Student t-test for normal distributions was applied in the comparative analysis of telomerase activity, telomere shortening rate (Table S3 and Table S4) and percentage of short telomeres among the familial breast cancer groups (Figure 4).

Spearman correlation test was used to establish whether correlation between variables were statistically significant (Figure 1).

Statistical calculations were performed using SPSS version 18 (SPSS Inc, Chicago, Illinois) and Graph pad Prism 5.03(San Diego, California). Nominal two-sided p-values less than 0.05 were considered statistically significant. Graphics were performed using Graph pad Prism 5.03 and Microsoft Office Excel 2007.

RESULTS

Controls

We evaluated the telomere-length distribution in 330 healthy women as a function of age in order to obtain a regression line to adjust the t/s values from both the familial breast cancer and the sporadic series. As expected, we found a decrease in telomere-length with age. (Figure S1).

Sporadic cases

We tested whether chemotherapy itself has an effect on telomere shortening. To address this hypothesis we evaluated the telomere-length distribution of patients included in the “During

treatment" category. We observed a strong correlation between telomere shortening and treatment duration (r=−0.43; p=3.71E-05) (Figure 1a). We did the same evaluation in the "Post treatment" category, and we observed that the distribution had the opposite shape, with a significant positive correlation between telomere-length and time after treatment (r=0.17; p=0.02) (Figure 1b).

We next did a comparative analysis of telomere-length during different periods of the treatment time line, (Figure 2). We compared the median telomere-length of each group, with the median telomere-length of the control group. The telomere-length (t/s values adjusted by age) in patients before treatment did not differ compared to controls (Figure 2, black line). From the beginning of the treatment, we observed a shortening effect that became statistically significant in patients treated for more than 90 days and remained significantly shortened until 360 days after the treatment. Patients whose samples were extracted later than 360 days after the end of the treatment tended to recover normal telomere-length values, and did not show significant differences when compared to controls. The results of this analysis are summarized in Table S2.

In patients treated with therapy based in taxane derivatives (Table 1), we observed a more significant telomere shortening effect in those treated with FEC+T/T+FEC (red line) compared to those treated with AC+T/T+AC (green line) however, the latter seemed to recover their telomere-length faster (Figure 2).

Familial Breast Cancer Cases

Cross-sectional study—We performed this analysis to explore both, the role of *BRCA1/2* mutations as telomere-length modifiers and the possible correlation between telomere shortening and cancer treatment. Healthy *BRCA1/2* mutation carriers (n=54) did not present shorter telomeres when compared to controls (n=330), while significantly shorter telomeres were found in affected *BRCA1/2* mutation carriers (n=50; p=0.044) and *BRCAX* patients (n=63; p=0.048) (Figure 3a).

In view of the behavior of telomeres in sporadic breast cancer cases according to the treatment status, we decided to reanalyze the data from the familial breast cancer series. We established two categories consisting of cancer patients from whom samples were extracted within two years from the beginning of the treatment, called "During treatment *BRCA1/2/X*", and a second group composed of patients whose samples were taken more than two years after the beginning of treatment, called "Post treatment-*BRCA1/2/X*". We used two years as a cut-off, because in the sporadic series we observed that the recovery phase starts approximately two years since diagnosis.

No significant differences were found between "Post treatment-*BRCA1/2/X*" patients and controls (Table2-controls$_1$). However, the "During treatment-*BRCA1/2/X*" group presented significant shortened telomere t/s values compared with the controls (p=0.0005) and the "Post treatment-*BRCA1/2/X*" groups (p=0.007) (Figure 3b).

We also evaluated the leukocyte telomerase activity in this cohort of patients (Figure 3c). We found that healthy *BRCA1/2* mutation carriers presented similar telomerase activities to the

healthy controls (Table 2-controls$_2$). Interestingly, all cancer patients, independently of the mutation type and the treatment time, presented significantly lower levels of telomerase activity, being patients "During treatment" the ones showing the lowest values (p=0.0009) (Table S3).

In parallel, we used High Throughput Q-FISH technology in order to validate our results using an alternative technology. We found the same results regarding telomere-length for the "During treatment-*BRCA1/2/X*" group (Figure 4a), confirming the presence of a significantly higher percentage of short telomeres (<3Kb) for this group of patients (p=0.01) compared to the control population (Table 2-controls$_2$) (Figure 4b).

Longitudinal study—We performed a longitudinal retrospective study in order to analyze telomere shortening rate in a set of 31 *BRCA1/BRCA2* mutation carriers with two independent blood samples taken separately by an average period of 6 years: 15 were healthy carriers, 9 affected carriers with the two samples obtained once the chemotherapy had finished, and 7 affected carriers in which the first sample was obtained "During treatment" and the second extraction point in the "Post treatment". Additionally we analyzed the telomere shortening rate in a set of 25 controls from which we also had samples taken at two time point (Table 2-controls$_3$).

Healthy *BRCA1/2* carriers presented a faster telomere shortening rate compared to the control group, although the differences were not significant; while "Post treatment-*BRCA1/2*" patients presented a telomere shortening rate very similar to the control group. By contrast, "During treatment-*BRCA1/2*" patients presented a different pattern, going from short telomeres at the first measurement, to normal telomeres 7 years later (Figure 5). In this case the elongation speed was very pronounced, and statistically different from the normal shortening of the control population (p=0.011). The results of this analysis are summarized in Table S4.

DISCUSSION

We previously reported that *BRCA1/2* might be telomere-length modifiers, because mutation carrier patients presented shorter telomeres than the control population and sporadic breast cancer cases [17]. However, two recent reports did not find any relationship between the presence of *BRCA1/2* mutations and telomere shortening, nor between telomere-length and an increased cancer risk [18, 19]. The three studies were done in a retrospective manner, and in none of them treatment status, which might constitute a confounding factor, was evaluated independently as a possible modifier of telomere-length. We tried to overcome this possible bias by working with two independent cohorts of women with breast cancer (sporadic and familial) and two different approaches (cross-sectional and longitudinal).

According to the results obtained in the sporadic set of patients treated with different chemotherapy schedules and followed for a maximum period of 1855 days, telomere shortening starts at 91-180 days after the beginning of treatment and reaches its maximum effect between 91-180 days after finishing treatment. Then a recovery phase starts, and it

lasts for a maximum of 1855 days after which the original telomere-length is recovered (Table S2). Similar results were observed in the familial breast cancer series in both, cross-sectional and longitudinal studies.

There are some reports suggesting a possible deleterious effect of chemotherapy on telomere-length and/or telomerase activity, although some of these seem to be contradictory.

The first authors, who addressed this question, reported significant telomere shortening accompanied by a significant reduction in telomerase activity in the blood cells of pediatric leukemia patients after the administration of cancer treatment [27]. Another early longitudinal study in breast cancer patients undergoing chemotherapy, reported a clear negative effect on different hematological parameters, including telomere shortening, after high doses of FEC +T [28]. On the other hand, in a recent longitudinal study performed in a set of 33 breast cancer patients undergoing AC+T/T+AC chemotherapy no changes were detected in telomere-length, at three and twelve months after the end treatment [29] .

It is probable that in this case patients were already at the “recovery phase” proposed in this study. Surprisingly, increased expression of the senescence markers *p16* and *ARF* was detected, which have been correlated with telomere damage in primary cells [30].

Engelhard et al. were the first to raise the question of whether telomere shortening is permanent or telomeres regain their initial length after discontinuation of chemotherapy [27].

In this regard, our results confirm there is a telomere recovery after treatment, although we have observed that the shortening effect and the time to reach the “recovery phase” varies depending on the treatment type, with a shortening effect more severe at the initial phase of the treatment for patients under the AC+T/T+AC regimen, while those treated with FEC +T/T+FEC present a more delayed “recovery phase”. It seems that telomere stability is affected by conventional chemotherapies in different manner depending on the specific drug mechanism of action (Alkylating agents, anti-replicative molecules, spindle poisons, anti-topoisomerase I and II) being the effects on the telomere heterogeneous.

Some authors have evaluated the role of several chemotherapy drugs *in vitro* and in cancer patients at a more mechanistic level [21, 31, 32]. For instance, the alkylating agent cyclophosphamide, was shown to induce in spermatogonial cells a significant increase in DNA damage, which was localized preferentially at telomeres. This telomere DNA damage was accompanied by telomere shortening and a significant reduction in both telomerase mRNA levels and significantly diminished telomerase activity [21]. These negative effects may be explained due to the high guanine content of the telomere sequence and the *TERC* gene, which may increase the risk of DNA-DNA crosslink damage by cyclophosphamide [21].

In another longitudinal study using 6 cycles of CHOP (cyclophosphamide, doxorrubicine, vincristine and Prednisone) in a cohort of 14 Non-Hodgkin lymphoma patients, significant telomere shortening was maintained up to 2 years, after the treatment ends. The same study evaluated the anti-metabolite drug 5-fluoracil alone in a set of 10 colon cancer cases. TL was measured 2 and 12 months after the end of the treatment showing an initial telomere attrition that was recovered after one year [31]. The authors propose a possible mechanism based on

whether these drugs are able to target hematopoietic stem cells, or only mature progenitors, to explain a long or a short-term effect in telomere shortening [31]. In addition, it is also known that mitotic inhibitors such as taxol, which are normally included in conventional breast cancer chemotherapy schedules, can causes telomere uncapping, triggering telomere dysfunction in cancer cells [32].

Taking all this evidences together we can assume some variation in the telomere dynamics during and after the treatment, depending which type of anticancer chemotherapy drugs are included in the patients treatment.

In the familial breast cancer model we followed both cross-sectional and longitudinal approaches in order to test whether the BRCA genes and chemotherapy are modifiers of telomere-length and/or telomerase activity.

In the cross-sectional approach we found similar results as in our previous study [17], familial cases presented shorter telomeres than controls; however, a substantial proportion of the samples had been taken during or after a short time of chemotherapy administration. When we corrected for treatment status we were not able to detect any effect of the *BRCA1/2* mutations on telomere shortening, neither in healthy carriers nor in post treated-*BRCA1/2* patients, suggesting that the treatment is the real telomere-length modifier (Figure 3b). These results could explain partially, the discrepancies reported in the literature regarding the role of the *BRCA1/2* genes as modifiers of telomere-length[17]. In a recent report by Pooley et al, *BRCA1/2* mutation carriers showed longer telomeres than controls, and the authors suggests that an increase in telomerase levels could be associated with this event [18]. However, in the present study we have not found higher levels of telomerase activity in healthy *BRCA1/2* patients, while treated patients (independently of their mutational status), presented both shorter telomeres and significant lower telomerase activity levels.

Regarding the longitudinal study, *BRCA1/2* affected carriers with two telomere-length measurements covering the “Post treatment” period, did not present significant differences in the shortening rate compared to healthy *BRCA1/2* carriers and/or controls. However, *BRCA1/2* patients, with the first sample taken during treatment and the second sample taken 7 years later (during the post treatment period) presented a recovery of telomere-length after chemotherapy, confirming our observations in the sporadic series (Fig 5).

To summarize, our study has focused on the effect of treatment on telomere-length in both familial and sporadic breast cancer cases. We cannot rule out that *BRCA*1 and *BRCA2* might be minor modifiers of telomere-length, but it appears that treatment is the true cause of telomere shortening. The rates of telomere shortening and recovery may vary depending on the treatment. These results stress the need to perform prospective and retrospective studies, considering the variability found as a consequence of the treatment status (untreated, during treatment and post treatment) of the patients, to obtain conclusive results about the relationship between telomere-length and disease.

Supplementary Material

Refer to Web version on PubMed Central for supplementary material.

ACKNOWLEDGEMENTS

We thank Alicia Barroso and Victoria Fernandez for their technical support. This work was partially funded by project FIS PI12/00070 from the Carlos III Health Institute and the Spanish Network on Rare Diseases (CIBERER). By project SAF2012–35779 (Spanish Ministry of Economy and Competiveness). M.A.B.'s laboratory is funded with the Spanish Ministry of Science and Innovation, projects SAF2008-05384 and 2007-A-200950 (TELOMARKER), European Research Council Advanced grant GA#232854, the Körber Foundation, Botín Fundation, and Lilly Fundation.

REFERENCES

1. Blackburn EH. Switching and signaling at the telomere. Cell. Sep 21; 2001 106(6):661–673. [PubMed: 11572773]
2. Blasco MA. Telomeres and human disease: ageing, cancer and beyond. Nat Rev Genet. Aug; 2005 6(8):611–622. [PubMed: 16136653]
3. Muezzinler A, Zaineddin AK, Brenner H. A systematic review of leukocyte telomere length and age in adults. Ageing Res Rev. Mar; 12(2):509–519. [PubMed: 23333817]
4. Harley CB, Futcher AB, Greider CW. Telomeres shorten during ageing of human fibroblasts. Nature. May 31; 1990 345(6274):458–460. [PubMed: 2342578]
5. Kong CM, Lee XW, Wang X. Telomere shortening in human diseases. FEBS J. Jul; 280(14):3180–3193. [PubMed: 23647631]
6. Wentzensen IM, Mirabello L, Pfeiffer RM, Savage SA. The association of telomere length and cancer: a meta-analysis. Cancer Epidemiol Biomarkers Prev. Jun; 20(6):1238–1250. [PubMed: 21467229]
7. Fyhrquist F, Silventoinen K, Saijonmaa O, et al. Telomere length and cardiovascular risk in hypertensive patients with left ventricular hypertrophy: the LIFE study. J Hum Hypertens. Dec; 25(12):711–718. [PubMed: 21697896]
8. Willeit P, Willeit J, Kloss-Brandstatter A, Kronenberg F, Kiechl S. Fifteen-year follow-up of association between telomere length and incident cancer and cancer mortality. JAMA. Jul 6; 306(1): 42–44. [PubMed: 21730239]
9. Willeit P, Willeit J, Mayr A, et al. Telomere length and risk of incident cancer and cancer mortality. JAMA. Jul 7; 304(1):69–75. [PubMed: 20606151]
10. Shao L, Wood CG, Zhang D, et al. Telomere dysfunction in peripheral lymphocytes as a potential predisposition factor for renal cancer. J Urol. Oct; 2007 178(4 Pt 1):1492–1496. [PubMed: 17707063]
11. Wu X, Amos CI, Zhu Y, et al. Telomere dysfunction: a potential cancer predisposition factor. J Natl Cancer Inst. Aug 20; 2003 95(16):1211–1218. [PubMed: 12928346]
12. Weischer M, Nordestgaard BG, Cawthon RM, Freiberg JJ, Tybjaerg-Hansen A, Bojesen SE. Short telomere length, cancer survival, and cancer risk in 47102 individuals. J Natl Cancer Inst. Apr 3; 105(7):459–468. [PubMed: 23468462]
13. Savage SA, Gadalla SM, Chanock SJ. The long and short of telomeres and cancer association studies. J Natl Cancer Inst. Apr 3; 105(7):448–449. [PubMed: 23468461]
14. Cunningham JM, Johnson RA, Litzelman K, et al. Telomere length varies by DNA extraction method: implications for epidemiologic research. Cancer Epidemiol Biomarkers Prev. Nov; 22(11):2047–2054. [PubMed: 24019396]
15. Aviv A, Hunt SC, Lin J, Cao X, Kimura M, Blackburn E. Impartial comparative analysis of measurement of leukocyte telomere length/DNA content by Southern blots and qPCR. Nucleic Acids Res. Nov 1.39(20):e134. [PubMed: 21824912]
16. Aviv A, Valdes AM, Spector TD. Human telomere biology: pitfalls of moving from the laboratory to epidemiology. Int J Epidemiol. Dec; 2006 35(6):1424–1429. [PubMed: 16997848]
17. Martinez-Delgado B, Yanowsky K, Inglada-Perez L, et al. Genetic anticipation is associated with telomere shortening in hereditary breast cancer. PLoS Genet. Jul.7(7):e1002182. [PubMed: 21829373]

18. Pooley KA, McGuffog L, Barrowdale D, et al. Lymphocyte telomere length is longer in BRCA1 and BRCA2 mutation carriers but does not affect subsequent cancer risk. Cancer Epidemiol Biomarkers Prev. Mar 18.
19. Killick E, Tymrakiewicz M, Cieza-Borrella C, et al. Telomere length shows no association with BRCA1 and BRCA2 mutation status. PLoS One. 9(1):e86659. [PubMed: 24489760]
20. Li P, Hou M, Lou F, Bjorkholm M, Xu D. Telomere dysfunction induced by chemotherapeutic agents and radiation in normal human cells. Int J Biochem Cell Biol. Sep; 44(9):1531–1540. [PubMed: 22728163]
21. Liu M, Hales BF, Robaire B. Effects of four chemotherapeutic agents, bleomycin, Etoposide, Cisplatin, and cyclophosphamide, on DNA damage and telomeres in a mouse spermatogonial cell line. Biol Reprod. 90(4):72. [PubMed: 24571982]
22. Milne RL, Osorio A, Cajal TR, et al. The average cumulative risks of breast and ovarian cancer for carriers of mutations in BRCA1 and BRCA2 attending genetic counseling units in Spain. Clin Cancer Res. May 1; 2008 14(9):2861–2869. [PubMed: 18451254]
23. Diez O, Osorio A, Duran M, et al. Analysis of BRCA1 and BRCA2 genes in Spanish breast/ovarian cancer patients: a high proportion of mutations unique to Spain and evidence of founder effects. Hum Mutat. Oct; 2003 22(4):301–312. [PubMed: 12955716]
24. Osorio A, Endt D, Fernandez F, et al. Predominance of pathogenic missense variants in the RAD51C gene occurring in breast and ovarian cancer families. Hum Mol Genet. Jul 1; 21(13): 2889–2898. [PubMed: 22451500]
25. Cawthon RM. Telomere measurement by quantitative PCR. Nucleic Acids Res. May 15.2002 30(10):e47. [PubMed: 12000852]
26. Canela A, Vera E, Klatt P, Blasco MA. High-throughput telomere length quantification by FISH and its application to human population studies. Proc Natl Acad Sci U S A. Mar 27; 2007 104(13): 5300–5305. [PubMed: 17369361]
27. Engelhardt M, Ozkaynak MF, Drullinsky P, et al. Telomerase activity and telomere length in pediatric patients with malignancies undergoing chemotherapy. Leukemia. Jan; 1998 12(1):13–24. [PubMed: 9436916]
28. Schroder CP, Wisman GB, de Jong S, et al. Telomere length in breast cancer patients before and after chemotherapy with or without stem cell transplantation. Br J Cancer. May 18; 2001 84(10): 1348–1353. [PubMed: 11355946]
29. Sanoff HK, Deal AM, Krishnamurthy J, et al. Effect of cytotoxic chemotherapy on markers of molecular age in patients with breast cancer. J Natl Cancer Inst. Apr.106(4):dju057. [PubMed: 24681605]
30. Jacobs JJ, de Lange T. p16INK4a as a second effector of the telomere damage pathway. Cell Cycle. Oct; 2005 4(10):1364–1368. [PubMed: 16177573]
31. Diker-Cohen T, Uziel O, Szyper-Kravitz M, Shapira H, Natur A, Lahav M. The effect of chemotherapy on telomere dynamics: clinical results and possible mechanisms. Leuk Lymphoma. Sep; 54(9):2023–2029. [PubMed: 23240911]
32. Lu Y, Leong W, Guerin O, Gilson E, Ye J. Telomeric impact of conventional chemotherapy. Front Med. Dec; 7(4):411–417. [PubMed: 24155095]

Europe PMC Funders Author Manuscripts

Europe PMC Funders Author Manuscripts

a)

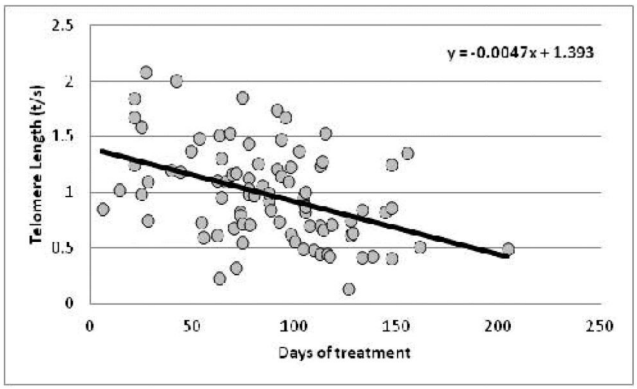

b)

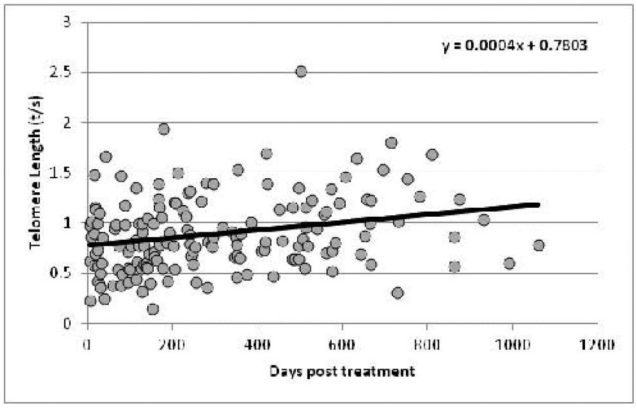

Figure 1.

a) Correlation between telomere-length (t/s) and treatment time (r=−0.43; p=3.71E-05). b) Correlation between telomere-length (t/s) and time after treatment (r=0.17; p=0.02).

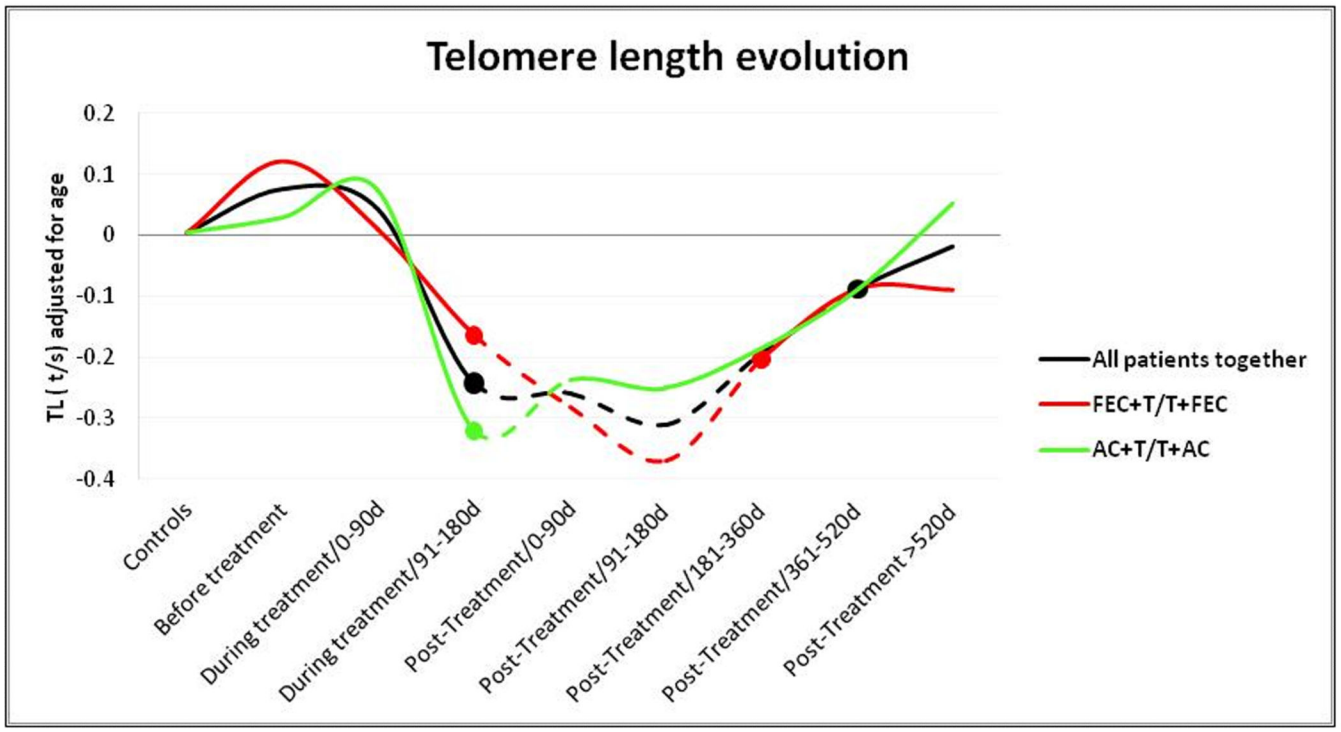

Figure 2.

Telomere-length evolution during treatment and after treatment. Mann Whitney test was used to determine significant differences between controls and the different subgroups. The discontinuous lines represent significantly shortened telomeres compared to controls for all the patients together (black line) and for the two major drug schedules (red and green lines).

Europe PMC Funders Author Manuscripts

Europe PMC Funders Author Manuscripts

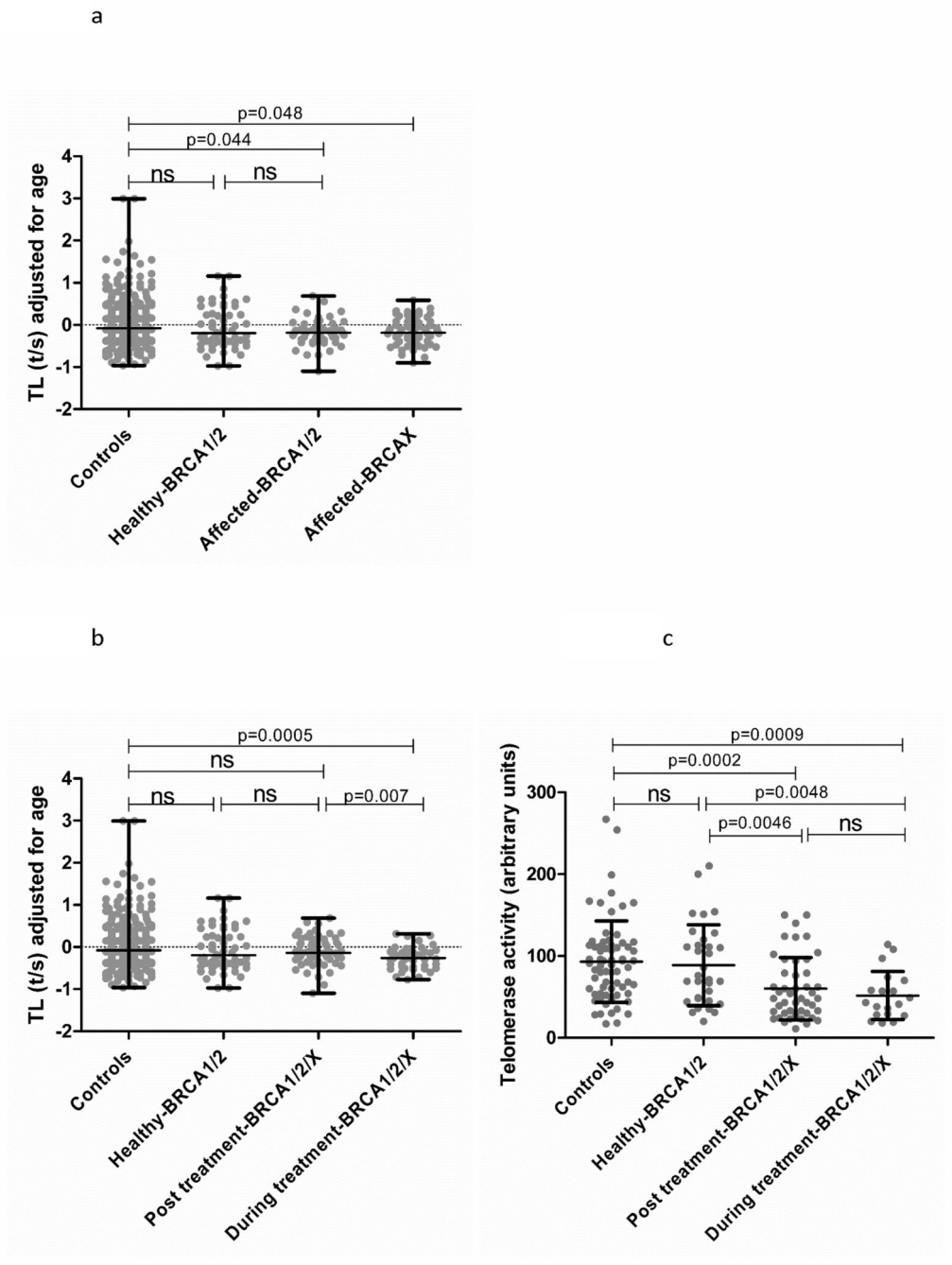

Figure 3.

a) Distribution of telomere-length (t/s) values adjusted for age for the familial breast cancer groups according to mutational status. The Mann Whitney test was used to test for significant differences in telomere-length between controls and the different subgroups. b) Distribution of telomere-length (t/s) values adjusted for age for the familial breast cancer groups according to treatment status (Mann Whitney test). c) Comparative analysis of telomerase activity levels in the familial breast cancer series; Student's unpaired t-test was used to determine significant differences among groups.

Europe PMC Funders Author Manuscripts

a

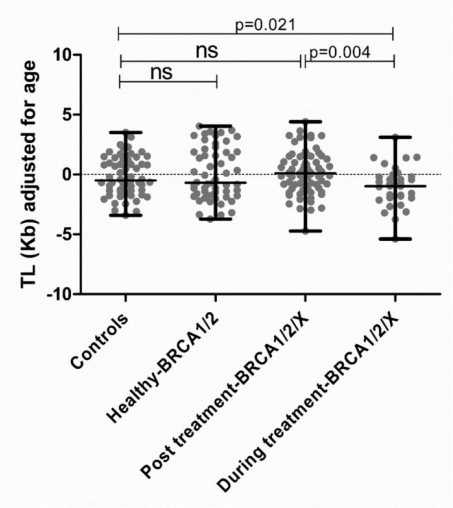

b

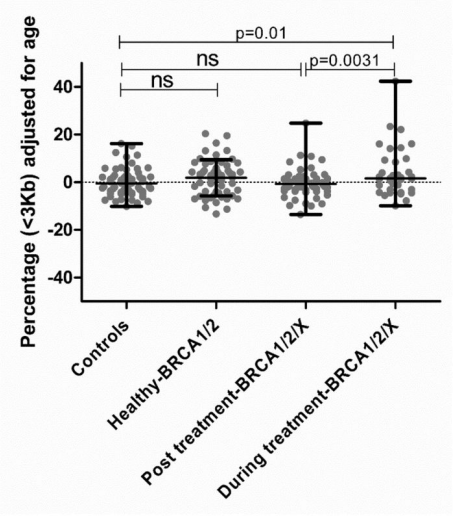

Figure 4.

a) Comparative analysis regarding telomere-length (adjusted Kb) in the familial breast cancer series (Unpaired Student t-test). b) Comparative analysis regarding content of short telomeres (<3Kb) in the familial breast cancer series (Unpaired Student t-test).

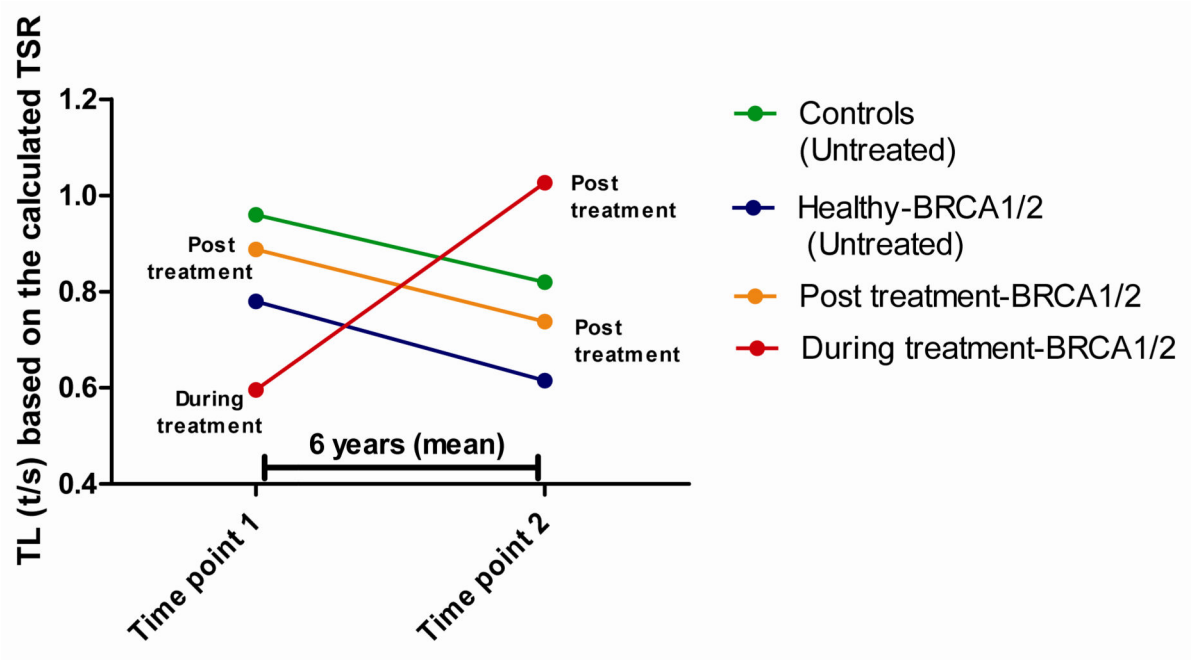

Figure 5.

Theoretical telomere-length (TL) evolution based on two telomere-length measurements along the time (average 6 years). We observed a similar behavior for controls, Healthy *BRCA1/2* carriers and Post treatment affected patients carrying *BRCA1/2* mutations regarding telomere shortening rate, ranging from 0.028 to 0.033 t/s per year. Strikingly patients with control samples during treatment and post treatment presented an opposite elongation pattern, of −0.086 t/s year.

Europe PMC Funders Author Manuscripts

Europe PMC Funders Author Manuscripts

Table 1

Details regarding the two main Taxane subgroup schedules

	During treatment			After treatment		
Drug/Combination	**n**	**Me-days treatment**	**Range/days** *	**n**	**Me-Days post treatment**	**Range/days** #
AC+T/T+AC	24	88	0-204	42	166.5	14-1855
FEC+T/T+FEC	63	85.5	0-161	124	281	1-1219

Me-days treatment: Median number of treatment days; Me-days post treatment: Median post treatment follows up in days; A: Doxorubicin; C: Cyclophosphamide; F: 5-Fluorouracil; E: Epirubicin; T: Paclitaxel

*Days counted from the first day of treatment.

#Days counted from last day of treatment.

Europe PMC Funders Author Manuscripts

Table2

General table with relevant information of the sporadic and familial breast cancer series

	n	Non Treated	Treated	Pos Treated	Age Median (y)	Age (Range)	Gap (years)	Telomere Length	Telomere Shortening Rate	Telomerase activity	High Throughput QFISH
Controls$_1$	330	330	-	-	43	19-77y		+		-	-
Sporadic	266	13	88	165	50	30-81y	-	+	-	-	-
Familial	236	54	45	68	50	20-87y	-	+	-	+	+
Controls$_2$	69/62	-	-	-	50	19-87y	-	-	-	+	+
Healthy-*BRCA1/2*	54	54	-	-	42	20-84y	-	+	-	+	+
Post treated-*BRCA1/2*	35	-	-	35	54	32-87y	-	+	-	+	+
Post treated-*BRCAX*	33	-	-	33	51	32-72y	-	+	-	+	+
During treatment-*BRCA1/2/X*	45	-	*	-	45	26-69y	-	+	-	+	+
Familial (2 time points)	56	40	7	9	-	-	6	-	+	-	-
Controls$_3$	25	25	-	-	35	22-55y	5	-	+	-	-
Healthy-*BRCA1/2*	15	15	-	-	29	19-61y	6	-	+	-	-
Post treated-*BRCA1/2*	9	-	-	9	47	35-58y	6	-	+	-	-
During treatment-*BRCA1/2*	7	-	7	-	46	29-61y	7	-	+	-	-

Controls 1: Set of control used for obtain the adjustment line for the age; *Controls 2*: Comprise the set of Healthy family members without mutations in *BRCA1/2* used as controls for the Telomerase activity (n=69) and High Throughput QFISH (n=62), comparative analysis; *Controls 3*: Controls that presented 2 samples, separated in time. These controls have been used to calculate the Telomere Shortening Rate of controls and to perform the comparative analysis;

*From a total of 45 "During treatment-*BRCA1/2/X*"patients, 15 were *BRCA1/2* and 30 *BRCAX*.

Figure S1

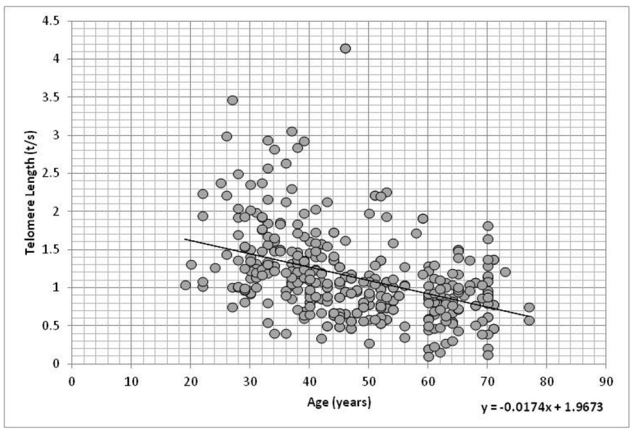

Figure S1: Telomere Length distribution in peripheral blood leukocytes as a function of age for the control women population (n = 330), measured by q-PCR. The regression line for control is drawn (y=-0.0174*X+1.96) (r =0, 2633).

Table S1 Characteristics of Taxane-based schedules .

Taxol schedule	Treatment strategy	n	Taxanes (mg/m2)	Days of treatment	Other drugs (mg/m2)	Days of treatment
AC+T	Adjuvant	51	80	60-80	(60/600)	80-100
T+AC	Neoadjuvant	15	80	60-80	(60/600)	80-100
FEC90+T	Adjuvant	134	100	60-80	(600/90/600)	80-100
T+FEC90	Neoadjuvant	53	80	60-80	(600/90/600)	80-100

A: Doxorubicin; C: Cyclophosphamide; F: 5-Fluorouracil; E: Epirubicin; T: Paclitaxel

Table S2 Comparative analysis between controls and sporadic breast cancer cases: before, during and after finishing chemotherapy.

	n	t/s adjusted for age	p-value
Controls	330	-0.077	ns
Pre-treatment	13	0.012	ns
During treatment 0-90d*	44	0.0715	ns
During treatment 91-180d	42	-0.273	0.0038
Post-treatment 0-91d#	33	-0.22	0.0007
Post-treatment 91-180d	35	-0.389	0.0001
Post-treatment 181-360d	38	-0.306	0.0093
Post-treatment 361-520d	24	-0.135	ns
Post-treatment >520d	37	-0.008	ns

p-value: Mann Whitney test was used to test for significant differences among the groups with controls (ns) Non significant differences.

* Days counted from the first day of treatment.

Days counted from last day of treatment.

Table S3 Comparative analysis of the telomerase activity among the familial breast cancer groups.

	n	Telomerase	p-value*
Controls	69	93.1	-
Healthy-BRCA1/2	32	88.8	ns
Affected-BRCA1	12	61.1	0.04
Affected-BRCA2	11	54.5	0.01
Affected-BRCAX	23	62.3	0.002
During treatment-BRCA1/2/X	19	51.8	0.0009

p-value*: Unpaired Student's t-test was used to establish the significance of the differences between the control group and the other groups

Table S4 Telomere shortening rate per year among the familial breast cancer groups.

	n	Gap (years)	Median age	Age range	Telomere Shortening Rate	p-value*
Controls	25	5	35	22-55y	0.028	-
Healthy-BRCA1/2	15	6	29	35-61y	0.033	ns
Post treatment-BRCA1/2	9	6	47	35-58y	0.03	ns
During treatment-BRCA1/2	7	7	46	29-61y	-0.086	0.01

p-value*: Unpaired Student's t-test was used to establish the significance of the differences between the control group and the other groups

ARTICLE 2

Molecular insights into the *OGG1* gene, a cancer risk modifier in *BRCA1* and *BRCA2* mutations carriers.

Authors: Carlos Benitez-Buelga, Tereza Vaclová, Sofia Ferreira, Miguel Urioste, Lucia Inglada-Perez, Nora Soberón, Maria A. Blasco, Ana Osorio, and Javier Benitez.

Publication date: May 2016
Journal: Oncotarget
Ref: 3; 7(18): 25815–25825.
Personal contribution: Collection, control and preparation of the samples, SNP genotyping, *OGG1* mRNA expression studies, cell culture, statistical analysis, preparation of the manuscript.

In a recent study published by our group, we identified a polymorphism (rs2304277) in the 3´UTR region of the *OGG1* gene that modify the risk of developing ovarian cancer for *BRCA1* mutation carriers

In order to explain at a molecular level this association, we studied the possible implication of this polymorphism on *OGG1* transcriptional regulation and its contribution on genome and telomere instability.

We have worked with two independent sample sets: A series of hereditary breast and ovarian cancer patients with a heterogeneous BRCA mutational status, and with panel of lymphoblastoid cell lines derived from patients with *BRCA1* mutations or non-carriers controls.

We found similar results in both cases: The presence of the polymorphisms as associated to a decrease of the transcriptional levels of *OGG1*. In addition, we also found a synergistic effect between the mutation and the polymorphism that was associated with higher levels of genome and telomere instability. Those individuals or cell lines that had both genetic events (mutation in *BRCA1* / *BRCA2* and the polymorphism rs2304277) had accelerated telomeric shortening associated with a short TL phenotype. In addition, the presence of the polymorphism was associated with a higher γH2AX signal intensity, especially for those cells carrying the *BRCA1* mutation.

These results suggest that this variant could be associated to a higher cancer risk in *BRCA1* mutation carriers, due to an *OGG1* transcriptional down regulation and its effect on genome /telomere instability. And points to a possible synthetic lethality relationship between *BRCA1* and *OGG1*.

Impact Factor (IF) = 5.008

Molecular insights into the *OGG1* gene, a cancer risk modifier in *BRCA1* and *BRCA2* mutations carriers

Carlos Benitez-Buelga[1], Tereza Vaclová[1], Sofia Ferreira[1], Miguel Urioste[2,5], Lucia Inglada-Perez[3,5], Nora Soberón[4], Maria A. Blasco[4], Ana Osorio[1,5], Javier Benitez[1,5]

[1]Human Genetics Group, Spanish National Cancer Research Center (CNIO), Madrid 28029, Spain

[2]Familial Cancer Clinical Unit, Spanish National Cancer Research Center (CNIO), Madrid 28029, Spain

[3]Endocrine Cancer Group, Spanish National Cancer Research Center (CNIO), Madrid 28029, Spain

[4]Telomere and Telomerase Group, Spanish National Cancer Research Center (CNIO), Madrid 28029, Spain

[5]Spanish Network on Rare Diseases (CIBERER), Madrid 28029, Spain

Correspondence to: *Javier Benitez,* ***e-mail:*** *jbenitez@cnio.es*

Keywords: *BRCA1 and BRCA2, telomere shortening, OGG1 polymorfism, cancer risk modifier, DNA damage*

Received: *January 28, 2016* ***Accepted:*** *March 07, 2016* ***Published:*** *March 22, 2016*

ABSTRACT

We have recently shown that rs2304277 variant in the *OGG1* glycosidase gene of the Base Excision Repair pathway can increase ovarian cancer risk in *BRCA1* mutation carriers. In the present study, we aimed to explore the role of this genetic variant on different genome instability hallmarks to explain its association with cancer risk.

We have evaluated the effect of this polymorphism on *OGG1* transcriptional regulation and its contribution to telomere shortening and DNA damage accumulation. For that, we have used a series of 89 *BRCA1* and *BRCA2* mutation carriers, 74 BRCAX cases, 60 non-carrier controls and 23 lymphoblastoid cell lines (LCL) derived from *BRCA1* mutation carriers and non-carriers.

We have identified that this SNP is associated to a significant *OGG1* transcriptional down regulation independently of the BRCA mutational status and that the variant may exert a synergistic effect together with *BRCA1* or *BRCA2* mutations on DNA damage and telomere shortening.

These results suggest that this variant, could be associated to a higher cancer risk in *BRCA1* mutation carriers, due to an *OGG1* transcriptional down regulation and its effect on genome instability.

INTRODUCTION

Carrying an inherited mutation in the *BRCA1* or *BRCA2* genes increases a woman's lifetime risk of developing breast and ovarian cancers although there are considerable differences in disease manifestation. At the age of 70, cumulative cancer risk for *BRCA1* and *BRCA2* mutation carriers ranges from 43% to 88% for breast cancer development, and from 11% to 59% for ovarian cancer [1, 2].

In the context of *BRCA1* and *BRCA2* mutation carriers, it has been shown that other factors such as single nucleotide polymorphisms (SNPs) in genes from other DNA repair pathways could cause a higher genomic instability, hence increasing the cancer risk predisposition [3–6]. In this regard, a well-known synthetic lethal interaction is described between the *BRCA1* and *BRCA2* genes and the poly ADP ribose polymerase (*PARP1*), involved in the Base Excision Repair (BER) pathway [7]. BER corrects oxidative lesions in the DNA bases, which represent the major portion of endogenous DNA damage due to chemical reactions during cellular metabolism [8]. These lesions cause different types of DNA damage including DNA single-strand breaks (SSBs) or DNA double-strand breaks (DSBs) which are the principal source of genomic instability [9, 10]. In the presence of a defective *BRCA1* or *BRCA2* background, this accumulation of double-strand DNA breaks can persist and lead to cell cycle arrest or cell death; making BRCA-deficient cells extremely sensitive to PARP inhibitors (PARPi).

In addition, telomere instability/shortening occurring during oxidative and inflammatory stress can be

explained by the strong tropism for guanine (G) oxidation at the telomere sequence (TTAGGG) [11]. For this reason, BER pathway is essential to maintain telomere integrity in mammals [12]. In fact, cellular changes due to BER defects have been implicated in a multitude of diseases, ranging from cardiovascular diseases, arthritis, cancer, as well as aging and age-related disorders [13, 14].

SNPs in genes involved in the BER pathway have been reported to modify ovarian and breast cancer risk in *BRCA1* and *BRCA2* mutation carriers. In particular, one of the most recent examples was described by our group for a SNP (rs2304277) in the *OGG1* (8-guanine DNA glycosylase) gene that was associated with increased ovarian cancer risk in *BRCA1* mutation carriers [5]. The *OGG1* gene encodes for a key enzyme involved in the first steps of BER that removes a highly mutagenic base, 8-oxodeoxyguanosine, generated by oxidative stress [15].

In this study, by using two independent sample sets with different *BRCA* status, we have explored the role of this polymorphism on *OGG1* transcriptional regulation and its possible implication on genome instability. With this, we would like to explain the cancer risk modifier effect that this gene exerts in carriers of *BRCA1* and *BRCA2* mutations.

RESULTS

SNP frequency in FBOC and LCL

We genotyped the SNP rs2304277 in both, FBOC and LCLs sample sets, to perform genotype/phenotype studies (role of the SNP on: *OGG1* mRNA expression, telomere studies, and DNA damage). In the FBOC samples, we identified 36% of the samples (81/223) carrying the variant. The same frequency was reported in our previous study analyzing more than 23000 cases and controls [5].

The different group of cases and controls presented similar frequencies that are summarized in Supplementary Table S1. No significant differences were found among groups.

From a total of 23 cell lines, 9 harbored the SNP (39%). From 16 of the LCL with *BRCA1* mutation 7 LCL harbored the SNP (43%) and from the 7 non-carrier controls, 2 had the variant (33%) (Supplementary Table S2).

Expression of *OGG1* in FBOC, Gtex server and LCLs

In order to know if the SNP could affect gene expression, we first analyzed in the FBOC series the *OGG1* mRNA expression levels considering both, the BRCA mutational status and the presence or absence of the *OGG1* variant to stratify and compare expression values among groups (Figure 1a).

First, we did an independent lineal regression analysis in BRCA1/2 mutation carriers to test whether cancer status (individuals with or without cancer antecedents) could affect *OGG1* mRNA levels; because it did not affect, we decided to include healthy and affected BRCA1/2 mutation carriers in the same group (BRCA1/2) for expression studies, Supplementary Table S3.

In the comparative analysis, we detected an *OGG1* mRNA down regulation in individuals harboring the variant. This down regulation was statistically significant when we stratified all the FBOC individuals by the presence of the variant (with/without) regardless the BRCA status (BRCA1/2, BRCAX and non-carrier controls), p=0.011. Although. we were not able to detect significant differences within each mutational group (non carrier controls, *BRCA1/2* and BRCAX*)* probably due to the reduced sample size (Figure 1a); a complementary lineal regression analysis confirmed a significant down regulation associated to the SNP in the non carrier controls (β=-0.63);p=0.049), in BRCA1/2 (β=-0.57;p=0.027) and a trend in the BRCAX group(β=-0.34;p=0.123), suggesting that the variant could be associated *per se* to lower *OGG1* mRNA levels independently of the BRCA mutational group.

In parallel, we tested *in silico* the SNP effect on transcriptional regulation in different tissues using the Gtex eQTL web server (http://www.gtexportal.org). Interestingly, we observed down regulation for whole blood, uterus, vagina and ovary, but only the last one presented a significant *OGG1* transcriptional down regulation (p=0.023), Supplementary Table S4. Ovary is the tissue where this variant was originally found to be associated to an increased cancer risk [5].

Finally, we measured *OGG1* mRNA basal levels among the 23 LCL considering the BRCA status, and presence or absence of the SNP. Only when we group all LCL together considering the presence of the SNP we are able to detect significant down regulation (p=0.04) Figure 1b, probably because the sample size was too small to detect significant association p-values of *OGG1* mRNA down regulation within groups (*BRCA1* non carriers LCLs and *BRCA1* LCLs).

Telomere length studies in FBOC

We explored the role of this variant on TL maintenance. Hence we measured TL and percentage of short telomeres by HT QFISH in the blood cells from FBOC patients and non-carrier controls to establish genotype/phenotype associations.

We first evaluated the TL distribution in 60 healthy women as a function of age to obtain a regression line to adjust the TL from FBOC samples. As expected, we found a decrease in TL with age, Supplementary Figure S1.

Because mean TL is strongly heritable [16] and our series contains related individuals, we used a single member (genotype) from each family for both, BRCA status and presence or absence of the SNP for the analysis.

Whenever possible, we used the index-case of the family and if this sample was not available, we used the latest genotype included in the family as common criteria of the study.

Chemotherapy status, another possible confounding factor that alters TL was corrected to perform this analysis [17]. We eliminated those cancer patients who were undertaking chemotherapy or those within a window of 2 years since the last cycle of chemotherapy. In total, 13 BRCA1/2 cases and 26 BRCAX cases were excluded.

Hence, we used a total of 44 controls (19 harboring the SNP), 21 *BRCA1* carriers (10 harboring the SNP), 28 *BRCA2* carriers (9 harboring the SNP), 1 patient harboring mutation in both genes and 38 BRCAX (15 harboring the SNP).

First, we did an independent lineal regression analysis in BRCA1/2 mutation carriers to test whether cancer status (individuals with or without cancer antecedents) could affect TL and percentage of short telomeres; because it did not affect these 2 factors (Supplementary Table S3), we decided to include healthy and affected BRCA1/2 mutation carriers in the same group (BRCA1/2) for telomere studies.

In the comparative analysis, Mann Whitney U test revealed no significant differences neither in adjusted TL nor in percentage of short telomeres between controls harboring and not harboring the variant (Figure 2a & Figure 2b). However, we observed significant shorter TL among BRCA1/2 carriers harboring the variant compared to those BRCA1/2 carriers not harboring the SNP (p=0.003) or controls (p=0.009), Figure 2a. Additionally, increased percentage of short telomeres were detected in BRCA1/2 mutation carriers harboring the SNP compared to the control group (p=0.018), Figure 2b. In the group of BRCAX cases we did not detect any effect of the SNP on TL although we found a significant increased percentage of short telomeres (p=0,009) compared to controls, Figure 2a and Figure 2b.

Then, we analyzed all FBOC patients together considering the presence/absence of the variant to test the effect of the SNP alone, regardless the BRCA mutational status. We were not able to observe significant differences on TL but we detected a significant increased percentage of short telomeres in the group harboring the SNP (p=0.016), Figure 2a and Figure 2b.

Linear regression analysis revealed that TL was significantly modified by the presence of the SNP in the group of patients harboring mutations in *BRCA1* or *BRCA2* genes (BRCA1/2) (β= -1.438; C.I (-2.554 – (-0.323); p=0.013), Supplementary Table S3; but not in the non-carrier controls or BRCAX groups (data not shown).

Hence, we stratified BRCA1/2 patients according to the SNP and we compared the linear model between each of the groups (BRCA1/2 with/without the SNP and controls). Significant differences were detected in BRCA1/2 carriers harboring the SNP when compared to those not harboring the SNP (p=0.010) or controls (p=0.034), Figure 2c. In fact, we observed a faster

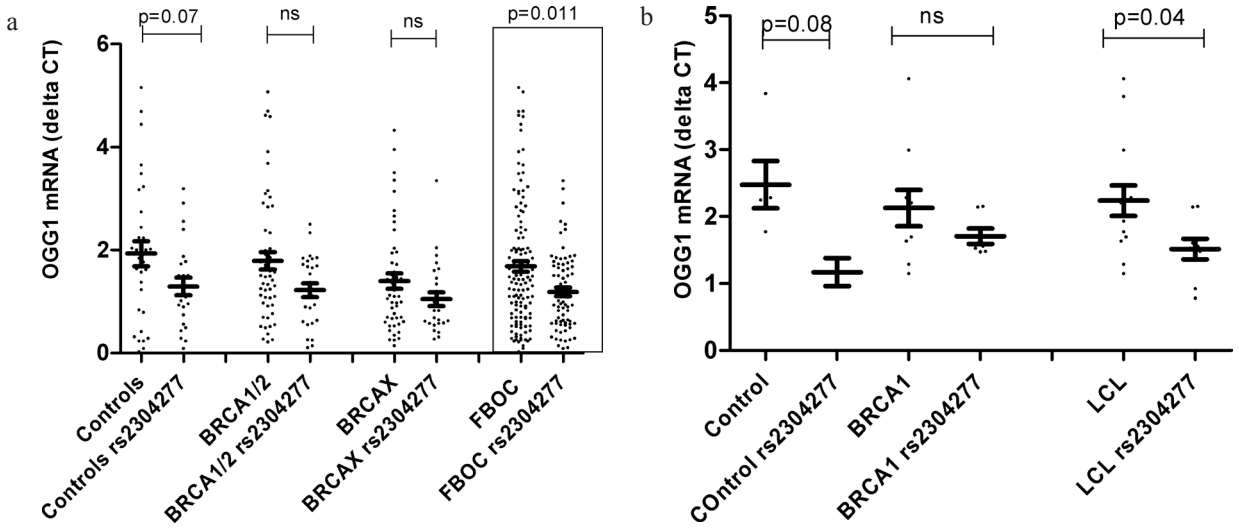

Figure 1: a. Comparative analysis relative to the *OGG1* mRNA expression levels between FBOC groups (*BRCA1 & BRCA2,* BRCAX) and controls according the presence of the *OGG1* SNP. Control group harbouring the variant showed a statistical trend of lower *OGG1* mRNA levels (p=0.07); while we didn't detect significant differences in *OGG1* transcriptional levels within *BRCA1* and *BRCA2* group due to the presence of the SNP (p=0.11). When all FBOC samples, were stratified according to the presence of the SNP, we observed significant lower *OGG1* mRNA expression levels in the individuals harbouring the variant (p=0.011). Line at mean with standard error mean (SEM) **b. Transcriptional mRNA basal levels of *OGG1* in Lymphoblastoid cell lines (LCLs)**. Each dot at the graph, represent the mean OGG1 mRNA values from two independent measurements (two clones of each sample) for most LCL analyzed (20/23), for 3 samples we could measure only once. We found that LCL harbouring the SNP presented significant lower *OGG1* mRNA levels when compared to those who did not harbour the SNP (p=0.04). Line at mean with standard error mean (SEM).

telomere shortening (slope) in the group of patients harboring both, the BRCA1/2 mutation together with the SNP, compared to those who did not harbor the SNP, or the control group, Figure 2c (legend).

Telomere length study in LCLs

We compared telomere shortening during normal replication among the *BRCA1* LCLs to confirm experimentally the faster telomere shortening (slopes) observed in the FBOC patients who harbored the BRCA1/2 mutation together with the variant. Additionally, we measured and compared the accumulation of short telomeres along the cell culture.

Due to technical issues and the differences in growth rate, we could only use a set of 8 out of the 16 LCLs harboring mutation in *BRCA1* gene to follow the

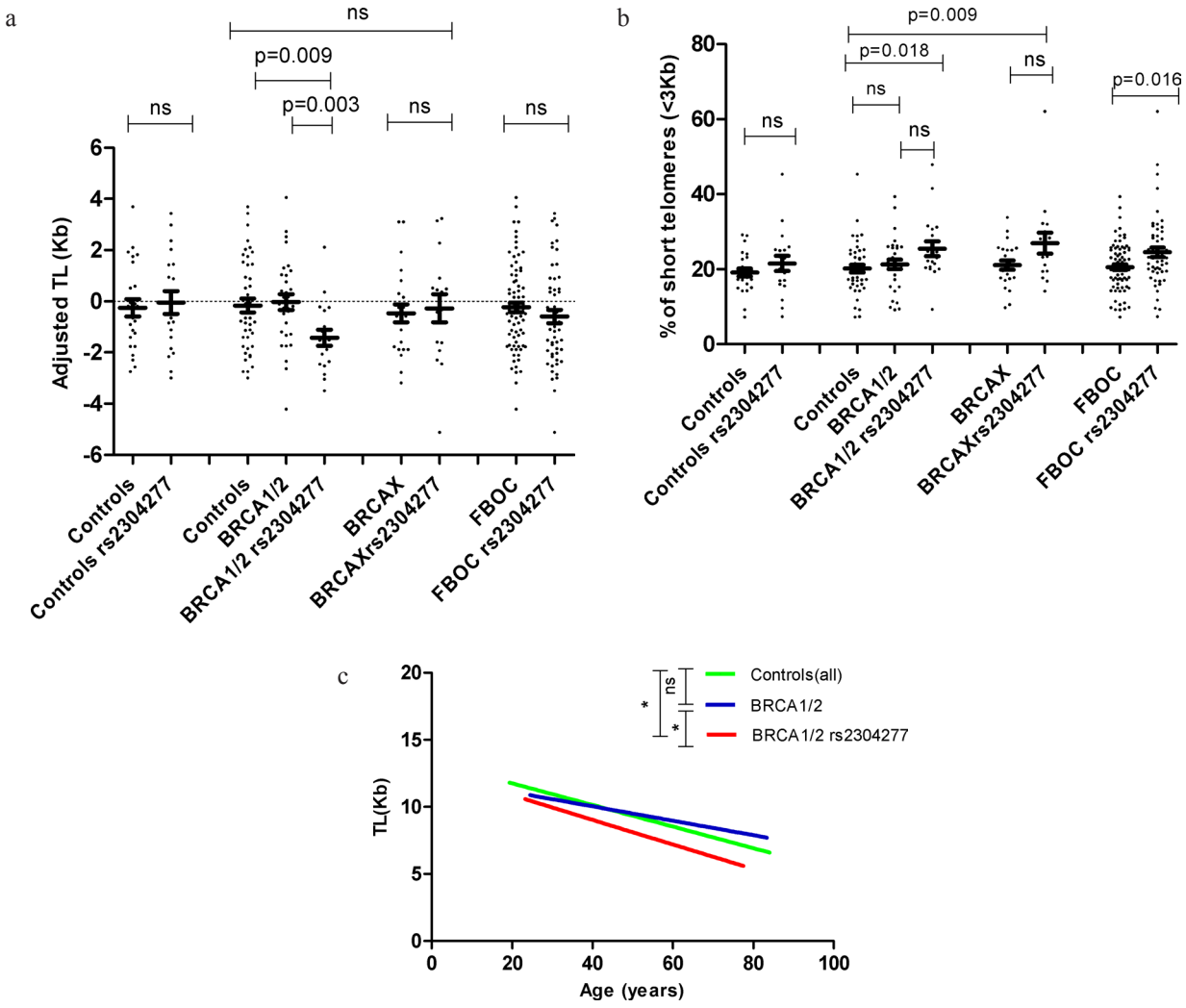

Figure 2: a. Distribution of the TL (Kb) values adjusted for age according to mutational status. We did not detect significant differences in TL for the control group due to the presence of the SNP; while TL was significantly shorter in BRCA1/2 mutation carriers harbouring the variant when compared to non carriers of the SNP (p=0.003) or controls(0.009). We were not able to find any difference in TL among the BRCAX group of patients. Additionally we stratify all the FBOC samples according to the presence of the variant and we did not detect any significant difference in TL between carriers and non carriers. Line at mean with standard error mean (SEM) **b. Comparative analysis among FBOC genotypes regarding the percentage of short telomeres (<3Kb)**. We did not detect significant differences in the percentage of short telomeres neither in the control nor in the BRCA1/2 groups when the variant was present; however BRCA1/2 or BRCAX harbouring the variant presented significant higher % of short telomeres compared to controls(all)(p=0.018; p=0.009). Additionally we stratify all the FBOC samples according to the presence of the variant, and we could detect a significant higher % of short telomeres in those samples harbouring the SNP (p=0.016) Line at mean with standard error mean (SEM) **c. Telomere shortening lines in BRCA1 or BRCA2 mutations carriers group (BRCA1/2) with and without the variant, and the non-carriers controls.** TL (Kb) is represented in this graph according to age (years). Regression line is draw in green colour for controls (y=-0.080*age+13.367), blue colour for BRCA1/2 patients (y=-0.537*age+12.188) and red colour for BRCA1/2 with the variant (y=-0.0918*age+12.705). F-test: BRCA1/2 *vs* BRCA1/2 rs2304277 (p=0.010); Controls *vs* BRCA1/2 rs2304277 (p=0.034).

telomere shortening during 55 passages. From the 8 LCL with mutation in *BRCA1* gene 3 presented also the SNP.

Our results revealed significant faster telomere shortening after 55 cell culture passages, in the group of samples harboring *BRCA1* mutation together with the SNP (p=0.033). This result is similar from the previous obtained in patients suggesting that this event is taking place only when *BRCA1* mutation and the variant are together, Figure 3a. We could also confirm a significant accumulation of short telomeres in the LCL harboring the *BRCA1* mutation together with the variant after 55 passages of cell culture (p=0.03), Figure 3b.

DNA damage

To test the possible contribution of the SNP to a higher DNA damage we measured the mean γH2AX intensity signal in the cell nucleus at basal conditions (first passage and no irradiation).

We plotted all the γH2AX values from the LCL in a cumulative frequency histogram to establish a damage threshold above which we observed an exponentially increase in the γH2AX intensity values, which indicates the cells with a clear nuclear DNA damage. We established the threshold in 95 arbitrary units of γH2AX of nuclear intensity (Figure 4a).

Then, we calculated the frequency of damaged cells among LCLs with different genotypes and the intensity of the nuclear γH2AX signal in these cells to evaluate the possible impact of the *OGG1* SNP on DNA damage. We found minimum differences in the percentage of damaged cells associated to the presence of the SNP (5.8% and 6.3% in LCLs with and without the SNP, respectively). However, the intensity of the damage was significantly higher in LCLs harboring the SNP (p=0.010) compared to those not harboring the variant, Figure 4b.

DISCUSSION

We have previously found that the *OGG1* SNP rs2304277may be a modifier of cancer risk in *BRCA1* mutation carriers [5]. *OGG1* belongs to the BER pathway that plays an important role correcting DNA lesions originated by oxidative stress. These lesions are the principal source of genomic instability and can drive to cancer development. In this study we have shown how this variant can contribute to increase cancer risk in *BRCA1* carriers, by reducing the mRNA *OGG1* expression levels, increasing the DNA damage as a consequence of genomic instability generated, and shortening the telomeres in a synergic way with the *BRCA1* mutation.

Because rs2304277 is located 1.8Kb downstream of 3'UTR region of the *OGG1* and post transcriptional modifications, like potential illegitimate microRNA target site [18, 19], could be altering normal *OGG1* mRNA regulation, we decided to explore the role of this SNP on transcriptional regulation using two set of samples. The first set consisted in 223 blood samples from controls and FBOC patients with a heterogeneous BRCA mutational status (*BRCA1, BRCA2* and BRCAX) and the second was a panel of 23 LCLs derived from *BRCA1* mutation carriers and non-carrier controls. The percentage of heterozygotes for

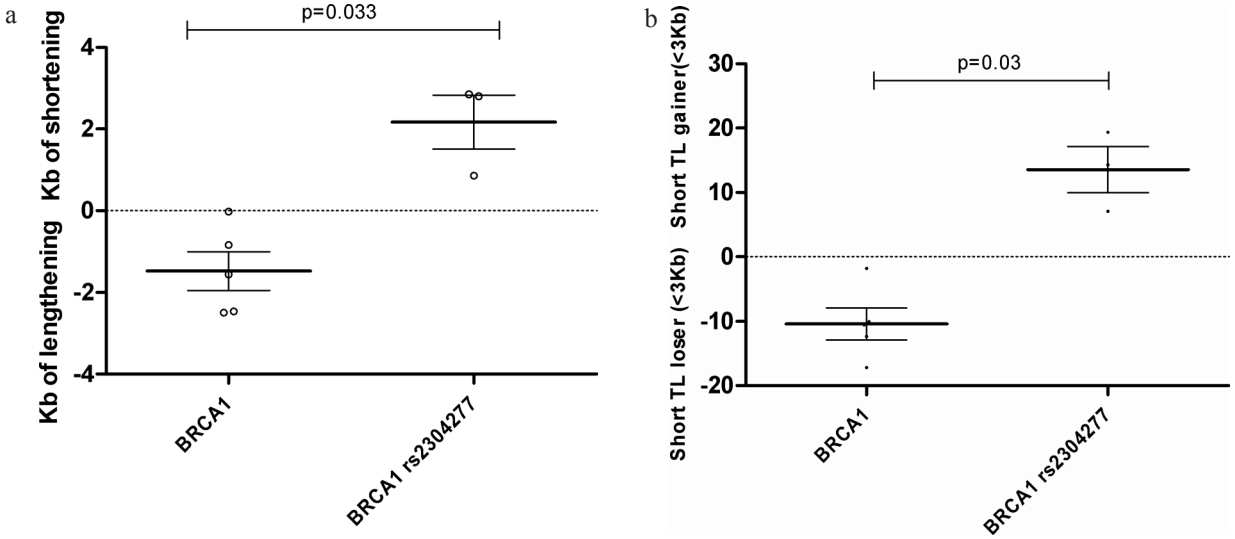

Figure 3: We measured TL differences between passage nº1 and passage nº55 for each LCL, to calculate telomere shortening/ lengthening in Kb and the gain or lose of critical short telomeres(<3Kb) a. Telomere length lose or gain after 55 passages of culture among *BRCA1* mutated LCLs. Significant telomere shortening in LCL harbouring *BRCA1* mutation together with the SNP was detected after 55 passages compared to those not harbouring the variant (p=0.033). Line at mean with standard error means (SEM) **b. Percentage of critical short telomeres gain or lose after 55 passages of culture among among *BRCA1* mutated LCLs.** Significant increased amount of short telomeres was found in the LCL harbouring BRCA1 mutation together with the SNP after 55 passages compared to those not harbouring the variant (p=0.03). Line at mean with standard error means (SEM).

the SNP in the FBOC and LCL set of samples was 36% and 39%, respectively, which was the expected frequency [5].

We confirmed in both sample sets (FBOC series and LCL) significant lower expression of *OGG1* mRNA transcript associated to the SNP, independently of BRCA mutational status, (Figure 1a & Figure 1b). We extended the analysis using Gtex eQTL dB (http://www.gtexportal.org) looking for the SNP effect over *OGG1* mRNA levels in different tissues and we found significant down regulation in ovary (p=0.023) tissue where this SNP was initially found to be associated to a higher cancer risk, Supplementary Table S4.

These results suggest that this cancer risk variant is likely associated with mRNA *OGG1* transcriptional down regulation which can potentially lead to higher genome instability due to a defective 8-oxoG repair capacity. In this way, the aberrant accumulation of 8-oxoG was previously associated with faster development of lung adenocarcinoma in *OGG1* knock-out mice models [20] while in transgenic mice it was demonstrated that over expression of *OGG1* attenuated breast cancer progression and metastasis through a reduction in the oxidative damage [21]. All these data suggest a critical role of this gene in cancer development and progression which, together with BRCA mutations could result in higher genome instability and increased cancer risk.

Given the role of the BER pathway and in particular the *OGG1* enzyme on telomere repair [11, 22], we explored the impact of this SNP on some features related to telomere biology considered as hallmarks of genome instability, such as telomere shortening or the percentage of critically short telomeres. We found in the linear regression analysis, that the SNP may be a TL modifier for *BRCA1* and *BRCA2* mutations carriers (p=0.013). Carriers of BRCA1/2 mutations and *OGG1* SNP presented a significant shorter TL compared to controls (p=0.009) and mutation carriers not harboring the SNP (p=0.003) (Figure 2a), likely due to an accelerated telomere shortening during life-time (Figure 2c). We also found an increase of short telomeres in those individuals harboring the SNP, regardless the BRCA mutational status (p=0.016) (Figure 2b).

These results were experimentally validated in our LCL set by measuring TL after 55 passages. We could confirm a significant faster telomere shortening in the group of samples harboring a *BRCA1* mutation together the SNP (p=0.033) (Figure 3a), which correlated with a significant accumulation of short telomeres after a total of 55 cell culture passages (p=0.03) (Figure 3b). Our results point to a synergistic effect of the SNP and the *BRCA1* mutation on telomere shortening. This telomere instability may be due to the cell tropism for the accumulation of oxidative lesions at the telomeric region [23, 24] in the context of defective BER performance [22] triggered by the SNP effect on *OGG1* down regulation. In this sense other authors have reported that SNPs located in the 3'UTR region of *OGG1* could be associated with a lower 8-oxoG repair activity being particularly sensitive to the cellular redox status. [25, 26]

The region represented by the SNP has been previously spotted by other authors who also found associations with different cancer types [27–29]. Then,

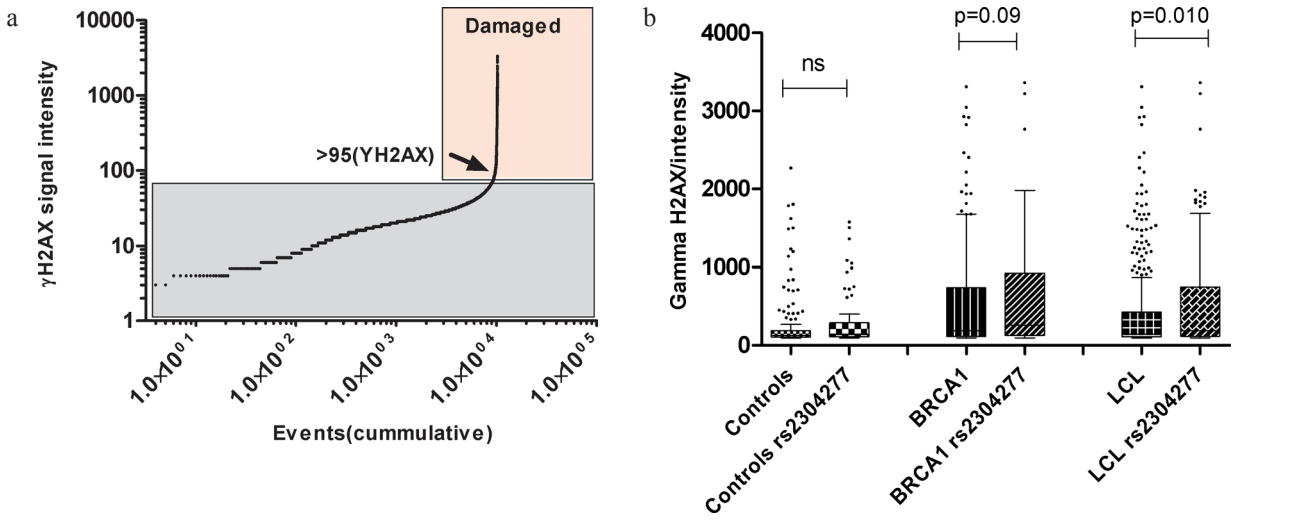

Figure 4: a. Threshold of γH2AX nuclear intensity damage. We selected the intensity value of 95(arbitrary units) as a cut of to establish the damaging signal intensity because this was the value in where the distribution change shape exponentially, indicating which are the normal and the abnormal (damaging)values. **b. Comparative analysis regarding the signal intensity of γH2AX at the nucleus among the LCL genotypes.** The effect of the variant is not significant in the control group (p>0.05) while in the group of cells carrying mutation in BRCA1, we found higher γH2AX signal intensity when the variant was present (p = 0.09). We stratified all the 23 LCL according the presence of the variant and we detected significant higher γH2AX intensity in the carriers of the variant (p =0.010). Line at mean with standard error means (SEM).

Table 1: Description of the analyzed series and the different studies performed

Families (n)	Healthy carriers	Affected carriers	[c] Non-carriers controls	Total	Median age, (range)	SNP Genotyping	Expression studies	[d]TL studies
BRCA1, (24)	18	20	13	51	45, (23-78y)	51	48	30
BRCA2, (25)	27	21	25	73	50, (22-87y)	73	64	46
[a]BRCA1 + BRCA2, (1)	1	2	1	4	54, (42-61y)	4	4	3
[b] BRCAX, (71)	-	74	21	95	49, (20-85y)	95	92	53
Total FBOC, (121)	46	117	60	223	49, (18-87y)	223	209	132

[a] Refers to a family harboring mutations in both BRCA1 and BRCA2 genes.
[b] Non BRCA1 or BRCA2 families.
[c] Non carrier controls were composed by family relatives without any antecedents of cancer and negative for BRCA1 or BRCA2 mutations.
[d] Sample size used in TL studies after heritability correction and exclusion of patients who were undertaking chemotherapy (see manuscript in results section, TL studies in FBOC).

we tested whether this SNP could have an impact on DNA damage, measured in this case by γH2AX, a DNA damage marker of DSB [30].

Using the LCL panel, we compared the percentage of damaged cells and its nuclear γH2AX signal intensity among different genotypes at basal conditions (first passage and no irradiation). Despite we found a similar percentage of damaged cells among LCLs with and without the variant (5.8% and 6.3%, respectively), we could detect that those LCLs harboring the SNP, presented significantly higher γH2AX signal intensity at the nucleus, pointing to a more profound DNA damage (p=0.010) (Figure 4b). These results are similar to other reported in the literature establishing association between SNPs in *OGG1* at the same gene region with an increased DNA damage/genome instability due to an impaired BER performance [6, 25-27, 31, 32]

In summary, we have identified that the *OGG1* SNP itself contributes to a higher nuclear DNA damage intensity, probably due to a defective BER performance triggered by *OGG1* transcriptional down regulation. Additionally, our results suggest a synergistic effect between *BRCA1* or *BRCA2* mutations with the SNP rs2304277 on specific telomere instability hallmarks, such as telomere shortening and the accumulation of short telomeres, when both genetic events are present in the cell. These molecular processes could explain the relation between this SNP and *BRCA1* or *BRCA2* mutations, on cancer risk.

MATERIALS AND METHODS

Familial breast and ovarian cancer (FBOC)

We studied two different set of samples: A first group, was composed by 223 individuals belonging to 121 families meeting high risk criteria and screened for deleterious mutations in *BRCA1* and *BRCA2* genes, as previously reported [1]. 24 carried a deleterious mutation in *BRCA1*, 25 in *BRCA2*, 1 family harbored both *BRCA1* and *BRCA2* mutations and 71 did not carry any mutation (*BRCAX*).

Sixty individuals were used as non-carrier controls: They were relatives of BRCA1/2 carriers, who didn't have any personal cancer antecedent and didn't harbor the corresponding familial mutation in *BRCA1* or *BRCA2* genes. General characteristic of this series are described in Table 1.

All cases and controls signed an appropriate informed consent and the proposal was approved by the ethics committee at the Fuenlabrada University Hospital.

We used this set of samples (BRCA1/2 carriers, BRCAX cases and controls) to calculate the percentage of heterozygotes harboring the SNP, to quantify the *OGG1* mRNA levels in peripheral blood, and to perform telomere studies using fresh blood cells, Table 1.

Lymphoblastoid cell lines

A second set of 23 LCLs was established by Epstein Barr virus transformation of peripheral blood lymphocytes from sixteen healthy women carrying heterozygous mutations in *BRCA1* and seven non-carrier relatives used as controls. Mutational analysis had been previously performed by Sanger sequencing, Supplementary Table S2. None of the women included in the study had personal antecedents of cancer. This LCL panel has been previously described by our group [33]. Cell lines were cultured in RPMI-1640 media (Sigma-Aldrich) supplemented with non-heat-inactivated 20% fetal bovine serum (Sigma-Aldrich), penicillin-streptomycin (Gibco) and Fungizone (Gibco). The cultures were carried out in 25 cm2 flasks (Corning) at 37°C in 5% CO2 atmosphere and cell lines were maintained in exponential growth by daily dilution to 10^6 cells/ml of full media.

We used this set of samples to measure *OGG1* mRNA expression levels, DNA damage at basal conditions and whenever possible telomere shortening and the percentage of short telomeres gained/lost after 55 passages of cell culture.

SNP genotyping

The SNP rs2304277, showed the strongest association to cancer risk among all the SNP covering the gene (tagged or imputed) that were included in our previous study [5]. This SNP is located 1.8 kb downstream the 3′UTR (untranslated region) of the gene. Despite we did not find better results for a more plausible causal SNP, we could detect that SNPs in high linkage disequilibrium (LD) with rs2304277, presented similar cancer association direction and p-values [5]. Hence, we considered rs2304277 as a good representative of that gene region, which is detailed in Supplementary Table S5.

DNA was extracted from patient's peripheral blood (FBOC) and from cultured LCLs using MagNAPure LC 2.0 (Roche Diagnostics, Indianapolis, Indiana) following manufacturer's conditions. DNA quantification and quality was assessed by NanoDrop® (ND-1000 V3.7.1).

Flanking region of the rs2304277 was amplified using PCR method with the following primers: *OGG1* "rs2304277-G>A"-F: 5' GACCTTTCTCGGACCCCATA 3'*OGG1* "rs2304277-G>A"-R: 5' ACTCCTCCCCAT CCCTACC 3' and the product was genotyped using Sanger method using ABI3700.

RNA expression analysis

Using TRIzol Reagent (Ambion®, Life Techonogies) according to manufacturer's instructions, RNA was extracted from peripheral blood cells. Both RNA quantity and quality were assessed by NanoDrop® (ND-1000 V3.7.1).

1 µl of cDNA at a final concentration 10-20 ng/µl was loaded in triplicate, with GoTaq® qPCR MasterMix 1x (Promega); *OGG1* cDNA primers (F/R) and *GAPDH* cDNA primers (F/R) in final concentration of 500nM. All the mentioned reagents were used following manufacture's conditions. Delta Delta Ct method was run in ABI quant studio S7.

cDNA-*OGG1*-F:5' CTCCACTCCTGCCCTGTG 3'

cDNA-*OGG1*-F:5' AGAGAAAAGGCATTCGATGG 3'

cDNA-*GAPDH*-F: 5' CTCCACTCCTGCCCTGTG 3'

cDNA-*GAPDH*-F: 5' AGAGAAAAGGCATTCGA TGG3'

Telomere length measurement (TL)

High throughput quantitative fluorescence *in situ* hybridization (HT-QFISH) with automated fluorescence microscopy was performed as previously described [34]. Briefly, Peripheral Blood Mononuclear cells (PBMCs) were separated by Histopaque-1070 (Sigma-Aldrich) gradient centrifugation. Cells were then counted and plated (80 000 – 100 000 cells/well in clear bottomed black-well 96-well plates precoated with 0.001% (poly) L-lysine solution (Sigma-Aldrich, St. Louis, MO) for 30 minutes at 37ºC. 4´,6-diamino-2-phenylindole (DAPI) was used for nucleus staining and a fluorescent peptide nucleic acid (PNA) Cy3 probe against telomeric repeats was used for telomere detection. TL values were analyzed using individual telomere spots in a per cell basis (Approximately 90000 telomere spots per sample, which represents around 3500 cells). Fluorescence intensities were then converted into Kb using L5178-R, L5178-S and CCRF-CEM cells as calibration standards, which have stable telomere lengths of 79.7 Kb, 10.3Kb and 7.5 kb, respectively[35]. Samples were analyzed in duplicate, or triplicate in the case of calibration standards. A TL <3Kb was defined as short. The load of short telomeres was estimated as the percentage of short telomeres (number of short telomeres divided by total number of measured telomeres) in each participant.

DNA damage

LCLs were cultured 4 hours before fixation with 4% paraformaldehyde (Electron Microscopy Sciences, Hatfield, Philadelphia, USA). Two hours before fixation, cells were counted and seeded into a poly-L-lysine-coated (Sigma-Aldrich) µCLEAR bottom 96-well plate (Greiner Bio-One) at a density of 75,000 cells per 100ul full media per well. LCL were then left for 2 hours in order to attach to the surface of the wells, fixed for 15 min at room temperature, permeabilized in 0.5% Triton X-100 in PBS for 20 minutes at 4°C and stained with primary and secondary antibodies and 4′,6-Diamidino-2-phenylindole dihydrochloride (DAPI) to visualize nuclei. To detect γ-H2AX we used mouse monoclonal anti-phospho-histone H2AX antibody (Millipore; #05-636). Alexa Fluor 488 from molecular probes (Invitrogen; #A-11034) was used, and fluorescent images were automatically taken for each well of the 96-well plate using an Opera High-Content Screening System (Perkin Elmer). Pictures were taken under non-saturating conditions using a 40x magnification lens to calculate the γ-H2AX nuclear signal intensity.

Statistical analysis

Pearson's chi-squared test was used to calculate whether differences in the frequency of the SNP among the FBOC groups were significant, Supplementary Table S1.

Telomere length (Kb) was adjusted to the age, using the best fit line controls (y= -0.067* age (years) +12.785). The difference between the actual and the predicted value was calculated for each sample.

For the comparative analysis we have considered healthy or affected (patients with cancer antecedents) *BRCA1* and *BRCA2* mutation carriers in a single group BRCA1/2. We performed an independent linear regression analysis, using cancer status as a binary variable to test whether it could affect significantly *OGG1* mRNA expression, TL or percentage of short telomeres (Supplementary Table S3).

Kolmogorov-Smirnov test was used to evaluate if the data sets were normally distributed. For the comparative analysis (*OGG1* mRNA expression, Telomere studies and γH2AX nuclear intensity signal), statistically significant differences were assessed by Mann-Whitney U test for not normal distributions (Figures: 1a, 1b, 2a, 2b, 3a, 3b, 4b) and complementary, using lineal regression analysis whenever necessary:

· Regarding the expression studies, lineal regression model including as explanatory variable *OGG1* SNP, was run to test whether this variable could affect *OGG1* mRNA levels in each FBOC group (BRCA1/2 carriers, BRCAX cases and non-carriers controls).

· In relation with the TL studies, a linear regression model was created including as explanatory variables age and the SNP among the different genotypes. Then, if significant differences were found, a separate model was created for each of the genotypes: i) Controls (all) ii) BRCA1/2 carriers harboring the variant iii) BRCA1/2 carriers without the variant. Significant differences among the models were tested with F-test (Figure 2c).

For all the analysis, bilateral p values less than $p<0.05$ where considered significant.

Statistical calculations were done by SPSS version 18 (SPSSI« Inc, Chicago, Illinois), the R project for statistical computing, GraphPad Prim 5.03 (San Diego, California), and graphics were performed by GraphPad Prim 5.03 (San Diego, California)

ACKNOWLEDGMENTS

We thank Alicia Barroso for her technical assistance, Diego Megias for his counseling on γH2AX results interpretation.

The Genotype-Tissue Expression (GTEx) Project was supported by the Common Fund of the Office of the Director of the National Institutes of Health. Additional funds were provided by the NCI, NHGRI, NHLBI, NIDA, NIMH, and NINDS. Donors were enrolled at Biospecimen Source Sites funded by NCI\SAIC-Frederick, Inc. (SAIC-F) subcontracts to the National Disease Research Interchange (10XS170), Roswell Park Cancer Institute (10XS171), and Science Care, Inc. (X10S172). The Laboratory, Data Analysis, and Coordinating Center (LDACC) was funded through a contract (HHSN268201000029C) to The Broad Institute, Inc. Biorepository operations were funded through an SAIC-F subcontract to Van Andel Institute (10ST1035). Additional data repository and project management were provided by SAIC-F (HHSN261200800001E). The Brain Bank was supported by a supplements to University of Miami grants DA006227 & DA033684 and to contract N01MH000028. Statistical Methods development grants were made to the University of Geneva (MH090941 & MH101814), the University of Chicago (MH090951, MH090937, MH101820, MH101825), the University of North Carolina - Chapel Hill (MH090936 & MH101819), Harvard University (MH090948), Stanford University (MH101782), Washington University St Louis (MH101810), and the University of Pennsylvania (MH101822). The data used for the analyses described in this manuscript were obtained from: [insert, where appropriate] the GTEx Portal on 01/12/2015 and/or dbGaP accession number phs000424.vN.pN on 01/12/2015.

FUNDING

J.B.'s laboratory is partially funded by the Spanish Ministry of Health PI12/00070 supported by FEDER funds, and the Spanish Research Network on Rare diseases (CIBERER). C.B-B is granted by the PI12/00070. M.A.B.'s laboratory is funded with the Spanish Ministry of Science and Innovation, projects SAF2008-05384 and 2007-A-200950 (TELOMARKER), European Research Council Advanced grant GA#232854, the Körber Foundation, Fundación Botín and Fundación Lilly. MU is supported by the Spanish Ministry of Health PI14/00459 with FEDER funds.

CONFLICTS OF INTEREST

The authors declare no conflicts of interest.

REFERENCES

1. Milne RL, Osorio A, Cajal TR, Vega A, Llort G, de la Hoya M, Diez O, Alonso MC, Lazaro C, Blanco I, Sanchez-de-Abajo A, Caldes T, Blanco A, Grana B, Duran M, Velasco E, et al. The average cumulative risks of breast and ovarian cancer for carriers of mutations in BRCA1 and BRCA2 attending genetic counseling units in Spain. Clin Cancer Res. 2008; 14:2861-2869.
2. Antoniou A, Pharoah PD, Narod S, Risch HA, Eyfjord JE, Hopper JL, Loman N, Olsson H, Johannsson O, Borg A, Pasini B, Radice P, Manoukian S, Eccles DM, Tang N, Olah E, et al. Average risks of breast and ovarian cancer associated with BRCA1 or BRCA2 mutations detected in case Series unselected for family history: a combined analysis of 22 studies. Am J Hum Genet. 2003; 72:1117-1130.
3. Antoniou AC, Sinilnikova OM, Simard J, Leone M, Dumont M, Neuhausen SL, Struewing JP, Stoppa-Lyonnet D, Barjhoux L, Hughes DJ, Coupier I, Belotti M, Lasset C,

Bonadona V, Bignon YJ, Rebbeck TR, et al. RAD51 135G->C modifies breast cancer risk among BRCA2 mutation carriers: results from a combined analysis of 19 studies. Am J Hum Genet. 2007; 81:1186-1200.

4. Osorio A, Milne RL, Alonso R, Pita G, Peterlongo P, Teule A, Nathanson KL, Domchek SM, Rebbeck T, Lasa A, Konstantopoulou I, Hogervorst FB, Verhoef S, van Dooren MF, Jager A, Ausems MG, et al. Evaluation of the XRCC1 gene as a phenotypic modifier in BRCA1/2 mutation carriers. Results from the consortium of investigators of modifiers of BRCA1/BRCA2. Br J Cancer. 2011; 104:1356-1361.
5. Osorio A, Milne RL, Kuchenbaecker K, Vaclova T, Pita G, Alonso R, Peterlongo P, Blanco I, de la Hoya M, Duran M, Diez O, Ramon YCT, Konstantopoulou I, Martinez-Bouzas C, Andres Conejero R, Soucy P, et al. DNA glycosylases involved in base excision repair may be associated with cancer risk in BRCA1 and BRCA2 mutation carriers. PLoS Genet. 2014; 10:e1004256.
6. Krupa R, Sobczuk A, Poplawski T, Wozniak K and Blasiak J. DNA damage and repair in endometrial cancer in correlation with the hOGG1 and RAD51 genes polymorphism. Mol Biol Rep. 2011 ; 38:1163-1170.
7. Farmer H, McCabe N, Lord CJ, Tutt AN, Johnson DA, Richardson TB, Santarosa M, Dillon KJ, Hickson I, Knights C, Martin NM, Jackson SP, Smith GC and Ashworth A. Targeting the DNA repair defect in BRCA mutant cells as a therapeutic strategy. Nature. 2005; 434:917-921.
8. Friedberg EC. DNA damage and repair. Nature. 2003; 421:436-440.
9. Caldecott KW. Single-strand break repair and genetic disease. Nat Rev Genet. 2008; 9:619-631.
10. Khanna KK and Jackson SP. DNA double-strand breaks: signaling, repair and the cancer connection. Nat Genet. 2001; 27:247-254.
11. Wang Z, Rhee DB, Lu J, Bohr CT, Zhou F, Vallabhaneni H, de Souza-Pinto NC and Liu Y. Characterization of oxidative guanine damage and repair in mammalian telomeres. PLoS Genet. 2010; 6:e1000951.
12. Zhou J, Fleming AM, Averill AM, Burrows CJ and Wallace SS. The NEIL glycosylases remove oxidized guanine lesions from telomeric and promoter quadruplex DNA structures. Nucleic Acids Res. 2015; 43:4039-4054.
13. Brenerman BM, Illuzzi JL and Wilson DM, 3rd. Base excision repair capacity in informing healthspan. Carcinogenesis. 2014; 35:2643-2652.
14. Bliksoen M, Baysa A, Eide L, Bjoras M, Suganthan R, Vaage J, Stenslokken KO and Valen G. Mitochondrial DNA damage and repair during ischemia-reperfusion injury of the heart. J Mol Cell Cardiol. 2015; 78:9-22.
15. Hegde ML, Hazra TK and Mitra S. Early steps in the DNA base excision/single-strand interruption repair pathway in mammalian cells. Cell Res. 2008; 18:27-47.
16. Pooley KA, Bojesen SE, Weischer M, Nielsen SF, Thompson D, Amin Al Olama A, Michailidou K, Tyrer JP, Benlloch S, Brown J, Audley T, Luben R, Khaw KT, Neal DE, Hamdy FC, Donovan JL, et al. A genome-wide association scan (GWAS) for mean telomere length within the COGS project: identified loci show little association with hormone-related cancer risk. Hum Mol Genet. 2013; 22:5056-5064.
17. Benitez-Buelga C, Sanchez-Barroso L, Gallardo M, Apellaniz-Ruiz M, Inglada-Perez L, Yanowski K, Carrillo J, Garcia-Estevez L, Calvo I, Perona R, Urioste M, Osorio A, Blasco MA, Rodriguez-Antona C and Benitez J. Impact of chemotherapy on telomere length in sporadic and familial breast cancer patients. Breast Cancer Res Treat. 2015; 149:385-394.
18. Clop A, Marcq F, Takeda H, Pirottin D, Tordoir X, Bibe B, Bouix J, Caiment F, Elsen JM, Eychenne F, Larzul C, Laville E, Meish F, Milenkovic D, Tobin J, Charlier C, et al. A mutation creating a potential illegitimate microRNA target site in the myostatin gene affects muscularity in sheep. Nat Genet. 2006; 38:813-818.
19. Brewster BL, Rossiello F, French JD, Edwards SL, Wong M, Wronski A, Whiley P, Waddell N, Chen X, Bove B, Hopper JL, John EM, Andrulis I, Daly M, Volorio S, Bernard L, et al. Identification of fifteen novel germline variants in the BRCA1 3'UTR reveals a variant in a breast cancer case that introduces a functional miR-103 target site. Hum Mutat. 2012; 33:1665-1675.
20. Sakumi K, Tominaga Y, Furuichi M, Xu P, Tsuzuki T, Sekiguchi M and Nakabeppu Y. Ogg1 knockout-associated lung tumorigenesis and its suppression by Mth1 gene disruption. Cancer Res. 2003; 63:902-905.
21. Yuzefovych LV, Kahn AG, Schuler MA, Eide L, Arora R, Wilson GL, Tan M and Rachek LI. Mitochondrial DNA repair through OGG1 activity attenuates breast cancer progression and metastasis. Cancer Res. 2016 ;76:30-4.
22. Lu J and Liu Y. Deletion of Ogg1 DNA glycosylase results in telomere base damage and length alteration in yeast. EMBO J. 2010; 29:398-409.
23. von Zglinicki T, Pilger R and Sitte N. Accumulation of single-strand breaks is the major cause of telomere shortening in human fibroblasts. Free Radic Biol Med. 2000; 28:64-74.
24. Coluzzi E, Colamartino M, Cozzi R, Leone S, Meneghini C, O'Callaghan N and Sgura A. Oxidative stress induces persistent telomeric DNA damage responsible for nuclear morphology change in mammalian cells. PLoS One. 2014; 9:e110963.
25. Berger F, Vaslin L, Belin L, Asselain B, Forlani S, Humbert S, Durr A and Hall J. The impact of single-nucleotide polymorphisms (SNPs) in OGG1 and XPC on the age at onset of Huntington disease. Mutat Res. 2013; 755:115-119.

26. Cardin R, Piciocchi M, Sinigaglia A, Lavezzo E, Bortolami M, Kotsafti A, Cillo U, Zanus G, Mescoli C, Rugge M and Farinati F. Oxidative DNA damage correlates with cell immortalization and mir-92 expression in hepatocellular carcinoma. BMC Cancer. 2012; 12:177.

27. Yuan T, Wei J, Luo J, Liu M, Deng S and Chen P. Polymorphisms of base-excision repair genes hOGG1 326cys and XRCC1 280His increase hepatocellular carcinoma risk. Dig Dis Sci. 2012; 57:2451-2457.

28. Yuan W, Xu L, Feng Y, Yang Y, Chen W, Wang J, Pang D and Li D. The hOGG1 Ser326Cys polymorphism and breast cancer risk: a meta-analysis. Breast Cancer Res Treat. 2010; 122:835-842.

29. Wei B, Zhou Y, Xu Z, Xi B, Cheng H, Ruan J, Zhu M, Hu Q, Wang Q, Wang Z, Yan Z, Jin K, Zhou D, Xuan F, Huang X, Shao J, et al. The effect of hOGG1 Ser326Cys polymorphism on cancer risk: evidence from a meta-analysis. PLoS One. 2011; 6:e27545.

30. Valdiglesias V, Giunta S, Fenech M, Neri M and Bonassi S. gammaH2AX as a marker of DNA double strand breaks and genomic instability in human population studies. Mutat Res. 2013; 753:24-40.

31. Erculj N, Zadel M and Dolzan V. Genetic polymorphisms in base excision repair in healthy slovenian population and their influence on DNA damage. Acta Chim Slov. 2010; 57:182-188.

32. Moritz E, Pauly K, Bravard A, Hall J, Radicella JP and Epe B. hOGG1-Cys326 variant cells are hypersensitive to DNA repair inhibition by nitric oxide. Carcinogenesis. 2014; 35:1426-1433.

33. Vaclova T, Gomez-Lopez G, Setien F, Bueno JM, Macias JA, Barroso A, Urioste M, Esteller M, Benitez J and Osorio A. DNA repair capacity is impaired in healthy BRCA1 heterozygous mutation carriers. Breast Cancer Res Treat. 2015; 152:271-282.

34. Canela A, Vera E, Klatt P and Blasco MA. High-throughput telomere length quantification by FISH and its application to human population studies. Proc Natl Acad Sci U S A. 2007; 104:5300-5305.

35. McIlrath J, Bouffler SD, Samper E, Cuthbert A, Wojcik A, Szumiel I, Bryant PE, Riches AC, Thompson A, Blasco MA, Newbold RF and Slijepcevic P. Telomere length abnormalities in mammalian radiosensitive cells. Cancer Res. 2001; 61:912-915.

SUPPLEMENTARY FIGURES AND TABLES

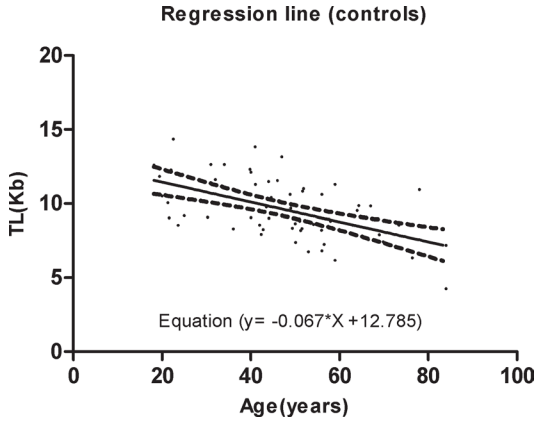

Supplementary Figure S1: TL distribution in peripheral blood leukocytes as a function of age for the control women population (n = 60), measured by HT QFISH. The regression line for control is drawn controls (y= -0.067* age + 12.785).

Supplementary Table S1: List of lymphoblastoid cell lines (LCL)

LCL [a]	BRCA1 mutation[b]	Mutation type[c]	Exon	[d]Age	[e]rs2304277	
06S179-L[1]	Wild type	-	-	31	Wt	
09S797-L[2]	Wild type	-	-	27	Wt	
10S889-L[3]	Wild type	-	-	20	Wt	
11S66-L[4]	Wild type	-	-	30	G>A	
11S534-L[5]	Wild type	-	-	50	G>A	
11S954-L	Wild type	-	-	35	Wt	
11S375-L	Wild type	-	-	23	Wt	
05S1303-L[1]	p.Ala1708Glu	Missense	18	59	Wt	*
06S1159-L	c.5123C > A; p.Ala1708Gluf	Missense	18	37	G>A	
10S1202-L	c.5123C > A; p.Ala1708Glu	Missense	18	53	Wt	
10S890-L[3]	c.5123C > A; p.Ala1708Glu	Missense	18	25	Wt	*
11S65-L[6]	c.5117G > A; p.Gly1706Glug	Missense	18	31	G>A	
11S67-L[6]	c.5117G > A; p.Gly1706Glu	Missense	18	34	Wt	
07S1291-L	c.3239T > A; p.Leu1080X	Nonsense/TRC	11	34	G>A	*
09S798-L[2]	c.2410C > T; p.Gln804X	Nonsense/TRC	11	24	Wt	
09S546-L	c.212 + 1G > A; p.?	Splice/TRC	5	42	G>A	*
11S376-L[7]	c.212 + 1G > A; p.?	Splice/TRC	5	39	Wt	*
11S384-L[7]	c.212 + 1G > A; p.?	Splice/TRC	5	75	Wt	*
06S1167-L	c.3331_3334delCAAG; p.Gln1111	Frameshift/TRC	11	33	Wt	
09S491-L	c.815_824dup10; p.Thr276	Frameshift/TRC	11	24	G>A	
10S1177-L[4]	c.68_69delAG; p.Glu23	Frameshift/TRC	2	27	G>A	*
10S44-L	c.4309delT; p.Ser1437	Frameshift/TRC	13	22	Wt	*
11S1004-L[5]	c.981_982delAT; p.Cys328X	Frameshift/TRC	11	25	G>A	

[a] 1–7 LCL from relatives of the same family (sisters or mother & daughter).
[b] Mutation nomenclature based on GenBank reference sequences NM_007294.3 with numbering starting at the A of the first ATG, following the journal guidelines (www.hgvs.org/mutnomen); p.?, unknown protein nomenclature (variant causing skipping of exon 5 of *BRCA1*).
[c] -: Refers to the non-carrier control; TRC: Stands for truncating mutation.
[d] Age of the woman at the time of extraction of the blood sample from which the LCL was established.
[e] G>A indicate the polymorphism (rs2304277).
* For those cells used in the experiment of telomere shortening along 55 passages.

Supplementary Table S2: Table with information regarding the SNPs within the block of Linkage disequilibrium (LD) >0.8 with the SNP rs2304277

SNP in LD>0.8 with rs2304277			
SNPs	**Gene**	**Location***	**r^2(LD)**
rs3219008	*OGG1*	intronic	0.86
rs2075747	*OGG1*	intronic	0.93
rs2072668	*OGG1*	intronic	0.85
rs1052133	*OGG1*	Missense/ 3-UTR	0.83
rs4021704	*OGG1/ CAMK1*	intronic	0.98
rs2304277	*OGG1/ CAMK1*	Downstream 3-UTR(*OGG1*)	*1.00*
rs7609858	*OGG1/ CAMK1*	intronic	0.99
rs6763347	*OGG1/ CAMK1*	intronic	1.00
rs73021455	*OGG1/ CAMK1*	intronic	0.90
rs66482970	-	-	0.89
rs57081507	-	-	0.89
rs67055061	-	-	0.90
rs14204	TADA3	3'-UTR	0.83
rs6809452	*TADA3*	intronic	0.88
rs7610826	*TADA3*	intronic	0.87
rs7618535	*TADA3*	intronic	0.87
rs7618636	*TADA3*	intronic	0.88
rs7621556	*TADA3*	intronic	0.88

*In some cases the SNP can cover more than 1 location depending on the gene isoform. (due to limited space only one gene location is available at the table).

Supplementary Table S3: Samples distribution and heterozygous frequency of the *OGG1* variant rs2304277

FBOC	Sample size	Heterozygotes frequency (%)
FBOC*	220	
FBOC rs2304277	81	36
Controls	60	
Controls rs2304277	26	43
BRCA1	38	
BRCA1 rs2304277	13	36
BRCA2	48	
BRCA2 rs2304277	16	34
BRCAX	74	
BRCAX rs2304277	26	35

No significant differences were found among the groups. * We have excluded individuals harboring mutations in both *BRCA1* and *BRCA2* genes simultaneously (n=3), none of them harbor the SNP. Hence, the total sample size is 223.

Supplementary Table S4: Lineal regression analysis in BRCA1/2 mutation carriers

Dependent variables	Independent variables	β coeff	p-values	95% C.I ((Lower)-(Upper limit))
OGG1 mRNA	SNP	-0.591	0.027	((-1.113)-(-0.070))
	Cancer	0.148	0.549	((-0.342)-(0.639))
TL(Kb)	SNP	-1.438	0.013	((-2.554)-(-0.323))
	Cancer	-0.115	0.832	((-1.199)-(0.969))
Short telomeres (%)	SNP	-0.030	0.990	((-4.886)-(4.825))
	Cancer	-0.908	0.700	((-5.625-(3.810))

We included as dependent variables *OGG1* mRNA, TL (Kb) and percentage of short telomeres (%), and as independent variables, the SNP and the cancer status. β coefficients quantify how much the 2 independent variables (*OGG1* SNP and cancer status) modify *OGG1* mRNA levels, TL (Kb) and the percentage of short telomeres and also the modification direction. C.I stands for confidence interval.

Supplementary Table S5: Gtex information summary, regarding *OGG1* transcriptional down regulation when rs2304277 is present (5 different tissues)

Gene Symbol	SNP	[a]p-value	Tissue
OGG1	rs2304277	0.57	Cells - EBV-transformed lymphocytes
OGG1	rs2304277	0.22	Uterus
OGG1	rs2304277	0.16	Vagina
OGG1	rs2304277	0.45	Whole Blood
OGG1	rs2304277	0.023	Ovary

[a]Nominal eQTL p-values were generated for each SNP-gene pair using a two-tailed t test, testing the alternative hypothesis that the beta (slope of the linear regression model) deviates from the null hypothesis of β=0.

ARTICLE 3

Variation in the NEIL2 DNA glycosylase gene is associated oxidative with DNA damage in BRCA2 mutation carriers.

Authors: Carlos Benitez-Buelga, Juan Miguel Baquero, Jose Luis Garcia Gimenez, Lucia Inglada-Perez, Nora Soberón, Miguel Urioste, Federico Pallardo, Maria A. Blasco, Ana Osorio, Javier Benítez.

Journal: Submitted to International Journal of Cancer
Publication Date: -
Ref: -
Personal contribution: Collection, control and preparation of the samples, SNP genotyping, *NEIL2* mRNA expression studies, telomere oxidation studies, statistical analysis, preparation of the manuscript.

We have recently shown how common genetic variations in some genes of the Base Excision Repair (BER) pathway can modify breast and ovarian cancer susceptibility risk for *BRCA1* and *BRCA2* mutation carriers. Previously, we studied one of these cancer variants in the DNA glycosylase *OGG1* gene, and we found that cancer susceptibility risk might be explained by a transcriptional down-regulation associated with the Single Nucleotide Polymorphism (SNP) and its contribution to a higher telomere and genome instability. In this report, we studied a second variant (rs804271) localized in the promoter region of the DNA glycosylase gene *NEIL2* that also acts as a cancer risk modifier We studied the role of this polymorphism on transcriptional regulation and enzyme activity to establish possible associations with oxidative DNA damage, telomere dysfunction and oxidative stress.

To that end, we used a series of 88 *BRCA1* and *BRCA2* mutation carriers, 87 BRCAX cases and 86 non-carrier controls. We found that SNP rs804271 is associated with significant *NEIL2* transcriptional upregulation independently of the BRCA mutational status and telomere instability in carriers of *BRCA1* mutation. In addition, we found that this SNP is associated, for *BRCA2* mutation carriers, with a significant accumulation of oxidative lesions at the telomere which suggest that for this specific group the SNP could have an impact on the performance of the NEIL2 enzyme, which may help to explain the cancer risk association.

Our results suggest that cancer risk association of this SNP among BRCA2 mutation carriers, could be driven by a deficient NEIL2 enzyme performance, and its contribution on oxidative DNA damage.

Genetic variation in the *NEIL2* DNA glycosylase gene is associated with oxidative DNA damage in *BRCA2* mutation carriers.

Carlos Benitez-Buelga[1], Juan Miguel Baquero[1], José Luis García-Giménez[2, 3], Lucia Inglada-Perez[4], Nora Soberón[5], Miguel Urioste[3, 6], Federico V. Pallardó[2, 3], María A. Blasco[5], Ana Osorio[1, 3], Javier Benítez[1, 3]

[1] Human Genetics Group, Spanish National Cancer Research Center (CNIO), Madrid 28029, Spain

[2] Department of Physiology, Faculty of Medicine and Dentistry, FIHCUV-Incliva, Universitat de Valencia, Mixt Unit CIPF-INCLIVA. E46010 Valencia, Spain

[3]Spanish Network on Rare Diseases (CIBERER), Spain

[4] Endocrine Cancer Group, Spanish National Cancer Research Center (CNIO), Madrid 28029, Spain

[5] Telomere and Telomerase Group, Spanish National Cancer Research Center (CNIO), Madrid 28029, Spain

[6] Familial Cancer Clinical Unit, Spanish National Cancer Research Center (CNIO), Madrid 28029, Spain

Correspondence to: *Javier Benitez,* ***e-mail:*** *jbenitez@cnio.es*

Keywords: *BRCA1 and BRCA2, telomere shortening, NEIL2 polymorphism cancer risk modifier, oxidative DNA damage*

We have recently shown how common genetic variations in some genes of the Base Excision Repair (BER) pathway can modify breast and ovarian cancer susceptibility for *BRCA1* and *BRCA2* mutation carriers.

In this report, we studied a second variant (rs804271) localized at the promoter region of the DNA glycosylase gene NEIL2 that also acts as a "cancer risk modifier" for *BRCA2* mutation carriers. To understand the molecular basis of this association, we studied the role of this polymorphism on transcriptional regulation and enzyme activity to establish possible associations with oxidative DNA damage, telomere dysfunction and oxidative stress.

To that end, we used a series of 88 *BRCA1* and *BRCA2* mutation carriers, 87 BRCAX cases and 86 non-carrier controls. We found that SNP rs804271 is associated with significant *NEIL2* transcriptional up-regulation independently of the BRCA mutational status and with telomere instability for *BRCA1* mutation carriers. In addition, we found that for *BRCA2* mutation carriers, this SNP is associated with a significant accumulation of oxidative lesions at the telomere, suggesting that for this specific group the SNP could have a negative impact on the performance of the NEIL2 enzyme. Such changes may help to explain this SNP in relation with its cancer risk modifier effect for *BRCA2* mutation carriers.

INTRODUCTION

The tumor suppressor genes *BRCA1* and *BRCA2* maintain genomic stability through their involvement in homologous recombination double-stranded break DNA repair [1].

Carrying a mutation in the *BRCA1* or *BRCA2* genes increases a woman's lifetime risk of developing breast and ovarian cancer, although there are considerable differences in disease manifestation. At the age of 70, cumulative cancer risk for *BRCA1* and *BRCA2* mutation carriers ranges from 43% to 88% for breast cancer development, and from 11% to 59% for ovarian cancer [2,3]. This high variability is the consequence of other genetic modifiers and/or environmental factors.

Given the relation of synthetic lethality that exists between one of the components of the Base Excision Repair (BER) pathway, *PARP1* (poly[ADP-ribose] polymerase 1), and both *BRCA1* and *BRCA2* [4] genes, it is likely that other members of the BER pathway exhibit a similar behavior. Following this hypothesis, we recently described that common genetic variants in genes involved in BER might increase a woman's lifetime risk of developing breast and ovarian cancers if she is a *BRCA1* or *BRCA2* mutation carrier [5]. In particular, two Single Nucleotide Polymorphisms (SNPs) located in the *OGG1* and *NEIL2* genes were identified as cancer risk modifiers in *BRCA1* and *BRCA2* mutation carriers, respectively [5]. Although the molecular mechanism underlying the cancer risk association is not clear yet, both SNPs were in transcriptional regulatory regions of genes encoding DNA glycosylase enzymes, which play an important role in the first steps of the BER pathway.

The BER pathway is responsible for correcting oxidative and alkylation lesions in DNA bases, and these lesions represent the majority of endogenous DNA damage due to chemical reactions during cellular metabolism [6]. If they are not repaired, these lesions can evolve into DNA single-strand breaks (SSBs) or DNA double-strand breaks (DSBs), which are the principal source of genomic instability [7,8]. In addition, due to the strong tropism for guanine (G) oxidation at the telomere sequence (TTAGGG) the BER pathway is essential for maintaining telomere integrity in mammals [9,10]. In humans, there are several DNA glycosylases with different DNA-structure/substrate affinities. The OGG1enzyme, is active only on duplex DNAs [11]. In contrast, NEIL2 shows preferential activity on bubble DNA or single-stranded DNA regions[12].

Since genetic and telomere instability are associated with cancer risk [13,14,15], it is likely that if cancer risk modifiers SNPs in DNA glycosylase genes could alter normal transcriptional levels or function, they could affect negatively to the general performance of the BER pathway. This would contribute to increased levels of genome/telomere instability and hence to a higher cancer risk, especially in individuals harboring mutations in the *BRCA1* or *BRCA2* gene.

As an example, we previously observed that the variant rs2304277, located in the 3'-untranslated region (UTR) of *OGG1*, was associated with a constitutive transcriptional down-regulation of the gene. Moreover, in individuals harboring the *OGG1* polymorphism together with a mutation in either *BRCA1* or *BRCA2*, the transcriptional down-regulation resulted in both, genome and telomere instability [16], which could explain the increased cancer risk associated with the presence of this SNP among *BRCA1* mutation carriers.

Similarly, the breast cancer variant rs804271 is localized within the *NEIL2* promoter region (5'- UTR), and forms part of several transcription-factor binding motifs that are responsive to oxidative stress [17]. It has previously been reported that common genetic variation within this region is associated with transcriptional downregulation of *NEIL2* mRNA levels or with higher levels of mutagen-induced genetic damage and repression of the transcriptional response to oxidative stress [18].

Hence, we have explored in a set of familial breast and ovarian cancer (FBOC) patients with a heterogeneous BRCA status, the role of this cancer polymorphism in relation to *NEIL2* transcriptional dysregulation, telomere oxidative DNA damage, oxidative stress susceptibility and telomere shortening to explain its cancer risk modifier effect.

MATERIAL AND METHODS

Familial breast and ovarian cancer (FBOC) group

We studied a group composed of 261 individuals belonging to 144 families meeting high-risk criteria, and screened for deleterious mutations in the *BRCA1* and *BRCA2* genes, as reported previously [3]. Of these families, 25 carried a deleterious mutation in the *BRCA1* gene, 25 in *BRCA2*, 1 family harbored both *BRCA1* and *BRCA2* mutations, and 94 did not carry any mutation in neither of these two genes (BRCAX).

Eighty-six individuals were used as non-carrier controls: they were relatives of *BRCA1/2* mutation carriers who did not have personal cancer antecedents and did not harbor the corresponding familial mutation in the *BRCA1* or *BRCA2* genes.

All cases and controls signed an appropriate informed consent form and the ethics committee of the hospital involved (Fuenlabrada University Hospital) approved the proposal.

We used this set of samples to calculate the SNP frequency, to quantify *NEIL2* mRNA levels in peripheral blood, to perform telomere studies using fresh blood cells, to measure the accumulation of oxidative DNA damage at telomeres (blood DNA), and to evaluate susceptibility to oxidative stress in plasma samples (Table 1).

SNP genotyping

Single Nucleotide Polymorphism rs1466785, located in the *NEIL2* gene is a cancer risk modifier for *BRCA2* mutation carriers [5]. Imputation using *1000 Genomes* data showed that there were several SNPs in strong linkage disequilibrium (LD) with rs1466785, the original SNP reported in Osorio et al[5]. Of these, we considered rs804271 to be the best candidate, given that it showed the most significant associations and that there existed epidemiological and functional data supporting its putative role in cancer [5].

The SNP rs804271 is located at the promoter region of the *NEIL2* gene, within a previously described transcriptional regulatory region[17]. Indeed, 18 proteins are predicted to interact with that region and 3 motifs, all of which are binding regions for transcription factors (E2F, Sin3Ak-20 and YY1), are predicted to be altered in the presence of this polymorphism (http://archive.broadinstitute.org/mammals/haploreg/haploreg.php).

DNA was extracted from peripheral blood of FBOC patients using MagNAPure LC 2.0 (Roche Diagnostics, Indianapolis, Indiana) following the manufacturer's instructions. DNA quantification and quality was assessed by NanoDrop® (ND-1000 V3.7.1). A specific Taqman probe for rs804271 was used to genotype the presence/absence of the polymorphism among the sample collection. Allelic discrimination assays were conducted using the 7900HT Fast Real-Time PCR System (Applied Biosystems).

RNA expression analysis

RNA was extracted from peripheral blood cells using TRIzol Reagent (Ambion®, Life Techonogies) according to the manufacturer's instructions.

NanoDrop® (ND-1000 V3.7.1) was used to assess both RNA quantity and quality. Two microliters of cDNA at a final concentration of 10-20 ng/µl were mixed in triplicate with GoTaq® qPCR MasterMix 1x (Promega), NEIL2 cDNA primers (F/R) and

GAPDH cDNA primers (F/R) at final concentrations of 500nM. Primers used were: *NEIL2* (F: GTCACACCCACCTGTGACAT; R: GCACTCAGGACTGAACCGAG) and *GAPDH* (F: CCTGCACCACCAACTGCTTA; R: CCATCACGCCACAGTTTCC).

All reagents were used following the manufacturer's instructions. qPCR was done using the QuantStudio S6 system (Applied Biosystems).

Oxidative stress studies

Oxidative DNA damage within telomeres

We used a qPCR-based method to evaluate the oxidative DNA damage within telomeric DNA [19], based on differences in PCR kinetics between DNA template digested by formamidopyrimidine-DNA glycosylase (FPG) and undigested DNA. Quantitative real-time amplification of genomic DNA was performed as described by O'Callaghan et al[20].

Immunodetection of oxidized proteins

Oxidized proteins in plasma samples were detected as previously described [21] by measuring the levels of carbonylated proteins. Carbonyl groups on the side chains of proteins in plasma samples were derivatized to 2,4-dinitrophenylhydrazone (DNP-hydrazone) by reaction with 2,4-dinitrophenylhidrazine (DNPH), according to the procedure of Shacter *et al*[22]. Briefly, 5 µg of proteins were denatured with 5 µl of 12% SDS. Next, 10 µl of 10 mM DNPH in 10% (v/v) trifluoroacetic acid was added to the protein solution. The reaction mixture was neutralized and prepared for SDS–PAGE by adding 7.5 µl of 2 M Tris base containing 30% (v/v) glycerol. Derivatized samples were spotted onto a nitrocellulose membrane.

The membrane was blocked with 5% bovine serum albumin (BSA) prepared in phosphate-buffered saline (PBS)–0.1% Tween 20 for 1 h. Afterwards, the membrane was incubated with a rabbit anti-DNP antibody as described by the manufacturer of the OxyBlot kit (OxyBlot Protein Oxidation Detection kit; Millipore, Billerica, MA, USA). Images were captured using an ImageQuant LAS-4000 (GE Healthcare Life Sciences; Chicago IL, USA). Signal density of each sample was analyzed with ImageJ software (NIH Image, NIH, Bethesda, USA).

Analysis of lipid peroxidation by HPLC-UV detection

Lipid peroxidation was determined by measuring malondialdehyde (MDA) as described previously[23]. Plasma samples were mixed with 0.44 M phosphoric acid and 42 mM thiobarbituric acid (TBA) and incubated in a water bath at 95 ºC for 1 h to hydrolyze lipoperoxides and liberate malondialdehyde. Samples were cooled immediately and diluted 1:1 with alkaline methanol, allowing MDA-TBA_2 adduct formation. Afterwards, samples were centrifuged (13,000 g, 5 min at 4 ºC) and 200 µL of supernatant was mixed 1:1 with 50 mM KH_2PO_4 pH 3.5. The supernatant was separated by HPLC on RP C18 columns using an isocratic method (Phase A consisting of 50 mM KH_2PO_4, pH 6.8, and acetonitrile (ACN); KH_2PO_4:ACN 83:17; and Phase B consisting of an ACN:water 70:30 mixture). MDA-TBA_2 adduct was detected under UV-vis at 532 nm.

Telomere length measurement (TL)

High throughput quantitative fluorescence in situ hybridization (HT-QFISH) with automated fluorescence microscopy was performed as previously described[24].

Briefly, Peripheral Blood Mononuclear cells (PBMCs) were separated by Histopaque-1070 (Sigma-Aldrich) gradient centrifugation. Cells were counted and plated (80 000 – 100 000 cells/well in clear bottomed black-well 96-well plates pre-coated with 0.001% (poly) L-lysine solution (Sigma-Aldrich, St. Louis, MO) for 30 minutes at 37ºC. 4′,6-diamino-2-phenylindole (DAPI) was used for nucleus staining and a fluorescent peptide nucleic acid (PNA) Cy3 probe against telomeric repeats was used for telomere detection. TL values were analyzed using individual telomere spots in a per cell basis (Approximately 90000 telomere spots per sample, which represents around 3500 cells).

Fluorescence intensities were then converted into Kb using L5178-R, L5178-S and CCRF-CEM cells as calibration standards, which have stable TL of 79.7 Kb, 10.3Kb and 7.5 kb, respectively. Samples were analyzed in duplicate, or triplicate in the case of calibration standards. A TL <3Kb was defined as short telomere. The load of short telomeres was estimated as the percentage of short telomeres (number of short telomeres divided by total number of measured telomeres) in each participant.

Statistical analysis

Pearson's chi-squared test was used to calculate whether differences in the frequency of the SNP among the FBOC groups were significant.

We performed linear regression analysis to test whether cancer antecedents in *BRCA1* and *BRCA2* mutation carriers were associated with any of the variables we evaluated in this report, but we did not find significant differences (Significant p-values <0.05) between healthy *BRCA1* and *BRCA2* carriers or cancer cases. Hence, we did not stratify for cancer status in these groups (Supplementary Table S1).

We considered heterozygotes and homozygotes (GT/TT) as a single group, to evaluate the effect of the SNP for each of the studied variables, as the cancer modifier effect of rs804271 is dominant for *BRCA2* mutation carriers[5].

In the supplementary tables, from 4 to 7, linear regression analysis was used to test whether the SNP (model 1), the BRCA status (model 2) or the combination of both events (model 3) significantly modified each of the studied variables among FBOC individuals. In addition, the SNP effect within BRCA groups or controls was tested in model 4. Two-sided p-values less than $p<0.05$ where considered significant.

The Kolmogorov-Smirnov test was used to evaluate if the data sets were normally distributed. For comparative analysis (Figure 1a), significance was assessed by the Mann-Whitney U test for non-normal distributions. Two-sided p-values less than $p<0.05$ where considered significant.

Statistical calculations were done using SPSS version 18 (SPSS Inc., Chicago, Illinois) and GraphPad Prism 5.03 (San Diego, California); graphs were made using GraphPad Prism 5.03.

RESULTS

SNP frequency in FBOC

We genotyped rs804271 among FBOC individuals and we found a SNP frequency of 0.40 as reported in ensemble for European population (http://www.ensembl.org). This frequency, was similar among the different case/control groups (Supplementary Table S2).

Expression of *NEIL2* in FBOC and GTEx

The GTEx eQTL web server (http://www.gtexportal.org) was used to evaluate whether rs804271 was associated with changes on *NEIL2* mRNA levels for different tissues. We found significant increased *NEIL2* mRNA levels for several tissues, including breast ($p<0.0001$), ovary ($p<0.0001$), and blood ($p<0.0001$) (Supplementary Table S3).

Next, we evaluated BRCA and/or SNP status over *NEIL2* mRNA transcriptional levels in our FBOC series. To that end, we performed linear regression analysis to confirm that the rs804271 was also associated with significant higher *NEIL2* mRNA levels ($\beta=0.023$; $p= 0.003$). The SNP effect (upregulation) on *NEIL2* mRNA levels was similar for each BRCA mutational group, and is detailed on (Supplementary Table S4).

These results suggest that rs804271, in the *NEIL2* promoter region, activates *NEIL2* transcription, and that potential inter-individual variability could be partially explained by the presence or absence of common genetic variants in the *NEIL2* gene promoter.

DNA glycosylase activity at the telomere

Because the NEIL family is involved in the recognition and excision of oxidized bases at the telomeres [10,25] and this region is especially susceptible to DNA oxidation[26], we evaluated the SNP effect on DNA glycosylase activity by measuring the accumulation of oxidative DNA damage at the telomere in our FBOC sample set (Figure 1a).

Linear regression analysis revealed that the genotype combining the *BRCA2* mutation together with rs804271 was significantly associated with oxidative DNA damage accumulation at the telomeres, as compared to any other group ($\beta=0.51$; $p= 6.9*10^{-6}$).

These results suggest that among *BRCA2* mutation carriers the presence of the variant reduces *NEIL2* enzyme activity, leading to an accumulation of oxidative DNA damage that can be detected at the telomere region (Figure 1b).

A detailed table with the complete lineal regression analysis can be found at Supplementary Table S5 with all genotype combinations.

Oxidative stress studies

Since oxidative stress induces oxidative DNA damage [27], we evaluated whether higher levels of oxidative DNA damage could be explained by chronic oxidative stress susceptibility for *BRCA2* mutations carriers harboring the variant.

To that end, we used plasma from FBOC individuals to evaluate two oxidative stress biomarkers widely used [28,29] consisting on plasma oxidized proteins (protein carbonylation) and lipid hydroperoxide malondialdehyde (MDA).

We performed linear regression analysis to evaluate the effect of the SNP on these two biomarkers. The analysis was performed among the different FBOC genotypes, and results are detailed in Supplementary Table S6.

Among *BRCA2* mutations carriers, we found no significant association of the SNP with higher levels of oxidative stress susceptibility, suggesting that the accumulation of oxidative DNA damage at the telomere, observed for this specific group is not caused by basal oxidative stress susceptibility, but as consequence of a deficient activity of glycosylases, as described in the previous section.

Interestingly, we found higher MDA levels for *BRCA1* mutation carriers harboring the SNP in *NEIL2*. Supplementary Table S6.

Telomere length (TL) studies in FBOC

We decided to explore the possible involvement of the SNP in *NEIL2* (rs804271) on telomere instability by measuring TL, percentage of short telomeres and telomerase activity in blood cells of FBOC series.

Because mean TL is strongly heritable [30] and our series is mainly composed of families, we decided to use a single genotype for both the BRCA and SNP status for each family:

When a genotype was repeated in several members within the same family, only the index-case was considered; whenever the index-case was not available only the last family member registered to participate in the study, from a group of redundant genotypes, was included to perform statistical analyses.

We previously demonstrated that chemotherapy shortens TL [31], and we therefore corrected for chemotherapy status in this analysis. We excluded patients who were undergoing chemotherapy from the analysis, as well as those for whom less than 2 years had passed since their last cycle of chemotherapy. Chemotherapy effect on TL in FBOC cases, was also tested by linear regression analysis (β=-0.14; p=0.024).

Telomere length (Kb) was adjusted for age using a best-fit line (y= -0.0674∗age (years) +12.631; (Figure S1)). The difference between the actual and the predicted value was calculated for each sample.

In addition, since TL is significantly correlated with telomerase activity in our series (R=+0.29; p= 0.01), we evaluated the possible effect of the rs804271 on telomerase activity. Cancer cases treated with chemotherapy were excluded for this analysis.

After the correction of these variables, we performed lineal regression analysis to test the effect of the SNP on TL, among the different FBOC genotypes.

Overall, we found that the presence of the SNP was associated to a decreased TL (β=-0.26; p= 0.004), increased levels of short telomeres (β=+0.25; p= 0.005) and lower telomerase activity (β=-0.17; p= 0.16).

When rs804271 was tested for each BRCA mutational group, we only found a significant effect among *BRCA1* mutation carriers: Reduced TL (adjusted by age) among *BRCA1* (β=-0.54; p= 0.007), accumulation of short telomeres (β=0.45; p= 0.02) and telomerase activity (β=-0.57; p= 0.034).

A detailed table with the complete linear regression analysis can be found at (Supplementary Table 7), with all genotype combinations.

DISCUSSION

We have previously shown that the SNP (rs2304277) located in the 3'UTR of the *OGG1* gene, and encoding a DNA glycosylase from the BER pathway, can increase cancer risk in *BRCA1* mutation carriers [5], by reducing *OGG1* mRNA levels and increasing genome/telomere instability in a synergistic way with the *BRCA1* mutation [14].

In the present study, we have tried to gain molecular insights into the breast cancer modifier SNP (rs804271) in the gene *NEIL2*, in a set of 261 FBOC patients with a heterogeneous BRCA status (*BRCA1* and *BRCA2* mutation carriers, *BRCAX*, and non-carrier controls). This SNP, which is located in the promoter region of the gene, increases the risk of developing breast cancer among *BRCA2* mutation carriers [5], but the molecular

mechanism underlying this association is unknown. Previous characterization of the *NEIL2* promoter region showed that *NEIL2* transcription is influenced by certain SNPs located 5′ upstream of the start site [18]. The results presented in this report, support these findings and suggest that rs804271 is associated with constitutive transcriptional activation of *NEIL2*.

First, we checked the effect of rs804271 on *NEIL2* mRNA levels in different tissues using Gtex eQTL dB (http://www.gtexportal. org), and we found a significant upregulation associated with the presence of the SNP in several tissues including breast, ovary and blood ($p<0.0001$) (Supplementary Table S3).

Then, we validated these results in our FBOC series and we found significantly increased *NEIL2* mRNA levels in individuals harboring the SNP ($p=0.003$), suggesting that it is associated with transcriptional activation of the *NEIL2* gene (Supplementary Table S4).

Since NEIL2 is an important enzyme of the BER, and it has been recently reported to be the gene most frequently displaying copy number variation loss, and is significantly down-regulated in several tumors [32], it is unlikely that *NEIL2* transcriptional activation could be the causal explanation for the cancer modifier effect of this polymorphism among *BRCA2* mutation carriers.

As an alternative hypothesis, it could be possible that this SNP reduced the activity of NEIL2 leading to an accumulation of oxidative lesions at telomeres and a *NEIL2* transcriptional activation by a positive feedback mechanism.

Because NEIL2 is involved in oxidative DNA damage repair at the telomeres [10,25] and this region is very susceptible from being oxidized, we have evaluated the telomere oxidation levels to assess the constitutive oxidative DNA repair capacity

among the different FBOC genotypes. Strikingly, we have found that *BRCA2* mutation carriers presented significantly higher levels of oxidation at the telomeres (Supplementary Table S5 and/or Figure 1a), and those levels were mainly explained by the subgroup of patients harboring the *NEIL2* SNP (Figure 1a & Figure 1b), suggesting that oxidative DNA repair is compromised when the rs804271 is present together with a *BRCA2* mutation. Because oxidative stress induces oxidative DNA damage [27], we evaluated whether higher levels of oxidative DNA damage for *BRCA2* mutations carriers harboring the variant, could be explained by chronic oxidative stress susceptibility. We found no association with basal oxidative stress susceptibility for *BRCA2* mutation carriers, with or without the SNP (Supplementary Table S6). In support for a functional role of this polymorphism on the performance of the NEIL2 enzyme, it was previously reported in the literature that this polymorphism rs804271 (previously ss74800505) was associated with significantly increased mutagen-induced genetic damage [18].

Although, a functional effect on transcription was initially expected, since this SNP is in the promoter region of *NEIL2*, our result suggest that this polymorphism may be associated with a reduced enzymatic activity exclusively for *BRCA2* mutation carriers, which lead to an accumulation of oxidative DNA damage. This scenario, could be the molecular mechanism explaining the cancer modifier effect of this SNP for *BRCA2* mutation carriers.

In relation with the role of this SNP among *BRCA1* mutation carriers, we found to be significantly associated with higher MDA levels in plasma. This result, correlated with a higher telomere instability reflected on reduced TL (β=-0.34; p= 0.01), accumulation of short telomeres (β=0.45; p= 0.024) and lower telomerase activity levels (β=-0.57; p= 0.034), Supplementary Table S7. In relation with these results, previous

studies have demonstrated that *BRCA1* protein is also involved in the response to oxidative stress [32–34] through its interaction with NFR2, a key player that regulates antioxidant signaling response and cell proliferation[35]. Since oxidative stress correlates with telomere shortening[33], it was not surprising to find this telomere phenotype for *BRCA1* mutation carriers, although the SNP is not associated with cancer risk for this group.

Altogether, our results suggest that rs804271, located in the promoter region of the gene *NEIL2*, has a functional effect on *NEIL2* mRNA transcription and on telomere maintenance, although is unlikely to be related to the cancer risk modifier effect of the SNP for *BRCA2* mutation carriers. In contrast, we have found that the SNP contributes significantly to oxidative DNA damage at telomeres exclusively for *BRCA2* mutation carriers, suggesting that the effect of this SNP on cancer risk could be driven by its effect on the enzyme activity.

ACKNOWLEDGMENTS

We thank Alicia Barroso and Victoria Fernandez for their technical assistance. The Genotype-Tissue Expression (GTEx) Project was supported by the Common Fund of the Office of the Director of the National Institutes of Health. Additional funds were provided by the NCI, NHGRI, NHLBI, NIDA, NIMH, and NINDS. Donors were enrolled at Biospecimen Source Sites funded by NCI/SAIC-Frederick, Inc. (SAIC-F) subcontracts to the National Disease Research Interchange (10XS170), Roswell Park Cancer Institute (10XS171), and Science Care, Inc. (X10S172). The Laboratory, Data Analysis, and Coordinating Center (LDACC) were funded through a contract (HHSN268201000029C) to The Broad Institute, Inc. Biorepository operations were funded through an SAIC-F subcontract to the Van Andel Institute (10ST1035). Additional data repository and project management were provided by SAIC-F (HHSN261200800001E). The Brain Bank was

supported by supplements to University of Miami grants DA006227 & DA033684 and to contract N01MH000028. Statistical Methods development grants were made to the University of Geneva (MH090941 & MH101814), the University of Chicago (MH090951, MH090937, MH101820, MH101825), the University of North Carolina - Chapel Hill (MH090936 & MH101819), Harvard University (MH090948), Stanford University (MH101782), Washington University St Louis (MH101810), and the University of Pennsylvania (MH101822). The data used for the analyses described in this manuscript were obtained from: [insert, where appropriate] the GTEx Portal on 01/12/2015 and/or dbGaP accession number phs000424.vN. pN on 01/12/2015.

FUNDING

J.B.'s laboratory is partially funded by the Spanish Ministry of Health PI12/00070, supported by FEDER funds, and the Spanish Research Network on Rare diseases (CIBERER). C.B-B is supported by FIS PI12/00070. J.M.B is supported by grant FPU15/01978 from the Spanish Ministry of Education, Culture and Sport. M.A.B.'s laboratory is funded by the Spanish Ministry of Science and Innovation, projects SAF2008-05384 and 2007-A-200950 (TELOMARKER), European Research Council Advanced Grant GA#232854, the Körber Foundation, Fundación Botín and Fundación Lilly. MU is supported by the Spanish Ministry of Health PI14/00459 with FEDER funds. FVP's laboratory is partially funded by the Spanish Research Network on rare diseases (CIBERER) and Fundación INCLIVA and the Generalitat Valenciana. The study was partially supported by the Spanish Ministry of Economy and Competitiveness (MINECO) SAF2014-57680-R.

BIBLIOGRAPHY

1. Roy R, Chun J, Powell SN. BRCA1 and BRCA2: different roles in a common

pathway of genome protection. *Nat Rev Cancer [Internet]* 2012;12:68–78. Available from: http://www.nature.com.ezp-prod1.hul.harvard.edu/nrc/journal/v12/n1/full/nrc3181.html

2. Antoniou A, Pharoah PDP, Narod S, Risch HA, Eyfjord JE, Hopper JL, Loman N, Olsson H, Johannsson O, Borg Å, Pasini B, Radice P, et al. Average Risks of Breast and Ovarian Cancer Associated with BRCA1 or BRCA2 Mutations Detected in Case Series Unselected for Family History: A Combined Analysis of 22 Studies. *Am J Hum Genet [Internet]* 2003;72:1117–30. Available from: http://linkinghub.elsevier.com/retrieve/pii/S0002929707606405

3. Milne RL, Osorio A, Cajal TRY, Vega A, Llort G, De La Hoya M, Díez O, Carmen Alonso M, Lazaro C, Blanco I, Sánchez-de-Abajo A, Caldés T, et al. The average cumulative risks of breast and ovarian cancer for carriers of mutations in BRCA1 and BRCA2 attending genetic counseling units in Spain. *Clin Cancer Res* 2008;14:2861–9.

4. Helleday T. The underlying mechanism for the PARP and BRCA synthetic lethality: Clearing up the misunderstandings. *Mol. Oncol.*2011;5:387–93.

5. Osorio A, Milne RL, Kuchenbaecker K, Vaclov?? T, Pita G, Alonso R, Peterlongo P, Blanco I, de la Hoya M, Duran M, D??ez O, Ram??n y Cajal T, et al. DNA Glycosylases Involved in Base Excision Repair May Be Associated with Cancer Risk in BRCA1 and BRCA2 Mutation Carriers. *PLoS Genet* 2014;10.

6. Wallace SS. Base excision repair: A critical player in many games. *DNA Repair (Amst)* 2014;19:14–26.

7. Caldecott KW. Single-strand break repair and genetic disease. *Nat Rev Genet [Internet]* 2008;9:619–31. Available from:

http://www.pubmedcentral.nih.gov/articlerender.fcgi?artid=2756414&tool=pmcentrez&rendertype=abstract\nhttp://www.ncbi.nlm.nih.gov/pubmed/18414403\nhttp://www.pubmedcentral.nih.gov/articlerender.fcgi?artid=PMC2756414\nhttp://www.nature.com/doifinder/10.103

8. Khanna KK, Jackson SP. DNA double-strand breaks: signaling, repair and the cancer connection. *Nat Genet [Internet]* 2001;27:247–54. Available from: http://www.ncbi.nlm.nih.gov/pubmed/11242102

9. Wang Z, Rhee DB, Lu J, Bohr CT, Zhou F, Vallabhaneni H, de Souza-Pinto NC, Liu Y. Characterization of oxidative guanine damage and repair in mammalian telomeres. *PLoS Genet* 2010;6:28.

10. Zhou J, Fleming AM, Averill AM, Burrows CJ, Wallace SS. The NEIL glycosylases remove oxidized guanine lesions from telomeric and promoter quadruplex DNA structures. *Nucleic Acids Res* 2015;43:4039–54.

11. Hazra TK, Das A, Das S, Choudhury S, Kow YW, Roy R. Oxidative DNA damage repair in mammalian cells: A new perspective. *DNA Repair (Amst)* 2007;6:470–80.

12. Dou H, Mitra S, Hazra TK. Repair of Oxidized Bases in DNA Bubble Structures by Human DNA Glycosylases NEIL1 and NEIL2. *J Biol Chem* 2003;278:49679–84.

13. Negrini S, Gorgoulis VG, Halazonetis TD. Genomic instability--an evolving hallmark of cancer. *Nat Rev Mol Cell Biol [Internet]* 2010;11:220–8. Available from: http://www.ncbi.nlm.nih.gov/pubmed/20177397\nhttp://www.nature.com/nrm/journal/v11/n3/pdf/nrm2858.pdf

14. Sarek G, Marzec P, Margalef P, Boulton SJ. Molecular basis of telomere dysfunction in human genetic diseases. *Nat Struct Mol Biol [Internet]* 2015;22:867–74. Available from: http://dx.doi.org/10.1038/nsmb.3093

15. Kong CM, Lee XW, Wang X. Telomere shortening in human diseases. *FEBS J [Internet]* 2013;280:3180–93. Available from: http://www.ncbi.nlm.nih.gov/pubmed/23647631

16. Benitez-Buelga C, Vaclová T, Ferreira S, Urioste M, Inglada-Perez L, Soberón N, Blasco MA, Osorio A, Benitez J. Molecular insights into the OGG1 gene, a cancer risk modifier in BRCA1 and BRCA2 mutations carriers. *Oncotarget [Internet]* 2016;Available from: http://www.ncbi.nlm.nih.gov/pubmed/27015555

17. Kinslow CJ, El-Zein RA, Rondelli CM, Hill CE, Wickliffe JK, Abdel-Rahman SZ. Regulatory regions responsive to oxidative stress in the promoter of the human DNA glycosylase gene NEIL2. *Mutagenesis* 2010;25:171–7.

18. Kinslow CJ, El-Zein RA, Hill CE, Wickliffe JK, Abdel-Rahman SZ. Single nucleotide polymorphisms 5??? upstream the coding region of the NEIL2 gene influence gene transcription levels and alter levels of genetic damage. *Genes Chromosom Cancer* 2008;47:923–32.

19. O'Callaghan NJ, Dhillon VS, Thomas P, Fenech M. A quantitative real-time PCR method for absolute telomere length. *Biotechniques* 2008;44:807–9.

20. O'Callaghan N, Baack N, Sharif R, Fenech M. A qPCR-based assay to quantify oxidized guanine and other FPG-sensitive base lesions within telomeric DNA. *Biotechniques* 2011;51:403–12.

21. García-Giménez JL, Ledesma AMV, Esmoris I, Romá-Mateo C, Sanz P, Viña J,

Pallardó F V. Histone carbonylation occurs in proliferating cells. *Free Radic Biol Med* 2012;52:1453–64.

22. Shacter E, Williams JA, Lim M, Levine RL. Differential susceptibility of plasma proteins to oxidative modification: Examination by western blot immunoassay. *Free Radic Biol Med* 1994;17:429–37.

23. Breusing N, Grune T, Andrisic L, Atalay M, Bartosz G, Biasi F, Borovic S, Bravo L, Casals I, Casillas R, Dinischiotu A, Drzewinska J, et al. An inter-laboratory validation of methods of lipid peroxidation measurement in UVA-treated human plasma samples. *Free Radic Res* 2010;44:1203–15.

24. Canela A, Vera E, Klatt P, Blasco M a. High-throughput telomere length quantification by FISH and its application to human population studies. *Proc Natl Acad Sci U S A [Internet]* 2007;104:5300–5. Available from: http://www.pubmedcentral.nih.gov/articlerender.fcgi?artid=1828130&tool=pmcentrez&rendertype=abstract

25. Chakraborty A, Wakamiya M, Venkova-Canova T, Pandita RK, Aguilera-Aguirre L, Sarker AH, Singh DK, Hosoki K, Wood TG, Sharma G, Cardenas V, Sarkar PS, et al. Neil2-null mice accumulate oxidized DNA bases in the transcriptionally active sequences of the genome and are susceptible to innate inflammation. *J Biol Chem* 2015;290:24636–48.

26. Raschenberger J, Lamina C, Haun M, Kollerits B, Coassin S, Boes E, Kedenko L, Köttgen A, Kronenberg F. Influence of DNA extraction methods on relative telomere length measurements and its impact on epidemiological studies. *Sci Rep [Internet]* 2016;6:25398. Available from: http://www.nature.com/articles/srep25398

27. Toyokuni S, Okamoto K, Yodoi J, Hiai H. Persistent oxidative stress in cancer. *FEBS Lett* 1995;358:1–3.

28. Nielsen F, Mikkelsen BB, Nielsen JB, Andersen HR, Grandjean P. Plasma malondialdehyde as biomarker for oxidative stress: Reference interval and effects of life-style factors. *Clin Chem* 1997;43:1209–14.

29. Pirincciogluu AG, G??kalp D, Pirincciogluu M, Kizil G, Kizil M. Malondialdehyde (MDA) and protein carbonyl (PCO) levels as biomarkers of oxidative stress in subjects with familial hypercholesterolemia. *Clin Biochem* 2010;43:1220–4.

30. Broer L, Codd V, Nyholt DR, Deelen J, Mangino M, Willemsen G, Albrecht E, Amin N, Beekman M, de Geus EJC, Henders A, Nelson CP, et al. Meta-analysis of telomere length in 19 713 subjects reveals high heritability, stronger maternal inheritance and a paternal age effect. *Eur J Hum Genet [Internet]* 2013;21:1163–8. Available from: http://www.pubmedcentral.nih.gov/articlerender.fcgi?artid=3778341&tool=pmcentrez&rendertype=abstract

31. Benitez-Buelga C, Sanchez-Barroso L, Gallardo M, Apellaniz-Ruiz M, Inglada-Perez L, Yanowski K, Carrillo J, Garcia-Estevez L, Calvo I, Perona R, Urioste M, Osorio A, et al. Impact of chemotherapy on telomere length in sporadic and familial breast cancer patients. *Breast Cancer Res Treat* 2015;149:385–94.

32. Hildrestrand G a, Neurauter CG, Diep DB, Castellanos CG, Krauss S, Bjørås M, Luna L. Expression patterns of Neil3 during embryonic brain development and neoplasia. *BMC Neurosci* 2009;10:45.

33. Houben JMJ, Mercken EM, Ketelslegers HB, Bast A, Wouters EF, Hageman GJ, Schols AMWJ. Telomere shortening in chronic obstructive pulmonary disease.

Respir Med 2009;103:230–6.

Figure 1

a)

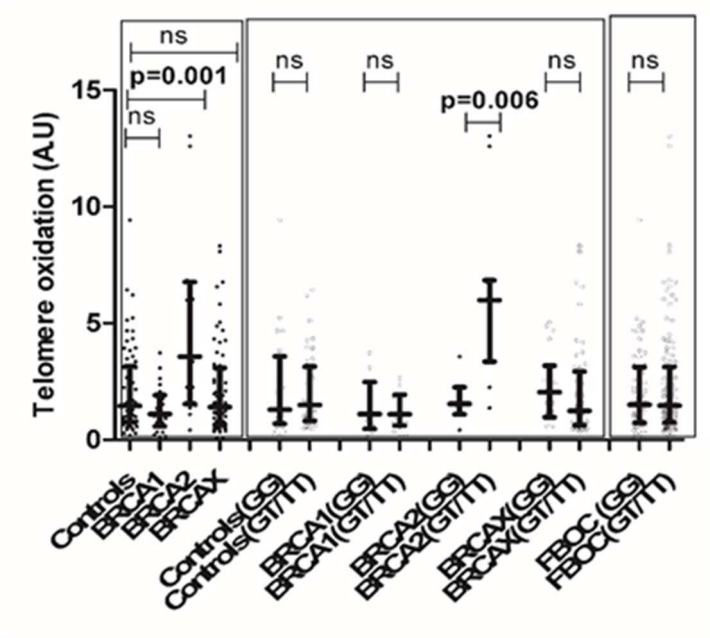
ns
p=0.001
ns
ns
ns
ns
p=0.006
ns
Telomere oxidation (A.U)
15
10
5
0
Controls
BRCA1
BRCA2
BRCAX
Controls(GG)
Controls(GT/TT)
BRCA1(GG)
BRCA1(GT/TT)
BRCA2(GG)
BRCA2(GT/TT)
BRCAX(GG)
BRCAX(GT/TT)
FBOC(GG)
FBOC(GT/TT)

b)

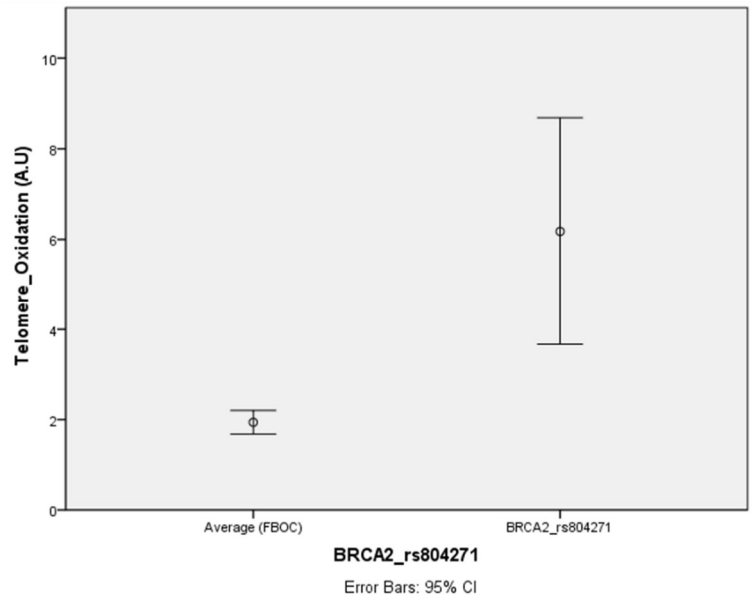
Telomere_Oxidation (A.U)
10
8
6
4
2
0
Average (FBOC)
BRCA2_rs804271
BRCA2_rs804271
Error Bars: 95% CI

Table 1: FBOC series information.

	Families (n)	Healthy carriers (n)	Cancer cases (n)	rs804271 genotyped (n)	NEIL2 mRNA (n)	Telomere oxidation (n)	Carbonylation (n)	Malondihal dehyde (n)	*Telomere studies (n)	Telomerase (n)
BRCA1	25	22	20	42	24	25	29	16	42	27
BRCA2	25	23	23	46	30	19	27	16	46	30
BRCAX	94	0	87	87	55	70	27	12	87	31
Controls	na	0	0	86	29	63	15	17	53	23

Information regarding number of healthy *BRCA1* and *BRCA2* mutation carriers or cancer cases and the sample size for each experimental section.* Telomere studies: The same sample size was used for both TL and percentage of short telomeres quantification.

Supplementary Figure 1 TL distribution in peripheral blood leukocytes as a function of age for the control women population (n = 60), measured by HT QFISH. The regression line for control is drawn controls (y= 0.067* age +12.785)

Supplementary Table S1: Lineal Regression analysis in FBOC Samples: Cancer effect on the studies variables

Independent Variable	Dependent variable	β coeff	p-value
Cancer status	NEIL2 mRNA	-0.13	0.111
	Telomere Oxidation	-0.079	0.238
	Carbonylation	-0.091	0.356
	Malondihaldehyde	-0.197	0.241
	Telomere length	0.005	0.938
	Short Telomeres (%)	0.122	0.061
	Telomerase	-0.151	0.111

We included as dependent variables *NEIL2* mRNA levels, telomere oxidation, carbonylation and MDA, TL (Adjusted by age) & % of short telomeres, telomerase. As independent variables, we included cancer status. β coefficients quantify how much the independent variable (cancer status) modifies the dependent variables, and it shows the direction of the modification.

Supplementary Table S2: Heterozygous/ homozygous frequency of the *NEIL2* variant rs804271 (G>T).

	GG	GT	TT
FBOC*	**0.36**	**0.49**	**0.16**
BRCA1	0.40	0.45	0.15
BRCA2	0.43	0.43	0.14
BRCAX	0.30	0.59	0.11
Controls	0.34	0.50	0.16

* Familial breast and ovarian cancer patients.

Supplementary Table S3: Gtex information summary, regarding *NEIL2* transcriptional up-regulation when rs804271 is present (17 different tissues).

Gencode Id	Gene Symbol	SNP Id	P-Value	Effect Size	Tissue
ENSG00000154328.11	NEIL2	rs804271	2.6e-20	0.49	Nerve - Tibial
ENSG00000154328.11	NEIL2	rs804271	3.8e-15	0.42	Artery - Tibial
ENSG00000154328.11	NEIL2	rs804271	2.3e-14	0.48	Heart - Atrial Appendage
ENSG00000154328.11	NEIL2	rs804271	3.3e-14	0.38	Adipose - Subcutaneous
ENSG00000154328.11	NEIL2	rs804271	1.2e-12	0.36	Thyroid
ENSG00000154328.11	NEIL2	rs804271	1.4e-12	0.33	Cells - Transformed fibroblasts
ENSG00000154328.11	NEIL2	rs804271	1.6e-11	0.39	Artery - Aorta
ENSG00000154328.11	NEIL2	rs804271	3.9e-11	0.69	Ovary
ENSG00000154328.11	NEIL2	rs804271	4.6e-11	0.34	Whole Blood
ENSG00000154328.11	NEIL2	rs804271	9.3e-11	0.29	Muscle - Skeletal
ENSG00000154328.11	NEIL2	rs804271	5.6e-7	0.46	Brain - Caudate (basal ganglia)
ENSG00000154328.11	NEIL2	rs804271	7.6e-7	0.62	Pituitary
ENSG00000154328.11	NEIL2	rs804271	0.0000048	0.29	Heart - Left Ventricle
ENSG00000154328.11	NEIL2	rs804271	0.0000084	0.39	Vagina
ENSG00000154328.11	NEIL2	rs804271	0.000014	0.22	Esophagus - Muscularis
ENSG00000154328.11	NEIL2	rs804271	0.000016	0.28	Breast - Mammary Tissue
ENSG00000154328.11	NEIL2	rs804271	0.000021	0.23	Stomach

aNominal eQTL p-values were generated for each SNP-gene pair using a two-tailed t test, testing the alternative hypothesis that the beta (slope of the linear regression model) deviates from the null hypothesis of $\beta=0$.

Supplementary Table S4: Linear regression models to test the SNP effect on *NEIL2* transcription.

		Dependent variable NEIL2 mRNA Expression	
	Independent Variable	**β coeff**	**p-value**
Model 1	**rs804271**	**0.23**	**0.003**
Model 2	**Controls**	0.04	0.580
	BRCA1	-0.06	0.401
	BRCA2	-0.02	0.732
	BRCAX	0.03	0.678
Model 3	**rs804271**	**β coeff**	**p-value**
Controls		0.12	0.4
BRCA1		**0.42**	**0.04**
BRCA2		0.18	0.322
BRCAX		**0.28**	**0.03**
Model 4	**Controls*rs804271**	-0.14	0.31
	BRCA1*rs804271	-0.083	0.55
	BRCA2*rs804271	-0.014	0.91
	BRCAX*rs804271	0.0091	0.543

Model 1: Where *NEIL2* mRNA levels is the dependent variable, and rs804271, the independent variable. **Model 2:** Where *NEIL2* mRNA levels is the dependent variable, and BRCA mutational status the independent variable (Controls, *BRCA1, BRCA2,* BRCAX). **Model 3:** Where NEIL2 mRNA levels is the dependent variable, and the rs804271 is the independent variable. The model is applied after stratification in each mutational group (Controls*, BRCA1, BRCA2*, BRCAX). **Model 4:** Where NEIL2 mRNA levels is the dependent variable, and the BRCA status, the SNP and combination of both genetic events together, (interaction terms: Controls*SNP; BRCA1*SNP; BRCA2*SNP and BRCAX*SNP) are independent variables. The table shows the β value & the p-value of the interaction term. β coefficients quantify how much the dependent variable (NEIL2 mRNA levels) modifies the dependent variables, and it shows the direction of the modification.

Supplementary Table S5: Linear regression models to test the SNP effect on telomere oxidation.

		Dependent variable **Telomere oxidation**	
	Independent Variable	**β coeff**	**p-value**
Model 1	**rs804271**	-0.06	0.372
Model 2	**Controls**	0.24	0.746
	BRCA1	-0.13	0.06
	BRCA2	**0.22**	**4.41*10exp-4**
	BRCAX	-0.08	0.248
Model 3		**β coeff**	**p-value**
Controls	**rs804271**	-0.16	0.18
BRCA1		-0.11	0.622
BRCA2		**0.60**	**0.008**
BRCAX		-0.03	0.81
Model 4	**Controls*rs804271**	-0.14	0.301
	***BRCA1*rs804271**	-0.05	0.552
	***BRCA2*rs804271**	**0.51**	**6.9*10exp-6**
	BRCAX*rs804271	-0.14	0.331

Model 1: Where telomere oxidation levels is the dependent variable, and rs804271, the independent variable. **Model 2:** Where telomere oxidation levels is the dependent variable, and BRCA mutational status the independent variable (Controls, *BRCA1, BRCA2*, BRCAX). **Model 3:** Where telomere oxidation levels is the dependent variable, and the rs804271 is independent variable. This model is applied for each BRCA mutational group (Controls, *BRCA1, BRCA2*, BRCAX) after stratification for each mutational group. **Model 4:** Where telomere oxidation levels is the dependent variable, and the BRCA status, the SNP and combination of both genetic events together (Controls*rs804271; *BRCA1** rs804271; *BRCA2** rs804271 and BRCAX*SNP) are independent variables. Although in the table is only shown the β value & the p-value of the combined variable. β coefficients quantify how much the dependent variable (telomere oxidation levels) modifies the dependent variables, and it shows the direction of the modification.

Supplementary Table S6: Linear regression models to test the SNP effect on protein carbonylation and lipid peroxidation (MDA).

		Dependent variables			
		Carbonylation		**MDA**	
	Independent Variable	**β coeff**	**p-value**	**β coeff**	**p-value**
Model 1	**rs804271**	-0.07	0.499	0.19	0.202
Model 2	**Controls**	0.11	0.226	0.15	0.287
	BRCA1	-0.15	0.869	0.082	0.574
	BRCA2	-0.08	0.355	-0.13	0.367
	BRCAX	-0.09	0.315	-0.12	0.390
Model 3		**β coeff**	**p-value**	**β coeff**	**p-value**
Controls		-0.24	0.241	-0.11	0.679
BRCA1	**rs804271**	0.12	0.499	**0.65**	**0.042**
BRCA2		0.00	0.971	0.012	0.974
BRCAX		-0.27	0.121	-0.34	0.301
Model 4	**Controls*rs804271**	-0.33	0.054	-0.31	0.251
	***BRCA1*rs804271**	0.11	0.466	**0.64**	**0.002**
	***BRCA2*rs804271**	0.06	0.411	-0.21	0.285
	BRCAX*rs804271	-0.03	0.837	-0.26	0.165

Model 1: Where protein carbonylation and lipid peroxidation (MDA) are the dependent variables, and rs804271, the independent variable. **Model 2:** Where protein carbonylation and lipid peroxidation (MDA) are the dependent variables, and BRCA mutational status the independent variable (Controls, *BRCA1, BRCA2*, BRCAX). **Model 3:** Where protein carbonylation and lipid peroxidation (MDA) are the dependent variables, and the rs804271 is independent variable. This model is applied for each BRCA mutational group (Controls*, BRCA1, BRCA2*, BRCAX) after stratification for each mutational group. **Model 4:** Where protein carbonylation and lipid peroxidation (MDA) are the dependent variable, and the BRCA status, the SNP and combination of both genetic events together (Controls*rs804271; *BRCA1** rs804271; *BRCA2** rs804271 and

BRCAX*SNP) are independent variables. Although in the table is only shown the β value & the p-value of the combined variable. β coefficients quantify how much the 2 dependent variables (protein carbonylation and lipid peroxidation (MDA) modifies the dependent variables, and it shows the direction of the modification

Supplementary Table S7: Lineal regression models to test the SNP effect on telomere length, accumulation of short telomeres and telomerase activity.

		Dependent variables					
		TL		% short telomeres		Telomerase	
	Independent Variable	β coeff	p-value	β coeff	p-value	β coeff	p-value
Model 1	**rs804271**	**-0.26**	**0.004**	**0.25**	**0.005**	-0.17	0.16
Model 2	**Controls**	0.15	0.063	-0.09	0.27	-0.03	0.761
	BRCA1	-0.13	0.13	0.04	0.89	0.13	0.18
	BRCA2	-0.03	0.691	-0.017	0.83	-0.06	0.58
	BRCAX	-0.02	0.81	0.08	0.34	-0.11	0.28
Model 3		**β coeff**	**p-value**	**β coeff**	**p-value**	**β coeff**	**p-value**
Controls		-0.29	0.06	0.27	0.17	-0.07	0.63
BRCA1	**rs804271**	**-0.54**	**0.007**	**0.45**	**0.02**	**-0.57**	**0.035**
BRCA2		**-0.12**	**0.52**	0.14	0.71	0.09	0.742
BRCAX		-0.09	0.69	-0.06	0.813	na	na
Model 4	**Controls*rs804271**	-0.027	0.56	-0.019	0.903	0.14	0.395
	***BRCA1*rs804271**	**-0.26**	**0.056**	**0.22**	**0.14**	-0.10	0.457
	***BRCA2*rs804271**	0.15	0.30	-0.12	0.394	-0.18	0.242
	BRCAX*rs804271	0.15	0.405	-0.10	0.572	-0.21	0.15

Model 1: Where telomere length, accumulation of short telomeres and telomerase activity are the dependent variables, and rs804271, the independent variable. **Model 2:** Where telomere length, accumulation of short telomeres and telomerase activity are the dependent variables, and BRCA mutational status the independent variable (Controls, *BRCA1, BRCA2*, BRCAX). **Model 3:** Where telomere length, accumulation of short telomeres and telomerase activity are the dependent variables, and the rs804271 is independent variable. This model is applied for each BRCA mutational group (Controls, *BRCA1, BRCA2*, BRCAX) after stratification for each mutational group. **Model 4:** Where telomere length, accumulation of short telomeres and telomerase activity are the dependent variables, and the BRCA status, the SNP and combination of both genetic events together (Controls* rs804271; *BRCA1** rs804271; *BRCA2** rs804271 and BRCAX*SNP) are independent variables. Although in the table is only shown the β value & the p-value of the combined variable. β coefficients quantify how much the 2 dependent variables (protein carbonylation and lipid peroxidation (MDA) modifies the dependent variables, and it shows the direction of the modification.

FIGURE LEGENDS

Figure 1 Telomere oxidation comparative analysis among FBOC series.
a) Left panel: Telomere oxidation in the different groups according to the BRCA mutational status (*BRCA1, BRCA2* or BRCAX) was compared with controls. **Middle panel:** Telomere oxidation in the according the BRCA mutational status (*BRCA1, BRCA2* or BRCAX) and controls, stratified according the absence or presence of the variant in *NEIL2* (non-carriers (GG) / carriers (GT/TT). **Right panel:** Telomere oxidation in all FBOC individuals stratified according to the absence or presence of the variant in *NEIL2*. Bars show the mean and the standard deviation.

b) *BRCA2* harboring the rs804271 (n=11) mutation carriers compared to the mean telomere oxidation values from the whole FBOC series (n=166).

Supplementary figure Figure 1 TL distribution in peripheral blood leukocytes as a function of age for the control women population (n = 60), measured by HT QFISH. The regression line for control is drawn controls (y= 0.067* age +12.785)

TABLE LEGENDS

Table 1: FBOC series information. Information regarding number of healthy *BRCA1* and *BRCA2* mutation carriers or cancer cases and the sample size for each experimental section.* Telomere studies: The same sample size was used for both TL and percentage of short telomeres quantification.

Supplementary Table S1: Lineal Regression analysis in FBOC Samples
We included as dependent variables *NEIL2* mRNA levels, telomere oxidation, carbonylation and MDA, TL (Adjusted by age) & % of short telomeres, telomerase. As independent variables, we included cancer status. β coefficients quantify how much the independent variable (cancer status) modifies the dependent variables, and it shows the direction of the modification.

Supplementary Table S2: Heterozygous/ homozygous frequency of the *NEIL2* variant rs804271 (G>T).* Familial breast and ovarian cancer patients.

Supplementary Table S3: Gtex information summary, regarding *NEIL2* transcriptional up-regulation when rs804271 is present (16 different tissues).
aNominal eQTL p-values were generated for each SNP-gene pair using a two-tailed t test, testing the alternative hypothesis that the beta (slope of the linear regression model) deviates from the null hypothesis of β=0.

Supplementary Table S4: Linear regression models to test the SNP effect on NEIL2 transcription. **Model 1:** Where *NEIL2* mRNA levels is the dependent variable, and rs804271, the independent variable. **Model 2:** Where *NEIL2* mRNA levels is the dependent variable, and BRCA mutational status the independent variable (Controls, *BRCA1, BRCA2,* BRCAX). **Model 3:** Where NEIL2 mRNA levels is the dependent variable, and the rs804271 is the independent variable. The model is applied after stratification in each mutational group (Controls*, BRCA1, BRCA2*, BRCAX). **Model 4:** Where NEIL2 mRNA levels is the dependent variable, and the BRCA status, the SNP and combination of both genetic events together, (interaction terms: Controls*SNP; BRCA1*SNP; BRCA2*SNP and BRCAX*SNP) are independent variables. The table shows the β value & the p-value of the interaction term. β coefficients quantify how much the dependent variable (NEIL2 mRNA levels) modifies the dependent variables, and it shows the direction of the modification.

Supplementary Table S5: Linear regression models to test the SNP effect on telomere oxidation. **Model 1:** Where telomere oxidation levels is the dependent variable, and rs804271, the independent variable. **Model 2:** Where telomere oxidation levels is the dependent variable, and BRCA mutational status the independent variable (Controls, BRCA1, BRCA2, BRCAX). **Model 3:** Where telomere oxidation levels is the dependent variable, and the rs804271 is independent variable. This model is applied for each BRCA mutational group (Controls*, BRCA1, BRCA2*, BRCAX) after stratification for each mutational group. **Model 4:** Where telomere oxidation levels is the dependent variable, and the BRCA status, the SNP and combination of both genetic events together (Controls*SNP; BRCA1*SNP; BRCA2*SNP and BRCAX*SNP) are independent variables. Although in the table is only shown the β value & the p-value of the combined variable. β coefficients quantify how much the dependent variable (telomere oxidation levels) modifies the dependent variables, and it shows the direction of the modification.

Supplementary Table S6: Linear regression models to test the SNP effect on protein carbonylation and lipid peroxidation (MDA). Model 1: Where protein carbonylation and lipid peroxidation (MDA) are the dependent variables, and rs804271, the independent variable. **Model 2:** Where protein carbonylation and lipid peroxidation (MDA) are the dependent variables, and BRCA mutational status the independent variable (Controls, *BRCA1, BRCA2*, BRCAX). **Model 3:** Where protein carbonylation and lipid peroxidation (MDA) are the dependent variables, and the rs804271 is independent variable. This model is applied for each BRCA mutational group (Controls*, BRCA1, BRCA2*, BRCAX) after stratification for each mutational group. **Model 4:** Where protein carbonylation and lipid peroxidation (MDA) are the dependent variable, and the BRCA status, the SNP and combination of both genetic events together (Controls*SNP; BRCA1*SNP; BRCA2*SNP and BRCAX*SNP) are independent variables. Although in the table is only shown the β value & the p-value of the combined variable. β coefficients quantify how much the 2 dependent variables (protein carbonylation and lipid peroxidation (MDA)) modifies the dependent variables, and it shows the direction of the modification.

Supplementary Table S7: Lineal regression models to test the SNP effect on telomere length, accumulation of short telomeres and telomerase activity. Model 1: Where telomere length, accumulation of short telomeres and telomerase activity are the dependent variables, and rs804271, the independent variable. **Model 2:** Where telomere length, accumulation of short telomeres and telomerase activity are the dependent variables, and BRCA mutational status the independent variable (Controls, *BRCA1, BRCA2*, BRCAX). **Model 3:** Where telomere length, accumulation of short telomeres and telomerase activity are the dependent variables, and the rs804271 is independent variable. This model is applied for each BRCA mutational group (Controls*, BRCA1, BRCA2*, BRCAX) after stratification for each mutational group. **Model 4:** Where telomere length, accumulation of short telomeres and telomerase activity are the dependent variables, and the BRCA status, the SNP and combination of both genetic events together (Controls*SNP; BRCA1*SNP; BRCA2*SNP and BRCAX*SNP) are independent variables. Although in the table is only shown the β value & the p-value of the combined variable. β coefficients quantify how much the 2 dependent variables (protein carbonylation and lipid peroxidation (MDA)) modifies the dependent variables, and it shows the direction of the modification.

ARTICLE 4

Synthetic lethality in *BRCA1* deficient breast cancer cell lines after OGG1 drug inhibition.

Authors: Carlos Benitez-Buelga; Torkild Visnes; Armando Cázares-Körner; Juan Miguel Baquero; Tereza Vaclova; Ana Osorio; Thomas Helleday; Javier Benítez.
Journal: -
Publication Date: In preparation
Personal contribution: Sample preparation, proliferation studies, telomere oxidation protocol, phosphorylated γH2AX Immunofluorescence, statistical analysis and manuscript preparation.

We have recently shown that the Single Nucleotide Polymorphism (SNP) rs2304277, located in the 3´ untranslated region (UTR) of the DNA glycosylase *OGG1* from the Base Excision Repair Pathway (BER), modify cancer risk in patients harboring mutations in the *BRCA1* gene (Osorio *et al*. 2014). This association may be explained by a synthetic lethal/sickness interaction between these 2 genes. Indeed, we identified that the SNP, was associated to a constitutive OGG1 transcriptional downregulation that leads to both, genome and telomere instability in those patients harboring *BRCA1* and *BRCA2* mutations, explaining the contribution of this polymorphism to cancer risk (Benitez-Buelga *et al*. 2016). In order to explore the biological link between BER and the homologous recombination (HR) DNA repair pathway, we have tested the pharmacological inhibition of OGG1 enzyme, by using a panel of novel OGG1 inhibitors, in a set of *BRCA1* and *BRCA2* deficient cancer cell lines.

We have identified that in cells with the same genetic background, the inactivation of *BRCA1* make cells very sensitive to OGG1 inhibitors. This inhibition in proliferation, after the treatment with OGG1 inhibitors, correlated with oxidative DNA damage accumulation and with phosphorylated γH2AX-foci formation at the nucleus in *BRCA1* deficient cancer cells.

These preliminary results, points to a synthetic lethal interaction between *BRCA1* and *OGG1*, and open a new framework for the treatment of *BRCA1* derived tumors.

SYNTHETIC LETHALLITY IN *BRCA1* DEFICIENT BREAST CANCER CELL LINES AFTER OGG1 DRUG INHIBITION

Carlos Benitez-Buelga[1]; Torkild Visnes[2]; Armando Cázares-Körner[2]; Juan Miguel Baquero[1]; Tereza Vaclova[1]; Ana Osorio[1],*; Thomas Helleday[2]; Javier Benitez[1],*

[1] Human Genetic Group, Spanish National Cancer Research Institute (CNIO), and 3 Spanish Network on Rare Diseases (CIBERER) Madrid, Spain.

[2]Medical Biochemistry and Biophysics, Division of Translational Medicine and Chemical Biology, Karolinska Institutet, Stockholm, Sweden.

*Spanish Network on Rare Diseases (CIBERER), Madrid 28029, Spain

We have recently shown that the Single Nucleotide Polymorphism (SNP) rs2304277, located in the 3' untranslated region (UTR) of the DNA glycosylase *OGG1* from the Base Excision Repair Pathway (BER), modify cancer risk in patients harboring mutations in the *BRCA1* gene [1]. This association is likely explained by a synthetic lethal/sickness interaction between these two genes. Indeed, we identified that the SNP was associated to a constitutive hOGG1 transcriptional downregulation that leads to both genome and telomere instability in those patients harboring *BRCA1* and *BRCA2* mutations explaining the contribution of this polymorphism to cancer risk[2]. In order to explore the biological link between BER and the homologous recombination (HR) DNA repair pathway, we have tested the pharmacological inhibition of OGG1 enzyme by using a panel of novel OGG1 inhibitors* in a set of *BRCA1* and *BRCA2* deficient cancer cell lines.

We have identified that in cells with the same genetic background, the inactivation of BRCA1 make cells very sensitive to OGG1 inhibitors. This inhibition in proliferation, after the treatment with OGG1 inhibitors, correlated with oxidative DNA damage accumulation and with GammaH2AX-foci formation at the nucleus in *BRCA1* deficient cancer cells.

These preliminary results point to a synthetic lethal interaction between *BRCA1* and *OGG1*, and open a new framework for the treatment of *BRCA1* mutated tumors.

*OGG1 inhibitors have been develop entirely by Thomas Helleday lab (Scilifelab, KI). And are currently in process of being patented.

INTRODUCTION

Synthetic lethality can be defined as a type of genetic interaction where the co-occurrence of two genetic events results in organism or cellular death[3]. Similarly, a genetic combination that yields non-lethal growth impairment is called synthetic sickness, and it is usually grouped together with synthetic lethal interactions. Although it is best known in the context of loss-of-function mutants, combinations of other types of perturbations such as genetic polymorphisms (SNPs), gene over-expression, action of chemical compounds or environmental changes can also result in synthetic lethality/sickness[2,4].

One of the most representative examples is the synthetic lethal interaction displayed by *BRCA1* or *BRCA2* loss of-function mutants and pharmacological inhibition of the Poly [ADP-ribose] polymerase 1 (PARP-1). While BRCA1 and BRCA2 are key enzymes of the homologous recombination (HR) pathway, PARP1 enzyme assists in the repair of single-strand DNA nicks at the latest steps of the base excision repair (BER) and it is also able to repair double strand breaks when necessary. In the presence of a defective *BRCA1* or *BRCA2* background and PARP inhibitors, accumulation of double-strand DNA breaks (DSBs) can persist and lead to cell cycle arrest or cell death, making BRCA-deficient cells extremely sensitive to PARP inhibitors (PARPi)[5,6].

Recently, the PARP inhibitor Olaparib was FDA-approved for mono-therapy, in BRCA1 and/or BRCA2 ovarian cancer patients[7]. However, resistance to PARPi has been observed in an important number of patients and at least 5 independent mechanisms of resistance to PARP inhibitors have been described in vivo until now [8–10]. Hence, it is important to find alternative treatments and in this regard it is likely that other members of the BER pathway could have the potential of being targeted to generate novel inhibitors, with similar anticancer properties as Olaparib based on synthetic lethality/sickness for *BRCA1* and/or *BRCA2* derived tumors.

Recently, we identified one SNP in a DNA glycosylase gene (*OGG1*) whose activity is required at the early steps of BER pathway. This SNP confers a higher risk to develop ovarian cancer among *BRCA1* mutation carriers[1].

We have tried to explain this cancer association at a molecular level and we have found that the *OGG1* SNP is associated with a constitutive *OGG1* transcriptional down-regulation, which contributes to a higher genome and telomere instability, especially in those cells harboring mutations in *BRCA1* and *BRCA2* genes [2], pointing to a synthetic lethal interaction between both genetic events. Similarly to the action of PARP inhibitors, *OGG1* and DNA glycosylase could be a potential therapeutic target for *BRCA1* and *BRCA2* related tumors.
In general, inhibitors of BER show clinical benefit in two very different treatment protocols:

The first, and similar to PARP inhibitors, applies as mono-therapy for tumors that have specific genetic deficiencies, usually in another DNA repair pathway[11–13].For example, AP endonuclease-1 (APE1) inhibitors were shown to be synthetically lethal in BRCA and ATM deficient cancer cells resulting in accumulation of DNA DSBs and G2/M cell cycle arrest[14].

The second approach is the combination of BER inhibitors with other drugs. For example, several groups have shown that the loss of the DNA glycosylase *OGG1* sensitized cells to PARP1 inhibitors[15,16].

Taking all this information together we have targeted theDNA glycosylase *OGG1* using a novel set of small molecule *OGG1* inhibitors developed at Thomas Helleday's laboratory, to test if BRCA1/2 deficient cancer cells are sensitized by these novel compounds.

MATHERIAL & METHODS

BRCA1 AND *BRCA2* DEFICIENT CELLS

Breast cancer cell line MDA-MB-231, derived from a sporadic breast cancer tumor, was obtained from the Cancer Epigenetics Group at the Bellvitge Institute for Biomedical Research (Barcelona, Spain). MDA-MB-231 was transduced by BRCA1-specific short-hairpin RNAs (shRNAs) or control shRNA (shScramble) and these newly generated cell lines were then used to confirm a synthetic lethal interaction between BRCA1 and OGG1. BRCA1 gene down-regulation was performed in MDA-MB-231 cell line using shRNAmir target gene set obtained from Open Biosystems (13 human GIPZ lentiviral shRNAmir individual clones; #RHS4531).

Six different shRNA constructs were transduced, and one of them (sh1), which provided the best knockdown efficiency, was selected to silence BRCA1 in the breast cancer cell line (MDA-MB-231shBRCA1).

Details in Supplementary figure 1a and figure1b/ **Tereza Vaclová, Doctoral Thesis,2015** . https://repositorio.uam.es/bitstream/handle/10486/665000/vaclova_tereza.pdf?sequence=1

The *BRCA1* deficient commercial breast cancer cell line MDA-MB-436, was obtained from ATCC (ATCC® HTB-130™). Finally, pancreatic *BRCA2* deficient PL45 was obtained from the Epithelial Carcinogenesis Group, at the Spanish Cancer Research Center (CNIO).

VIABILITY ASSAY

MDA-MB-231 and MDA-MB-231 shBRCA1 or MDA-MB-436 and PL45 cells were seeded in 96- or 384-well plates (in duplicates) 4 h prior to OGG1 inhibitors treatment for 5 days. The treatment consisted of a dilution series of active and control inactive OGG1 inhibitors (16 different molecules) starting at 100 µM. This initial concentration was used to generate a 1:2 dilution series, including 8 points. These dilution series was used to evaluate and compare the half maximal inhibitory concentration (IC50) for each cell line. Three independent experiments were performed.

RESAZURIN PROLIFERATION ASSAY

Resazurin sodium salt (Sigma-Aldrich) was added at a final concentration of 0.1 mg/ml to the cell growth media. The plates were then incubated for 6 h before fluorescence readout at 535/590 nm in an Hidex Sense plate reader. The absorbance was normalized against background levels and the data processed in MS Excel by standard techniques before statistical analysis in XLfit (ID Business Solutions, Surrey, UK) to generate combination index plots.

OXIDATIVE DNA DAMAGE WITHIN TELOMERES

We used a qPCR-based method to evaluate the oxidative stress within telomeric DNA [17], based on differences in PCR kinetics between DNA template digested by human purified Oxoguanine glycosylase (OGG1) plus Apurinic/apyrimidinic endonuclease (APE1) and undigested DNA. OGG1is a monofunctional DNA glycosylase that is specific for oxidized purines, principally 8-oxoG, producing apurinic sites (AP), which APE1 converts into single-strand breaks (SSBs).

These SSBs inhibit PCR reactions, thus, the ΔCT after digesting DNA by OGG1 / APE1 (CT digested – CT undigested) is proportional to the oxidative damage in the amplified region.

A total amount of 400 ng of genomic DNA was incubated with 12 and 6 units of OGG1or APE1, respectively in OGG1/APE1 buffer. Also, a control incubated with OGG1/APE1 buffer but without OGG1/APE1 (replaced with H_2O), was prepared. All samples were set up on ice, then incubated at 37°C overnight (i.e., for 16 h) to allow complete digestion to occur. The digestion was verified by gel electrophoresis.

The quantitative real-time amplification of genomic DNA was performed as described by O'Callaghan et al[17]. Delta Ct method was run in an ABI Quant studio 7 and all samples were loaded and analyzed in triplicate. Cycling conditions were 10 min at 95°C, followed by

40 cycles of 95°C for 15 s and 60°C for 1 min. Three independent experiments were performed.

γH2AX IMMUNOFLUORESCENCE

MDA-MB-231 or MDA-MB-231 shBRCA1 cells were seeded on glass coverslips in 24-well plates. Once cells attached to the coverslip (12 hours), cells were treated for 5d with TH5487 OGG1 inhibitor. Then cells were washed and incubated for 30 s with ice cold 0.1% Triton-X in PBS to pre-extract soluble protein and then fixed in 4% paraformaldehyde at room temperature for 10 min.

Cells were washed again with PBS and incubated for 10 min with 5% bovine serum albumin (BSA), 0.1% Tween-20 in PBS. Cells were then incubated overnight at 4°C with primary antibody, anti-phospho-γH2AX (S139; 1:1000; Millipore) .The cells were then washed and incubated with secondary antibody anti-mouse IgG Alexa Fluor® 488 (1:1000, Life technologies). DNA was stained with 100 nM 4, 6 diamidino-2-phenylindole for 15 min. Finally, coverslip were mounted over the microscope slides and were processed for confocal microscope analysis. A total of 10 field were evaluated, each field contained around 50 cells. Pictures of each field were taken and measured using ImageJ software.

INHIBITORS

OGG1 inhibitors are in the process of being patented. Hence, chemical structures and/or biochemical information from these compounds is strictly confidential and protected under a material transfer agreement (MTA) signed between CNIO and Scilifelab, KI.

RESULTS

OGG1 INHIBITORS SENSITIZE *BRCA1* INACTIVATED BREAST CANCER CELL LINES

First we compared the drug inhibitory effect of 16 active and inactive control OGG1 inhibitors, in MDA-MB-231 with functional BRCA1 protein versus MDA-MB-231 with constitutive small hairpin-mediated *BRCA1* knockdown. We found that all but one OGG1 inhibitor with sub-micromolar potency in the biochemical assay sensitize significantly more MDA-MB-231shBRCA1 compared to MDA-MB-231 with functional BRCA1 protein ($p=0.00097$)) (Figure 1 & Table 1), while OGG1 inhibitors with poorer biochemical potency (TH1796 and TH8020 were not toxic at all. Inactive control compounds were generally tolerated well by both cell lines. We repeated the proliferation studies including two additional commercial cells lines; MDA-MB-436 is a *BRCA1* deficient breast cancer cell line, while PL45 is a pancreatic *BRCA2* deficient cancer cell line. This time we used a 10 μM single dose of TH5487 during 5 days to compare OGG1 inhibitor sensitivity among these BRCA1/2 deficient cell lines.

We have validate that MDA-MB436 breast cancer cells were significantly sensitized after 5 days of TH5487 exposure ($p=0.002$) (Figure 2). In contrast, we were not able to see the same effect in *BRCA2* deficient PL45 pancreatic cancer cells (Figure 2).

OGG1 INHIBITORS INDUCES TELOMERE OXIDATIVE DAMAGE

We have adapted the original method from Nathan 2011 to detect oxidation at the telomere as a double strategy[18]. First, to detect oxidative DNA damage as a constitutive hallmark of genome instability, and second as a method for detecting the efficacy of the inhibitor in living cells. Since *OGG1* remove 8-oxodG lesions, we expect that during the cell culture, in the presence of OGG1 inhibitors cells will accumulate more oxidative lesions in the DNA compared to those cells growing without OGG1 inhibitors. Since BER is active throughout the entire cell cycle[19], we expected to see changes in oxidative damage accumulation after 24hours of OGG1 inhibitor exposure, equivalent to one doubling round for MDA-MB-231 and MDA-MB-231shBRCA1 cells.

When we compared MDA-MB-231 & MDA-MB-231shBRCA1 cells we observed similar levels of telomere oxidative DNA damage. After 24 hours of OGG1 inhibitor treatment, both cell types presented an increased accumulation of telomere oxidative DNA damage although this increment was not significant (Figure 3). On the other hand we have observed that telomere DNA oxidation was significantly increased in *BRCA1* inactivated cells after the treatment with OGG1 inhibitors, compared to those with functional BRCA1 protein,($p=0.003$) (figure3).These results suggest that in living cells the inhibitors are blocking the OGG1 enzymatic activity, especially in *BRCA1* deficient cells.

γH2AX IMMUNE-FLUORESCENCE (IF)

Because oxidative lesions can be converted into DSBs if not repaired in a *BRCA1* or *BRCA2* deficient setting[20], and we have detected a significant accumulation of oxidative lesions after 24hours exposure to TH5487 in *BRCA1* inactivated MDA-MB-231 we have evaluated γH2AX as marker for DSBs.

We have used the same set of cells (MDA-MB-231 & MDA-MB-231shBRCA1) in two different conditions: Cells unexposed or exposed to TH5487 during 5 days, time that was previously used to see an effect on proliferation. We have evaluated the contribution of TH5487 on DNA damage. These two cell lines have an identical genetic background, but the *BRCA1* inactivation in the case of MDA-MB-231shBRCA1.

We have detected that in MDA-MB-231 the exposure to TH5487 lead to γH2AX induction. In contrast in the case of the MDA-MB-231sh*BRCA1* it was possible to observe a basal γH2AX induction, in both untreated and treated cells, likely caused by a defective HR DNA repair system (shBRCA1) (Figure 4).

Finally, we could confirm a decrease in proliferation after the treatment with OGG1 inhibitors that for both cell types; although it was more severe for MDA-MB-231sh*BRCA1.*

DISCUSSION

Previously we have described that common polymorphisms in transcriptional regulatory regions of OGG1 DNA glycosylase, can modify ovarian cancer risk for *BRCA1* mutation carriers[1]. The molecular mechanism underlying this association is unclear although this polymorphism is also associated with lower *OGG1* transcript levels and with genome and telomere instability among *BRCA1* and *BRCA2* mutations carriers[2]. Under the hypothesis of a possible synthetic lethal/sickness interaction between *BRCA1* and *OGG1* to explain the molecular basis of this cancer association, we tested whether the pharmacological inhibition of OGG1 could sensitize

BRCA1 or *BRCA2* deficient cancer cells, similar as occurred with the recent FDA-approved Olaparib (PARP1 inhibitors) for *BRCA1* and *BRCA2* derived tumors.

We have tested a set of novel molecules that effectively inhibit OGG1 enzymatic activity *in vitro* (Data not shown) in a breast cancer cell line (MDA-MB-231) with functional BRCA1 protein and in the same cell line with *BRCA1* inactivated through shRNA constructs, MDA-MB-231sh*BRCA1*.

We have observed, that for this specific model the entire set of molecules sensitized preferentially MDA-MB-231sh*BRCA1* after 5 days of treatment compared to MDA-MB-231 with functional BRCA1 protein (Figure & Table1). In addition, we have confirmed this result in another *BRCA1* deficient breast cancer commercial cell line (MDA-MB-436); in contrast, the pancreatic *BRCA2* deficient cancer cell line PL45 was not sensitized at all by OGG1 inhibitors (Figure2).

To explain the sensitization observed in *BRCA1* deficient cells after pharmacological inhibition of OGG1, we have evaluated oxidative DNA damage accumulation and its conversion into DSBs in both MDA-MB-231 & MDA-MB-231sh*BRCA1* cells (Figure3).

To study the accumulation of oxidative DNA damage, we have modified a previously described protocol to detect oxidative lesions (8-oxoG) at the telomere region[17]. We can use this method to quantify the effectiveness of the OGG1 inhibitor molecule TH5487 in cultured cells.

After 24 hours exposure to 10 µM TH5487 we could observe higher levels of oxidative damage at the telomere in both MDA-MB-231 and MDA-MB-231sh*BRCA1*, suggesting that cells exposed to OGG1 inhibitor TH5487 cannot effectively repair endogenous oxidative DNA damage generated during cell culture, leading to an accumulation of these lesions at the telomere (Figure 3).

Accumulation of oxidative lesions was significantly higher in MDA-MB-231 shBRCA1 compared to MDA-MB-231 breast cancer cells which suggest a role for *BRCA1* in the repair of oxidative lesions at the telomere region. In relation with this, *BRCA1* contributes to the repair of the 8-oxoguanine oxidative damage in human cells[21] protecting against oxidative DNA damage being converted into double-strand breaks during DNA replication[20]. Hence, it is likely that *BRCA1* could be involved in the oxidative DNA damage repair at telomeres, since there are evidence of BRCA1 protein interacting at telomeric regions [22,23].

Finally, we could confirm by IF that after 5 days of TH5487 exposure, MDA-MB-231 presented an induction of γH2AX nuclear signal and foci formation, figure 4. This may suggest that the inhibition of OGG1 could first lead to an accumulation of oxidative damage, that later is converted into DSBs contributing to a higher genome instability.

Taking into account that DSBs are the most dangerous perturbation for DNA, and because *BRCA1* is a protein essential in the HR DNA that repairs DSBs, we believe that this could be the mechanistic explanation behind the effects observed in proliferation in MDA-MB-231sh*BRCA1* when exposed to TH5487, OGG1 inhibitor.

In summary, in the present report we have described how in cells with the same genetic background, inactivation of *BRCA1* make cells very sensitive to OGG1 inhibitors. This effect in proliferation correlates with an accumulation of oxidative damage and γH2AX nuclear induction, and all together these evidences, together with previous ones[1] points to a synthetic lethal interaction between *OGG1* and *BRCA1*.

REFERENCES

1. Osorio A, Milne RL, Kuchenbaecker K, Vaclov?? T, Pita G, Alonso R, Peterlongo P, Blanco I, de la Hoya M, Duran M, D??ez O, Ram??n y Cajal T, et al. DNA Glycosylases Involved in Base Excision Repair May Be Associated with Cancer Risk in BRCA1 and BRCA2 Mutation

Carriers. *PLoS Genet* 2014;10.
2. Benitez-Buelga C, Vaclová T, Ferreira S, Urioste M, Inglada-Perez L, Soberón N, Blasco MA, Osorio A, Benitez J. Molecular insights into the OGG1 gene, a cancer risk modifier in BRCA1 and BRCA2 mutations carriers. *Oncotarget [Internet]* 2016;Available from: http://www.ncbi.nlm.nih.gov/pubmed/27015555
3. Boone C, Bussey H, Andrews BJ. Exploring genetic interactions and networks with yeast. *Nat Rev Genet [Internet]* 2007;8:437–49. Available from: http://www.ncbi.nlm.nih.gov/pubmed/17510664
4. Luo J, Solimini NL, Elledge SJ. Principles of Cancer Therapy: Oncogene and Non-oncogene Addiction. *Cell*2009;136:823–37.
5. Fong PC, Boss DS, Yap TA, Tutt A, Wu P, Mergui-Roelvink M, Mortimer P, Swaisland H, Lau A, O'Connor MJ, Ashworth A, Carmichael J, et al. Inhibition of poly(ADP-ribose) polymerase in tumors from BRCA mutation carriers. *N Engl J Med [Internet]* 2009;361:123–34. Available from: http://www.ncbi.nlm.nih.gov/pubmed/19553641
6. Helleday T. The underlying mechanism for the PARP and BRCA synthetic lethality: Clearing up the misunderstandings. *Mol. Oncol.*2011;5:387–93.
7. Ledermann JA, El-Khouly F. PARP inhibitors in ovarian cancer: Clinical evidence for informed treatment decisions. *Br J Cancer [Internet]* 2015;113:S10–6. Available from: http://www.nature.com/doifinder/10.1038/bjc.2015.395
8. Lord CJ, Ashworth A. Mechanisms of resistance to therapies targeting BRCA-mutant cancers. *Nat Med [Internet]* 2013;19:1381–8. Available from: http://www.ncbi.nlm.nih.gov/pubmed/24202391
9. Fojo T, Bates S. Mechanisms of resistance to PARP inhibitors-three and counting. *Cancer Discov* 2013;3:20–3.
10. Bouwman P, Jonkers J. Molecular pathways: How can BRCA-mutated tumors become resistant to PARP inhibitors? *Clin Cancer Res* 2014;20:540–7.
11. Audeh MW, Carmichael J, Penson RT, Friedlander M, Powell B, Bell-McGuinn KM, Scott C, Weitzel JN, Oaknin A, Loman N, Lu K, Schmutzler RK, et al. Oral poly(ADP-ribose) polymerase inhibitor olaparib in patients with BRCA1 or BRCA2 mutations and recurrent ovarian cancer: A proof-of-concept trial. *Lancet* 2010;376:245–51.
12. Mendes-Pereira AM, Martin SA, Brough R, McCarthy A, Taylor JR, Kim JS, Waldman T, Lord CJ, Ashworth A. Synthetic lethal targeting of PTEN mutant cells with PARP inhibitors. *EMBO Mol Med* 2009;1:315–22.
13. Martin SA, McCabe N, Mullarkey M, Cummins R, Burgess DJ, Nakabeppu Y, Oka S, Kay E, Lord CJ, Ashworth A. DNA Polymerases as Potential Therapeutic Targets for Cancers Deficient in the DNA Mismatch Repair Proteins MSH2 or MLH1. *Cancer Cell* 2010;17:235–48.
14. Sultana R, McNeill DR, Abbotts R, Mohammed MZ, Zdzienicka MZ, Qutob H, Seedhouse C, Laughton CA, Fischer PM, Patel PM, Wilson DM, Madhusudan S. Synthetic lethal targeting of DNA double-strand break repair deficient cells by human apurinic/apyrimidinic endonuclease inhibitors. *Int J Cancer* 2012;131:2433–44.
15. Dziaman T, Ludwiczak H, Ciesla JM, Banaszkiewicz Z, Winczura A, Chmielarczyk M, Wisniewska E, Marszalek A, Tudek B, Olinski R. PARP-1 expression is increased in colon adenoma and carcinoma and correlates with OGG1. *PLoS One* 2014;9.
16. Alli E, Sharma VB, Sunderesakumar P, Ford JM. Defective repair of oxidative DNA damage in triple-negative breast cancer confers sensitivity to inhibition of poly(ADP-ribose) polymerase. *Cancer Res* 2009;69:3589–96.
17. O'Callaghan NJ, Dhillon VS, Thomas P, Fenech M. A quantitative real-time PCR method for absolute telomere length. *Biotechniques* 2008;44:807–9.
18. O'Callaghan N, Baack N, Sharif R, Fenech M. A qPCR-based assay to quantify oxidized guanine and other FPG-sensitive base lesions within telomeric DNA. *Biotechniques* 2011;51:403–12.

19. Dianov GL, Hübscher U. Mammalian base excision repair: The forgotten archangel. *Nucleic Acids Res.*2013;41:3483–90.
20. Fridlich R, Annamalai D, Roy R, Bernheim G, Powell SN. BRCA1 and BRCA2 protect against oxidative DNA damage converted into double-strand breaks during DNA replication. *DNA Repair (Amst)* 2015;30:11–20.
21. Le Page F, Randrianarison V, Marot D, Cabannes J, Perricaudet M, Feunteun J, Sarasin A. BRCA1 and BRCA2 are necessary for the transcription-coupled repair of the oxidative 8-oxoguanine lesion in human cells. *Cancer Res* 2000;60:5548–52.
22. Acharya S, Kaul Z, Gocha AS, Martinez AR, Harris J, Parvin JD, Groden J. Association of BLM and BRCA1 during telomere maintenance in ALT cells. *PLoS One* 2014;9.
23. Badie S, Carlos AR, Folio C, Okamoto K, Bouwman P, Jonkers J, Tarsounas M. BRCA1 and CtIP promote alternative non- homologous end-joining at uncapped telomeres. *EMBO J* 2015;34:410–24.

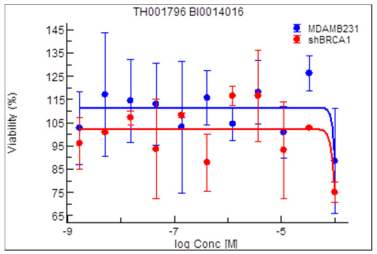
TH001796 BI0014016
MDAMB231
shBRCA1
Viability (%)
log Conc [M]

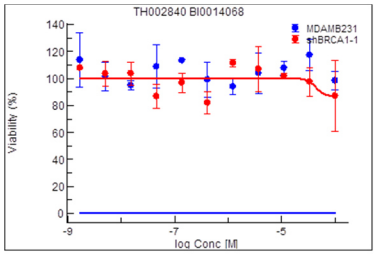
TH002840 BI0014068
MDAMB231
shBRCA1-1
Viability (%)
log Conc [M]

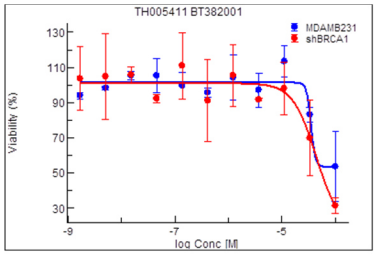
TH005411 BT382001
MDAMB231
shBRCA1
Viability (%)
log Conc [M]

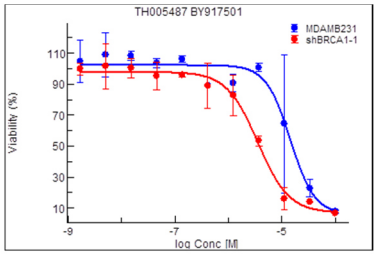
TH005487 BY917501
MDAMB231
shBRCA1-1
Viability (%)
log Conc [M]

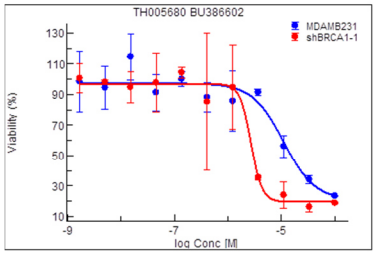
TH005680 BU386602
MDAMB231
shBRCA1-1
Viability (%)
log Conc [M]

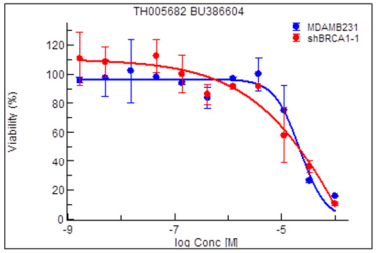
TH005682 BU386604
MDAMB231
shBRCA1-1
Viability (%)
log Conc [M]

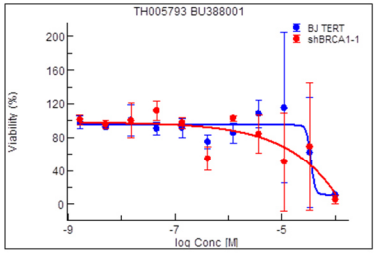
TH005793 BU388001
BJ TERT
shBRCA1-1
Viability (%)
log Conc [M]

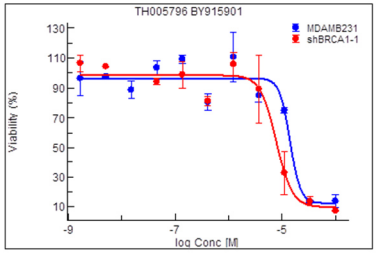
TH005796 BY915901
MDAMB231
shBRCA1-1
Viability (%)
log Conc [M]

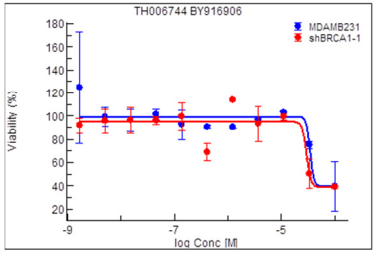
TH006744 BY916906
MDAMB231
shBRCA1-1
Viability (%)
log Conc [M]

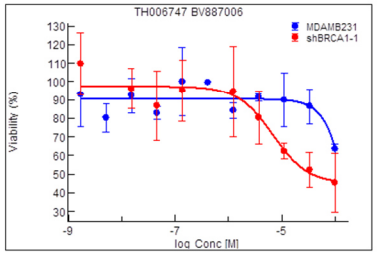
TH006747 BV887006
MDAMB231
shBRCA1-1
Viability (%)
log Conc [M]

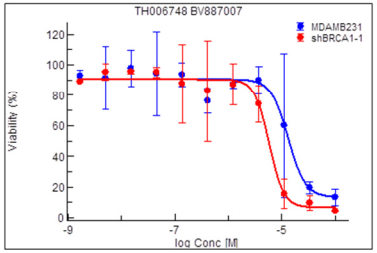
TH006748 BV887007
MDAMB231
shBRCA1-1
Viability (%)
log Conc [M]

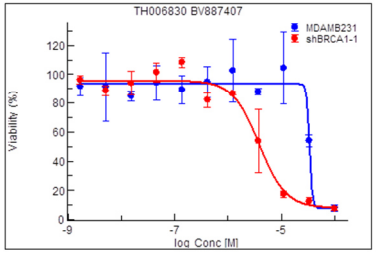
TH006830 BV887407
MDAMB231
shBRCA1-1
Viability (%)
log Conc [M]

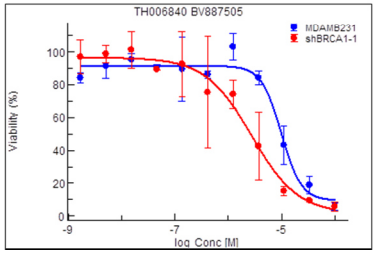
TH006840 BV887505
MDAMB231
shBRCA1-1
Viability (%)
log Conc [M]

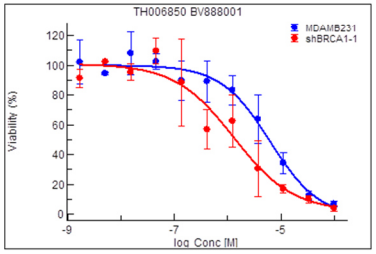
TH006850 BV888001
MDAMB231
shBRCA1-1
Viability (%)
log Conc [M]

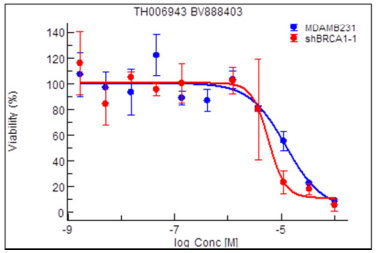
TH006943 BV888403
MDAMB231
shBRCA1-1
Viability (%)
log Conc [M]

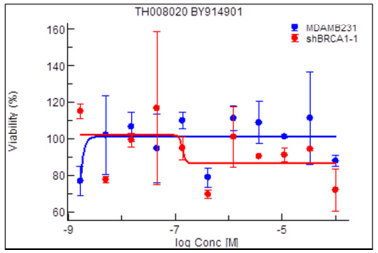
TH008020 BY914901
MDAMB231
shBRCA1-1
Viability (%)
log Conc [M]

Figure1, A set of 16 molecules were initially tested. Proliferation curves, with decreasing concentration of different compounds are plotted in this figure. In the first and the second panel were cells treated with decreasing concentration of DMSO (TH001796 and TH002840), and in the last panel cells were treated with an analog that has not any *OGG1* inhibition properties (TH008020). Then, 13 molecules with *in vitro* OGG1 inhibition properties, were tested for MDA-MB-231 (Blue lines) and MDA-MB-231shBRCA1. In most of the cases, the molecules showed a stronger and specific inhibition properties for MDA-MB-231shBRCA1 compared with MDA-MB-231 with both BRCA1 functional alleles.

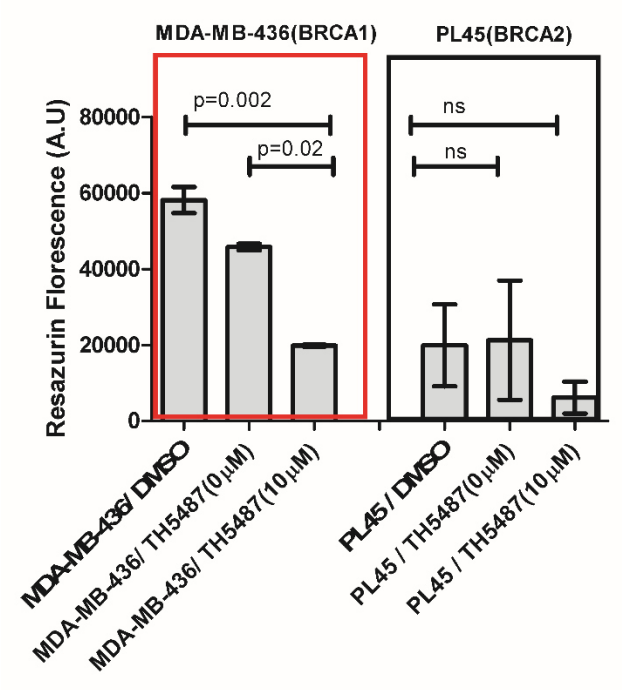

Figure 2 Comparative analysis regarding the effect of TH5487 OGG1 inhibitor in the proliferation of 2 commercial BRCA1 and BRCA2 deficient cancer cells. A single dose of 10 µMolar of TH5487 was exposed to cancer cells during 5 days, and fluorescence values (Resazurin) were compared between treated cells, non-treated (0 µMolar) or treated just with the vehicle in which the drug is dissolved (DMSO).BRCA1 defective breast cancer cells are significantly sensitive to OGG1 inhibitor TH5487 (p=0.002), while BRCA2 deficient cells were not significantly sensitive to the compound.

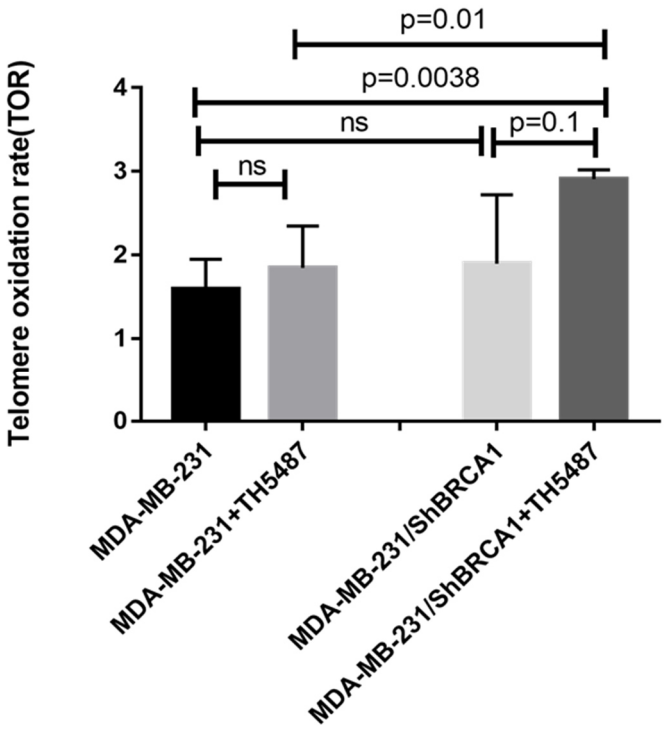

Figure 3 Accumulation of oxidative DNA damage in MDA-MB-231 Vs MDA-MB-231 (sh1) against BRCA1 in basal conditions, and after 5days treatment with the OGG1 inhibitor (TH5487). OGG1 inhibitor TH5487 induces telomere oxidation in *BRCA1* inactivated cells after 24hours of treatment at a 10µM single dose of TH5487.

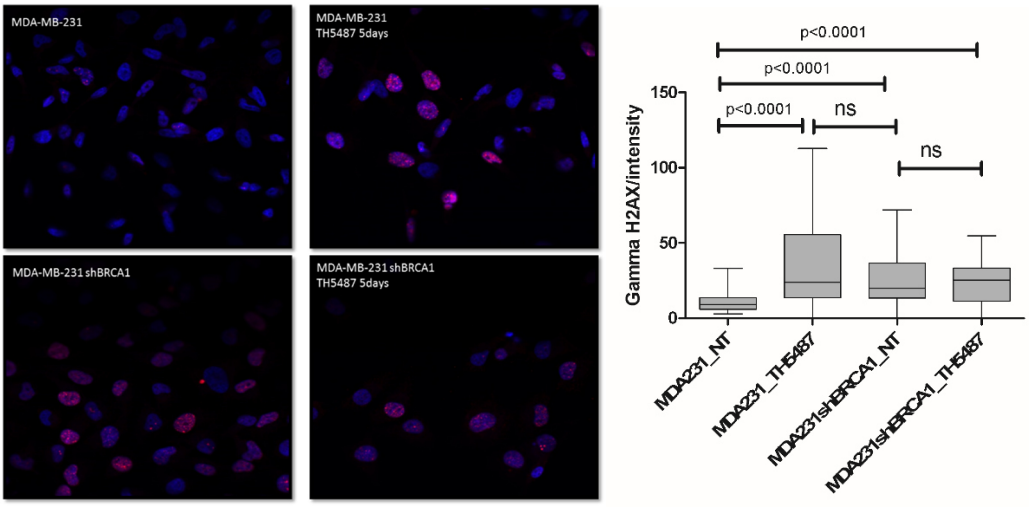

Figure 4 γH2AX immune-fluorescence in MDA-MB-231 *Vs* MDA-MB-231 (sh1) against BRCA1 in basal conditions, and after 5days treatment with the OGG1 inhibitor (TH5487).

Compound ID	Biochemical IC50 (µM)	Cellular EC50 (µM) MDA-MB-231	IC50 (µM)/MDA-MB-231shBRCA1
TH1796	9.5	>99	>99
TH2840[c]	> 99	>99	>99
TH5411[c]	> 99	34.78	43.53
TH5487	0.465	14.37	3.54
TH5680	0.848	11.02	2.7
TH5682	0.728	21.82	12.1
TH5793	0.488	34.61	22.6
TH5796	0.766	14.03	7.79
TH6744	0.683	34.32	29.5
TH6747[b]	> 99	>99	6.76[a]
TH6748	0.886	13.08	5.77
TH6830	0.603	33.65	3.8
TH6840	0.551	9.84	2.73
TH6850	0.379	6.25	1.31
TH6943	0.149	12.17	5.75
TH8020	2.92	>99	>99

Table1 Comparision of biochemical IC50 values of tested OGG1 inhibitors to cellular EC50 values for MDA-MD-231 with or without BRCA1 knockdown. TH5487, used for follow up experiments, is displayed in red. a) Plateau at 40% viability. b) TH6748 is inactive *in vitro*, but have the possibility to be converted to an active compound *in cellulo*. c) TH2840 and TH5411 are inactive compounds that are structural similar chemical controls for the active OGG1 inhibitors.

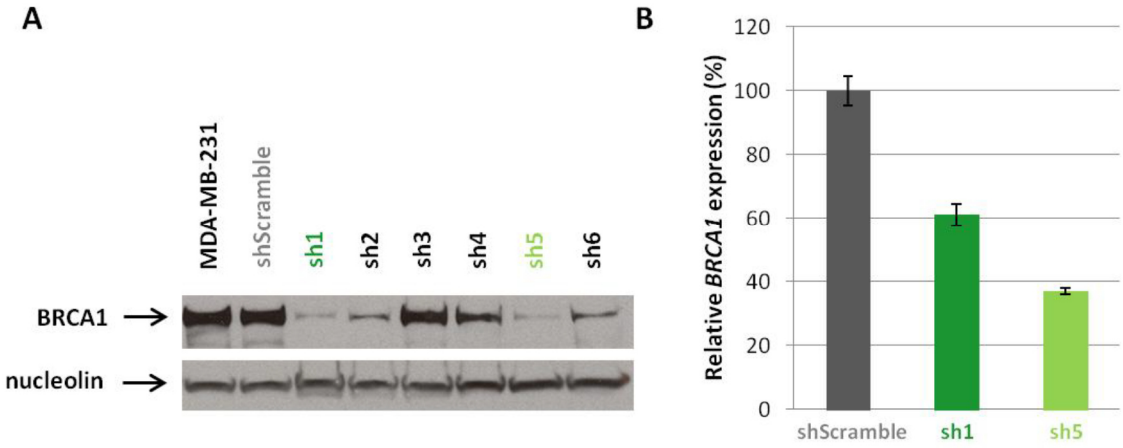

Supplementary figure 1. *BRCA1* silencing ability of a set of human GIPZ lentiviral shRNAmir. A) Western blot analysis of BRCA1 protein expression in MDA-MB-231 cells, parental or transduced with 6 *BRCA1*-specific shRNA clones (sh1–6) or control shRNA (shScramble). Nucleolin was used as a loading control for nuclear proteins. **B)** Relative *BRCA1* mRNA expression in cells overexpressing non-targeting shRNA or BRCA1-specific sh1 or sh5.

EXAMPLES OF TELOMERE LENGTH DYSREGULATION AS A CAUSE OF CANCER/DISEASE DEVELOPMENT

Defects in genes involved in telomere maintenance (shelterin complex or telomerase) result in a wide spectrum of overlapping symptoms (Kirwan & Dokal 2008), which converge in disruption of telomere length regulation and end protection, and finally in disease manifestation. In article 5 and article 6, two examples of telomere length dysregulation caused by defects in genes from the shelterin or telomerase complex are described. In these examples, disease manifestation is not exclusively associated with telomere shortening. Telomere length equilibrium is maintained by both telomerase and the shelterin complex, and aberrant telomere elongation or shortening can converge in disease manifestation.

Personal contribution

In these two articles, I contributed by measuring TL (qPCR) in samples of interest, and doing the corresponding statistical analyses.

ARTICLE 5

A mutation in the *POT1* gene is responsible for cardiac angiosarcoma in TP53-negative Li-Fraumeni-like families.

Authors: Calvete O, Martinez P, Garcia-Pavia P, **Benitez-Buelga C**, Paumard-Hernández B, Fernandez V, Dominguez F, Salas C6, Romero-Laorden N, Garcia-Donas J, Carrillo J, Perona R, Triviño JC, Andrés R, Cano JM, Rivera B, Alonso-Pulpon L, Setien F, Esteller M, Rodriguez-Perales S, Bougeard G, Frebourg T, Urioste M, Blasco MA, Benítez J.

Journal: Nature Communications
Publication Date: September 2015
Ref: 25; 6:8383
Personal contribution: Telomere measurement by qPCR, statistical analysis and the corresponding part of the manuscript.

Cardiac angiosarcoma (CAS) is a rare malignant tumour whose genetic basis is unknown. Here we show, by whole-exome sequencing of a TP53-negative Li–Fraumeni-like (LFL) family including CAS cases, that a missense variant in *POT1* (protection of telomeres 1) gene is responsible for CAS. The same gene alteration is found in two other LFL families with CAS, supporting the causal effect of the identified mutation. We extend the analysis to TP53-negative LFL families with no CAS and find the same mutation in a breast AS family. The mutation is recently found once in 121,324 studied alleles in ExAC server but it is not described in any other database or found in 1,520 Spanish controls. *In silico* structural analysis suggests how the mutation disrupts POT1 structure. Functional and in vitro studies demonstrate that carriers of the mutation show reduced telomere-bound POT1 levels, abnormally long telomeres and increased telomere fragility.

Impact factor (IF): 11.08

nature COMMUNICATIONS

ARTICLE

Received 6 Apr 2015 | Accepted 14 Aug 2015 | Published 25 Sep 2015

DOI: 10.1038/ncomms9383 OPEN

A mutation in the *POT1* gene is responsible for cardiac angiosarcoma in *TP53*-negative Li–Fraumeni-like families

Oriol Calvete[1,2,*], Paula Martinez[3,*], Pablo Garcia-Pavia[4,5], Carlos Benitez-Buelga[1], Beatriz Paumard-Hernández[1], Victoria Fernandez[1], Fernando Dominguez[4], Clara Salas[6], Nuria Romero-Laorden[7], Jesus Garcia-Donas[7], Jaime Carrillo[8], Rosario Perona[2,8], Juan Carlos Triviño[9], Raquel Andrés[10], Juana María Cano[11], Bárbara Rivera[12,†], Luis Alonso-Pulpon[4], Fernando Setien[13], Manel Esteller[13,14,15], Sandra Rodriguez-Perales[16], Gaelle Bougeard[17], Tierry Frebourg[17], Miguel Urioste[2,12], Maria A. Blasco[3,**] & Javier Benítez[1,2,**]

Cardiac angiosarcoma (CAS) is a rare malignant tumour whose genetic basis is unknown. Here we show, by whole-exome sequencing of a *TP53*-negative Li–Fraumeni-like (LFL) family including CAS cases, that a missense variant (p.R117C) in *POT1* (*protection of telomeres 1*) gene is responsible for CAS. The same gene alteration is found in two other LFL families with CAS, supporting the causal effect of the identified mutation. We extend the analysis to *TP53*-negative LFL families with no CAS and find the same mutation in a breast AS family. The mutation is recently found once in 121,324 studied alleles in ExAC server but it is not described in any other database or found in 1,520 Spanish controls. *In silico* structural analysis suggests how the mutation disrupts POT1 structure. Functional and *in vitro* studies demonstrate that carriers of the mutation show reduced telomere-bound POT1 levels, abnormally long telomeres and increased telomere fragility.

[1] Human Genetics Group, Spanish National Cancer Research Center (CNIO), Melchor Fernandez Almagro 3, Madrid 28029, Spain. [2] Center for Biomedical Network Research on Rare Diseases (CIBERER), Madrid 28029, Spain. [3] Telomeres and Telomerase Group, Spanish National Cancer Research Center (CNIO), Madrid 28029, Spain. [4] Department of Cardiology. Hospital Universitario Puerta de Hierro, Mahadahonda, Madrid 28222, Spain. [5] Department of Cardiovascular Development and Repair, Centro Nacional de Investigaciones Cardiovasculares (CNIC), Madrid 28029, Spain. [6] Department of Pathology. Hospital Universitario Puerta de Hierro Majadahonda, Madrid 28222, Spain. [7] Oncology Department, Clara Campal Comprehensive Cancer Center, Sanchinarro, Madrid 28050, Spain. [8] Department of Experimental Models of Human Disease. Instituto Investigaciones Biomédicas (CSIC/UAM), Madrid 28029, Spain. [9] Bioinformatic Unit, Sistemas Genómicos, Paterna 46980, Spain. [10] Medical Oncology Service, Hospital Universitario Lozano Blesa, Zaragoza 50009, Spain. [11] Medical Oncology Service, Hospital General de Ciudad Real, Ciudad Real 13005, Spain. [12] Familial Cancer Clinical Unit, Spanish National Cancer Research Center (CNIO), Madrid 28029, Spain. [13] Cancer Epigenetics and Biology Program (PEBC), Bellvitge Biomedical Research Institute (IDIBELL), Barcelona 08908, Spain. [14] Department of Physiological Sciences II, School of Medicine, University of Barcelona, Barcelona 08007, Spain. [15] Institució Catalana de Recerca i Estudis Avançats (ICREA), Barcelona 08010, Spain. [16] Cytogenetics Unit, Spanish National Cancer Research Center (CNIO), Madrid 28029, Spain. [17] Genetics Department, Rouen University Hospital, Rouen 76000, France. * These authors contributed equally to this work. ** These authors jointly supervised this work. † Present address: Department of Human Genetics, McGill University, Montreal, Québec, Canada QC H3A 0G4. Correspondence and requests for materials should be addressed to M.U. (email: murioste@cnio.es) or to M.A.B. (email: mblasco@cnio.es) or to J.B. (email: jbenitez@cnio.es).

The incidence of primary cardiac tumours is estimated to be between 0.001 and 0.003% in general population[1]. Cardiac angiosarcoma (CAS) is a very rare malignant tumour that represents <10% of cardiac malignancies Patients are generally diagnosed at advanced stages with very poor prognosis and short survivals[2]. Patients with sporadic AS had a 5-year survival rate of 14% while familial cancer patients had a mean survival time of 4 months. Age of familial CAS onset shows a wide range but most patients affected are younger than 65 years of age[2]. Information about familial CAS is very scarce and as far as we now, only two families have been reported presenting both an earlier age of onset than sporadic[3,4] No genes responsible for these cases have been identified so far, thus humpering early diagnosis and effective treatment, which involves surgical excision combined with chemotherapy, and heart transplantation only for patients with no evidence for metastasis.

On the other hand, Li–Fraumeni syndrome (LFS) is characterized by the presence of different types of tumours including sarcomas and ASs in multiple locations such as liver, spleen, breast, head and neck, and rarely heart[5]. In most cases, LFS is triggered by the mutations in the *TP53* gene (>80%), which is the causal gene that confers susceptibility to the development of different tumours. In addition, Li–Fraumeni-like (LFL) families have similar clinical presentation and family characteristics. However, they are generally diagnosed at a later age of onset and rarely associated with mutations in *TP53* (<20% of cases)[6,7].

Here we describe the identification by whole-exome sequencing of *POT1* (*protection of telomeres* 1) gene as responsible of *TP53*-negative LFL families with CAS, as well as other tumour types.

POT1 is a component of the so-called shelterin complex (POT1, TRF1, TRF2, TIN2, TPP1 and RAP1) that binds to telomeres and has fundamental roles in chromosome stability and regulation of telomerase activity at chromosome ends[8,9].

POT1 possesses two N-terminal OB domains, which confer to this protein high specificity for single-stranded DNA sequence 5′-TAGGGTTAG-3′, thereby binding to the telomeric G-strand overhang[10–12]. In addition, POT1 binds through its C terminus to TPP1 and anchors POT1 to the shelterin complex at telomeres[13–15]. POT1 regulates telomere length (TL) by preventing telomerase access to telomeres by sequestering the DNA terminus[12,16,17]. POT1 loss-of-function mutations have been related with telomere lengthening and chromosomal instability[18,19]. Recently, germline mutations in the *POT1* gene were found in familial melanoma and glioma tumours[20–22], as well as in somatic chronic lymphocytic leukemia (CLL)[23].

Here we identify a new missense variant in *POT1* (p.R117C) as responsible of LFL locus specifically associated with CAS and demonstrate that mutation carriers show reduced telomere-bound POT1 levels, abnormally long telomeres and increased telomere fragility, highlighting a new role of *POT1* as a high susceptibility gene in familial cancer and opening therapeutical opportunities for prognosis and treatment in families with CAS.

Results

Whole-exome sequencing (WES) and candidate variant studies. A *TP53*-negative LFL Spanish family with three CAS cases and eight members with different tumours across generations were ascertained from the Cancer Genetic Consultancy of CNIO, (Fig. 1 and Table 1). Two members affected by CAS (II-10 and III-13) were selected for WES (Fig. 1; Methods for details). About

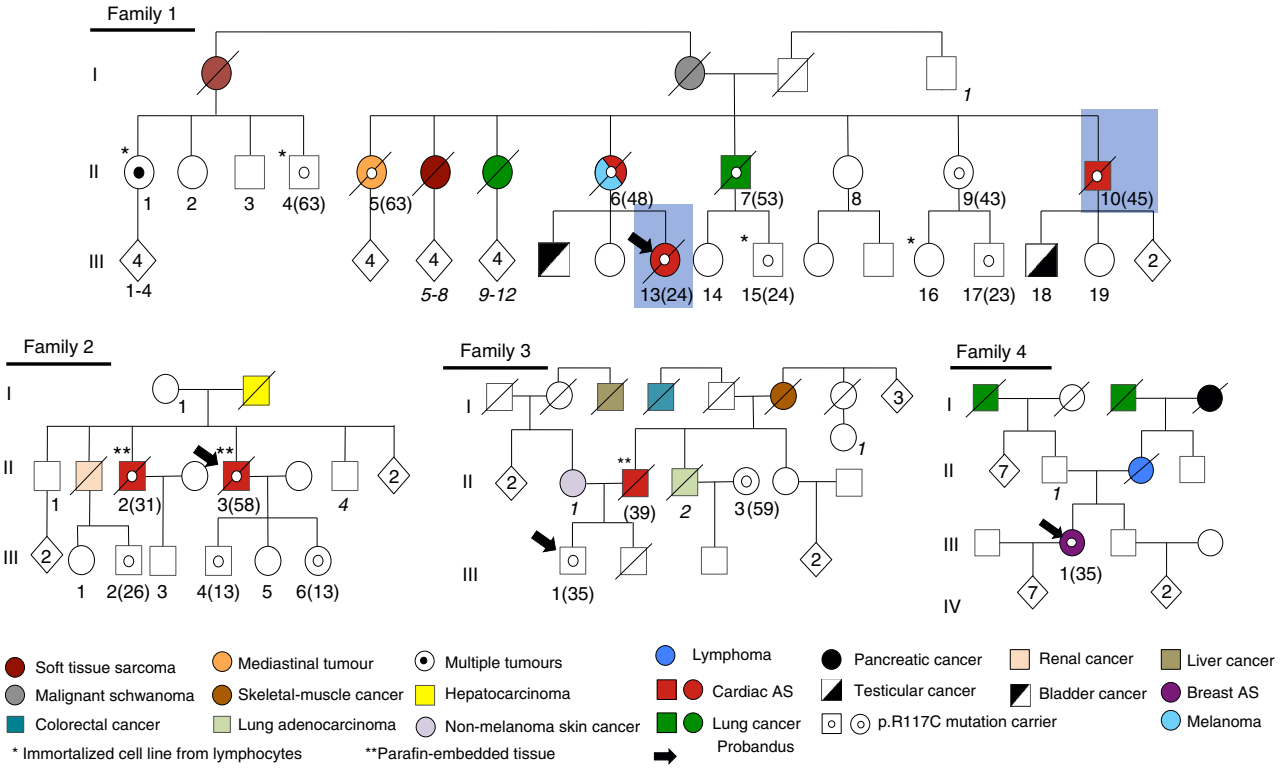

Figure 1 | Pedigrees of *TP53*-negative LFL families. Families 1, 2 and 3 have three, two and one members with cardiac angiosarcomas (CAS), respectively. CAS and other tumours are shown (colour code below the Fig.). Exomes of blue-squared CAS cases were sequenced. One member of family 4 presented with breast angiosarcoma. Only family members of whom DNA samples were available are numbered (1–19) in bold and italics. Age of onset (CAS cases) and age of sample (mutation carriers) is shown in brackets. Age of onset of other tumours is shown in the Table 1. '*' indicates immortalized lymphocyte cell lines from family 1: II-1 and II-4 (64- and 65-years old, respectively) and III-15 and III-16 (34- and 35-years old, respectively). '**' indicates paraffin-embedded tumour tissue available. Black arrows show the probandus for each family.

Table 1 | Tumour types of different members of the studied families.

p.R117C	Family		Tumour type									
			Sarcoma				Breast	CNS	Melanoma	Lung	Other	Multiple primary tumours*
			Angiosarcoma	Soft	Bone	NS						
Present	1	Carriers	3 CAS (24,45,58)**	1 (69)		1 (93)			1 (48)	2 (47,61)		1 melanoma + CAS
		NT		1 (56)						1 (43)		
	2	Carriers	2 CAS (32,41)									
		NT									1 liver (54) 1 kidney (50)	
	3	Carriers	2 CAS (40)									
	4	Carriers	1 breast (32)								1 PTC (35)	1 BA + PTC
		NT									1 lymphoma (38)	
Not Present	5			3 (41,45,50)			1 (U)	2 astroc. (12,24)			1 NHL neurofibromas (24)	1 astroc. + NHL + CM
	6			1 (42)				1 astroc. (12)			1 CRC (40)	
	7				2 (45,49)						2 stomach (65,68), 2 CCR (27,71)	
	8			1 (2)			1 (44)		1 (63)		1 CRC (58)	
	9			1 (21)			2 (45, 45)					
	10			2 (2,15)			1 (45)				1 EC (16) 1 CRC (26)	1 STS + EC + CRC
	11			2 (13,38)			1 (35)					1 STS + BC
	12			2 (54,68)								
	13				1 (7)		1 (28) 1 bilateral (35,39)	1 (54)			1 kidney	1 CM
	14			1 (U)			2 (U)	1 GBM (U)			1 stomach, 1 ovarian 1 NHL	1 BC + STS
	15		1 breast (22)				2 (43,50)				1 head&neck (45) 1CRC (70)	
	16		1 chest wall (56)				1 bilateral (48,61) 1 (80)				1 peritoneum (58)	1 CM + AS
	17		1 breast (32)								1 ALL (15)	1 ALL + BA
	18		1 breast (57)				2 (49,58)				1 prostate (51)	1 CM + BA
	19		2 bilateral breast (37,39)				1 (50)			1 (60)		
	20		1 breast (42)				1 bilateral (37,45) 1 (64)					1 CM + BA + BC
	21		1 thigh (17)	1 (U)								
	22		1 breast (15)									

ALL, acute lymphoblastic leukemia; AS, angiosarcoma; astroc., astrocytic tumour; BA, breast angiosarcoma; BC, breast cancer; CAS, cardiac angiosarcoma; CM, cutaneous melanoma; CNS, central nervous system; CRC, colorectal cancer; EC, endometrial cancer; GBM, glioblastoma multiforme; NHL, non-Hodgkin Lymphoma; NS, not specified; NT, not tested; PTC, papillary thyroid carcinoma; STS, soft tissue sarcoma; U, unknown.
Tumours of the members of family 1 without DNA sample were NT. Age at diagnosis is shown in brackets.
*Multiple primary tumours refer to tumour types described in one individual.

85% of target regions were observed with coverage $>20\times$. After filtering according to our homemade pipeline and GATK-based variant calling (Methods), we only found 394 variants in common between both samples, which were used for downstream filtering. Ten variants fulfilled our prioritization criteria, taking forward annotation and putative damaging effects into account (Supplementary Table 1). After Sanger validation and segregation studies in other members of this family, variants annotated in *POT1* (Chr7:124503601G>A), *SPEG* (chr2:220355477) and *EIF2AK* (chr2:37347280) were validated. We decided to further study *POT1*, as other germline and somatic mutations of this gene were recently found in familial melanoma and glioma tumours[20–22], as well as in CLL[23], respectively. *POT1* variant found in both CAS members (p.R117C) was highly deleterious and was neither described in the Exome variant server, Ensembl, dbSNP, 1000 genomes and COSMIC databases nor present in melanoma and glioma families with *POT1* mutations[20–22]. The variant was recently found once (heterozygous) in 121,324 studied alleles (frequency: 8.2×10^{-6}) in ExAC server. p.R117C mutation was not found in 1,520 Spanish control individuals.

We could study the complete *POT1* gene in two additional Spanish LFL families with CAS (Fig. 1, families 2 and 3) and strikingly, we found the same variant p.R117C. Then, we extended the study of the POT1 gene to 19 probands belonging to *TP53*-negative LFL families, with no CAS. Nine of them had developed different AS types and 10 presented with sarcomas (Table 1). We found one Spanish family with breast AS and other tumours carrying the same mutation.

We assessed the founder effect of the mutation, by performing haplotype studies with seven single nucleotide polymorphisms (SNPs) covering the gene (Methods). Six different haplotypes were found from the analysis of control Spanish families. Only families 1 and 2 had enough members for this study and both presented the most frequent haplotype (42%) (Supplementary Table 2).

***In silico* studies**. The p.R117 position is highly conserved across selected representative species that suggest the same residue for the last common ancestor within the phylogeny (Fig. 2a).

p.R117C mutation was located within the OB1/OB2 domains of the protein, similarly to the germline mutations found in familial melanoma and glioma[20–22] (Table 2). Tolerance to independent amino acid (aa) substitutions was calculated in a heat map representation using PredictProtein[24] showing a highly deleterious effect (Fig. 2b).

Position p.117 was found to be part of a short linear peptide motif of a disordered/unstructured region based on previous predictions[10] (hot loops), which have a critical conformation[25] and are related to alterations in predicted accessibility and protein flexibility. Thus, the PACC (predicted solvent accessibility in square Angstroem) was calculated for the residues of POT1^{R117C} protein model that were described to be located within the OB fold (from p.142 to p.152) and with stacking interaction to DNA (p.31, p.62, p.89, p.161, p223, p.245, p.266 and p.271) in POT1 protein according to the study by Lei *et al.*[10] Two residues (p.152 and p.266) had significantly different PACC scores in POT1^{R117C} protein model (Supplementary Table 3). p.152 and p.266 are oriented closed together and located at the border of domains OB1 and OB2. The consequence of this accessibility change predicts a disruption of the interaction between OB1 and OB2 in a putative three-dimensional model of the POT1^{R117C} protein (Fig. 2c).

To complete the study of these putative conformational changes observed in POT1^{R117C}, PACC scores for the same residues were calculated for predicted protein models encompassing previously described mutations in the OB1 domain in melanoma and glioma tumours (p.Y89C and p.Q94E[20], p.G95C[22], and p.R137H[21]). Moreover, we also included a protein model with a deletion from p.1 to p.126 residues (POT1$^{\Delta OB1}$) as described by Loayza and De Lange[12] and a second protein model encompassing a deletion of the whole OB1 domain (cd04497: hPOT1_OB1_like (E-value: 3.43e-45); interval from p.10 to p.141). Both p.152 and p.266 PACC score changes observed in POT1^{R117C} were not found in the rest of the studied protein models (Supplementary Table 3).

Finally, we searched for the putative protein–protein-binding regions of wild-type (wt) POT1 protein and 14 positions were found to be significantly relevant (threshold > 20) (Supplementary Table 4). The same positions were studied in all mutated protein models. A putative protein-binding region annotated in position p.499 was significantly lost in the POT1^{R117C} protein model (Supplementary Table 4). p.499 is a well-conserved position with high deleterious tolerance to aa change (86,4) at the conserved POT1 C terminus within the TPP1-binding domain (Fig. 2b)[13]. Interestingly, this protein-binding region was lost in the protein model with the deletion of the whole OB1 domain (from p.10 to p.141) but was unaffected in the other mutant models and POT1$^{\Delta OB1}$ (with a deletion in OB1 domain from p.1 to p.126) (ref. 12).

Expression and protein studies. To study whether the missense variant (p.R117C) affects POT1 transcriptional and protein levels, we performed quantitative PCR (qPCR) from complementary DNA (cDNA) and western blot (WB) analyses from primary lymphocytes (PL) from carriers and in non-carriers. We found no significant differences in *POT1* mRNA levels in PL from carriers compared with non-carriers (Supplementary Fig. 1). Similarly, we did not find significant differences in POT1 protein levels (two-tailed student's *t*-test, $P = 0.1$) as determined by WB (Supplementary Fig. 1). Next, we set to determine POT1 levels localized at telomeres by double immunofluorescence with POT1 and TRF1 antibodies (another telomere-binding protein from the shelterin complex used here to localize telomeres)[26]. To this end, we used immortalized lymphoblastoid cell lines (LCLs) derived from members II-1, II-4, III-15 and III-16 (Fig. 1, family 1). Immunofluorescence levels with anti-TRF1 antibody were similar for all family members independently of the carrier status (Fig. 3a,b). In contrast, the intensity of POT1 telomeric foci was significantly lower in p.R117C carriers (two-tailed student's *t*-test, $P < 0.0001$) than controls and there was also a decrease in the number of co-localizations (Fig. 3a,b).

To address the effect of this mutation on the binding of POT1 to telomeric chromatin *in vivo*, we performed chromatin immunoprecipitation (ChiP) with the four LCLs using antibodies against POT1, TRF1 and TRF2 (Methods). The hybridization signal of telomeric DNA immunoprecipitated with anti-TRF1 and anti-TRF2 (positive telomeric controls) was not significantly different in mutation carriers compared with non-carriers (Fig. 3c). However, a significant reduction of hybridization signal was observed in mutation carriers when telomeric DNA was immunoprecipitated with anti-POT1 antibodies (two-tailed student's *t*-test, $P = 0.004$).

POT1 is recruited to telomere through interaction with TPP1 (ref. 13). The reduced levels of telomere-bound POT1 observed in mutation carriers (Fig. 3a–c), as well as the *in silico* analysis (Supplementary Table 4) suggest that POT1^{R117C} might be defective in TPP1 binding. To test this, we performed co-immunoprecipitation assays with *in vitro*-translated MYC-tagged POT1^{R117C} and FLAG-tagged TPP1. As controls, we used MYC-tagged wt POT1 and a mutant MYC-POT1$^{\Delta OB1}$ that has been shown to be defective in single strand DNA binding but functional in its interaction with TPP1 (ref. 12). In addition, we also used a FLAG-tagged mutant TPP1^{OBD} that lacks both the POT1 and TIN2 interaction domain[27]. Equal amounts of the different MYC-POT1 and FLAG-TPP1 variants were mixed as indicated and TPP1-POT1 complexes immunoprecipitated with anti-MYC antibody (Fig. 3d; Supplementary Fig. 2). As expected, FLAG-TPP1 was pulled down with MYC-POT1 and MYC-POT1$^{\Delta OB1}$ while FLAG-TPP1^{OBD} was not detected with any of the *POT1* variants used in the assay. However, immunoprecipitation of MYC-POT1^{R117C} recovered FLAG-TPP1 to a much lesser extent than wt MYC-POT1. Indeed, FLAG-TPP1 was only faintly detected when the immunoblots were developed under long exposure time (Fig. 3d). These results confirmed that mutant POT1^{R117C} is affected in its ability to bind TPP1.

We next sought to determine whether the p.R117C substitution affected the ability of POT1 to bind to the 3′ end of the G-rich telomeric overhang, as suggested by the *in silico* analysis. *In vitro*-translated MYC-POT1, MYC-POT1$^{\Delta OB1}$ and MYC-POT1^{R117C} were incubated with radio-labelled telomeric single-stranded DNA (ssDNA) and with c-MYC (9E10) antibody. Visualization of the protein-DNA complexes by electrophoretic mobility shift assay confirmed that wt POT1 efficiently bound telomeric ssDNA, whereas POT1^{R117C} bound telomeric ssDNA less efficiently (Fig. 3e; Supplementary Fig. 2). As expected, POT1$^{\Delta OB1}$ was unable to bind to the telomeric sequence.

Studies in telomeres. In line with dysfunctional POT1 that is usually associated with increased DNA damage at telomeres (the so-called telomere-induced foci (TIF)) and occurrence of telomere fragility, we observed significantly increased multi-telomeric signal events (MTS) in mutation carriers compared with non-carriers (two-tailed student's *t*-test, $P < 0.0001$) (Fig. 3f) and an increase of positive cells for γH2AX (two-tailed student's *t*-test, $P = 0.05$) a DNA damage marker (Fig. 3g). Double immunofluorescence staining with γH2AX and TRF1 antibodies was performed to determine TIFs. The results showed a significant increase in the percentage of cells with more than five TIFs in carriers as compared with non-carriers (two-tailed student's *t*-test, $P = 0.003$) (Fig. 3g). Of note, we did not observe end-to end fusions in mutation carriers.

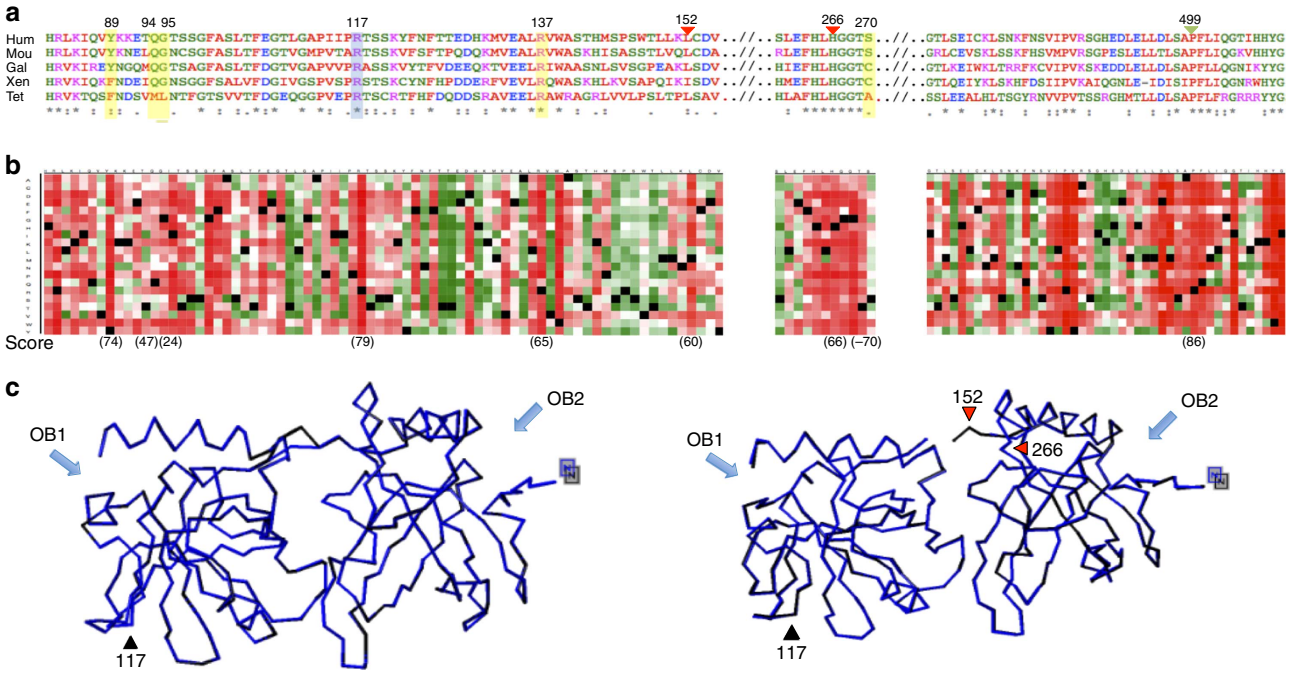

Figure 2 | *In silico* studies. (**a**) Amino acid conservation across representative phylogeny of POT1 orthologues (tet, *Tetraodon nigroviridis*; xen, *Xenopus laevis*; gal, *Gallus gallus*; hum, *Homo sapiens*; mou, *Mus musculus*). The mouse POT1a gene sequence was used in the alignment. Position p.117 is shown in blue; mutations described in previous studies are shown in yellow. Triangles indicate positions with putative conformational changes (red) and loss of TPP1-binding site (green) due to the p.R117C mutation. '*' indicates amino acid (aa) conserved in all POT1 orthologues. (**b**) Heat map representation shows the tolerance to independent aa substitutions (*y*-axis) for each position of the protein (*x*-axis). Dark red indicates the highest score for a deleterious effect (score 100); white indicates a small effect; green indicates a neutral effect/no effect (score −100); and black represents the corresponding wild-type residue. Deleteriousness effect score is shown for highlighted positions. (**c**) Putative tertiary structure. p.152 and p.266 residues change PACC score value driving a putative protein conformation change. Left: homology-based three-dimensional model of human POT1 (Uniprot, Q9NUX5). Right: structural impact of the p.R117C mutation using the same algorithm from Protein Model Portal (Uniprot, PSI_SBKB). Black triangle shows the loop where p.117 is located. Red triangles show the principal detected structural changes (p.152 and p.266). Blue arrows show OB1 and OB2 domains.

Table 2 | Deleterious germinal mutations described in the *POT1* gene.

Position	Allele	Exon	Amino acid change	Domain	Source
g.124503601	G>A	4	p.Arg117Cys	OB1	*
g.124503684	T>C	4	p.Tyr89Cys	OB1	Robles-Espinoza *et al.*[20]
g.124503670	G>C	4	p.Gln94Glu	OB1	
g.124493077	C>A	6	p.Arg273Leu	OB2	
g.124465412	C>T	14	Splice site	Telomere/TPP1 binding	
g.124503540	C>T	4	p.Arg137His	OB1	Shi *et al.*[21]†
g.124499043	C>T	5	p.Asp224Asn	OB2	
g.124493086	C>T	6	p.Ser270Asn	OB2	
g.124469308	C>G	13	p.Ala532Pro	Telomere/TPP1 binding	
g.124464052	C>G	15	p.Gln623His	Telomere/TPP1 binding	
g.124503667	C>A	4	p.Gly95Cys	OB1	
g.124481048	C>A	10	p.Glu450‡	Telomere/TPP1 binding	Bainbridge *et al.*[22]
g.124464068	TTA>T	15	p.Asp617Glu (fs)	Telomere/TPP1 binding	

fs, frame shift; POT1, protection of telomeres 1.
*Mutation described in the present study.
†Founder mutation.
‡Stop codon.

We evaluated the effect of the p.R117C mutation in TL. We measured it by qPCR in peripheral blood lymphocytes from members of family 1. TL values were adjusted for age. We consistently found longer telomeres in mutation carriers compared with non-carriers (two-tailed student's *t*-test, $P=0.02$) (Fig. 4a). TL was also calculated with fluorescence *in situ* hybridization quantitative detection (quantitative fluorescence *in situ* hybridization (qFISH))[28] and we validated that TL was significantly longer in mutation carriers compared with controls (two-tailed student's *t*-test, $P<0.0001$) (Fig. 4b). In addition, a higher percentage of short telomeres <3 kb was found in non-carriers compared with p.R117C mutant carriers comparing older members (II-1 and II-4, 64.5 old in average) (Fig. 4c). Otherwise, no significant differences among members of family 1 were found regarding *in vitro* telomeric repeat amplification (TRAP) telomerase activity (Fig. 4d).

Abnormal telomeres elongation could be the consequence of increased telomere recombination, to the so-called alternative

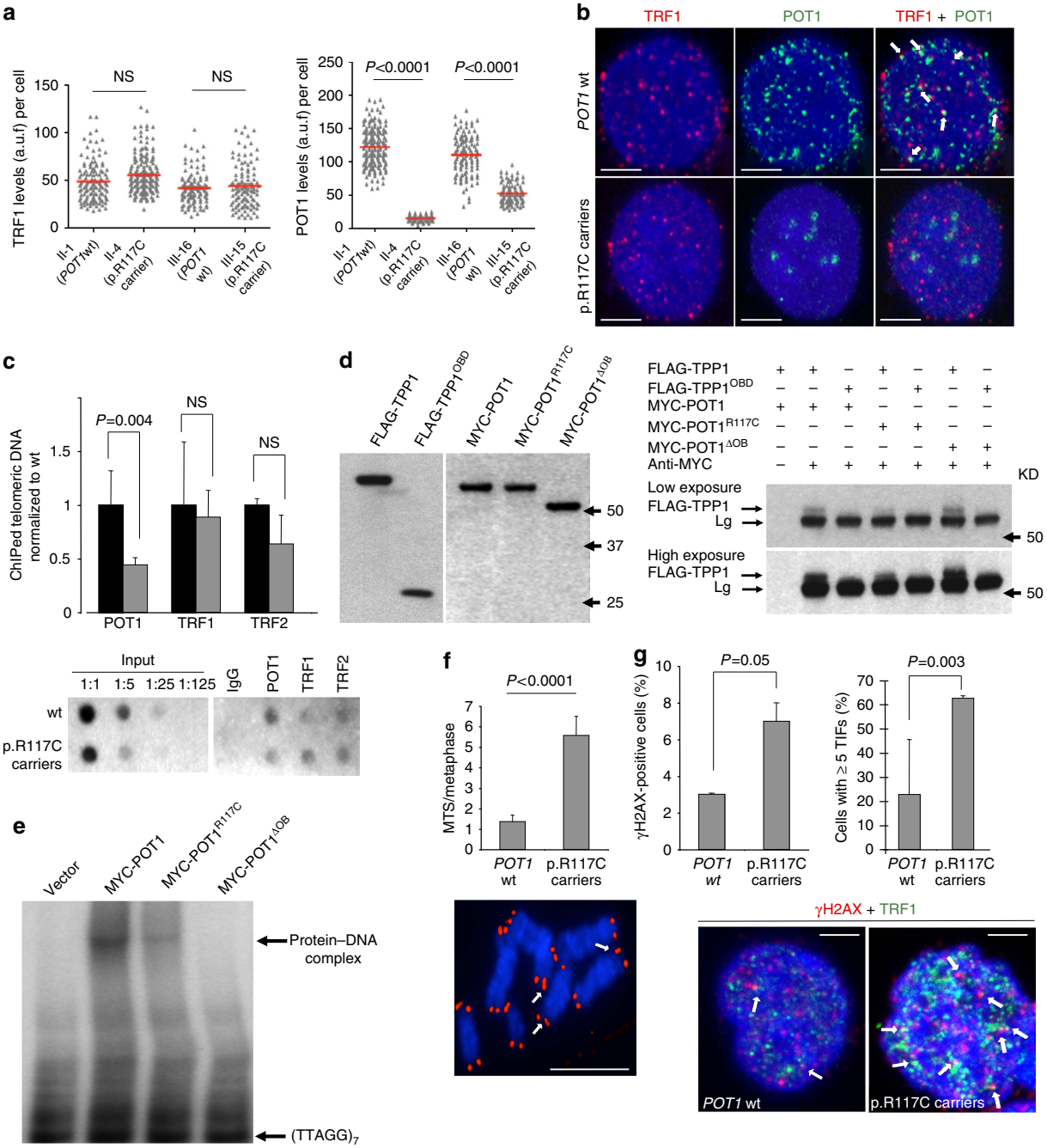

Figure 3 | *POT1*^{R117C} mutation affects telomere binding and induces telomeric damage. (**a**) Quantification of telomere-bound TRF1 (left panel) and POT1 (right panel) protein levels in immortalized LCLs corresponding to p.R117C carriers and non-carriers. Two independent experiments with replicated samples were performed. a.u.f., arbitrary units of fluorescence. (**b**) Representative images of TRF1 (red) and POT1 (green) double immunofluorescence in wild-type and p.R117C carriers. White arrows indicate colocalization of both proteins (yellow spots). Scale bar, 5 μm. (**c**) Quantification of telomeric DNA bound to POT1, TRF1 and TRF2 by ChIP analysis. IgG was used as negative control. Results were normalized to input chromatin. Black bars, wild-type; grey bars, p.R117C carriers. Two independent experiments from each genotype were performed. Lower panel: representative ChIP dot-blot is shown. (**d**) Left panel: western blot analysis of *in vitro*-translated FLAG-TPP1, FLAG-TPP1^{OBD}, MYC-POT1, MYC-POT1^{R117C} and MYC-POT1$^{\Delta OB1}$. Right Panel: p.R117C substitution decreased POT1 binding capacity to TPP1. Co-immunoprecipitation assays of the *in vitro*-translated proteins. FLAG-TPP1 was pulled down with MYC antibody and revealed by FLAG antibody. FLAG-TPP1 lacking the TIN2 and POT1 binding domain, FLAG-TPP1OBD, and a POT1 mutant lacking its OB1 domain were used as controls. Two exposures are showed. (**e**) p.R117C substitution decreased POT1 binding capacity to telomeric ssDNA. Electrophoretic mobility shift assay of [^{32}P]-labelled oligonucleotide (5′-TTAGGG-3′)$_7$ in the presence of the indicated *in vitro*-translated POT1 proteins. Data from two independent experiments are shown in **d**,**e**. (**f**) Upper panel: quantification of multitelomeric signal (MTS) events per metaphase in primary lymphocytes by telomeric FISH ($n=2$ in triplicate). Lower panel: example of MTS (white arrows). Red fluorescence shows telomere signals. Scale bar, 5 μm. (**g**) Quantification of cells positive for γH2AX (left) and per cent of cells with >5 telomeric induced foci (TIFs) (right) in immortalized LCLs ($n=2$ in triplicate). Lower panel: representative images of γH2AX and TRF1 immunofluorescence. White arrows show examples of TIFs (yellow spots) with anti-TRF1 (green fluorescence) and anti-γH2AX (red fluorescence). Scale bar, 5 μm. Values are expressed as mean + s.e. The two-tailed student's unpaired *t*-test was used for the statistical analysis, NS, not significant. DAPI (blue) was used for DNA labelling.

lengthening of telomeres (ALT). We evaluated this possibility by quantification of recombination events specifically at telomeric repeats, the so-called telomere sister chromatid exchanges (T-SCEs). We observed a similar frequency of T-SCE in mutations carriers (0.43 ± 0.14) compared with wt controls (0.29 ± 0.19) (Fig. 4e) ruling out a possible ALT mechanism of telomere elongation in lymphocytes.

Finally, paraffin-embedded tissues were also studied. Loss of heterozygosity of *POT1* locus was evaluated in four CAS tumours from families 1 and 2. Loss of heterozygosity was observed in only one of the studied cases while the other three cases presented a heterozygosis profile. The three CAS tumours from families 2 and 3 (one also with normal cardiac tissue) were also studied for ultra-bright spots (ubs) in telomeres. FISH for ubs in telomeres showed an increased number of ubs-positive signals (5.56 positive signals × 100/total signals on average) compared with normal tissue (0.68 positive signals × 100/total signals; Fig. 4f). This alteration correlated with the TL of tumours, which was highly increased compared with wt samples ($P = 0.0001$) and mutation carriers ($P = 0.0075$) adjusted for age (two-tailed student's *t*-test) (Fig. 4g).

***In vitro* experiments**. As the identified mutation is present in heterozygosis in all the analysed carriers, we hypothesize that POT1^{R117C} protein functions in a dominant-negative manner. To further validate this possibility, we create heterologous Hela cell lines using retroviral vectors to express wt *MYC-POT1*, *MYC-POT1*^{R117C} and *MYC-POT* $^{\Delta OB1}$ alleles[26] in the presence of endogenous POT1. Double immunofluorescence microscopy analysis with MYC and TRF1 antibodies of Hela cells showed that wt and mutant Myc-POT1$^{\Delta OB1}$ proteins but no cells expressing the MYC epitope alone (empty vector) show colocalization of both telomeric proteins MYC-POT1 and TRF1. Hela cells expressing MYC-POT1^{R117C} showed a similar pattern than those expressing the vector alone and only few cells presented few MYC foci that colocalized with TRF1 (Fig. 5a,b). Quantification of TRF1 nuclear intensity revealed no significant differences among Hela cells expressing either the empty vector or the wt and mutant *POT1* alleles (Fig. 5a,b). Decreased amount of telomere bound of MYC-POT1^{R117C} protein in Hela cells is in agreement with the decreased amount of protein observed in lymphocytes by immunofluorescence and ChIP analysis using POT1 antibodies (Fig. 3a–c).

To address, whether heterologously *MYC-POT1*^{R117C} over-expression recapitulates the observed effects in lymphocytes we analysed the functional effects of POT1^{R117C} expression in Hela cells. TL in Hela cells infected with retroviral empty vector, *MYC-POT1, MYC-POT1*^{R117C} and *MYC-POT1*$^{\Delta OB1}$ was measured by quantitative telomere FISH on metaphase spreads. Increased TL was observed in both Hela cells expressing *MYC-POT1*$^{\Delta OB1}$ and *MYC-POT1*^{R117C} compared with both cells infected with empty vector and *MYC-POT1* after 30 population doublings (Fig. 5c,f).

Finally, analysis of chromosome aberrations in metaphase spreads of the different transduced Hela cells, revealed a moderate but significant increase in MTS events in those expressing *MYC-POT1*^{R117C} and *MYC-POT1*$^{\Delta OB1}$ as compared with those expressing either the empty vector or wt *MYC-POT1* (Fig. 5d,f). In addition, an increase in γH2AX-positive cells was detected in Hela cells infected with *MYC-POT1*^{R117C} as compared with those harbouring either the empty vector, *MYC-POT1 wt* or *MYC-POT1*$^{\Delta OB1}$ (Fig. 5e).

Discussion

We have found a novel damaging missense variant (p.R117C) in the *POT1* gene in *TP53*-negative LFL families with CAS and other tumours. Mutations in *POT1* were recently associated with familial melanoma[20,21] and glioma[22] and as a driver for CLL[23], uncovering a new role of this gene not only as telomere protector, but also as one of the main responsible genes for development of different familial cancer types. The mutation was the same in the four studied families. Haplotype studies suggested a possible founder effect within the Spanish population although larger studies are necessary to confirm this issue.

There are several consequences of this mutation that we have demonstrated by *in silico*, *in vivo* and *in vitro* studies. Thus, *in silico* studies showed that the p.R117C substitution putatively disrupted the interaction between OB1 and OB2 (Fig. 2d) and affect the protein-binding site to TPP1 (Supplementary Table 4), which might result in the loss of capability of the POT1^{R117C} protein to interact with ssDNA and to be recruited to telomeres. The predicted conformation change might be explained as a consequence of the substitution of a polar basic aa (Arginine) with a non-polar thiol aa (Cysteine) at position p.117 with the capability to generate disulfide bonds.

In silico analyses were confirmed by *in vivo* assays analysing the binding of mutated POT1 protein to telomeres. Double immunofluorescence with POT1 and TRF1 in immortalized LCLs suggests that the variant has an important effect on the levels of POT1 at telomeres by showing significant decreased levels in mutation carriers. *In vitro* assays demonstrated that POT1^{R117C} is deficient at both, in TPP1 interaction and in telomeric ssDNA binding, affecting POT1 function.

Although the mutation was located within the OB1/OB2 domains of the protein, similarly to the germline mutations found in familial melanoma and glioma[20–22] (Table 2), it was specific of CAS. In fact, only a member from family 1 carrying the mutation (II-6) developed melanoma, and no members from reported families with melanoma or gliomas carrying *POT1* mutations presented CAS[20–22]. The fourth family (Fig. 1, family 4) did not have any member with CAS but the family structure was small and we cannot rule out the possibility that asymptomatic carriers of the mutation will develop a CAS in the future.

These findings stress the importance of POT1 domains in cancer development and raise the intriguing open question about the correlation between the genotype and the phenotype. Our *in silico* studies suggest that the putative conformational changes in POT1 proteins due to the mutations described in melanoma and glioma tumours are different from those observed for POT1^{R117C} (Supplementary Tables 3 and 4). Because POT1 is described in tight coordination with the rest of shelterin complex proteins, we cannot rule out that different conformational changes might have different effects on the shelterin complex function.

Similarly to other members of the shelterin complex, disruption of POT1 function was associated to increased DNA damage at telomeres and occurrence of telomere fragility[23]. In our case, defective POT1^{R117C} function has shown to lead to a moderate increase in MTS, and in telomere DNA damage, that could account for the genomic instability that these cases present. Moreover, increased TL was confirmed in mutation carriers. This is in agreement with previously described POT1 mutations in CLL and familial melanoma and glioma patients that showed abnormally elongated telomeres[20–23]. In our cases, TL was markedly different between mutation carriers and non-carriers within older members, suggesting that there was a cumulative effect in telomere elongation with age (Fig. 4b,c). Differences observed in the amount of telomeres shorter than 3 Kb in older members suggest a downfall in the telomere shortening through aging, indicating abnormal telomere biology in mutation carriers. We showed similar *in vitro* TRAP telomerase activity levels in both carriers and non-carriers, indicating no defects in telomerase assembly or function (Fig. 4d). Thus, the longer telomeres

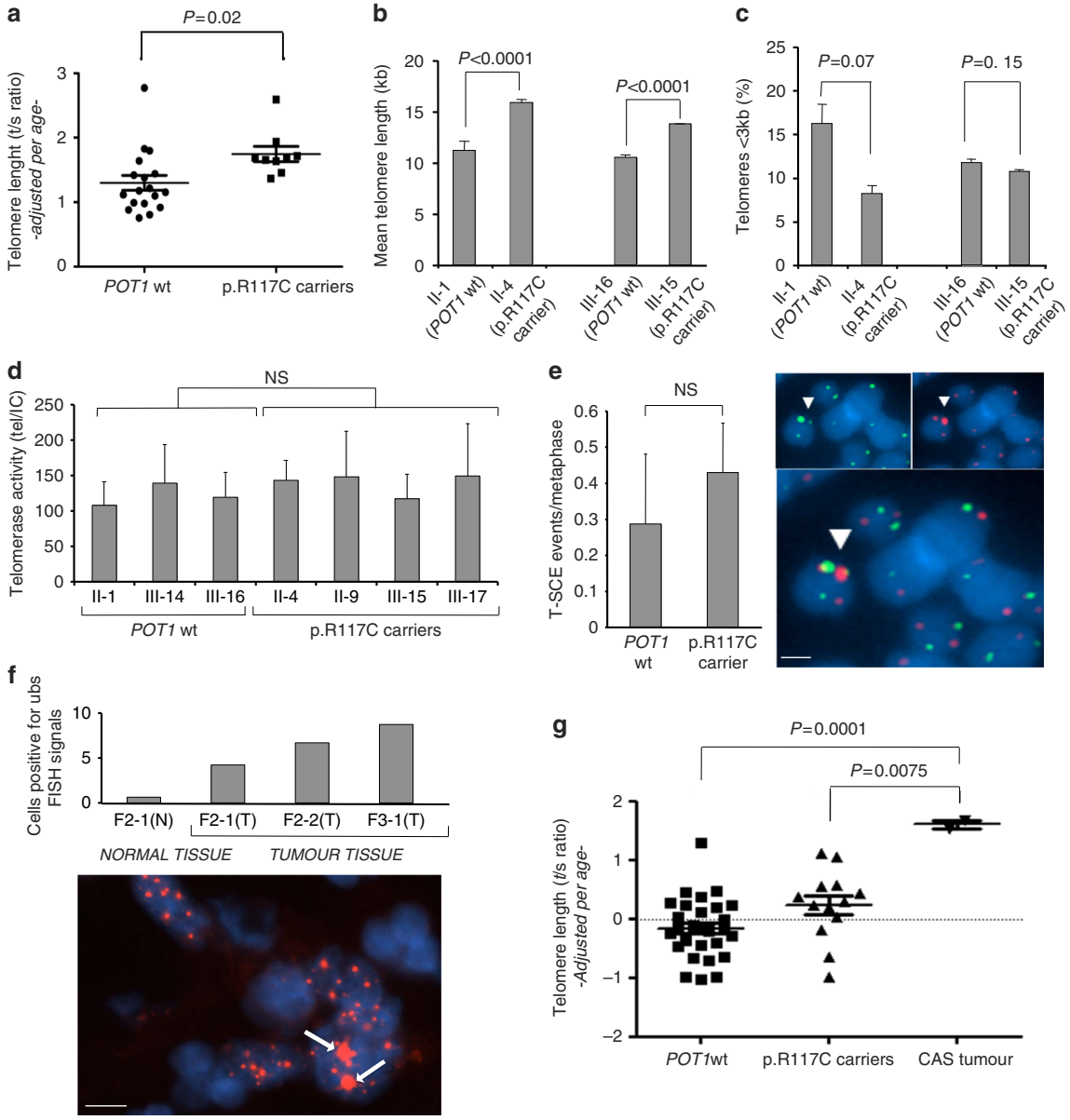

Figure 4 | POT1^{R117C} carriers present longer telomeres. (**a**) Telomere length (TL) analysis by qPCR (*t/s* ratio) for family 1 members ($n=29$). (**b**) TL analysis by qFISH of primary immortalized LCLs corresponding to non-carriers (II-1 and III-16) and p.R117C carriers (II-4 and III-15). (**c**) Percentage of telomeres shorter than 3 kb of primary immortalized LCLs corresponding to non-carriers (II-1 and III-16) and p.R117C carriers (II-4 and III-15). (**d**) TRAP Tel/IC ratio values for telomerase activity calculated from primary lymphocytes of different members of family 1 ($n=7$). In **b**–**d** two independent experiments with samples in triplicate were performed. (**e**) Left panel: number of telomere sister chromatid exchange (T-SCE) events/metaphase in primary lymphocytes by CO-FISH ($n=2$ individuals per genotype in triplicate). Right panels: representative CO-FISH images showing the leading (green) and lagging (red) telomere strands. T-SCEs are indicated with arrows. DAPI (blue) was used for DNA labelling. Below a magnified merge image is shown. Scale bar, 1 μm. (**f**) Upper panel: per cent of cells positive for ultra-bright spots (ubs) at telomeres by FISH in three different paraffin-embedded cardiac tumour (T) and normal (N) tissue samples carrying the mutation from members of family 2 (F2) and 3 (F3). Lower panel: examples of large red spots corresponding to positive signals (white arrows). DAPI (blue) was used for DNA labelling. Scale bar, 10 μm. (**g**) TL adjusted for age of wt and p.R117C carriers of all members of families 1, 2 and 3 and the 3 CAS tumours. DNA from CAS samples was extracted from paraffin-embedded tissues. Values are expressed as mean + s.e. and the two-tailed student's unpaired *t*-test was used for the statistical analysis, NS, not significant.

observed in mutation carriers are rather due to alterations in *in vivo* telomerase recruitment and function on telomeres. In fact, POT1 has been shown to be important to prevent telomerase access to telomeres by sequestering the DNA terminus[12,16,17]. We show that POT1^{R117C} is defective in both binding to TPP1 and binding to ssDNA telomeric DNA. It is therefore tempting to speculate that POT1^{R117C} fails to inhibit telomerase due to the reduced telomere-bound POT1^{R117C}, as well as to defective binding to telomeric G-strand overhang. In addition, given the defective binding of POT1^{R117C} to single G-strand overhang (Fig. 3d,e), telomeric damage could also stem from defective maintenance of the 3′ G-strand overhang needed for proper T-loop formation. Indeed, abnormal telomere elongation due to the consequence of increased telomere recombination (ALT) was ruled out as no differences in T-SCE were found in lymphocytes between carriers and non-carriers. Thus, lack of functional POT1 seems to affect telomere structure and expose them to abnormal elongation by a normal telomerase activity.

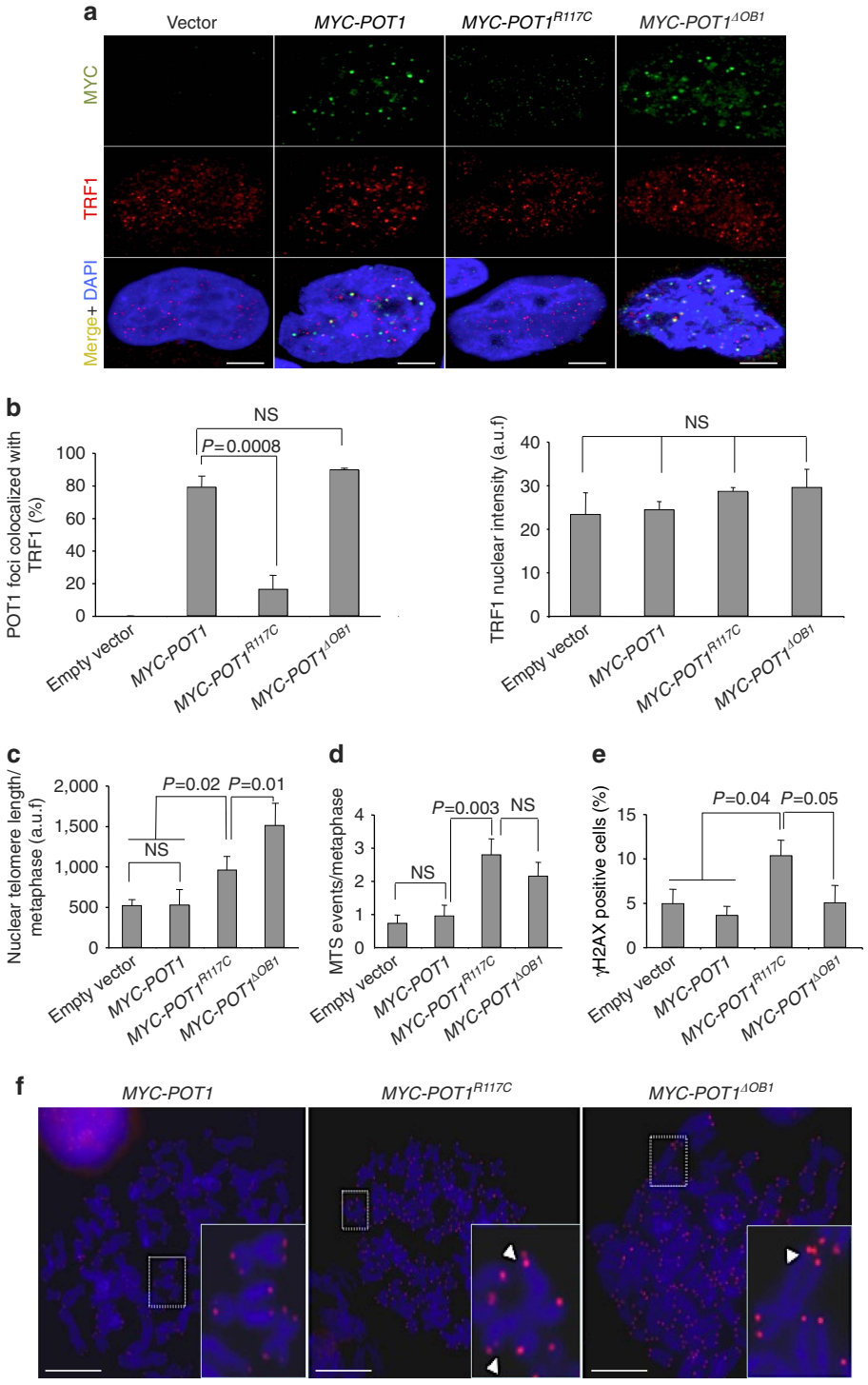

Figure 5 | Heterologous POT1^{R117C} expression induces telomere lengthening. (**a**) Representative images of MYC (green) and TRF1 (red) double immunofluorescence in Hela cells with endogenous expression of POT1 protein infected with retroviral empty vector, *MYC-POT1, MYC-POT1*^{R117C} and *MYC-POT1*$^{\Delta OB1}$. DAPI (blue) was used to DNA labelling. Scale bar, 5 μm. (**b**) Quantification of MYC-POT1 and TRF1 colocalization foci (left panel) and of nuclear TRF1 foci intensity (right panel) (a.u.f., arbitrary units of fluorescence) in Hela cells infected with retroviral empty vector, *MYC-POT1, MYC-POT1*^{R117C} and *MYC-POT1*$^{\Delta OB1}$. (**c**,**d**) Quantification of nuclear telomere length per metaphase (a.u.f) (**c**) and of multitelomeric signal (MTS) events/metaphase (**d**) in Hela cells infected with retroviral empty vector, *MYC-POT1, MYC-POT1*^{R117C} and *MYC-POT1*$^{\Delta OB1}$. (**e**) Per cent of γH2AX-positive cells in Hela cells infected with retroviral empty vector, *MYC-POT1, MYC-POT1*^{R117C} and *MYC-POT1*$^{\Delta OB1}$. (**f**) Representative qFISH images of metaphase spreads. Examples of MTS are shown in the magnified insets (arrow). Red fluorescence shows telomere signal. DAPI (blue) was used for DNA labelling. Scale bar, 5 μm. Two independent infections were performed. Values are expressed as mean + s.e. The two-tailed student's unpaired *t*-test was used for the statistical analysis, NS, not significant.

The telomeric phenotypes observed in lymphocytes from p.R117C variant carriers were validated by *in vitro* studies in Hela cell lines created using retroviral vectors expressing wt *MYC-POT1*, *MYC-POT1*^{R117C} and *MYC-POT1*$^{\Delta OB1}$ (ref. 26) in the presence of endogenous POT1. We confirmed that the POT1^{R117C} protein acts in a dominant-negative manner, analogous to that previously reported for the POT1^{DOB1} mutant[26], as well as for others *POT1* variants found in CLL[23]. In this system, we also detected decreased POT1^{R117C} protein levels at telomeres, moderate increase in MTS incidence, higher telomeric DNA damage and a telomere lengthening effect. So, it is tempting to speculate that telomere elongation induced by this mutation in *POT1* may constitute the underlying molecular mechanism favouring tumour incidence.

The identification of *POT1* mutation in CAS is important, since it provides the possibility for earlier diagnosis of people at risk. Currently this tumour is diagnosed in advanced stages when distant metastases are present and the survival is very poor, as surgical resection is not effective. Larger studies are necessary to fully assess the clinical spectrum associated with this mutation and other mutations along the whole *POT1* gene. Future work is needed to address POT1^{R117C} relation not only with familial but also with sporadic CAS and its role in LFL cases including ASs other than cardiac.

Methods

Patients. Index cases from LFL families negative for mutations and large deletions of the *TP53* gene were selected for this study. Three of our families had members affected with CAS plus other tumours (Fig. 1). The rest of the families fulfilled the LFL criteria but they did not have any member with a CAS tumour (Table 1). Families were selected from the Spanish National Cancer Research Center (CNIO), Hospital Puerta de Hierro and Clara Campal Center (Spain), and Rouen University Hospital (France). DNA from most of the family members and whenever possible total mRNA and protein were collected from lymphocytes.

A group of 1,520 samples from a Spanish control population was used for genotyping the POT1 variant by denaturing high performance liquid chromatography[29]. Heteroduplex was amplified with primers of the exon 4, which encompassed the candidate variant (Supplementary Table 5). Genotyping was performed with WAVE Nucleic Acid Fragment System from Transgeomics and Navigator Software. Amplification was performed with standard conditions ((95 °C, 5 min; (44 °C, 30 seg.; 64 °C, 30 seg.; 72 °C, 45 seg.) × 30 cycle; 72 °C, 10 min.).

The study was approved by the ethics committee of the different centres and informed consent was obtained from all participants.

Establishment of B LCLs. Lymphoblasts from different members of family 1 were immortalized: II-1 (aged 64), II-4 (aged 65), III-15 (aged 35) and III-16 (aged 34). LCLs were established by Epstein–Barr virus (EBV) transformation/infection of peripheral blood mononuclear cells (PBMC)[30]. PBMCs were incubated with B95-8 cell supernatant (containing EBV in the presence of 10 μg ml^{-1} of phytohemagglutinin in R.P.M.I1640 supplemented with 20% (v/v) heat-inactivated, foetal calf serum, 2 mM of L-Glutamine, 100 U ml^{-1} of penicillin, 100 μg ml^{-1} of streptomycin and 0.5 μg ml^{-1} of Amphotericin B (Gibco, Invitrogen)). Cells were plated and incubated at 37 °C, 5% CO_2 and routinely grown in R.P.M.I1640 culture medium supplemented with 10% heat-inactivated foetal calf serum, 2 mM of L-Glutamine, 100 U ml^{-1} of penicillin and 100 μg ml^{-1} of streptomycin.

Paraffin-embedded tissue samples. Paraffin-embedded tissue samples of CAS members from families 2 and 3 were collected (Fig. 1). DNA was extracted using the DNeasy Blood & Tissue Kit (Cat. No. 69504, Qiagen) following the manufacturer's instructions. Selected tumour tissue was evaluated a pathologist (C.S.).

Whole-exome sequencing. Exomes from two members of family 1 with CAS (II-10 and III-13) were captured and enriched using the SureSelect Human All Exon Kit (78 Mb) (Agilent Technologies). Enriched samples were paired-end sequenced on an Illumina Genome Analyzer II sequencing platform, using two lanes per sample and generating 78-bp-long reads. Filtering of reads and variant calling were done with the Rubioseq software suite of parallelized pipelines[31]. PCR duplicates, overrepresented sequences and low quality reads were filtered with a modular set of analyses considering per base and per sequence quality scores (Fastqc >30) and N content.

BWA files of short reads were aligned with the genome of reference (GRCh37/hg19). GATK-based variant calling was performed for aligned reads considering DP (read depth) values of >30 and QD (quality by depth) scores for a variant confidence of >1.00. A MAF <3% of was considered. Variants were also filtered by position (non-synonymous, essential splice site, frame shift or gain/loss of stops). Their potential damaging effect was assessed using the VEP[32] script software package (including Sift, Polyphen and Condel damage predictors) from Ensembl.

Filtered variants were prioritized for segregation studies when they were (i) previously described in other pathogenic processes (COSMIC database), (ii) annotated in genes with related functions or involved in tumourogenetic processes, and (iii) annotated in genes suggested to be related to cardiac function.

Prioritized variants from 10 candidate genes were validated by Sanger sequencing and segregation studies were performed among the different members of family 1. Candidate variants that were found in the three CAS cases and mediastinal tumour patients were selected. PCR was performed using standard conditions (95 °C, 5 min; (44 °C, 30 s.; * °C, 30 s.; 72 °C, 45 s) × 30 cycle; 72 °C, 10 min). *: °C annealing of the corresponding primer. Sequences of the primers are listed in Supplementary Table 5.

POT1 gene study. Sanger sequencing of the candidate *POT1* variant was performed in 19 probands from LFL families negative for *TP53* mutations. The entire *POT1* gene was sequenced for cases negative for the candidate mutation. The primers used for Sanger sequencing of the 15 exons are listed in Supplementary Table 5. PCR was performed using standard conditions ((95T °C, 5 min; (44T °C, 30 s; *T °C, 30 s; 72 °C, 45 s) × 30 cycle; 72T °C, 10 min). *: T °C annealing of the corresponding primer.

Haplotype study. A haplotype study was performed to confirm the possible founder effect of our variant. Seven SNPs covering the gene were used (Supplementary Table 2). Selected trios (parent and two offspring) from families 1 and 2 were studied to establish the haplotype carrying the mutation. Trios from 15 healthy Spanish families were used to determine the different haplotypes in the Spanish population and their frequencies. The primers used for Sanger sequencing of the seven SNPs are listed in Supplementary Table 5.

Real-time qPCR. Expression studies for *POT1* gene genes was performed with Real-Time qPCR with cDNA obtained from reverse transcription of 1,200 ng of total RNA from PBMCs using the High Capacity cDNA Reverse Transcription Kit (Applied Biosystems #4368814). PCR was carried out with ~25 ng μl^{-1} of cDNA and the POWER SYBR green PCR Master Mix (Applied Biosystems #4367659). Quantification was performed using Sequence Detection System 7900HT (Applied Biosystems). Expression levels were evaluated with the $\Delta\Delta C_t$ method[33] in triplicate and normalized to the expression levels of *GAPDH*, which was used as a standard. PCR was run with exon 10 forward primer and exon 11 reverse primer to avoid amplification of genomic DNA (Supplementary Table 5). PCR was performed using standard conditions (95T °C, 5 min; (44T °C, 30 seg.; 58T °C, 30 seg.; 72 °C, 45 seg.) × 30 cycle; 72T °C, 10 min).

Western blotting. WB was performed with 50 μg of total protein isolated from lysed PBMCs. Protein expression levels of POT1 were determined using rabbit polyclonal anti-POT1 antibody and normalized to GAPDH levels using anti-GAPDH antibody (Supplementary Table 6). The hybridization signal was quantified using ImageJ 1.43 u software (W. Rasband, the National Institutes of Health). Protein expression was evaluated with the $\Delta\Delta C_t$ method[33].

ChIP assay. ChIP assays were performed with LCLs from family 1. Cells in culture were cross-linked with formaldehyde (1%) during 15 min at room temperature. The cross linking reaction was stopped by addition of glycine (0.125 M) during 5 min. Cells were washed twice with cold PBS, collected by centrifugation and lysed in lysis buffer (1%SDS, 10 mM EDTA, 50 mM Tris-HCl pH 8.0, protease inhibitors (P8340, Sigma)). Protein/DNA extracts were sonicated and centrifuged at 14,000 r.p.m. for 15 min. Protein concentration was determined (DC protein assay, Bio-Rad), and chromatin from 200 μg total protein extract was used per immunoprecipitation with 4 μl of either anti-POT1, anti-TRF2 or anti-TRF1 antibody (Supplementary Table 6) and protein A/G PLUS-agarose beads (Santa Cruz Biotechnology, sc-2003)[34]. The immunoprecipitated DNA was transferred to a Hybond N$^+$ membrane using a dot-blot apparatus. The membrane was then hybridized with a telomeric probe containing 1.6 kb of 5′-TTAGGG-3′ repeats. Quantification of the signal was performed with ImageQuant software (Molecular Dynamics). The amount of telomeric DNA after ChIP was normalized to the total input telomeric DNA.

Bioinformatics tools to assess the *in silico* studies. Heat map representation of independent substitutions for each position of the protein and aa tolerance test was performed with PredictProtein[24]. Secondary structures (β-strands, α-helix and loops) of the putative POT1 model were based on REPROFSec prediction. The predictions of the annotation (minimum REPROFSEc score of 5) of conserved secondary structures and evolutionary profiles for POT1 carrying the p.R117C mutation were based on several original prediction methods (NORSnet,

DISOPRED2, PROFbval and Ucon) implemented in PredictProtein[24]. Solvent accessibility notation (PACC) was annotated using the PROFAcc prediction algorithm[35] also implemented in ProteinPredict[24]. Protein binding regions were found using the ISIS algorithm[36] and SomeNA predictor method (also implemented in ProteinPredict[24]). Annotation of residues was based on crystallography studies of POT1 (ref. 10). A homology-based three-dimensional model of human POT1 was taken from Uniprot (Q9NUX5). Protein modelling for POT1 carrying the p.R117C mutation (PSI_SBKB) was performed using the Protein model portal (available at http://www.proteinmodelportal.org/).

Real-time qPCR of TL. TL was measured by qPCR using DNA from blood samples. Quantification of TL (*t*/*s* ratio) was done through quantification of telomere repeat copy number (*t*) and the *36B4* reference gene (*s*)[37]. Telomere repeats were amplified with TEL primers (tel 1, 5′-GGTTTTTGAGGGTGAGG GTGAGGGTGAGGGTGAGGGT-3′; tel 2, 5′-TCCCGACTATCCCTATCCCTA TCCCTATCCCTATCC-CTA-3′), and *36B4* gene was amplified with 36B4u (5′-CAGCAAGTGGGAAGGTGTAATCC-3′) and 36B4d (5′-CCCATTCTATCA TCAACGGGTACAA-3′) primers[37]. The final TL value for each sample was determined under standard conditions in three independent measurements. Independent measurements had a correlation of r 0.80. The coefficient of variation was obtained for telomere (average 5%, range 1–50%) and *36B4* (average 1.7%, range 0.02–16%). TL values were adjusted for age by calculating a regression line with 330 DNA controls[38]. Each sample was adjusted for the difference between the observed TL and the predicted value using the regression line. Following this method we adjusted *t*/*s* values obtained by qPCR ($y = -0.0174x + 1.96$). PCR was performed using standard conditions (see real-time qPCR section).

High-throughput qFISH. Mononuclear cells (150,000) from PBMCs were plated in triplicate onto Poly-L-Lysine pre-coated Greiner 96-well plates for 4 h at 37 °C. Poly-L-Lysine was removed before cell addition (100,000 lymphocytes per well). When lymphocytes attached to the wells, cells were washed three times with PBS and then fixed during 1 h at room temperature with methanol/acetic acid (3:1 vol/vol). The plates were overnight dried at 37 °C. The cells were rehydrated in PBS during 15 min, fixed for 1 min in 4% formaldehyde, treated with pepsin (1 mg ml^{-1}, pH 2.0) at 37 °C for 10 min, washed with PBS, fixed for 1 min in 4% formaldehyde, washed with PBS and dehydrated in a ethanol series (70, 90, 100%). The Cy-3-labelled $(C_3TA_2)_3$ PNA probe (Perseptive Biosystems, Bedford, MA) was dissolved in a hybridization buffer containing 70% formamide/10 mM Tris pH 7.0/0.25% (w/v) blocking reagent (0.5 μg ml^{-1}) (Dupont, Boston, MA). The hybridization mixture was placed onto the wells, followed by DNA denaturation (5 min, 85 °C). After hybridization (2 h, room temperature), slides were washed twice with 70% formamide/0.1% BSA/10 mM Tris pH 7.2 for 15 min, followed by three washes of 5 min in TBS-Tween 0.08% containing DAPI (4′,6-diamidino-2-phenylindole). The cells were dehydrated in a ethanol series (70, 90, 100%) and air dried. Finally, Moviol mounting medium was added to the wells[28]. Wells were sealed (Alumaseal; Sigma-Aldrich) and stored at 4 °C in the dark. Samples were processed by High-throughput microscopy within 48 h after sample preparation by using the Opera-Acapella system (Perkin Elmer) for image acquisition and analysis[28]. TL values were calculated using individual telomere spots.

Telomeric FISH on metaphase spreads. Primary mononuclear cells from peripheral blood (PBMCs) were stimulated with 7.5 ng ml^{-1} 12-O-tetradecanoylphorbol-13-acetate in R.P.M.I medium supplemented with FBS, penicillin-streptomycin, β-mercaptoethanol, sodium pyruvate, nonessential aa and L-glutamine. Colcemid was added at a concentration of 0.1 μg ml^{-1} during 12 h. Cells were then recovered, subjected to hypotonic shock and fixed in methanol/acetic acid (3:1). QFISH hybridization on metaphase spreads was performed as described above for HT-QFISH[39]. Metaphase spreads were captured on a Leitz Leica DMRB fluorescence microscope. At least 10 metaphase spreads per subject were analysed, and chromosomal aberrations were quantified and represented as frequency per metaphase.

Measurement of T-SCE events by chromosome orientation FISH. Measurement of sister telomere recombination events (T-SCE) was performed using chromosome orientation FISH (CO-FISH). Mononuclear cells from peripheral blood (PBMCs) were stimulated as above and sub-cultured in the presence of BrdU (5′-bromo-2′-deoxyuridine; Sigma) at a final concentration of 1×10^{-5} M, and then allowed to replicate their DNA once at 37 °C for 24 h. Colcemid was added at a concentration of 0.1 μg ml^{-1} during the last 6 h. Cells were then recovered, subjected to hypotonic shock and fixed in methanol/acetic acid (3:1). CO-FISH was performed using first a telomeric $(5′\text{-CCCTAA-}3′)_7$ PNA probe labelled with Cy3 and then a second telomeric $(5′\text{-TTAGGG-}3′)_7$ PNA probe labelled with Alexa-488 (Supplementary Table 6)[40]. Metaphase spreads were captured on a fluorescence microscope (DMRB).

Retroviral expression. The pLPC-human *MYC-POT1* and pLPC-human *MYC-POT1$^{\Delta OB1}$* (deleted OB1 domain) plasmids were a gift of de Lange (Addgene plasmid 12387 and 13241)[12]. The POT1 variant encoding p.R117C change, *MYC-POT1^{R117C}*, was generated by site-directed mutagenesis of the pLPC-human *MYC-POT1* using the QuickChange XL site-directed mutagenesis kit (Agilent Technologies) using oligonucleotides hPOT1-R117C-F (5′-gggagcccctatcatacctTgc acttcaagcaagtat-3′) and hPOT1-R117C-R (5′-atacttgcttgaagtgcAaggtatgatagggct ccc-3′). Retroviruses were packaged in 293T cells (ATCC-CRL-3216) using pCL-Ampho packaging vector. Hela cells (ATCC-CCL-2) were seeded onto p-10 plates to 30% of confluency 24 h before infection. Three consecutive infections every 12 h were performed by adding 5 ml of viral supernatant. Cells were allowed to recover for 24 h in growth medium before undergoing selection with puromycin for 3 days. Cells then underwent serial passaging and collected at the indicated population doubling points.

Inmunofluorescence staining techniques. Lymphoblastoid (this work) and Hela (ATCC-CCL-2) cells were plated onto Poly-L-Lysine pre-coated coverslips, treated for 5 min with Triton X-100 buffer[41] for nuclear extraction, fixed for 10 min in 4% buffered formaldehyde, permeabilized with 0.2% PBS-Triton for 5 min and blocked with foetal bovine serum in PBS for 1 h. Samples were incubated o/n at 4 °C with the primary antibody at 1:250 dilution. TIFs were detected using rabbit polyclonal anti-TRF1 and a mouse monoclonal antibody raised against phospho-histone2 H2AX-Ser139 (γH2AX) (Supplementary Table 6). Telomeric POT1 and TRF1 foci were detected using a rabbit polyclonal anti-POT1 and a mouse monoclonal antibody anti-TRF1 (Supplementary Table 6). MYC-POT1 was detected using a mouse monoclonal c-MYC antibody. Slides were further incubated with 488-Alexa or 555-Alexa-labelled secondary antibodies (Supplementary Table 6). Slides were mounted in Vectashield with DAPI. Confocal microscopy was performed at room temperature with a laser-scanning microscope (TCS SP5; Leica) using a Plan Apo 63 Å-1.40 numerical aperture oil immersion objective (HCX; Leica). Maximal projection of Z-stack images generated using advanced fluorescence software (LAS) was analysed with the Definiens XD software package. The DAPI images were used to detect signals inside the nuclei.

TRAP analysis. Telomerase activity was measured using protein extract from PBMCs cultured in RPMI supplemented with 20% FBS and phytohemagglutinin during 4–5 days. Telomerase activity was determined under recommended standard conditions of the TRAPEZE Telomerase Detection S7700 Kit (Millipore) for TRAP using radioisotopic detection. Telomerase activity was determined in each sample using 0.5, 0.25 and 0.125 μg of protein extract and normalized with the internal control included in the assay[38].

Ultra-bright telomere spots in paraffin-embedded tissue. Ultra-bright telomere spots were detected by FISH on paraffin-embedded tissue slides. The Histology FISH Accessory Kit (DAKO) was used following the manufacturer's instructions. A telomere-specific PNA-Cy3-labelled probe (DAKO) was used for the detection of ubs[42]. Tissue images were captured using a CCD camera with focus motor (Photometrics SenSys camera) connected to a PC running the Cytovision image analysis system (Applied Imaging Ltd., UK) and Z-stack software.

G-strand binding and co-immunoprecipitation assays. The TNT-coupled reticulocyte lysate kit (Promega) was used to *in vitro* synthesize MYC-POT1, MYC-POT1^{R117C}, MYC-POT1$^{\Delta OB1}$, FLAG-TPP1 and FLAG-TPP1^{OBD} (refs 12,27). For co-immunoprecipitation assays, 3 μl of either MYC-POT1, MYC-POT1^{R117C} or MYC-POT1$^{\Delta OB1}$ with either 3 μl of either FLAG-TPP1 or FLAG-TPP1^{OBD} translation reaction and incubated at 37 °C for 20 min. About 500 μl of NETN buffer (20 mM Tris pH 8.0, 100 mM NaCl, 1 mM EDTA, 0.5% NP-40) and 1 μg of anti-MYC (9E10) were added to each protein mix and incubated at 4 °C. The antibody complexes were pulled down with protein A/G agarose beads, washed four times with NETN and eluted with 40 μl 2 × SDS loading buffer. The eluted proteins (10 μl) were separated by SDS–PAGE, transferred to nitrocellulose membranes and probed with a monoclonal FLAG antibody.

DNA-binding assays were performed in 20 μl reaction mixtures, 5 μl of each translation reaction was incubated with 10 nM 5′-[^{32}P]-labelled telomeric oligonucleotide containing seven TTAGGG repeats, 1 μg of the nonspecific competitor DNA poly (dI-dC) and 2 μl of anti c-MYC (9E10) (C-40, Santa Cruz Biotechnology) in binding buffer (25 mM HEPES-NaOH pH 7.5, 100 mM NaCl, 1 mM EDTA and 5% glycerol)[23]. Reactions were incubated for 10 min at room temperature, and protein-DNA complexes were analysed by electrophoresis on a 6% polyacrylamide Tris-borate EDTA gel run at 80 V for 3 h.

Statistics. Significance of expression differences among individuals grouped according to genotype (wt versus mutation carriers) was evaluated with the non-parametric Kolmogorov–Smirnov test to determine normal distribution of values within the groups. Student's *t*-test was used for comparison of normally distributed values among genotypes. Differences were considered to be significant when the exact *P* value was <0.05.

Study approval. Written informed consent was received from participants prior to inclusion in the study.

References

1. Butany, J. *et al.* Cardiac tumours: diagnosis and management. *Lancet Oncol.* **6,** 219–228 (2005).
2. Patel, S. D. *et al.* Primary cardiac angiosarcoma—a review. *Med. Sci. Monit.* **20,** 103–109 (2014).
3. Casha, A. R., Davidson, L. A., Roberts, P. & Nair, R. U. Familial angiosarcoma of the heart. *J. Thorac. Cardiovasc. Surg.* **124,** 392–394 (2002).
4. Keeling, I. M., Ploner, F. & Rigler, B. Familial cardiac angiosarcoma. *Ann. Thorac. Surg.* **82,** 1576 (2006).
5. Kamihara, J., Rana, H. Q. & Garber, J. E. Germline TP53 mutations and the changing landscape of Li–Fraumeni syndrome. *Hum. Mutat.* **35,** 1–40 (2014).
6. Silva, A. G. *et al.* The profile and contribution of rare germline copy number variants to cancer risk in Li–Fraumeni patients negative for TP53 mutations. *Orphanet J. Rare Dis.* **9,** 63 (2014).
7. Ognjanovic, S., Olivier, M., Bergemann, T. L. & Hainaut, P. Sarcomas in TP53 germline mutation carriers: a review of the IARC TP53 database. *Cancer* **118,** 1387–1396 (2012).
8. Bunch, J. T., Bae, N. S., Leonardi, J. & Baumann, P. Distinct requirements for Pot1 in limiting telomere length and maintaining chromosome stability. *Mol. Cell. Biol.* **25,** 5567–5578 (2005).
9. Patel, T. N. V., Vasan, R., Gupta, D., Patel, J. & Trivedi, M. Mini-review shelterin proteins and cancer. *Asian Pac. J. Cancer Prev.* **16,** 3085–3090 (2015).
10. Lei, M., Podell, E. R. & Cech, T. R. Structure of human POT1 bound to telomeric single-stranded DNA provides a model for chromosome end-protection. *Nat. Struct. Mol. Biol.* **11,** 1223–1229 (2004).
11. Baumann, P. & Cech, T. R. Pot1, the putative telomere end-binding protein in fission yeast and humans. *Science (New York, N.Y.)* **292,** 1171–1175 (2001).
12. Loayza, D. & De Lange, T. POT1 as a terminal transducer of TRF1 telomere length control. *Nature* **423,** 1013–1018 (2003).
13. Liu, D. *et al.* PTOP interacts with POT1 and regulates its localization to telomeres. *Nat. Cell Biol.* **6,** 673–680 (2004).
14. Kibe, T., Osawa, G. A., Keegan, C. E. & de Lange, T. Telomere protection by TPP1 is mediated by POT1a and POT1b. *Mol. Cell. Biol.* **30,** 1059–1066 (2010).
15. Chen, L.-Y., Liu, D. & Songyang, Z. Telomere maintenance through spatial control of telomeric proteins. *Mol. Cell. Biol.* **27,** 5898–5909 (2007).
16. Nandakumar, J. & Cech, T. R. Finding the end: recruitment of telomerase to telomeres. *Nat. Rev. Mol. Cell Biol.* **14,** 69–82 (2013).
17. Baumann, P. & Price, C. Pot1 and telomere maintenance. *FEBS Lett.*. **584,** 3779–3784 (2010).
18. He, H. *et al.* POT1b protects telomeres from end-to-end chromosomal fusions and aberrant homologous recombination. *EMBO J.* **25,** 5180–5190 (2006).
19. Hockemeyer, D., Daniels, J. P., Takai, H. & de Lange, T. Recent expansion of the telomeric complex in rodents: two distinct POT1 proteins protect mouse telomeres. *Cell* **126,** 63–77 (2006).
20. Robles-Espinoza, C. D. *et al.* POT1 loss-of-function variants predispose to familial melanoma. *Nat. Genet.* **46,** 478–481 (2014).
21. Shi, J. *et al.* Rare missense variants in POT1 predispose to familial cutaneous malignant melanoma. *Nat. Genet.* **46,** 482–486 (2014).
22. Bainbridge, M. N. *et al.* Germline mutations in shelterin complex genes are associated with familial glioma. *J. Natl. Cancer Inst.* **107,** dju384–dju384 (2014).
23. Ramsay, A. J. *et al.* POT1 mutations cause telomere dysfunction in chronic lymphocytic leukemia. *Nat. Genet.* **45,** 526–530 (2013).
24. Yachdav, G. *et al.* PredictProtein-an open resource for online prediction of protein structural and functional features. *Nucleic Acids Res.* **42,** W337–W343 (2014).
25. Linding, R. *et al.* Protein disorder prediction: Implications for structural proteomics. *Structure* **11,** 1453–1459 (2003).
26. De Lange, T. Shelterin: the protein complex that shapes and safeguards human telomeres. *Genes Dev.* **19,** 2100–2110 (2005).
27. Sexton, A. N., Youmans, D. T. & Collins, K. Specificity requirements for human telomere protein interaction with telomerase holoenzyme. *J. Biol. Chem.* **287,** 34455–34464 (2012).
28. Canela, A., Vera, E., Klatt, P. & Blasco, M. A. High-throughput telomere length quantification by FISH and its application to human population studies. *Proc. Natl Acad. Sci. USA* **104,** 5300–5305 (2007).
29. Michailidou, K. *et al.* Large-scale genotyping identifies 41 new loci associated with breast cancer risk. *Nat. Genet.* **45,** 353–361 361e1-2 (2013).
30. Martinez, M. *et al.* The Δ 4-desaturation pathway for DHA biosynthesis is operative in the human species: differences between normal controls and children with the Zellweger syndrome. *Lipids Health Dis.* **9,** 1–10 (2010).
31. Rubio-Camarillo, M., Gómez-López, G., Fernández, J. M., Valencia, A. & Pisano, D. G. RUbioSeq: a suite of parallelized pipelines to automate exome variation and bisulfite-seq analyses. *Bioinformatics (Oxford, England)* **29,** 1687–1689 (2013).
32. McLaren, W. *et al.* Deriving the consequences of genomic variants with the Ensembl API and SNP Effect Predictor. *Bioinformatics* **26,** 2069–2070 (2010).
33. Livak, K. J. & Schmittgen, T. D. Analysis of relative gene expression data using real-time quantitative PCR and the 2(− Delta Delta C(T)) Method. *Methods* **25,** 402–408 (2001).
34. García-Cao, M., O'Sullivan, R., Peters, A. H. F. M., Jenuwein, T. & Blasco, M. A. Epigenetic regulation of telomere length in mammalian cells by the Suv39h1 and Suv39h2 histone methyltransferases. *Nat. Genet.* **36,** 94–99 (2004).
35. Schlessinger, A. & Rost, B. Protein flexibility and rigidity predicted from sequence. *Proteins* **61,** 115–126 (2005).
36. Ofran, Y. & Rost, B. ISIS: interaction sites identified from sequence. *Bioinformatics* **23,** 13–16 (2007).
37. Cawthon, R. M. Telomere measurement by quantitative PCR. *Nucleic Acids Res.* **30,** e47 (2002).
38. Benitez-Buelga, C. *et al.* Impact of chemotherapy on telomere length in sporadic and familial breast cancer patients. *Breast Cancer Res. Treat.* **2,** 385–394 (2014).
39. Samper, E. *et al.* Normal telomere length and chromosomal end capping in poly(ADP-ribose) polymerase-deficient mice and primary cells despite increased chromosomal instability. *J. Cell Biol.* **154,** 49–60 (2001).
40. Samper, E., Goytisolo, F. A., Slijepcevic, P., van Buul, P. P. & Blasco, M. A. Mammalian Ku86 protein prevents telomeric fusions independently of the length of TTAGGG repeats and the G-strand overhang. *EMBO Rep.* **1,** 244–252 (2000).
41. Muñoz, P. *et al.* TRF1 controls telomere length and mitotic fidelity in epithelial homeostasis. *Mol. Cell. Biol.* **29,** 1608–1625 (2009).
42. Abedalthagafi, M. *et al.* The alternative lengthening of telomere phenotype is significantly associated with loss of ATRX expression in high-grade pediatric and adult astrocytomas: a multi-institutional study of 214 astrocytomas. *Modern Pathol.* **26,** 1425–1432 (2013).

Acknowledgements

We are grateful to T. de Lange (The Rockefeller University) and K. Collins (The University of California) for providing POT1 and TPP1 plasmids, respectively. J.B.'s laboratory is partially funded by the Spanish Ministry of Health PI12/00070, the Spanish Ministry of Science and Innovation (INNPRONTA 2012) and the Spanish Research Network on Rare diseases (CIBERER). O.C. is granted by the CIBERER and C.B.-B. by the PI12/00070 supported by FEDER funds. P.G.-P. is partially supported by the Spanish Ministry of Health PI11/0699, PI12/01941 and RD12/0042/0066. M.A.B.'s laboratory is funded with the Spanish Ministry of Science and Innovation, projects SAF2008-05384 and 2007-A-200950 (TELOMARKER), European Research Council Advanced grant GA#232854, the Körber Foundation, Fundación Botín and Fundación Lilly. R.P.' lab is partially funded by PI11/0949 Supported by FEDER funds.

Author contributions

J.B. and M.A.B. conceived the original idea and led the work. J.B., M.A.B., O.C. and P.M. designed the experiments and wrote the paper. O.C. carried out the WES variant calling/filtering, molecular genetic and *in silico* analyses. P.M. carried out the molecular, cellular and functional analysis. O.C. and P.M. contributed equally to this work. M.U., P.G.-P., F.D., N.-R.L., J.-G.D., R.A., J.M.C., L.A.-P., C.S were involved in CAS study and family selection. Samples collection: J.C., R.P. and C.B.-B. were involved in telomeres and telomerase studies. J.C.T. was involved in bioinformatics. B.P.-H., B.R., V.F., S.R.-P. were involved in molecular genetics and cytogenetics studies. M.U., P.G.-P. were involved in genetic counselling and clinical follow-up. F.S. and M.E. were involved in cell lines establishment. G.B., T.F., M.U. were involved in LFL families and samples collection.

Additional information

Acession codes. Whole genome sequencing data have been deposited in ArrayExpress under accession code E-MTAB-3858.

Supplementary Information accompanies this paper at http://www.nature.com/naturecommunications

Competing financial interests: The authors declare no competing financial interests.

Reprints and permission information is available online at http://npg.nature.com/reprintsandpermissions/

How to cite this article: Calvete, O. *et al.* A mutation in the *POT1* gene is responsible for cardiac angiosarcoma in *TP53*-negative Li–Fraumeni-like families. *Nat. Commun.* 6:8383 doi: 10.1038/ncomms9383 (2015).

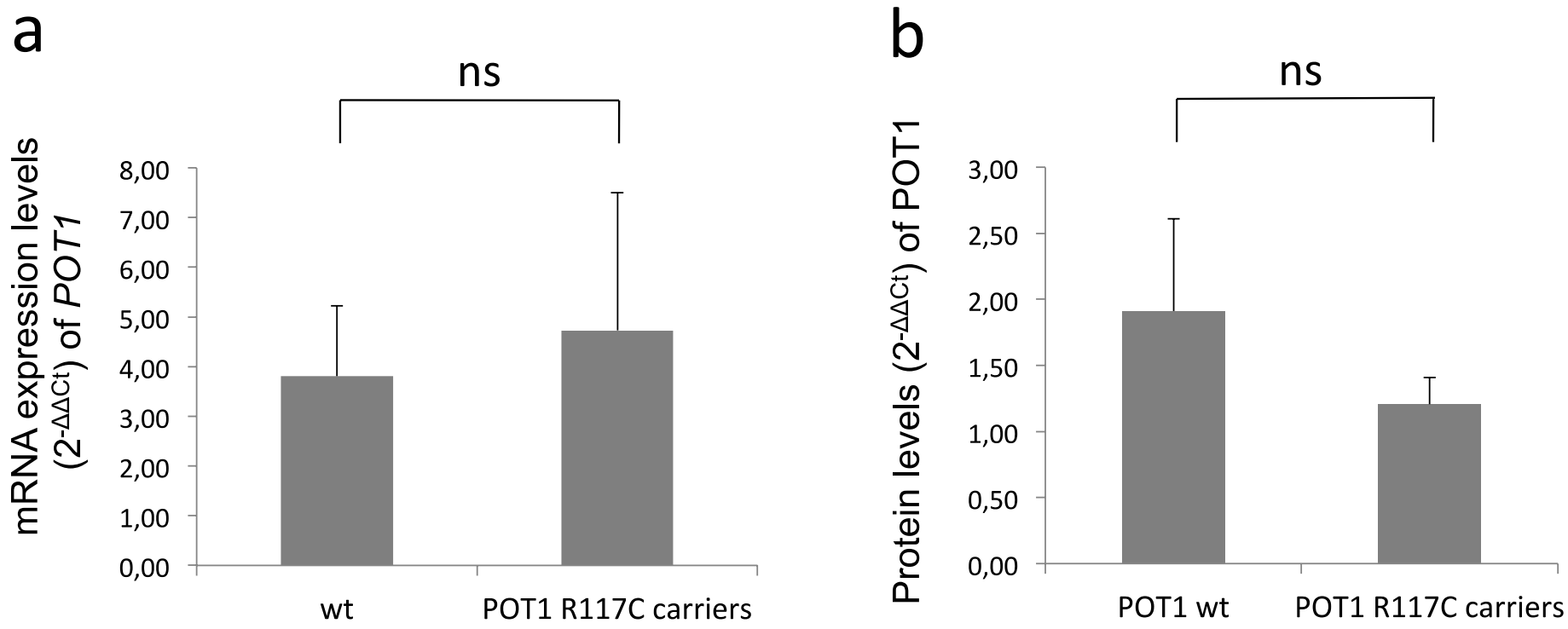

Supplementary Figure 1: Analyses of family 1 members. The T-student's t –test was used for the statistical analysis of normal distributed values. a) Comparison of mRNA expression levels between *POT1* wild type (wt) and p.R117C mutation carriers. normalized with *GAPDH* as control b) Values of POT1 protein levels for several members of family 1 (n=7) normalized for GAPDH control . There was a trend towards decreased POT1 levels in mutation carriers (1.91±0.69) compared with non-carriers (1.21±0.2) (p=0.1).

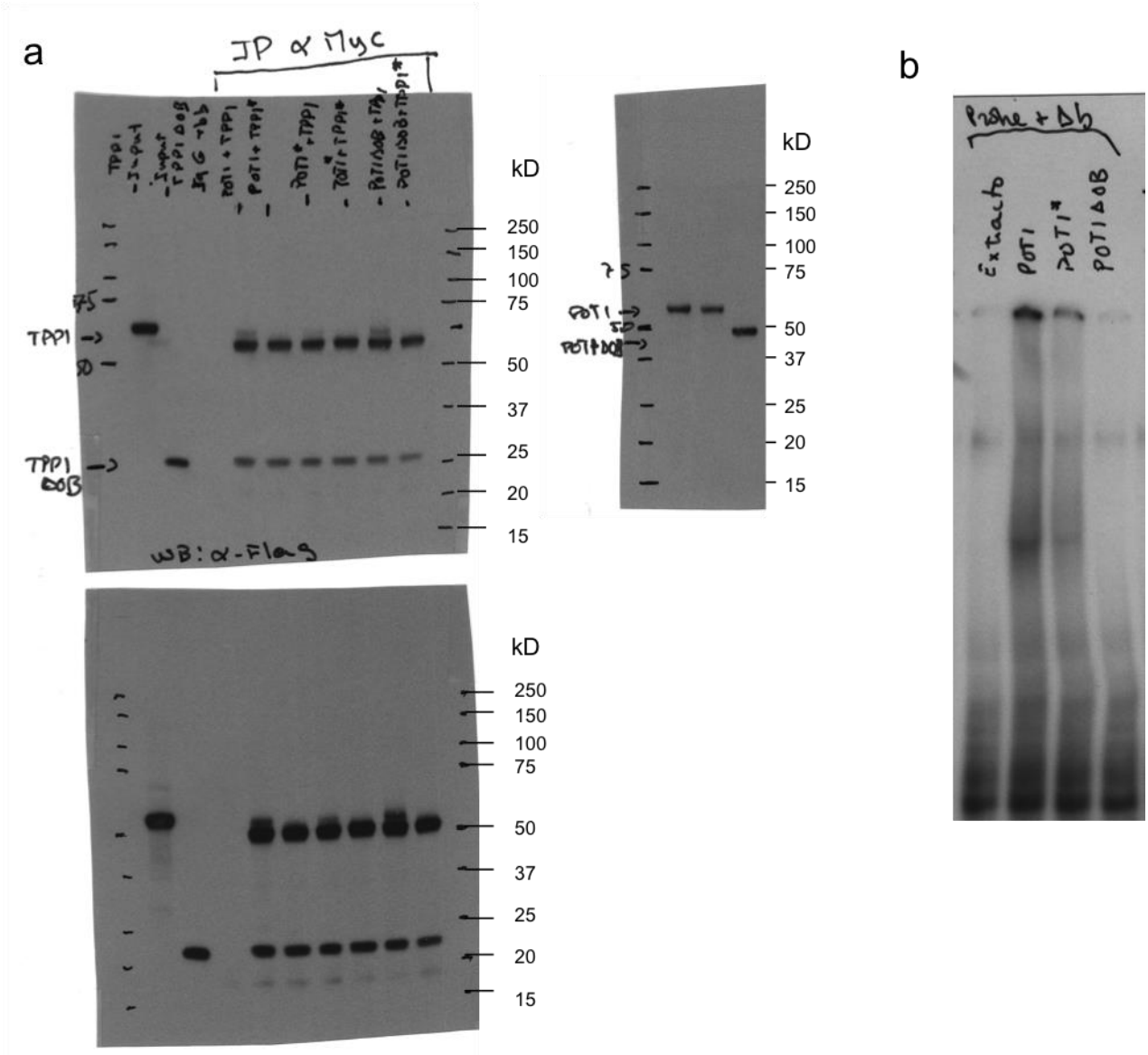

Supplementary Figure 2: Uncropped scans of the gels/blots. (a) Western blots presented in Figure 3d and (b) of the electrophoretic mobility shift assay (EMSA) presented in Figure 3e. The molecular weight ladder is shown to the right of each blot.

Supplementary Table 1: Candidate variants to study further segregation in members of family 1.

Prioritization Criteria	Variant position	GENE	Protein change	Function	Tissue expression	COSMIC/Pathology/
	chr1:1238583	*ACAP3*	Arg62Cys	arf-GAP with coiled-coil, ANK repeat and PH domain-containing protein 3	Lung	COSM527726
Described in COSMIC	chr15:71535077	*THSD4*	Thr185Met	A disintegrin and metalloproteinase with thrombospondin motifs-like protein 6	Lung	COSM555837
	chr7:5112796	*RBAK*	Leu227Phe	RB-associated KRAB zinc finger protein		pleomorphic sarcoma (RB1)
	chr7:124503601	*POT1*	Arg117Cys	Telomere end-binding protein	Blood/ nervous	Gastric carcinoma, melanoma, glioma
Function Related	chr2:37347280	*EIF2AK*	Ser316*	Apoptosis		*p53* related
	chr7:151945007	*MLL3*	Gly838Ser	Lysine N-methyltransferase 2C	Muscular	myeloid/lymphoid or mixed-lineage leukemia
	chr5:79030433	*CYMA5*	His1949Tyr		Cardiac	
Tissue Related	chr2:220355477	*SPEG*	Val3062Leu	Differentiation	Aortic	
	chr1:161721670	*DUSP12*	Phe158Ser	Protein-tyrosine phosphatase		
	chr10:81932595	*ANXA11*	Phe8Leu	Annexin		

*Stop codon

Supplementary Table 2: Haplotype frequency study for families 1and 2.

SNP	Position	Annotation	MAF	1*	2	3	4	5	6
rs67585224	124537476	Intron 1	0.21	A	C	A	A	A	C
rs68091803	124526331	Intron 2	0.20	T	T	T	T	T	T
rs7784168	124492038	Intron 6	0.28	C	C	T	T	T	T
rs7801661	124483222	Intron 8	0.21	T	C	T	T	T	T
rs35536751	124481185	Exon10	0.01	C	C	C	C	C	C
rs17246404	124462661	3'UTR	0.20	C	T	C	T	C	T
rs76436625	124462655	3UTR	0.12	T	T	T	T	C	T
Frequency				42.0%	21.1%	7.7%	7.7%	3.3%	2.2%

* Unique haplotype found in different members of families 1 and 2.

MAF: Minor Allele Frequency.

Supplementary Table 3: In silico PACC score of aa annotated in the OB fold and described stacking to DNA (T1-G10) [14] for POT1 proteins with mutations within OB1 domain (Categorization is shown in brackets).

Interaction	Postion (aa)	WT	p.Y89>C	p.Q94>G	p.G95>C	p.R117>C	p.R137>H	OBDelta*	OBDelta**
OB fold	146	122(E)	122(E)	122(E)	122(E)	122(E)	122(E)	122(E)	97(E)
	147	93(E)	117(E)	93(E)	93(E)	93(E)	117(E)	117(E)	93(E)
	148	45(I)	45(I)	45(I)	45(I)	45(I)	45(I)	95(E)	45(I)
	149	59(E)	59(E)	79(E)	59(E)	59(E)	59(E)	59(E)	59(E)
	150	19(I)	9(B)	19(I)	9(B)	9(B)	9(B)	9(B)	9(B)
	151	32(I)	32(I)	32(I)	32(I)	61(I)	9(B)	19(I)	49(I)
	152	86(E)	86(E)	86(E)	86(E)	0(B)	61(I)	86(E)	86(E)
T1; T2	62	0(B)	0(B)	0(B)	0(B)	0(B)	0(B)	-	-
A3; G4	89	26(I)	16(I)	26(I)	26(I)	26(I)	26(I)	-	-
G5; G6	31	0(B)	0(B)	0(B)	0(B)	0(B)	0(B)	-	-
T7	271	26(I)	26(I)	26(I)	26(I)	26(I)	26(I)	66(I)	66(I)
	161	0(B)	0(B)	0(B)	0(B)	0(B)	0(B)	0(B)	0(B)
	245	0(B)	0(B)	0(B)	0(B)	0(B)	0(B)	0(B)	0(B)
T8; A9	266	36(I)	0(B)	36(I)	22(I)	0(B)	0(B)	55(I)	22(I)
G10	223	0(B)	0(B)	0(B)	0(B)	0(B)	0(B)	0(B)	0(B)

*: 1-126 deletion; **: 10-141 deletion; (E): Exposed; (I): Intermediate; (B): Buried

Highlighted in grey: Most significant changes

Supplementary Table 4: In silico protein-protein interaction score for positions with significant acceptance in wt POT1 (threshold >20) for POT1 proteins with mutations within OB1 domain.

Position (aa)	WT	p.Y89>C	p.Q94>G	p.G95>C	p.R117>C	p.R137>H	OBDelta*	OBDelta**
1 (M)	26	26	26	26	28	24	NA	19
2 (S)	30	31	26	30	27	24	NA	10
3 (L)	27	25	25	28	25	21	NA	-23
39 (K)	26	24	24	24	24	22	NA	NA
91 (K)	26	29	29	28	31	29	NA	NA
253 (S)	33	28	35	34	30	36	38	32
254 (E)	28	19	24	25	31	31	21	28
255 (N)	34	23	26	28	36	36	29	38
341 (Q)	23	23	15	13	21	28	23	19
363 (R)	47	48	47	48	47	49	49	42
427 (K)	23	21	23	29	20	26	10	10
428 (N)	23	17	20	23	17	22	10	6
499 (H)	21	19	16	20	-24	15	18	-23
599 (A)	28	23	17	23	24	28	23	19

*: 1-126 deletion; **: 10-141 deletion; NA: Not applicable

Highlighted in grey: Most significant changes

Supplementary Table 5: Primers used for variant validation and further segregation and for *POT1* gene and haplotype studies.

Gene	Position of the variant	Forward	Reverse	TºC	Product size (bp)
ACAP3	chr1:1238583	GCTGGTGAAGCTGTGCAGT	GTAGGCTGTCAGCGAACCTC	57	338
THSD4	chr15:71535077	CCCTGGCAAGTATGGCTATG	ACTTGAAGCTGCAGGGTAGC	64	286
RBAK	chr7:5112796	TTCTAGCCAGCACCAGGAAG	CCCAAAAGGAAACAGCACCT	64	364
POT1	chr7:124503601	AATGATGCTCCGTCCACTTC	TGGTTCGTAGGTTGTGCATC	64	351
EIF2AK	chr2:37347280	ATGTTGGCCAGACTGGTTTC	CCGGAGTAGCTGGGACTACA	64	609
MLL3	chr7:151945007	TCAGTCACTCCAAAAATTGG	TGGCATTCTTCATTAACAGCA	65	260
CYMA5	chr5:79030433	GATGTTGGGAAAGCCAGAAA	GAATCTCCTTCCCCTCTGCT	59	350
SPEG	chr2:220355477	GCCACACTCCAGGGTTATTG	AAGATCGTGCCCTATGCTG	64	245
DUSP12	chr1:161721670	TGCAGGAGTCAGTCGAAGTG	TCTCAGGGATTGCTGGAAGT	64	405
ANXA11	chr10:81932595	GAGGAGGGGAGTGAGGAAAC	CACCAGCAGGAGACAGTGAA	64	326
Gene	**EXON**	**Forward**	**Reverse**	**TºC**	**Product size (bp)**
POT1	1	TTAGGCTGGAGATGGGTAAAA	CACATGTATCTATGTGTGTGGCATA	60	589
	2.1	CATGGATTTGCTGCTAATATGAT	AATGCATTTCCACTCCAAAAA	58	246
	2.2	AATTGTACCATTTATAAACAAAGTTC	GCATCAGTGTTGTTTGGCAAT	58	451
	3	TGCTTTAAAATATTGAAAGTCAGG	CAGTGAACAATACAGAGTTCTCTTCAA	58	238
	4	TGGTTCGTAGGTTGTGCATC	GGTGCTAACTTATAATTCCCAGTA	58	400
	5	TTTTTCAAAAGGATCATAAAACTACTC	AAAAATTGCTCTAACCCATTAAG	58	398
	6	CCACTTTCTAAATAACAAATGATCT	TCGGCTTAATCGATACCTTA	58	250
	7	TCTGGATTTTGTGGGTAGAGC	AGCAAGAACTAAACTGTCAATGTT	58	199
	8	AGCAACGCTCCATTGTTTTC	TGCTCATTACTGTGCCCATC	58	175
	9	GCCTAGCGTAATATTTTCTTAGC	CGTTTGTTTTATTATGGAAAATACTCA	60	500
	10	TCACGCTTACACCAAAATCG	GCAAAAGGAGTATTCTAACAAAACA	58	300
	11	CATTTTATTTGCACTACTTGAAGG	AGCACATGACCCCAGAACTT	60	248
	12	GCAGTAAAAAGTTATAACAAACAAGC	TCTGAATTGGCCAAACAACAT	60	494
	13	GCAGACTCATATGGTTTGATCTTTT	TCCTTTTAGGAACAAAGCAGGT	60	224
	14	TTTTGGAGTTGAGACCAGCA	GGGATTGTTAAAATATTCTTGCCTAC	60	298
	15	CAGAGTTATTTATTTTGTTTTAATGG	AAACTCAGGTCAGGAAAAGA	60	250
Gene	**Position of the SNP**	**Forward**	**Reverse**	**TºC**	**Product size (bp)**
POT1	rs67585224	TCCTGAGAACTGTCCTGAGAACT	AAAATATTCAAATTCACTAGGATGACA	57	205
	rs68091803	AGCCATGGGGAACAAGAATA	TTTTCACGAAAAATTCTAGCTAATGA	57	586
	rs7784168	TCTGGATTTTGTGGGTAGAGC	AGCAAGAACTAAACTGTCAATGTT	58	199
	rs7801661	GCCTAGCGTAATATTTTCTTAGC	CGTTTGTTTTATTATGGAAAATACTCA	62	500
	rs35536751	TCACGCTTACACCAAAATCG	GCAAAAGGAGTATTCTAACAAAACA	58	300
	rs17246404 rs76436625	AGAATATAGACTCTTGGTTCAAAACAT	CTTCTAGATTGAGGGCTTCCTG	57	150

.

Supplementary Table 6: Characteristics of the antibodies used for Western blotting and FISH studies.

Antibody	Reference	Clone	Working Concentrations	
			WB	IF
POT1*	Novus Biologicals: NB500-176	Rabbit Polyclonal	1:500	1:250
GAPDH	Homemade, CNIO	Monoclonal	1:500	-
TRF2*	Cell Signaling, #2645	Rabbit Polyclonal	-	-
TRF1	Homemade, CNIO	Rabbit Polyclonal	-	1:250
TRF1*	(TRF-78) (ab10579), ABCAM	Mouse monoclonal	-	1:250
γH2AX	Millipore, #05-636	Mouse Monoclonal	-	1:250
555-Alexa-donkey	Life technologies, A31572		-	1:400
488-Alexa-goat	Life technologies, A11017		-	1:400
FLAG	F3166 SIGMA	Mouse monoclonal	1:1000	-
c-MYC (9E10)	C-40, Santa Cruz Biotechnology	Mouse monoclonal	1:1000	1:500

*: 4 µL of antibody were used per IP Chip reaction; WB: Western Blot; IF: Inmunofluorescence

ARTICLE 6

Telomerase gene therapy rescues telomere length, bone marrow aplasia, and survival in mice with aplastic anemia.

Authors: Bär C, Povedano JM, Serrano R, **Benitez-Buelga C,** Popkes M, Formentini I, Bobadilla M, Bosch F, Blasco MA.

Journal: Blood
Publication Date: April 2016
Ref: 7; 127(14):1770-9
Personal contribution: Telomere measurement by qPCR, statistical analysis and the corresponding part of the manuscript.

Aplastic anemia is a fatal bone marrow disorder characterized by peripheral pancytopenia and marrow hypoplasia. The disease can be hereditary or acquired and develops at any stage of life. A subgroup of the inherited form is caused by replicative impairment of hematopoietic stem and progenitor cells due to very short telomeres as a result of mutations in telomerase and other telomere components. Abnormal telomere shortening is also described in cases of acquired aplastic anemia, most likely secondary to increased turnover of bone marrow stem and progenitor cells. Here, we test the therapeutic efficacy of telomerase activation by using adeno-associated virus (AAV)9 gene therapy vectors carrying the telomerase Tert gene in 2 independent mouse models of aplastic anemia due to short telomeres (Trf1- and Tert-deficient mice). We find that a high dose of AAV9-Tert targets the bone marrow compartment, including hematopoietic stem cells. AAV9-Tert treatment after telomere attrition in bone marrow cells rescues aplastic anemia and mouse survival compared with mice treated with the empty vector. Improved survival is associated with a significant increase in telomere length in peripheral blood and bone marrow cells, as well as improved blood counts. These findings indicate that telomerase gene therapy represents a novel therapeutic strategy to treat aplastic anemia provoked or associated with short telomeres.

Impact factor (IF) =11.82

GENE THERAPY

Telomerase gene therapy rescues telomere length, bone marrow aplasia, and survival in mice with aplastic anemia

Christian Bär,[1] Juan Manuel Povedano,[1] Rosa Serrano,[1] Carlos Benitez-Buelga,[2] Miriam Popkes,[1] Ivan Formentini,[3] Maria Bobadilla,[4] Fatima Bosch,[5] and Maria A. Blasco[1]

[1]Telomeres and Telomerase Group, Molecular Oncology Program and [2]Human Genetics Group, Spanish National Cancer Research Centre, Madrid, Spain; [3]Roche Pharma Research and Early Development, Neuroscience, Ophthalmology, and Rare Disease, Roche Innovation Center and [4]Roche Extending the Innovation Network Academia Partnering Program, F. Hoffmann-La Roche, Basel, Switzerland; and [5]Centre of Animal Biotechnology and Gene Therapy, Department of Biochemistry and Molecular Biology, School of Veterinary Medicine, Universitat Autònoma de Barcelona, Bellaterra, Spain

Key Points

- Telomerase gene therapy in a mouse model of aplastic anemia targets the bone marrow and provides increased and stable telomerase expression.
- Telomerase expression leads to telomere elongation and subsequently to the reversal of aplastic anemia phenotypes.

Aplastic anemia is a fatal bone marrow disorder characterized by peripheral pancytopenia and marrow hypoplasia. The disease can be hereditary or acquired and develops at any stage of life. A subgroup of the inherited form is caused by replicative impairment of hematopoietic stem and progenitor cells due to very short telomeres as a result of mutations in telomerase and other telomere components. Abnormal telomere shortening is also described in cases of acquired aplastic anemia, most likely secondary to increased turnover of bone marrow stem and progenitor cells. Here, we test the therapeutic efficacy of telomerase activation by using adeno-associated virus (AAV)9 gene therapy vectors carrying the telomerase *Tert* gene in 2 independent mouse models of aplastic anemia due to short telomeres (*Trf1*- and *Tert*-deficient mice). We find that a high dose of AAV9-*Tert* targets the bone marrow compartment, including hematopoietic stem cells. AAV9-*Tert* treatment after telomere attrition in bone marrow cells rescues aplastic anemia and mouse survival compared with mice treated with the empty vector. Improved survival is associated with a significant increase in telomere length in peripheral blood and bone marrow cells, as well as improved blood counts. These findings indicate that telomerase gene therapy represents a novel therapeutic strategy to treat aplastic anemia provoked or associated with short telomeres. (*Blood*. 2016;127(14):1770-1779)

Introduction

Aplastic anemia is a potentially life-threatening, rare, and heterogeneous disorder of the blood in which the bone marrow cannot produce sufficient new blood cells due to a marked reduction of immature hematopoietic stem and progenitor cells (HSPCs).[1,2] The main disease manifestations are pancytopenia and marrow hypoplasia, which can emerge at any stage of life but are more frequent in young individuals (age 10-25 years) and in the elderly (>60 years).[3] Aplastic anemia can be acquired or inherited. The acquired type is often of idiopathic origin and involves autoimmune processes but can also be triggered by environmental factors such as exposure to radiation, toxins, and viral infections.[4] The congenital form is rarer, and mutations in more than 30 genes involved in DNA repair, ribosome biogenesis, and telomere maintenance pathways have been identified to date.[5] A frequently observed clinical feature of aplastic anemia is the presence of short telomeres in subpopulations of peripheral blood cells (neutrophils in particular; less prominent in lymphocytes),[6] even in the absence of mutations in the telomere maintenance machinery.

Telomeres, the termini of vertebrate chromosomes, are specialized nucleoprotein structures composed of tandem repeat sequences (TTAGGG in vertebrates) bound by a 6-protein complex (TRF1, TRF2, TIN2, RAP1, TPP1, and POT1) known as shelterin.[7,8] Telomeres are essential for chromosome integrity by preventing telomere fusions and telomere fragility. Telomere length is controlled by the ribonucleoprotein enzyme telomerase, which can add telomeric sequences onto telomeres de novo. Because telomeres shorten with every cell division (a phenomenon known as the "end replication problem") and somatic cells do not express sufficient telomerase to compensate for this, telomeres shorten throughout life. When telomeres reach a critically short length, their protective function is impaired, eliciting a persistent DNA-damage response at chromosome ends, which leads to cellular senescence or cell death.[9,10] Hematopoietic stem cells, in contrast to most somatic cells, can activate telomerase; however, this is insufficient to prevent telomere attrition with aging, thus eventually leading to loss of the regeneration potential of hematopoietic stem cells.[11] In line with this, recipients of bone marrow transplants have shorter telomeres than their donors, suggesting that telomerase cannot fully compensate for the increased cell proliferation that occurs during the engraftment phase of the transplanted bone marrow.[12] Telomeres also show an accelerated rate of shortening in patients with aplastic anemia compared with

Submitted August 31, 2015; accepted January 27, 2016. Prepublished online as *Blood* First Edition paper, February 22, 2016; DOI 10.1182/blood-2015-08-667485.

The online version of this article contains a data supplement.

The publication costs of this article were defrayed in part by page charge payment. Therefore, and solely to indicate this fact, this article is hereby marked "advertisement" in accordance with 18 USC section 1734.

healthy individuals, most likely due to a higher than normal number of cell divisions in the aplastic anemia cases.[13]

Accelerated telomere shortening due to defects in telomerase or other telomere maintenance genes prematurely limits the proliferation potential of cells, including stem cells, leading to decreased tissue renewal capacity.[9,14] Highly proliferative tissues such as the hematopoietic system are particularly vulnerable to defects in telomere maintenance genes, leading to severe disorders such as aplastic anemia.[15] As an example, the telomeropathy dyskeratosis congenita (DKC) has been linked to mutations in 11 genes that encode components of the telomerase complex (*TERT*, *TERC*, *DKC1*, *NOP10*, and *NHP2*) or of the telomere capping complex shelterin (*TIN2*). Other genes altered in DKC encode for accessory proteins important for telomerase assembly and trafficking (*CTC1*, *ACD7* [alias *TPP1*], and *TCAB1*) or for telomere replication (*RTEL1*).[16] Mutated *PARN* was also recently linked to reduced messenger RNA (mRNA) levels of several key genes in telomere maintenance.[17] In all these cases, DKC is characterized by very short telomeres. DKC is a multisystem syndrome comprising diverse clinical features such as nail dystrophy, oral leukoplakia, abnormal skin pigmentation, and cerebellar hypoplasia.[16] The most severe complication, however, is the development of aplastic anemia in 80% of the cases, underlining that the clinical features are caused by excessive telomere shortening that eventually leads to the exhaustion of the stem cell reserve.[5]

These findings suggest that telomerase activation could be a good therapeutic strategy to treat those forms of aplastic anemia associated with a limited blood-forming capacity due to the presence of very short telomeres. We have previously developed a telomerase (*Tert*) gene therapy using adeno-associated virus (AAV)9 vectors,[18] which attenuated or reverted aging-associated telomere erosion in peripheral blood mononuclear cells (PBMCs).[18]

To test the efficacy of this strategy in the treatment of aplastic anemia, we first used a mouse model of aplastic anemia generated by us in which we depleted the TRF1 shelterin protein specifically in the bone marrow, leading to a bone marrow phenotype that recapitulates the main pathological findings of human aplastic anemia patients, including extreme telomere shortening.[19,20] In particular, partial depletion of the *Trf1* gene specifically in bone marrow causes severe telomere uncapping and provokes a persistent DNA-damage response at telomeres, which in turn leads to a fast clearance of those HSPCs deficient for *Trf1*. In this context, the remaining HSPCs that did not delete the *Trf1* gene undergo additional rounds of compensatory proliferation to regenerate the bone marrow, leading to very rapid telomere attrition. Thus, partial depletion of the bone marrow stem cell and progenitor compartments by *Trf1* deletion recapitulates the compensatory hyperproliferation and short telomere phenotype observed after bone marrow transplant or in other acquired forms of aplastic anemia, as well as in patients due to mutations in telomere maintenance genes. Interestingly, this mouse model allows adjustment of the rate of telomere shortening by modulating the frequency of *Trf1* deletion–mediated HSPC depletion, thus controlling the onset of bone marrow aplasia and pancytopenia.[19,20]

As an additional model to mimic the presence of very short telomeres specifically in the bone marrow, we transplanted irradiated wild-type mice with bone marrow from late (third)-generation (G3) telomerase-deficient *Tert*-knockout mice, which have short telomeres due to telomerase deficiency during 3 mouse generations.

Here, we tested telomerase activation by using gene therapy AAV vectors in both mouse models of aplastic anemia produced by short telomeres. Our results show that telomerase treatment is sufficient to attenuate telomere attrition and HSPC depletion with time, thus significantly preventing death by bone marrow failure.

Material and methods

Study approval

All experimental procedures with mice (*Mus musculus*) were approved by the Spanish National Cancer Research Center Instituto de Salud Carlos III Ethics Committee for Research and Animal Welfare. Mice were treated in accordance to the Spanish laws and the Federation of European Laboratory Animal Science Associations guidelines (approval file number CBA PA 87_2012).

Mice and animal procedures

Mice of pure C57/BL6 background were produced and housed at the specific-pathogen-free animal house of the Spanish National Cancer Research Center in Madrid, Spain. $Trf1^{lox/lox}$ *Mx1-Cre* and $Trf1^{lox/lox}$ *Mx1-wt* mice were generated as described previously.[21] First-generation (G1) $Tert^{-/-}$ mice were generated by intercrossing $Tert^{+/-}$. G3 $Tert^{-/-}$ mice were obtained by intercrossing G1 mice (to give second-generation [G2] mice) and subsequently intercrossing G2 mice.[22] Ten-week-old $Trf1^{lox/lox}$ *Mx1-Cre* or G3 $Tert^{-/-}$ mice were used as bone marrow donors for transplant into 8-week-old lethally irradiated (12 Gy) wild-type mice as described previously.[19,23] Two million cells were transplanted via tail vein injection at a donor-to-recipient ratio of 1:8, and mice were left for 30 days to allow bone marrow reconstitution. To induce Cre expression, mice were intraperitoneally injected with 15 μg/g body weight of polyinosinic: polycytidylic acid (pI:pC; Sigma-Aldrich) 3 times per week for a total of 5 weeks. After 1 week, mice were treated with the AAV9-*Tert* or AAV9-empty vector. Vectors were administered via tail vein injection at a concentration of 3.5×10^{12} viral genomes per mouse.

Gene therapy vector production

Viral vectors were generated[24] and purified as described previously.[25] Briefly, vectors were produced through triple transfection of HEK293T. Expression cassettes were under the control of the cytomegalovirus promoter and contained an SV40 polyA signal for *EGFP* and the cytomegalovirus promoter, and a 3′ untranslated region of the *Tert* gene as polyA signal for *Tert*. AAV9 particles were purified using 2 cesium chloride gradients, dialyzed against phosphate-buffered saline (PBS) and filtered.[25] Viral genome particle titers were determined by a quantitative real-time polymerase chain reaction (PCR) method.[26]

Histology

Bone marrow samples (sternum or tibia bone) were fixed in 4% paraformaldehyde and paraffin embedded after decalcification. Tissue sections (5 μm) were stained with hematoxylin and eosin. Immunohistochemistry was performed on deparaffinized sections. After antigen retrieval, samples were stained with anti–enhanced green fluorescent protein (EGFP) (rabbit anti-EGFP, 1:200, ab290; Abcam). EGFP-positive cells were counted in a semiautomated way using ImageJ software.

FACS

For sorting of HSPCs, whole bone marrow cells were extracted from the long bones (femur and tibia) as described previously.[23] Erythrocytes were lysed for 10 minutes in 10 mL of erythrocyte lysis buffer (Roche), washed once with 10 mL of PBS, and resuspended in fluorescence-activated cell sorting (FACS) buffer (PBS, 2 mM EDTA, 0.3% bovine serum albumin) containing Fc-block (1:400) at a concentration of 5 to 10×10^6 cells per 100 μL. Cells were incubated for 10 minutes and washed once in FACS buffer. Cells were then resuspended in FACS buffer at 20 to 25×10^6 cells per milliliter, and the antibody cocktail was added as follows: anti–Sca-1–PerCP-Cy5.5 (1:200), lin cocktail-eFluor450 (1:50) (all eBioscience), and anti–c-kit–APC-H7 (1:100) (BD Pharmingen). Cells were incubated for 30 minutes. After washing cells twice with PBS, 2 mL of 4,6 diamidino-2-phenylindole (DAPI; 2 mg/mL) was added and cells were sorted in a FACSAria IIU (Becton Dickinson, San Jose, CA) into HSPCs (lin^-, Sca-1^+, and c-kit^+) and lineage-positive fractions.

Colony-forming assay

A short-term colony-forming assay was performed by plating 1×10^4 and 2×10^4 freshly isolated mononucleated bone marrow cells in 35 mm dishes containing MethoCult media (both STEMCELL Technologies) following the manufacturer's protocol. All experiments were performed in duplicate, and the number of colonies was counted after 12 days of incubation at 37°C.

Blood counts

Peripheral blood was drawn from the facial vein (~50 μL) and collected into anticoagulation tubes (EDTA). Blood counts were determined using an Abacus Junior Vet veterinary hematology analyzer.

Quantitative real-time PCR and western blot analysis

Total RNA from whole bone marrow extracts or from bone marrow cells sorted by FACS was isolated using QIAGEN's RNeasy Mini Kit according to the manufacturer. Quantitative real-time PCR was performed using an ABI PRISM 7700 or QuantStudio 6 Flex (both Applied Biosystems). Primer sequences for *Tert* and reference genes *Act1* and *TBP* are as follows: Tert-forward 5′GGATTGCCACTGGCTCCG; Tert-reverse 5′TGCCTGACCTCCTCT TGTGAC; actin-forward 5′GGCACCACACCTTCTACAATG; actin-reverse 5′GTGGTGGTGAAGCTGTAG; TBP-forward 5′CTTCCTGCCACAATG TCACAG; TBP-reverse 5′CCTTTCTCATGCTTGCTTCTCTG.

Q-FISH telomere analysis

Quantitative FISH (Q-FISH) on paraffin-embedded tissue sections was performed as described previously.[27] Confocal images were acquired as stacks every 0.5 μm for a total of 1.5 μm using a Leica SP5-MP confocal microscope, and maximum projections were done with the Leica Application Suite–Advanced Fluorescence software. Telomere signal intensity was quantified in at least 6 images per mouse using Definiens software, with a specific script allowing for individual spot background correction.

High-throughput (HT)-Q-FISH on peripheral blood leukocytes was done using 120 to 150 μL of blood as described previously.[28] Confocal images were captured using the Opera High-Content Screening system (Perkin Elmer). Telomere length values were analyzed using individual telomere spots (>10 000 telomere spots per sample). The average fluorescence intensities of each sample were converted into kilobases using L5178-R and L5178-S cells as calibration standards, which have stable telomere lengths of 79.7 kb and 10.2 kb, respectively.[29] Samples were analyzed in duplicate.

Real-time PCR–based measurement of relative telomere length was done on genomic DNA isolated from whole bone marrow samples following a previously described protocol.[30,31]

Results

AAV9-*Tert* targets bone marrow and hematopoietic stem cells

First, we tested the ability of AAV9 vectors to transduce bone marrow cells upon mouse IV injection. In particular, to determine the location and percentage of transduced cells, we first treated wild-type mice with an AAV9-EGFP reporter virus (3.5×10^{12} viral genomes per mouse) via tail vein injections. We found that 2% of the BM cells were positive for EGFP upon immunohistochemistry with anti-EGFP antibodies in in middle bone sections, and this increased to 10% in bone regions adjacent to the joints, which showed the highest AAV9 transduction (Figure 1A-B). We then injected wild-type mice with the same amount of AAV9-*Tert* particles and determined *Tert* mRNA expression by quantitative real-time PCR in whole bone marrow isolates at 2 weeks and 8 months after virus injection. At 2 weeks posttreatment with the AAV9 vectors, *Tert* mRNA expression was significantly increased in the AAV9-*Tert*-treated mice compared with those treated with the AAV9-empty vector, and this increased expression was maintained up to 8 months after the initial treatment (Figure 1C-E). In agreement with the known tropism of the AAV9 serotype, we found a stronger induction of *Tert* in organs such as heart and liver, which are preferential AAV9 targets (supplemental Figure 1, available on the *Blood* Web site).[32] We then studied *Tert* mRNA expression specifically in the blood-forming compartments of the bone marrow. To this end, we performed FACS of c-kit$^+$ and Sca-1$^+$ HSPCs and lin$^+$ lineage-committed cells. We found a significant increase in *Tert* mRNA in HSPCs (10-fold) and lineage-committed bone marrow cells (3.5-fold) in AAV9-*Tert*-treated mice compared with mice treated with the empty vector (Figure 1F-G), demonstrating that bone marrow cells, including HSPCs, are targeted by *Tert* gene therapy. Of note, the higher expression in whole bone marrow compared with isolated hematopoietic cells (HPSCs and lin$^+$ cells) could suggest that additional bone marrow cells corresponding to the stroma (ie, adipocytes) may also be infected. In this regard, we previously demonstrated that adipocytes are efficiently targeted by AAV9.[33] Moreover, the relative lower fold changes in *Tert* in HSPCs compared with total bone marrow may also be due to higher levels of endogenous *Tert* in HPSCs compared with whole bone marrow. As a control, AAV9-*Tert* treatment of wild-type mice did not affect the relative numbers of lineage-positive or -negative cells or the proportion of HSPCs (supplemental Figure 2). Given the increased *Tert* expression in HSPCs, we next addressed whether this affected their proliferation/colony-forming potential. To this end, we performed a colony-forming cell assay (MethoCult). We observed a significantly increased number of colonies in the bone marrow from AAV9-*Tert*-treated mice compared with those treated with the empty vector (Figure 1H).

In summary, IV injection of AAV9 vectors administered at a high dose can target *Tert* to hematopoietic cells, including HSPCs.

AAV9-*Tert* treatment rescues survival in a mouse model of aplastic anemia

We next tested whether treatment with AAV9-*Tert* was effective in increasing survival upon induction of lethal aplastic anemia due to critically short telomeres. First, we used the conditional *Trf1* mouse model recently developed by us (*Trf1*$^{lox/lox}$ *Mx1-Cre* mice) in which we induce partial *Trf1* deletion specifically in the bone marrow.[19] To this end, we transplanted lethally irradiated wild-type mice with bone marrow isolated from *Trf1*$^{lox/lox}$ *Mx1-Cre* mice, followed by administration of pI:pC to induce the expression of Cre recombinase and *Trf1* deletion.[19,20] Genotyping confirmed that the new bone marrow solely consisted of donor cells with excisable *Trf1* (supplemental Figure 3). Thus, *Trf1*$^{lox/lox}$ *Mx1-Cre* mice allow study of the effects of *Trf1* depletion exclusively in the bone marrow. We previously showed that partial *Trf1* deletion in the bone marrow results in rapid death and removal of the *Trf1*-deleted cells, whereas cells that fail to delete *Trf1* undergo compensatory rounds of cell division, leading to rapid telomere shortening and replicative senescence, eventually resulting in bone marrow failure.[19,20]

Here, we induced *Trf1* deletion with pI:pC injections at a frequency of 3 times per week for 5 weeks, at which point these mice started to show signs of aplastic anemia.[19,20] One week after the last pI:pC injection, mice were treated with either the AAV9-*Tert* or AAV9-empty vector (Figure 2A). Mouse survival was monitored for 100 days after treatment with the AAV9 vectors (note: beyond 100 days after virus treatment, none of the mouse cohorts developed signs of aplastic anemia. At 120 days post–virus administration, all mice were euthanized for further analyses). Strikingly, AAV9-*Tert* treatment significantly increased survival: 87% of mice were still alive at 100 days after virus administration in the AAV9-*Tert*-treated group compared

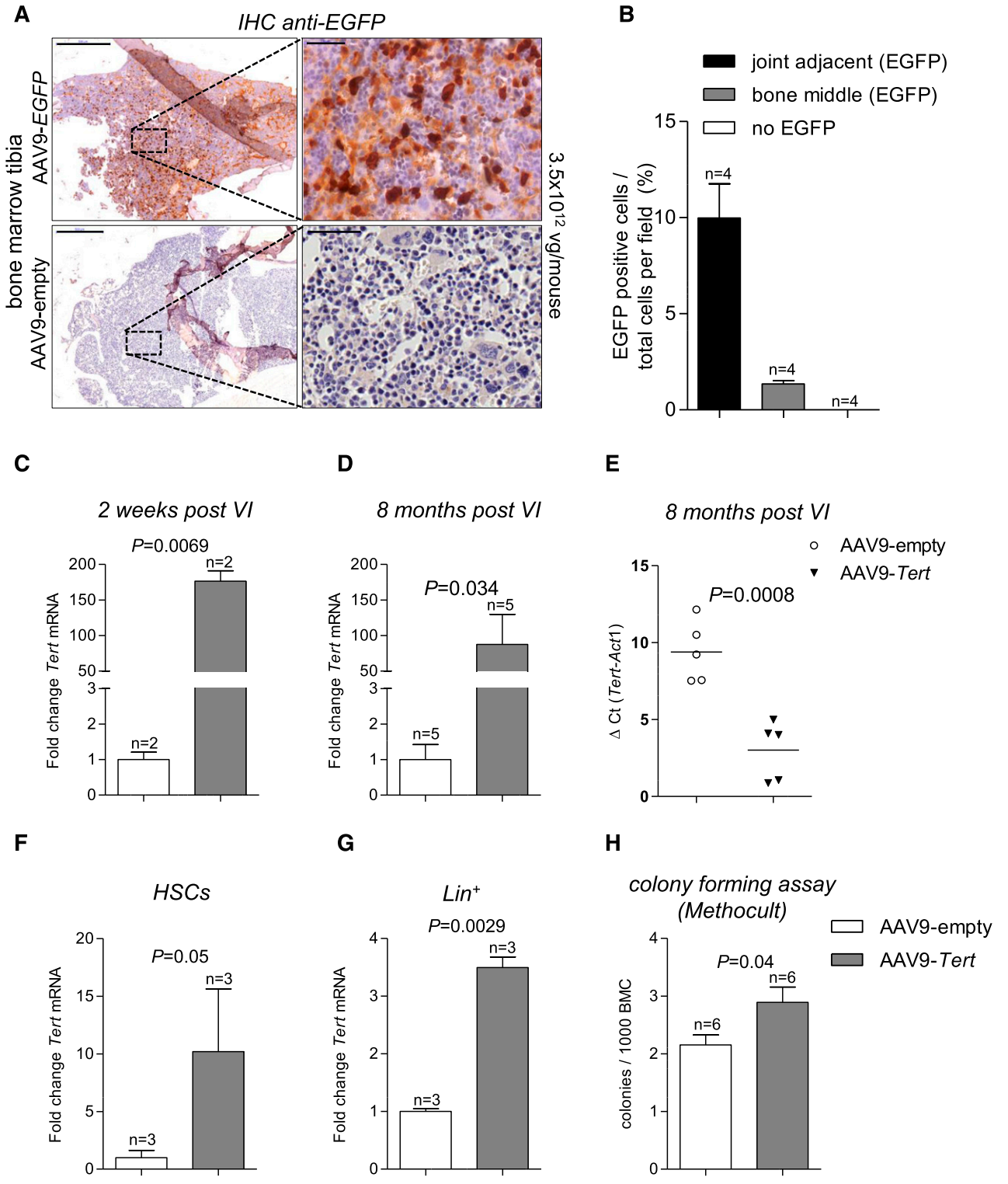

Figure 1. High dose of AAV9 particles targets bone marrow, including HSPCs. (A) Representative anti-EGFP immunohistochemistry (IHC) images of bone marrow corresponding to the tibia. Mice were injected with the AAV9-EGFP vector or AAV9-empty vector at a concentration of 3.5×10^{12} viral genomes (vg) per mouse. EGFP-positive cells were mainly located toward the end of the bones. Bars represent 500 μm (left) and 50 μm (right); hematoxylin and eosin stain. (B) Percentage of EGFP-positive cells relative to the total number of cells. Cells were separately counted in joint adjacent areas and in the middle of the bone. (C-D) *Tert* mRNA expression level in total bone marrow isolated 2 weeks (C) and 8 months (D) after VI with 3.5×10^{12} viral genomes per mouse. AAV9-*Tert* relative to the expression of mice injected with the same amount of AAV9-empty vector. (E) Δ Ct values (*Tert* minus *Act1*) of the quantitative real-time PCR shown in panel D. Quantitative real-time PCR determined relative *Tert* expression in HSPCs (HSCs) sorted by FACS (F) and lineage-committed cells (G). (H) Colony-forming assay in MethoCult with whole bone marrow cells isolated from mice injected with AAV9-*Tert* or AAV9-empty. For all experiments, n indicates number of mice. Data are mean ± SEM. Statistical analysis: 2-sided Student *t* test; *P* values are shown. SEM, standard error of the mean; VI, virus injection.

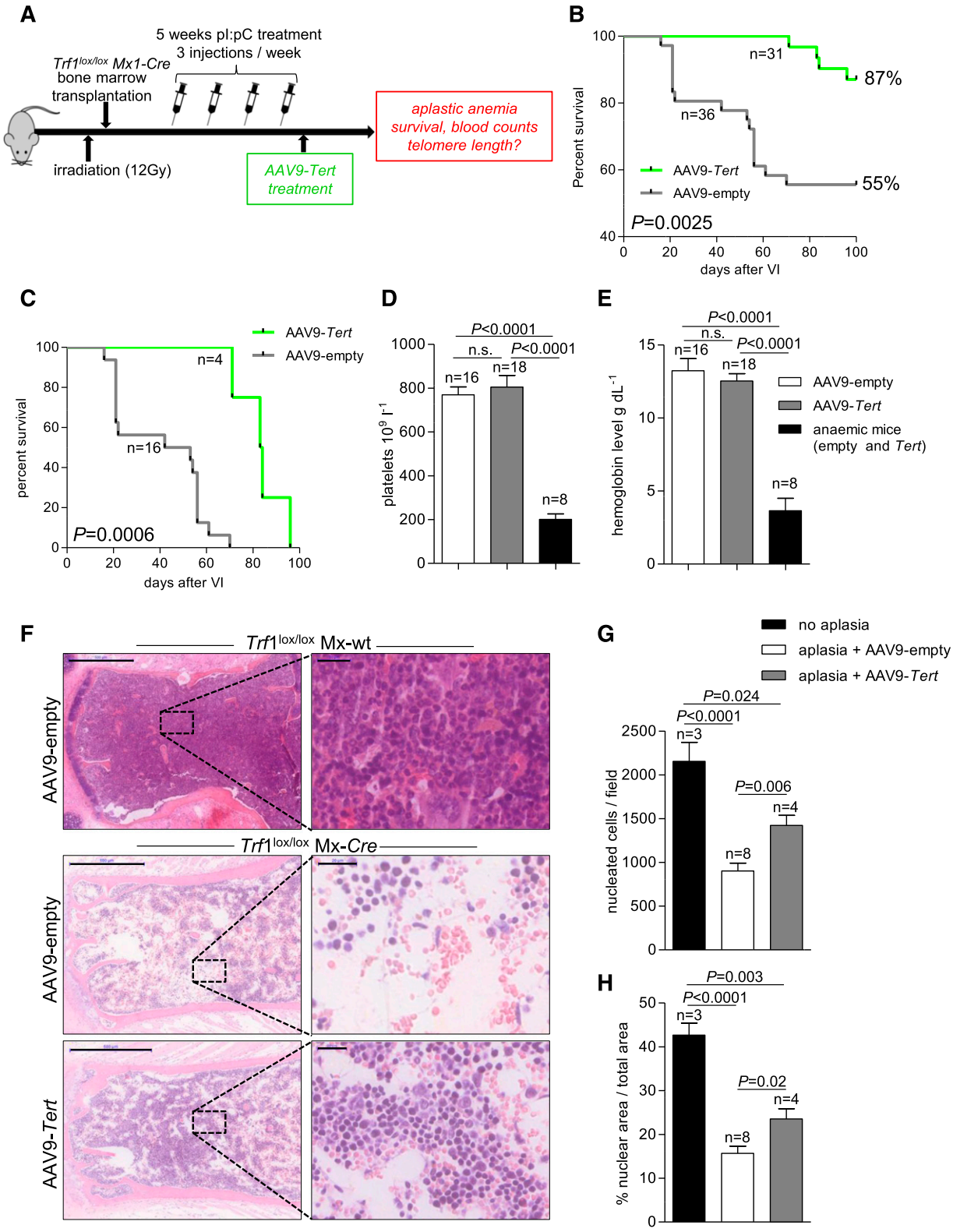

Figure 2. AAV9-*Tert* treatment rescues the aplastic anemia phenotype in *Trf1*$^{lox/lox}$ mice. (A) Experimental design. Mice were lethally irradiated and transplanted the following day with *Trf1*$^{lox/lox}$ *Mx1-Cre* bone marrow. After engraftment, *Cre* expression and *Trf1* excision was induced by pI:pC injections for 5 weeks. One week later, mice were injected with AAV9-*Tert* or AAV9-empty particles. (B) Kaplan-Meier survival curves showing that AAV9-*Tert* treatment significantly rescues mouse survival. (C) Kaplan-Meier survival curves considering only those animals that died of aplastic anemia within 100 days after virus treatment show significant protection of AAV9-*Tert* treatment from deaths due to aplastic anemia. Platelet counts (D) and hemoglobin levels (E) in mice of the AAV9-*Tert*-treated and AAV9-empty-treated groups showing clear signs of anemia compared with healthy mice from the same AAV9-*Tert*-treated and AAV9-empty-treated groups. (F) Representative bone marrow images of healthy controls (no Cre-mediated induction of *Trf1* deletion) and of mice with bone marrow aplasia. Genotypes and AAV9 treatments are indicated. Bars represent 500 μm (left) and 20 μm (right); hematoxylin and eosin stain. (G) Quantification of bone marrow cellularity expressed as number of nucleated cells per field. Four to 5 fields per mouse were counted. (H) Quantification of bone marrow cellularity expressed as the percentage of nuclear area (purple stain) to total areas per field. Four to 5 fields per mouse were counted. In all graphs, n indicates number of mice. Data are mean ± SEM. Statistical analysis: log-rank test in panels B and C; 2-sided Student *t* test in panels D, E, G, and H; *P* values are shown. n.s., not significant.

with only 55% of mice alive in the empty vector–treated group (Figure 2B). In particular, whereas only 4 of 31 mice (13%) treated with AAV9-*Tert* developed aplastic anemia, 16 of 36 mice (44%) died with clear signs of aplastic anemia in the group treated with the empty vector (Figure 2C). In both groups, aplastic anemia was determined as the cause of death in those mice showing a drastic drop in platelet counts and hemoglobin levels at the time of death (Figure 2D-E) and presenting with severe bone marrow hypoplasia and aplasia after postmortem histopathological analysis of bone marrow sections (Figure 2F). Interestingly, among those mice that died of aplastic anemia, we observed a tendency to show a milder bone marrow aplasia phenotype in the AAV9-*Tert*-treated group compared with the AAV9-empty-treated group, as indicated by higher bone marrow cellularity in the AAV9-*Tert*-treated group (Figure 2F). Quantification of the bone marrow cellularity confirmed a drastic decrease of cellularity in aplastic anemia mice compared with wild-type control mice. Of importance, the decrease in cellularity was significantly attenuated in the AAV9-*Tert*-treated cohort compared with the AAV9-empty-treated group (Figure 2G-H). Our results suggest that AAV9-*Tert* treatment of mice with induced severe telomere shortening significantly reduces mortality due to aplastic anemia.

Telomerase treatment reverses telomere shortening in peripheral blood and bone marrow cells in a mouse model of aplastic anemia

Because aplastic anemia in our mouse model is caused by extreme telomere shortening,[19,20] we next compared the dynamics of telomere length in mice treated with AAV9-*Tert* vs mice treated with the empty vector. To this end, we performed a longitudinal study to follow telomere length in peripheral blood (PBMCs) over time using telomere HT-Q-FISH technology.[34] To do so, we extracted blood at 4 different time points (time point 1, 30 days after bone marrow engraftment; time point 2, 5 weeks after pI:pC treatment; time point 3, 2 months after treatment with the AAV9 vectors; and time point 4, 4 months after treatment with the AAV9 vectors) (note: longitudinal telomere measurements were done on PBMCs from mice that did not develop aplastic anemia). In agreement with previous findings, we found a dramatic drop in telomere length of ~10 kb in all mice after induction of *Trf1* deletion with pI:pC and prior to treatment with the gene therapy vectors (Figure 3A; compare time points 1 and 2).[19,20] We observed a further drop in telomere length in those mice treated with the AAV9-empty vector when comparing time point 4 with time point 2 in this mouse cohort (Figure 3A-B). Importantly, during the same period of time, mice treated with AAV9-*Tert* showed a net increase in average telomere length of 10 kb when comparing time point 4 with time point 2 (Figure 3A-B). Indeed, throughout the course of the experiment, AAV9-empty-treated mice showed a total decrease in average telomere length of 12 kb, whereas mice treated with AAV9-*Tert* showed re-elongation of telomeres to a similar telomere length as before the induction of *Trf1* deletion by pI:pC treatment (Figure 3C). These findings indicate that AAV9-*Tert* treatment is sufficient to stop and even revert initial telomere shortening. To further confirm whether telomeres were elongated as the consequence of AAV9-*Tert* gene therapy specifically in the bone marrow, we performed Q-FISH analysis on bone marrow cross-sections at the end point of the experiment. In agreement with longer telomeres in peripheral blood cells in the AAV9-*Tert*-treated mice, we found that AAV9-*Tert*-treated mice also had significantly longer telomeres in the bone marrow compared with mice treated with the empty vector (Figure 3D-F). We confirmed the AAV9-*Tert*-mediated telomere elongation on independent samples using a real-time PCR assay for relative telomere length determination[30,31] (supplemental Figure 4A). Furthermore, in line with our hypothesis that aplastic anemia is the consequence of drastically shortened telomeres, mice treated with the AAV9-empty vector that developed aplastic anemia had significantly shorter telomeres than mice that were treated in the same manner but did not develop aplastic anemia (supplemental Figure 4B).

Of note, telomere length analysis on bone marrow sections or bone marrow DNA does not allow one to distinguish between various cell populations. However, the observed telomere elongation in PBMCs suggests a direct effect of AAV9-*Tert* on HSPCs.

Telomerase gene therapy of aplastic anemia produced by short telomeres resulting from *Tert* deletion improves blood counts and increases telomere length

To validate the therapeutic use of telomerase gene therapy in aplastic anemia provoked by short telomeres, we used an additional mouse model for modeling short telomere length in the hematopoietic system (in this case due to telomerase deficiency during several mouse generations): the *Tert*-deficient mouse model.[22] To this end, we irradiated wild-type mice and transplanted them with bone marrow from G3 *Tert*-knockout mice, which have short telomeres in all mouse tissues, including the bone marrow[22] (Figure 4A). First, we confirmed shorter telomeres in the G1 and G3 *Tert*-knockout bone marrow donors compared with the wild-type bone marrow donors by performing HT-Q-FISH analysis on PBMCs. In particular, *Tert* deficiency leads to progressive telomere shortening, with G3 mice having an average telomere length of ~25 kb compared with ~40 kb in the wild-type controls (Figure 4B). One month after transplantation of irradiated wild-type mice with G3 *Tert* knockout bone marrow, mice were divided in 2 groups and treated with either AAV9-*Tert* or AAV9-empty gene therapy vectors (3.5×10^{12} viral genomes per mouse) (Figure 4A). After treatment, we monitored mice during a follow-up period of 5 months and observed robust expression of *Tert* in the bone marrow in the AAV9-*Tert*-treated group (supplemental Figure 5). Importantly, in response to AAV9-*Tert* treatment, we observed an increase in survival compared with the AAV9-empty-treated group that almost reached statistical significance ($P = .058$) (Figure 4C). Upon mouse euthanasia, *Tert*-treated mice had significantly increased hemoglobin levels and higher erythrocyte and platelet counts compared with mice treated with the empty vector (Figure 4D-F). The same trend was observed for leukocyte counts, which were higher in AAV9-*Tert*-treated mice compared with the AAV9-empty group, although the trend did not reach statistical significance ($P = .09$) (Figure 4G). Lastly, to analyze the mechanism by which *Tert* gene therapy improved survival and blood counts in these mice, we followed longitudinally the telomere length in PBMCs in both mouse cohorts. To this end, we extracted blood before and 3 and 5 months after mice were injected with the viruses and performed HT-Q-FISH analysis. In line with the results obtained with the $Trf1^{lox/lox}$ mouse model (see "AAV9-*Tert* treatment rescues survival in a mouse model of aplastic anemia"), we found that AAV9-*Tert* treatment led to a net increase in average telomere length of 5.18 kb with time, whereas during the same period, mice treated with the AAV9-empty vector suffered a slight telomere shortening of −1.76 kb (Figure 5A-B). These findings were also confirmed by telomere Q-FISH analysis on bone marrow sections at 5 months after virus administration. In particular, we found significantly longer telomeres in the bone marrow of *Tert*-treated mice compared with mice treated with the empty vector (Figure 5C-D).

In summary, these results indicate that a single treatment with the AAV9-*Tert* vector in mice with previously shortened telomeres in the bone marrow due to telomerase deficiency is sufficient to increase

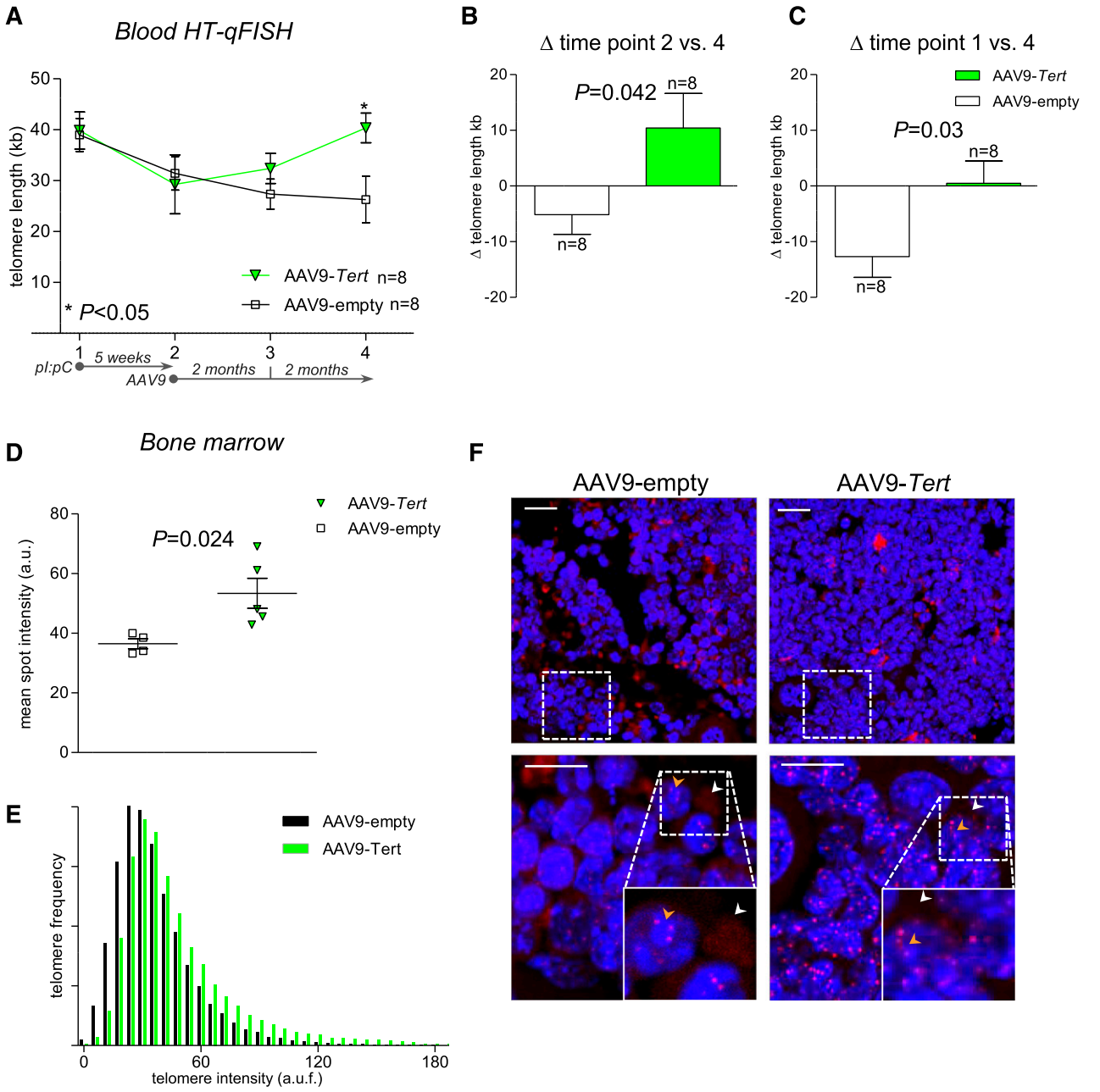

Figure 3. AAV9-*Tert* treatment causes telomere elongation in blood and bone marrow. (A) Longitudinal HT-Q-FISH analysis of telomere length in peripheral blood monocytes (*Trf1*$^{lox/lox}$ *Mx1-Cre*–transplanted mice; see also Figure 2A). Blood was extracted at 4 different time points (time point 1, before pI:pC treatment; time point 2, after 5 weeks of pI:pC treatment and before AAV9 injection; time point 3, 2 months after AAV9 injection; and time point 4, 4 months after AAV9 injection). Relative variation (Δ) of telomere length in AAV9-*Tert*-treated and AAV9-empty-treated animals between time points 2 and 4 (B) and between time points 1 and 4 (C). (D) Relative telomere length in bone marrow sections from AAV9-*Tert*-treated and AAV9-empty-treated mice shown as arbitrary units of fluorescence (a.u.f.). Each square and triangle represents the mean telomere length per nucleus of an individual mouse. (E) Frequency distribution blot of telomere length showing a higher abundance of short telomeres in the AAV9-empty-treated group compared with AAV9-*Tert*-treated mice (pooled data from panel D). (F) Representative images of bone marrow sections from AAV9-*Tert*-treated and AAV9-empty-treated mice used for Q-FISH analysis. Cell nuclei are stained blue (DAPI) and telomeres are stained red (Cy3). White arrowheads indicate nonspecific extranuclear signals and yellow arrowheads indicate specific telomere signals within DAPI-stained nuclei. Bars represent 20 μm (top) and 10 μm (bottom). In all graphs, n indicates number of mice. Data are mean ± SEM. Statistical analysis: 2-way analysis of variance in panel A; 2-sided Student *t* test in panels B and C; *P* values are shown. a.u., arbitrary units.

telomere length in the bone marrow and in blood. Telomerase gene therapy also improved blood counts and mouse survival.

Discussion

Here, we set out to test the hypothesis of whether increased expression of telomerase through systemic virus-based *Tert* delivery may delay or prevent the emergence of aplastic anemia provoked by short telomeres. We tested this hypothesis in 2 independent mouse models with very short telomeres specifically in the bone marrow due to either *Trf1* or *Tert* deficiency.[20,22]

The rationale for this study was based on our previous finding showing that systemic AAV9-*Tert* gene therapy in wild-type mice was sufficient to delay different age-related diseases and to significantly increase mouse life span by delaying telomere shortening with age in different tissues.[18] A 5-month longitudinal follow-up of these mice also

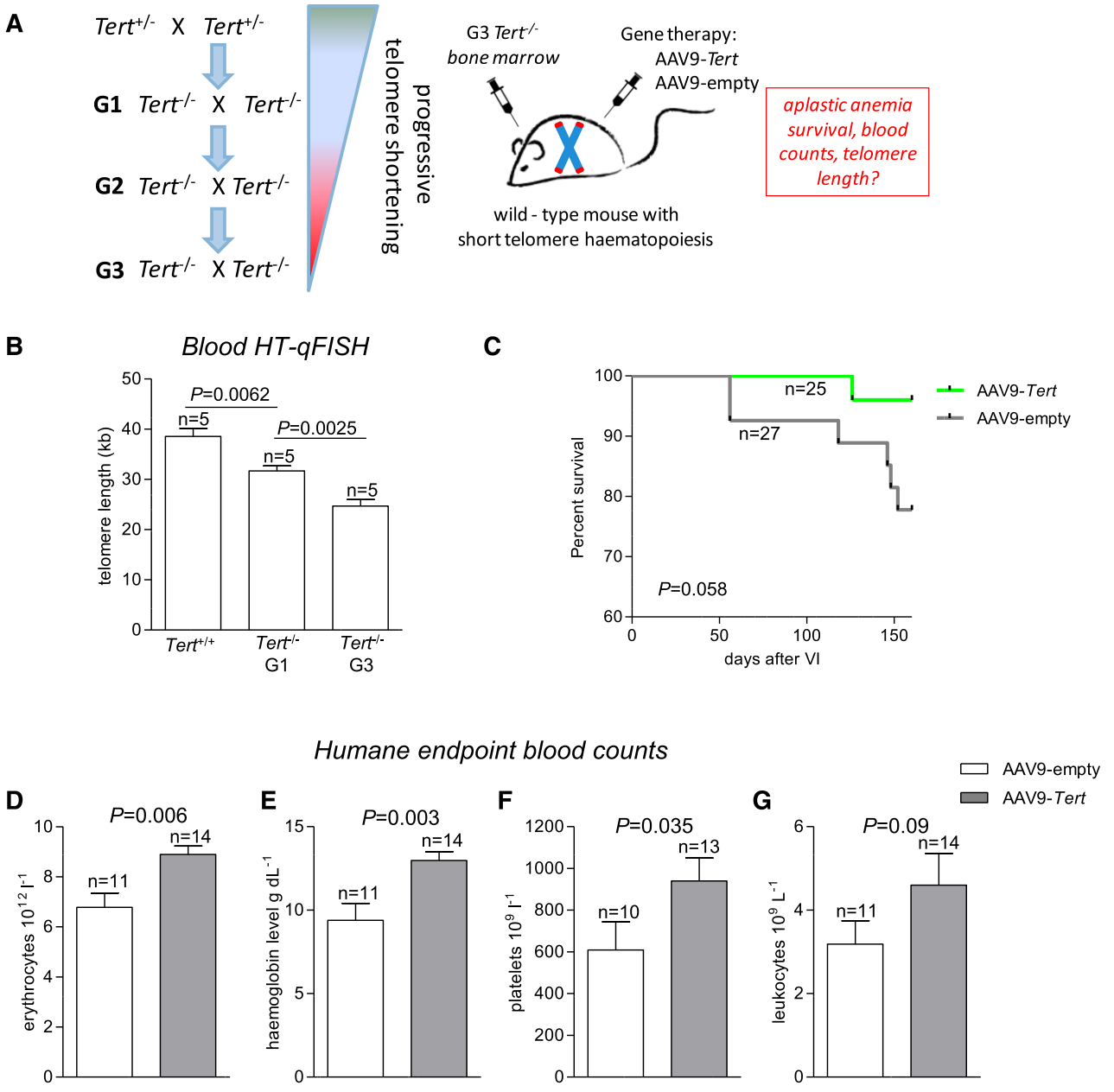

Figure 4. AAV9-*Tert* treatment improves blood counts in mice with short telomeres resulting from specific *Tert* deletion in the bone marrow. (A) Experimental design. G3 *Tert*$^{-/-}$ mice with short telomeres were generated by consecutive crosses of *Tert*-deficient mice. Bone marrow from these G3 mice was isolated and transplanted into irradiated wild-type mice. After engraftment, mice were injected with AAV9-*Tert* or AAV9-empty virus particles. (B) HT-Q-FISH analysis of telomere length in PBMCs from wild-type, G1 *Tert*$^{-/-}$, and G3 *Tert*$^{-/-}$ mice reveals progressive telomere shortening with consecutive mouse generations. (C) Kaplan-Meier survival curves show that AAV9-*Tert* treatment improves survival of mice with very short telomeres in the bone marrow due to *Tert* deficiency specifically in the bone marrow (irradiated wild-type mice transplanted with G3 *Tert*$^{-/-}$ bone marrow). AAV9-*Tert* compared with AAV9-empty treatment improves erythrocyte counts (D), hemoglobin levels (E), platelet counts (F), and leukocyte counts (G). In all graphs, n indicates number of mice. Data are mean ± SEM. Statistical analysis: log-rank test in panel A; 2-sided Student *t* test in panels B and E-H; *P* values are shown.

revealed increased telomere length in PBMCs from mice treated with telomerase gene therapy, suggesting that the vectors were also targeting the bone marrow.[18] This finding is in line with recent reports showing that AAV9 viral genome copies are readily detectable in bone marrow isolates even 20 weeks postinjection[35] and with the fact that FACS analysis of bone marrow from neonatal mice administered AAV9–green fluorescent protein show increased amounts of green fluorescent protein–positive cells.[36] Thus, *Tert* delivery via AAV9 may hold potential for treating aplastic anemia triggered or associated with short telomeres in the bone marrow, a common consequence of telomerase mutations in the so-called telomeropathies or telomere syndromes, as well as in some acquired cases of aplastic anemia.[37-39]

To demonstrate this, we first confirmed that a high dose (3.5×10^{12} viral genomes per mouse) of AAV9-EGFP reporter vector injected IV was able to transduce the bone marrow, as indicated by the presence of EGFP-positive cells. Furthermore, administration of the same amount of AAV9-*Tert* particles led to robust *Tert* expression in whole bone marrow isolates 2 weeks after treatment; this increased expression was maintained at 8 months posttreatment. To rule out the possibility that AAV9 may be targeting only bone marrow stroma cells, we

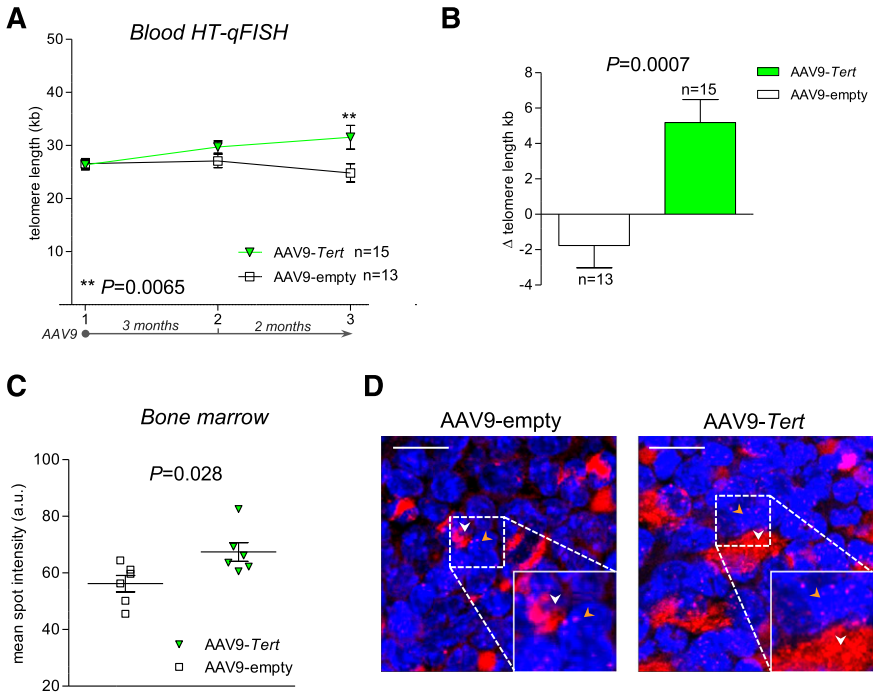

Figure 5. Telomerase gene therapy leads to telomere elongation in peripheral blood and bone marrow cells from mice with specific deletion of *Tert* in the bone marrow. (A) Longitudinal HT-Q-FISH analysis of telomere length in PBMCs of irradiated wild-type mice transplanted with bone marrow from G3 *Tert*$^{-/-}$ mice (see also Figure 4A). Blood was extracted at 3 different time points (time point 1, after G3 *Tert*$^{-/-}$ bone marrow engraftment and before AAV9 injection; time point 2, 3 months after AAV9 injection; and time point 3, 5 months after AAV9 injection). (B) Relative variation (Δ) of telomere length in AAV9-*Tert*-treated and AAV9-empty-treated animals between time points 1 and 3. (C) Telomere Q-FISH analysis on bone marrow sections from animals transplanted with G3 *Tert*$^{-/-}$ bone marrow and treated with AAV9-empty or AAV9-*Tert* for 5 months before euthanasia. Each square or triangle represents the mean telomere length per nucleus (expressed as arbitrary units of fluorescence) of an individual mouse. (D) Representative images of bone marrow sections from AAV9-*Tert*-treated and AAV9-empty-treated mice used for Q-FISH analysis. Cell nuclei are stained blue (DAPI) and telomeres are stained red (Cy3). White arrowheads indicate nonspecific extranuclear signals and yellow arrowheads indicate specific telomere signals within DAPI-stained nuclei. Bars represent 10 μm. For all experiments, n indicates number of mice. Data are mean ± SEM. Statistical analysis: 2-way analysis of variance in panel A; 2-sided Student *t* test in panels B and C; *P* values are shown.

demonstrated significantly increased *Tert* mRNA expression both in isolated hematopoietic stem cells (lin$^-$, Sca-1$^+$, c-kit$^+$) and in lineage-committed bone marrow cells (lin$^+$) from mice treated with AAV9-*Tert* compared with mice treated with the AVV9-empty vector. Importantly, bone marrow cells from AAV9-*Tert*-treated mice showed enhanced colony-forming abilities, suggesting that telomerase expression may increase the stem cell reserve.

Indeed, AAV9-*Tert* treatment of mice with aplastic anemia triggered by short telomeres resulting from marrow-specific *Trf1* deletion[19] significantly rescued mortality due to aplastic anemia, concomitant with telomere re-elongation in blood and bone marrow cells from these mice after telomerase treatment. We confirmed these findings by generating a second mouse model of aplastic anemia produced by short telomeres, in this case due to telomerase deficiency. In particular, we generated mice with *Tert* deficiency specifically in the bone marrow. In this case, the treatment of *Tert* gene therapy in mice with *Tert*-deficient bone marrow and short telomeres (irradiated wild-type mice transplanted with G3 *Tert*-knockout bone marrow) showed a moderate improvement of survival, which was not as dramatic as in the case of the *Trf1*-deficient bone marrow model. This result is likely due to the fact that in contrast to the *Trf1*-deletion model, which shows a very severe and rapid induction of aplastic anemia,[19,20] *Tert* deficiency leads to a variable penetrance of aplastic anemia with increasing mouse generations.[40,41] Similarly to the *Trf1*-deficient mouse model, *Tert* gene therapy of the *Tert*-deficient bone marrow mouse model also resulted in increased telomere length with time in peripheral blood cells and significantly improved blood counts. In both mouse models, improvement of blood counts can be interpreted as the consequence of improved stem cell reserve. This is in line with recently published data showing that genetic *Tert* re-activation in fifth-generation *Tert*$^{-/-}$ mice using a Cre-inducible system restored HSPC proliferation, concomitant with improved erythrocyte counts and hemoglobin levels.[42]

In summary, we provide proof of concept for a therapeutic effect of telomerase treatment using AAV9 gene therapy vectors in the treatment of aplastic anemia provoked by short telomeres. A strategy based on AAV9-*Tert* treatment may be beneficial not only in the correction of monogenic bone marrow disease such as in carriers of *Tert* mutations (we demonstrated improved blood counts in *Tert*-knockout mice) but also in other forms of aplastic anemia associated with short telomeres and hematopoietic stem cell depletion (eg, Fanconi anemia[43]). Generally, due to an excellent safety profile attributable to their low immunogenicity and the fact that they are nonintegrative, AAV vectors have become an attractive gene therapy tool, and many clinical trials using those vectors are already underway (see www.clinicaltrials.gov). However, despite the fact that AAV9 vectors carrying the *Tert* gene are nonintegrative and therefore unlikely to aid in the division of cancer cells, the association of many cancers with telomerase expression imposes specific safety concerns. In this regard, it is important to point out that in a previous study, a longer than 1-year follow-up of wild-type mice treated with AAV9-*Tert* did not show increased cancer; in fact, cancer onset was delayed in the same manner as other age-related diseases.[18] Nevertheless, subsequent studies should address the safety of this strategy in long-lived mammals such as primates. If those studies confirm our proof-of-principle findings, this gene therapy approach may also be adapted to treat hereditary forms of aplastic anemia caused by mutations other than *Tert* by replacing the gene to be delivered.

Acknowledgments

This study was funded by the Spanish Ministry of Economy and Competitiveness, the Fundación Botín, and the Roche Extending the Innovation Network Academia Partnering Program (M.A.B.).

Authorship

Contribution: M.A.B. conceived the original idea; M.A.B. and C.B. designed the experiments and wrote the paper; C.B. performed the majority of the experiments; R.S. performed the bone marrow

transplants and monitored the mice during all animal procedures; J.M.P., M.P., and C.B.-B. performed the experiments during the revision process; I.F. and M.B. contributed to scientific discussions and the experimental design; and F.B. provided the viral vectors.

Conflict-of-interest disclosure: The authors declare no competing financial interests.

The current affiliation for C.B. is Institute of Molecular and Translational Therapeutic Strategies, Hannover Medical School, Hannover, Germany.

Correspondence: Maria A. Blasco, Spanish National Cancer Research Center, Melchor Fernández Almagro 3, Madrid E-28029, Spain; e-mail: mblasco@cnio.es.

References

1. Scopes J, Bagnara M, Gordon-Smith EC, Ball SE, Gibson FM. Haemopoietic progenitor cells are reduced in aplastic anaemia. *Br J Haematol.* 1994;86(2):427-430.
2. Maciejewski JP, Anderson S, Katevas P, Young NS. Phenotypic and functional analysis of bone marrow progenitor cell compartment in bone marrow failure. *Br J Haematol.* 1994;87(2): 227-234.
3. Marsh JC, Ball SE, Cavenagh J, et al; British Committee for Standards in Haematology. Guidelines for the diagnosis and management of aplastic anaemia. *Br J Haematol.* 2009;147(1): 43-70.
4. Nakao S. Immune mechanism of aplastic anemia. *Int J Hematol.* 1997;66(2):127-134.
5. Dokal I, Vulliamy T. Inherited bone marrow failure syndromes. *Haematologica.* 2010;95(8): 1236-1240.
6. Brümmendorf TH, Maciejewski JP, Mak J, Young NS, Lansdorp PM. Telomere length in leukocyte subpopulations of patients with aplastic anemia. *Blood.* 2001;97(4):895-900.
7. Blackburn EH. Switching and signaling at the telomere. *Cell.* 2001;106(6):661-673.
8. de Lange T. Shelterin: the protein complex that shapes and safeguards human telomeres. *Genes Dev.* 2005;19(18):2100-2110.
9. Harley CB, Futcher AB, Greider CW. Telomeres shorten during ageing of human fibroblasts. *Nature.* 1990;345(6274):458-460.
10. Flores I, Canela A, Vera E, Tejera A, Cotsarelis G, Blasco MA. The longest telomeres: a general signature of adult stem cell compartments. *Genes Dev.* 2008;22(5):654-667.
11. Hiyama E, Hiyama K. Telomere and telomerase in stem cells. *Br J Cancer.* 2007;96(7):1020-1024.
12. Wynn RF, Cross MA, Hatton C, et al. Accelerated telomere shortening in young recipients of allogeneic bone-marrow transplants. *Lancet.* 1998;351(9097):178-181.
13. Ball SE, Gibson FM, Rizzo S, Tooze JA, Marsh JC, Gordon-Smith EC. Progressive telomere shortening in aplastic anemia. *Blood.* 1998; 91(10):3582-3592.
14. Flores I, Cayuela ML, Blasco MA. Effects of telomerase and telomere length on epidermal stem cell behavior. *Science.* 2005;309(5738): 1253-1256.
15. Vulliamy T, Marrone A, Dokal I, Mason PJ. Association between aplastic anaemia and mutations in telomerase RNA. *Lancet.* 2002; 359(9324):2168-2170.
16. Dokal I. Dyskeratosis congenita. *Hematology Am Soc Hematol Educ Program.* 2011;2011:480-486.
17. Tummala H, Walne A, Collopy L, et al. Poly(A)-specific ribonuclease deficiency impacts telomere biology and causes dyskeratosis congenita. *J Clin Invest.* 2015;125(5):2151-2160.
18. Bernardes de Jesus B, Vera E, Schneeberger K, et al. Telomerase gene therapy in adult and old mice delays aging and increases longevity without increasing cancer. *EMBO Mol Med.* 2012;4(8): 691-704.
19. Beier F, Foronda M, Martinez P, Blasco MA. Conditional TRF1 knockout in the hematopoietic compartment leads to bone marrow failure and recapitulates clinical features of dyskeratosis congenita. *Blood.* 2012;120(15):2990-3000.
20. Bär C, Huber N, Beier F, Blasco MA. Therapeutic effect of androgen therapy in a mouse model of aplastic anemia produced by short telomeres. *Haematologica.* 2015;100(10):1267-1274.
21. Martínez P, Thanasoula M, Muñoz P, et al. Increased telomere fragility and fusions resulting from TRF1 deficiency lead to degenerative pathologies and increased cancer in mice. *Genes Dev.* 2009;23(17):2060-2075.
22. Liu Y, Snow BE, Hande MP, et al. The telomerase reverse transcriptase is limiting and necessary for telomerase function in vivo. *Curr Biol.* 2000; 10(22):1459-1462.
23. Samper E, Fernández P, Eguía R, et al. Long-term repopulating ability of telomerase-deficient murine hematopoietic stem cells. *Blood.* 2002; 99(8):2767-2775.
24. Matsushita T, Elliger S, Elliger C, et al. Adeno-associated virus vectors can be efficiently produced without helper virus. *Gene Ther.* 1998; 5(7):938-945.
25. Ayuso E, Mingozzi F, Montane J, et al. High AAV vector purity results in serotype- and tissue-independent enhancement of transduction efficiency. *Gene Ther.* 2010;17(4):503-510.
26. Ayuso E, Blouin V, Lock M, et al. Manufacturing and characterization of a recombinant adeno-associated virus type 8 reference standard material. *Hum Gene Ther.* 2014;25(11):977-987.
27. Samper E, Goytisolo FA, Slijepcevic P, van Buul PP, Blasco MA. Mammalian Ku86 protein prevents telomeric fusions independently of the length of TTAGGG repeats and the G-strand overhang. *EMBO Rep.* 2000;1(3):244-252.
28. Canela A, Klatt P, Blasco MA. Telomere length analysis. *Methods Mol Biol.* 2007;371:45-72.
29. McIlrath J, Bouffler SD, Samper E, et al. Telomere length abnormalities in mammalian radiosensitive cells. *Cancer Res.* 2001;61(3):912-915.
30. Cawthon RM. Telomere measurement by quantitative PCR. *Nucleic Acids Res.* 2002; 30(10):e47.
31. Callicott RJ, Womack JE. Real-time PCR assay for measurement of mouse telomeres. *Comp Med.* 2006;56(1):17-22.
32. Inagaki K, Fuess S, Storm TA, et al. Robust systemic transduction with AAV9 vectors in mice: efficient global cardiac gene transfer superior to that of AAV8. *Mol Ther.* 2006;14(1):45-53.
33. Jimenez V, Muñoz S, Casana E, et al. In vivo adeno-associated viral vector-mediated genetic engineering of white and brown adipose tissue in adult mice. *Diabetes.* 2013;62(12):4012-4022.
34. Canela A, Vera E, Klatt P, Blasco MA. High-throughput telomere length quantification by FISH and its application to human population studies. *Proc Natl Acad Sci USA.* 2007;104(13): 5300-5305.
35. Huang J, Li X, Coelho-dos-Reis JG, Wilson JM, Tsuji M. An AAV vector-mediated gene delivery approach facilitates reconstitution of functional human CD8+ T cells in mice. *PLoS One.* 2014; 9(2):e88205.
36. Mattar CN, Wong AM, Hoefer K, et al. Systemic gene delivery following intravenous administration of AAV9 to fetal and neonatal mice and late-gestation nonhuman primates. *FASEB J.* 2015; 29(9):3876-3888.
37. Armanios M, Blackburn EH. The telomere syndromes. *Nat Rev Genet.* 2012;13(10): 693-704.
38. Calado RT, Young NS. Telomere diseases. *N Engl J Med.* 2009;361(24):2353-2365.
39. Kirwan M, Dokal I. Dyskeratosis congenita, stem cells and telomeres. *Biochim Biophys Acta.* 2009; 1792(4):371-379.
40. Herrera E, Samper E, Blasco MA. Telomere shortening in mTR-/- embryos is associated with failure to close the neural tube. *EMBO J.* 1999; 18(5):1172-1181.
41. Herrera E, Samper E, Martín-Caballero J, Flores JM, Lee HW, Blasco MA. Disease states associated with telomerase deficiency appear earlier in mice with short telomeres. *EMBO J.* 1999;18(11):2950-2960.
42. Raval A, Behbehani GK, Nguyen XT, et al. Reversibility of defective hematopoiesis caused by telomere shortening in telomerase knockout mice. *PLoS One.* 2015;10(7):e0131722.
43. Dokal I, Vulliamy T. Inherited aplastic anaemias/ bone marrow failure syndromes. *Blood Rev.* 2008; 22(3):141-153.

Supplementary Information

Supplementary Figure 1 l AAV9-*Tert* mRNA expression level. *Tert* expression (qPCR) in heart and liver tissue and peripheral blood cells 2 weeks after virus injection with $3.5x10^{12}$ vg/mouse AAV9-*Tert* relative to the expression of mice injected with the same amount of AAV9-empty vector.

Supplementary Figure 2 l AAV9-*Tert* treatment does not alter bone marrow constitution in wild-type mice. (A) Representative FACS analysis of HSCs. Single cell (doublet exclusion) (i) were next gated on forward and side scatter (FSC and SSC respectively) to eliminate debris and erythrocytes (ii). Including only viable cells on the basis of DAPI exclusion, lineage negative (Lin^-) cells were then separated (iii). c-Kit and Sca1 double positive cells were then sorted to obtain purified HSCs. (iv) **(B)** Bar graphs indicating the proportions of Lin+, Lin- and HSCs cells in total bone marrow isolates from mice treated with AAV9-*Tert* or AAV9-empty as indicated. No significant differences were observed, *P*-values are depicted. Statistical analysis: Two-tailed student's t-test. n = number of mice.

Supplementary Figure 3 l Bone marrow genotype of transplanted mice and pI:pC mediated *Trf1* excision. Genomic DNA from whole bone marrow cells of wild-type mice and mice transplanted with $Trf1^{lox/lox}$ *Mx1-Cre* bone marrow which were injected with pI:pC to induce *Trf1* excision was isolated. The *Trf1* locus was PCR amplified with

specific primers and PCR products were run on a 1% agarose gel. Lane 1-3 shows, in three individual animals, that the bone marrow consist only of the transgenic, donor bone marrow as seen by the presence of the 1.5kb $Trf1^{lox}$ and the 0.45kb $Trf1^{\Delta}$ excision fragment, while the 1.4kb band indicating the $Trf1^{WT}$ is absent in lane 1-3. In contrast only the 1.4kb $Trf1^{WT}$ fragment is detected in lane 4-5 where donor bone marrow was wild-type.

Supplementary Figure 4 l Relative telomere length. (A) Relative telomere length determined by real time PCR (T/S method) in bone marrow genomic DNA of mice transplanted with G3 *Tert* knock-out bone marrow and treated with AAV9-*Tert* or AAV9-empty as indicated. For the control genomic DNA of bone marrow from 3 wild-type mice was pooled. **(B)** Relative telomere lengths of bone marrow samples from mice treated with AAV9-empty virus indicate that mice with shorter telomeres are prone to develop aplastic anemia. Compared is the telomere length of mice that developed aplastic anemia (white bars) with those that did not (grey bars). Each bar represents the relative telomere length of one mouse. Statistical analysis: two-sided Student's t-test, P-value is shown.

Supplementary Figure 5 l AAV9-Tert leads to robust *Tert* expression in *tert* knock-out bone marrow. (A) Quantitative analysis of *Tert* mRNA expression level expressed as deltaCT values in total bone marrow isolated 1 month and **(B)** 4 months after virus injection (VI) with $3.5x10^{12}$ vg/mouse AAV9-*Tert* relative to the expression of mice

injected with the same amount of AAV9-empty vector. Data are mean ± SEM. Statistical analysis: two-sided Student's t-test, P-values are shown. n = number of mice.

Supplementary Figure 1

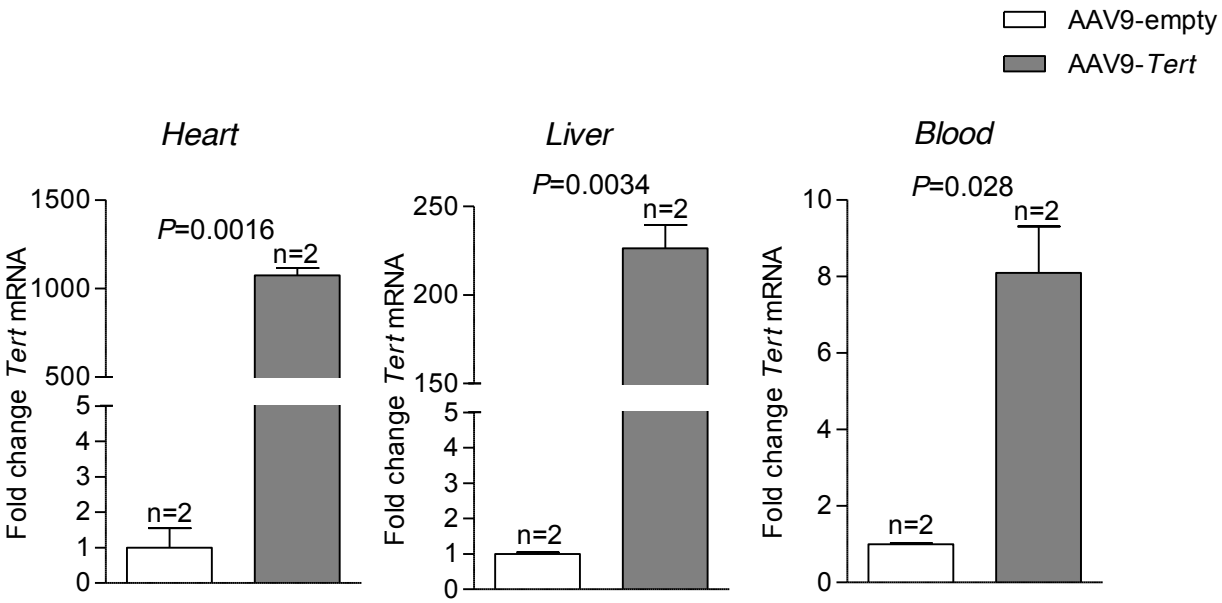

Supplementary Figure 2

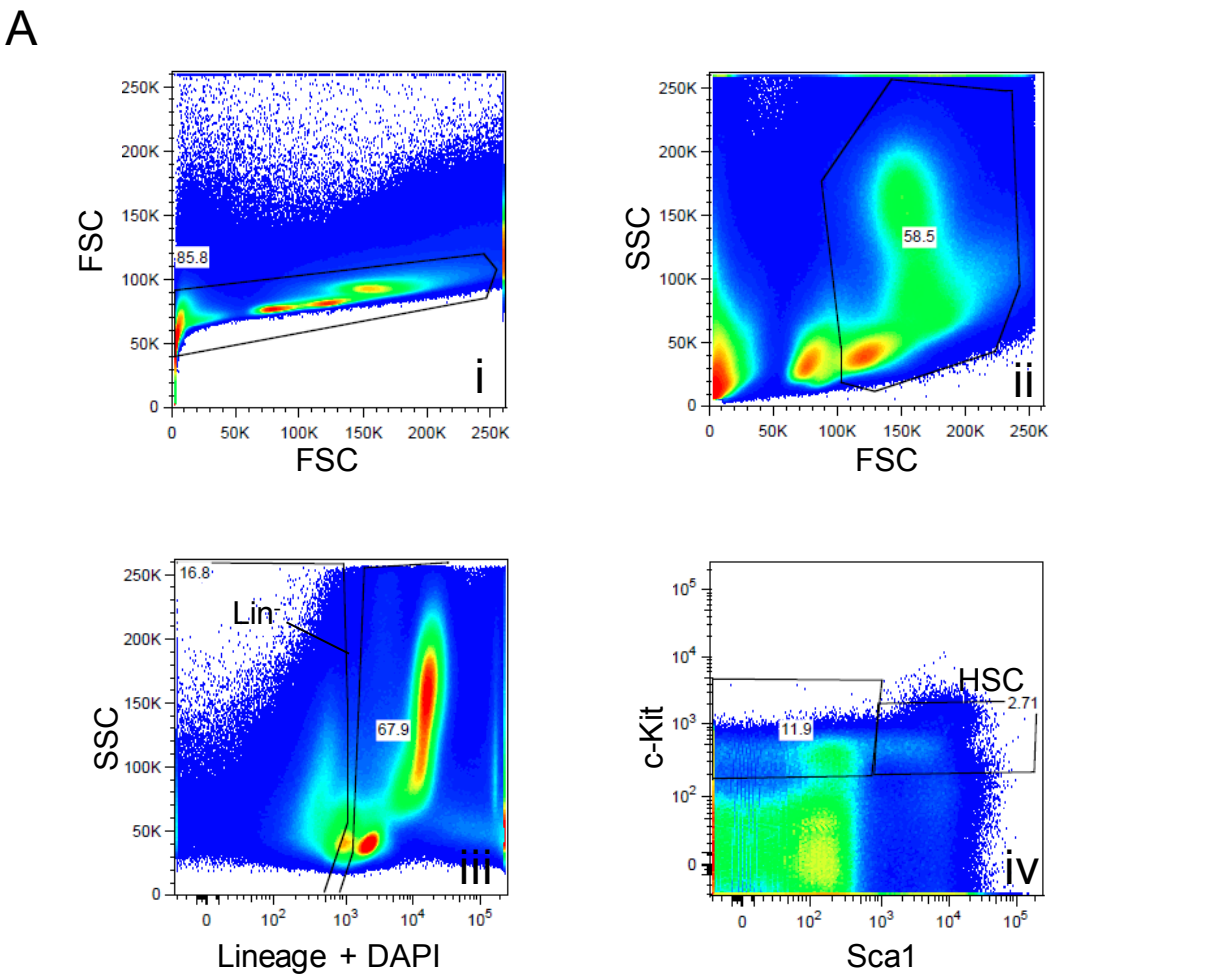

Supplementary Figure 3

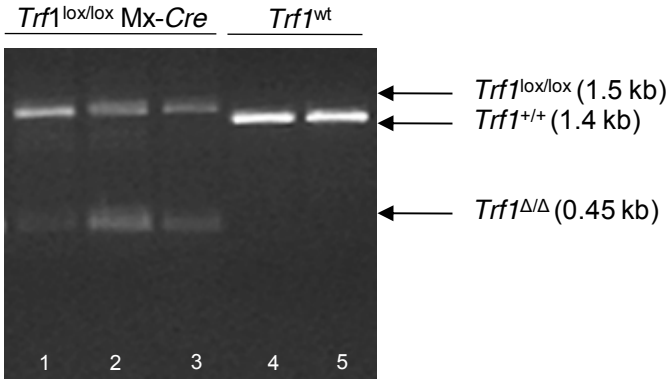

Agarose 1%

Supplementary Figure 4

A

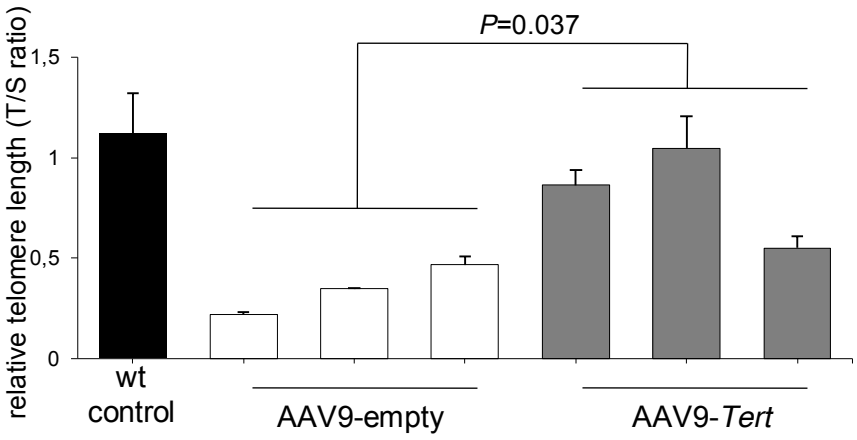

B

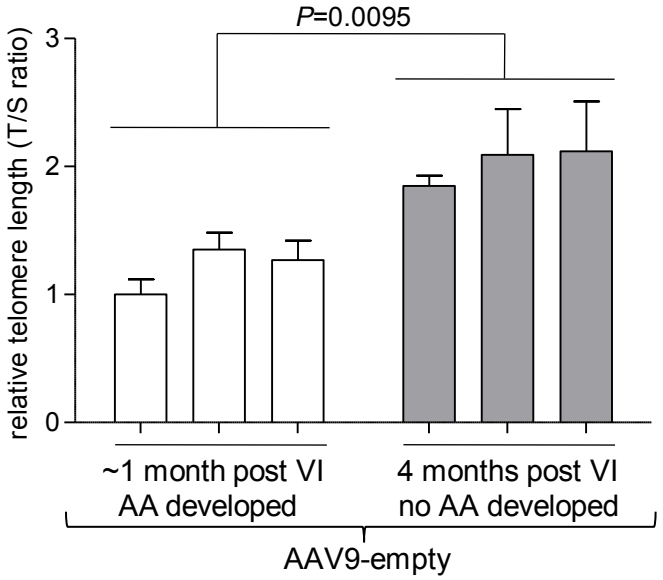

Supplementary Figure 5

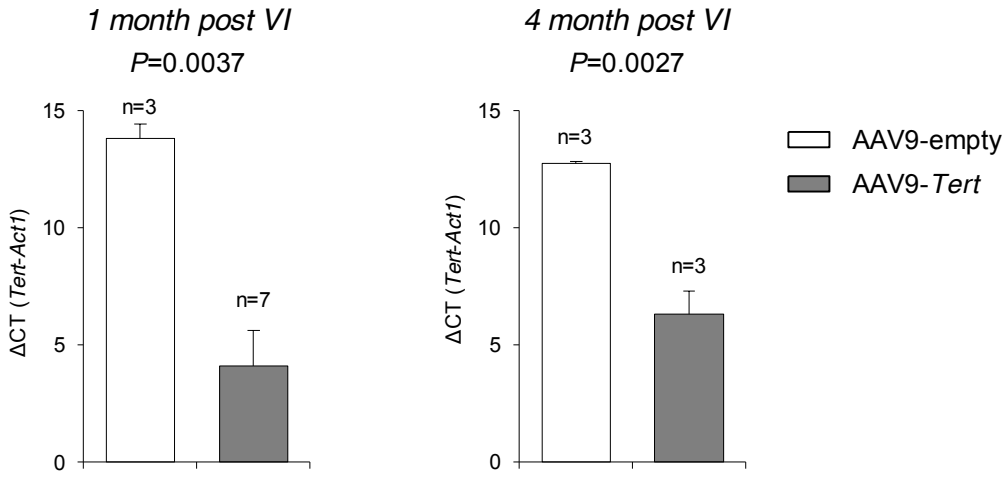

DISCUSSION

At the moment of writing this discussion, the search "telomere length cancer" in PubMed rendered 2524 academic entries. In spite of 30 years of research, it is still not clear whether TL in surrogate tissues such as blood can be used as a biomarker to predict cancer risk susceptibility. The reason is simple: TL regulation is complex and although telomere shortening can contribute to genome instability in some type of cancers, there are several environmental and genetic factors that determine TL for each individual.

The main focus of this thesis was the identification of environmental and genetic factors that modify TL, in order to improve TL association studies and gain a better understanding of TL regulation and its relation with cancer, especially in the context of FBOC.

As a potential exogenous TL modifier, the effect of chemotherapy on TL was evaluated in sporadic and in familial breast cancer patients, to assess whether it could be a confounding factor that may bias TL results in those association studies that use TL as a biomarker of disease susceptibility.

As potential genetic factors modifying TL, we evaluated the effect of two "cancer risk polymorphisms" in DNA glycosylases (BER pathway) in hereditary breast and ovarian cancer patients. We studied the role of these polymorphisms in TL regulation, telomerase activity, oxidative stress susceptibility, oxidative DNA damage at telomeres, and nuclear DNA damage. We wanted to explain the molecular mechanism behind the cancer modifier effect of these polymorphisms, but also to explore their involvement in TL regulation and telomere stability.

To this end, we first designed a prospective study to include and evaluate periodically individuals from families harboring a familial mutation in *BRCA1* or *BRCA2*, and from families without mutations in *BRCA1* or *BRCA2* (*BRCAX*). Evaluation consisted in filling out a questionnaire with information related to lifestyle and personal habits, as well as blood extraction to perform different biological studies (quantification of mRNA expression for *OGG1* and *NEIL2*, TL and telomerase activity measurement and oxidative stress evaluation).

In the first part of this Thesis, from article 1 to article 3, individuals from the familial breast / breast and ovarian cancer series (FBC/FBOC) also took part in the prospective study mentioned above.

As a consequence of our findings exploring those "cancer risk polymorphisms" and their relation with genome and telomere instability in *BRCA1* and *BRCA2* mutation carriers, we opened a new line of research. We considered the possibility that *OGG1* and *NEIL2* might display synthetic lethality together with *BRCA1* and *BRCA2*, respectively. We also considered the possibility that the DNA glycosylases OGG1 and NEIL2 might be candidates for being targeted as a treatment strategy for *BRCA1*- and *BRCA2*-derived tumors. We therefore started a collaboration with the Thomas Helleday laboratory (Karolinska Institutet, Stockholm) to further explore this hypothesis. Article 4 summarizes the results and findings in relation to this topic.

Finally, articles 5 and article 6 summarize the results of collaborations with other groups, and were included in this thesis to illustrate that cancer and disease susceptibility are not exclusively associated with telomere shortening. In fact, TL dysregulation due to mutations in genes directly associated with telomere maintenance presents different phenotypes, and both telomere shortening and telomere lengthening can converge in the manifestation of a disease.

EXOGENOUS FACTORS THAT MODIFY TELOMERE LENGTH: CHEMOTHERAPY

Article 1

Hereditary breast and ovarian cancer presents some characteristics that are common to certain telomeropathies, characterized by mutations in genes related with telomere biology (shelterin complex or telomerase).

Familial breast and ovarian cancer (FBOC) is predominantly associated with inherited mutations in two genes, *BRCA1* and *BRCA2*, which are tumor suppressor genes responsible for maintaining genome stability through their involvement in homologous recombination (HR) double-stranded break DNA repair (Roy *et al*. 2012). In addition, there is evidence to suggest that BRCA1 is localized at telomeres and may regulate TL and stability (Blasco 2005; Badie *et al*. 2010; Badie *et al*. 2015; Cabuy *et al*. 2009) and that BRCA2 protein may be involved in telomere replication (Badie *et al*. 2010).

As described earlier for dyskeratosis congenita (DKC) (Vulliamy *et al*. 2004), our group described a mechanism of genetic anticipation in hereditary breast cancer (Martinez-Delgado *et al*. 2011) driven by telomere shortening in *BRCA1* and *BRCA2* mutation carriers, and a subgroup of *BRCAX* cancer cases. These results suggested that BRCA1 and BRCA2 proteins, were likely involved in TL maintenance, and that telomere shortening was the causal mechanism explaining the cancer anticipation across generations. It also opened the possibility of looking for new cancer susceptibility genes associated with TL maintenance that could explain other BRCAX breast cancer families.

After this initial report, two independent reports using larger series of *BRCA1* and *BRCA2* hereditary breast cancer patients showed different results (Killick *et al*. 2014; Pooley *et al*. 2014). These three reports paint three different scenarios for the roles of the *BRCA1* and *BRCA2* mutations in TL regulation in relation with cancer risk development. In the first scenario, telomere shortening as a hallmark of genome instability may be associated with *BRCA1* and *BRCA2* mutations, and this would contribute to cancer risk development (Martinez-Delgado *et al*. 2011). In the second scenario, TL is not associated either with *BRCA1/BRCA2* mutations or cancer

risk (Killick *et al*. 2014). In the third scenario, longer telomeres are associated with *BRCA1* and *BRCA2* mutations, independently of cancer status (Pooley *et al*. 2014).

The three studies were done in a retrospective manner and in none of them treatment status, which might constitute a confounding factor, was evaluated independently as a possible modifier of TL. We tried to overcome this possible bias by working with two independent cohorts of women with breast cancer (sporadic and familial) and using two different approaches (cross-sectional and longitudinal). In addition, we measured TL by two independent methods and obtained similar results.

We used a series composed of 266 sporadic breast cancer patients, treated with conventional chemotherapy and with a follow-up of 5 years and detailed clinical and treatment records, to characterize the effect of the two major chemotherapy schedules (AC+T/T+AC and FEC+T/T+FEC) on TL (Table 1).

Overall, we found that TL was shortened by the effect of the chemotherapy, although this effect was not permanent, and TL could be recovered after the treatment:
Telomere shortening started at 91-180 days after the beginning of treatment and reached its maximum effect between 91-180 days after the end of treatment. Then, a recovery phase started, and it lasted for a maximum of 5 years. After this period, the original TL was recovered (Table S2). We detected some variations in the chemotherapy effects during the initial "telomere shortening phase" and during the "recovery phase", depending on the chemotherapy combination (Figure 2). These variations suggest that TL is affected by conventional chemotherapies in different ways, depending on the mechanism of action of the specific drug involved ((hypo-) alkylating agents, anti-replicative molecules, spindle poisons, anti-topoisomerase I and II). The effects of chemotherapeutic drugs on TL and telomerase activity in cell culture experiments with different cell lines have been the subject of a recent review and are summarized in Table below*.

Table* Effect of chemotherapeutic drugs on telomere length and telomerase activity in cultured cells (Bolzán 2016).

DRUG	TL	TELOMERASE ACTIVITY	CELL TYPE	REFERENCE
Cisplatin	↓	ND	Hela cells	(Ishibashi & Lippard 1998)
	ND	↓	Human testicular cancer cells	(Burger *et al*. 1997)
	ND	↓	Human endometrial cancer cells	(Basiak *et al*. 2002)
	↓	↓	Mouse spermatogonial cells	(Liu *et al*. 2014)

	↓	↑	Human ovarian cancer cells	(Kiyozuka *et al*. 2000)
	↓	↓	Human hepatoma cells	(Zhang *et al*. 2002)
	ND	↓	Human ovarian cancer cells	(Kunifuji *et al*. 2002)
	ND	↓	Human head and neck squamous cell carcinoma cell lines	(Kunifuji *et al*. 2002)
	ND	--	Human haematopoietic cancer cell lines	(Park *et al*. 1998)
Paclitaxel	↓	--	Mouse melanoma cells	(Asha S. Multani *et al*. 1999a)
	↓	--	Paclitaxel-requiring mutant CHO cells	(A S Multani *et al*. 1999b)
	↓	↓	Human pharynx tumor cells	(Mo *et al*. 2003)
	--	--	Human ovarian cancer cells	(Kiyozuka *et al*. 2000)
	↓	ND	Human pharynx tumor cells	(Johnston *et al*. 2003)
Doxorubicin	↓	↓	Human hepatoma cells	(Zhang *et al*. 2002)
	--	--	Human ovarian cancer cells	(Kiyozuka *et al*. 2000)
	--	↓	Human breast tumor cells	(Elmore *et al*. 2002)
	ND	↓	Human breast and stomach cancer cells	(Park *et al*. 1998)
	↓	↓	Human normal T-lymphocytes and fibroblasts	(Li *et al*. 2012)
	ND	↓	Human ovarian cancer cells	(Kunifuji *et al*. 2002)
	ND	--	Human testicular cancer cells	(Burger *et al*. 1997)
Cyclophosphamide	↓	↑	Human ovarian cancer cells	(Kiyozuka *et al*. 2000)
4OOH-CPA (**)	↓	↓	Mouse spermatogonial cells	(Liu *et al*. 2014)
5-Fluorouracil (5-FU)	ND	--	Human head and neck squamous cell carcinoma cell lines	(Lee *et al*. 2007)

↑: increasing effect (telomere elongation); ↓: decreasing effect (telomere shortening or erosion); --: no effect; ND: Not determined; **: 4-hydroperoxycyclophosphamide, a preactivated analog of cyclophosphamide.

Once we confirmed that chemotherapy was a TL modifier in sporadic breast cancer patients, we moved to the FBC model. We used both cross-sectional and longitudinal approaches to test whether the *BRCA* genes and chemotherapy are modifiers of TL and/or telomerase activity in these patients.

In the cross-sectional approach, we found similar results as in our previous study (Martinez-Delgado *et al*. 2011): familial cases presented shorter telomeres than controls. However, a substantial proportion of the samples were taken during or after a short time of chemotherapy administration. When we corrected for treatment status, we were not able to detect any effect of the *BRCA1* and/or *BRCA2* mutations on telomere shortening, neither in healthy carriers nor in post-treatment *BRCA1/2* patients. In contrast, patients "during treatment" exhibited shorter TL independently of the mutational status. This suggests that the treatment is the real TL modifier (Figure 3b). In addition, these results partially explain the discrepancies reported in the literature regarding the role of the *BRCA1* and *BRCA2* mutations as modifiers of TL (Martinez-Delgado *et al*. 2011) and point to chemotherapy as a factor that needs to be taken into consideration to obtain reliable results.

Although it is not clear yet whether *BRCA1* and/or *BRCA2* are involved in TL maintenance and their relation with cancer risk, recent studies suggest that mutations in these genes disrupt TL homeostasis and contribute to malignant transformation and cancer risk for *BRCA* mutant carriers (Uziel *et al*. 2016; Thorvaldsdottir *et al*, 2017).

To summarize, our study focused on the effect of cancer treatment on TL in both familial and sporadic breast cancer cases. We cannot rule out that *BRCA1* and *BRCA2* might be minor modifiers of TL, but it appears from our results that the treatment is the true cause of telomere shortening. The rates of telomere shortening and recovery may vary depending on the treatment. These results stress the need to perform prospective and retrospective TL association studies, considering the variability found as a consequence of the treatment status for cancer patients (untreated, during treatment and post treatment), to avoid reverse causation bias.

ENDOGENOUS FACTORS THAT MODIFY TL: "CANCER RISK POLYMORPHISMS" IN DNA GLYCOSYLASES OF THE BER PATHWAY

At the age of 70, cumulative cancer risk for *BRCA1* and *BRCA2* mutation carriers ranges from 43% to 88% for breast cancer development, and from 11% to 59% for ovarian cancer (Antoniou *et al*. 2003; Milne *et al*. 2008). This high variability is the consequence of other genetic and/or environmental factors that can modify cancer risk.

Regarding genetic factors, Single Nucleotide Polymorphisms (SNPs) located in the *OGG1* and *NEIL2* genes were identified as cancer risk modifiers for *BRCA1* and *BRCA2* mutation

carriers, respectively (Osorio *et al*. 2014). Although the molecular mechanism underlying the cancer risk association is still unknown, both SNPs were in transcriptional regulatory regions of genes encoding DNA glycosylase enzymes involved in the BER DNA repair pathway.

Oxidative DNA damage is repaired by the BER pathway, in which DNA glycosylases play an important role by recognizing and excising the oxidized bases in the DNA, at the very first step of the pathway (Dianov & Hübscher 2013). Later steps are also dependent on DNA glycosylases to finish the repair process. Oxidative DNA damage is especially challenging at telomere regions, because telomeres are prone to oxidation and because the complex structure of the telomeres makes access of the DNA repair machinery to telomeres difficult (Wallace 2014). Oxidative DNA damage at telomeres leads to telomere shortening, and proper BER performance is crucial to maintain TL homeostasis.

Hence, we tried to explain the molecular bases underlying their association with cancer in the context of *BRCA1* and *BRCA2* deficiency, taking into consideration that they could be TL modifiers given the role that these enzymes play in oxidative DNA damage repair, especially at the telomere region.

Article 2

The first SNP, rs2304277, was reported to be a modifier of ovarian cancer risk for *BRCA1* mutation carriers (Osorio *et al*. 2014). This SNP is located 1.8Kb downstream of the 3´UTR region of the DNA glycosylase OGG1 (BER). Polymorphisms that create potential illegitimate microRNA target sites (Clop *et al*. 2006; Brewster *et al*. 2012) may be involved in altering normal *OGG1* mRNA or protein levels. Indeed, by using the segRNA2.0 web server to identify functional RNA motifs, we found a new miRNA interaction region for miRNA-23a created by the SNP (not included as a result of this thesis). Interestingly, this miRNA is highly expressed in ovarian cancer (Vaksman *et al*. 2011).

We decided to explore the role of this SNP in transcriptional regulation using two sets of samples. The first set consisted of 223 blood samples from controls and FBOC patients with a heterogeneous BRCA mutational status (*BRCA1, BRCA2* and *BRCAX*), and the second was a panel of 23 lymphoblastoid cell lines (LCLs) derived from *BRCA1* mutation carriers and non-carrier controls.

We confirmed in both sample sets (FBOC series and LCLs) a significantly lower expression of *OGG1* mRNA transcripts associated with the SNP, independently of *BRCA* mutational status (Figure 1a & Figure 1b). We extended the analysis by consulting the Gtex eQTL database (http://www.gtexportal.org) for the effect of the SNP on *OGG1* mRNA levels in different tissues, and we found significant down-regulation in ovary tissue (p=0.023) where this SNP was initially found to contribute to cancer risk (Supplementary Table S4).

These results suggest that this cancer risk variant is likely associated with transcriptional down-regulation of *OGG1* mRNA, which could lead to higher genome/telomere instability due to a defective 8-oxoG repair capacity.

Given the role of the BER pathway and in particular the OGG1 enzyme in telomere repair (Wang *et al*. 2010; Lu & Liu 2010), we explored the impact of this SNP on some features related to telomere biology that are considered as hallmarks of genome instability, such as telomere shortening or the percentage of critically short telomeres. Using linear regression analysis, we found that the SNP may be a TL modifier for *BRCA1* and *BRCA2* mutation carriers (p=0.013). Carriers of BRCA1/2 mutations and the *OGG1* SNP presented a significantly shorter TL compared to both controls (p=0.009) and mutation carriers not harboring the SNP (p=0.003) (Figure 2a), likely due to accelerated telomere shortening during life (Figure 2c). These results were experimentally validated in our LCL set by measuring TL after 55 passages. We found significantly faster telomere shortening in the group of samples harboring a *BRCA1* mutation together with the SNP (p=0.033) (Figure 3a). Our results point to a synergistic effect of the SNP and the *BRCA1* mutation on telomere shortening. This may be due to the accumulation of oxidative lesions at the telomeric region (Ahmed *et al*. 2008; Coluzzi *et al*. 2014) triggered by a defective BER performance (Wang *et al*. 2010) due to this SNP and its effect on *OGG1* transcriptional down-regulation.

Using the LCL panel, we compared the percentage of damaged cells and nuclear γH2AX signal intensity among different genotypes under basal conditions (first passage and no irradiation). We found that LCLs harboring the SNP presented significantly higher γH2AX signal intensity at the nucleus (p=0.010) (Figure 4b), suggesting that this SNP contributes to DNA damage. These results are similar to others reported in the literature establishing an association between SNPs in *OGG1* at the same gene region and an increased DNA damage/genome instability due to impaired BER performance (Krupa *et al*. 2011; Berger *et al*. 2013; Cardin *et al*. 2012; Yuan *et al*. 2012; Moritz *et al*. 2014).

In summary, we found that the *OGG1* SNP itself contributes to increased nuclear DNA damage, probably due to a defective BER performance triggered by *OGG1* transcriptional down-regulation. Additionally, our results suggest a synergistic effect between *BRCA1* or *BRCA2* mutations and SNP rs2304277 on telomere shortening and telomere instability.

These results suggest a possible synthetic lethal interaction between *OGG1* from the BER pathway and *BRCA1* from the HR DNA repair pathways, although further studies are needed to confirm this hypothesis.

Article 3

The original study of Osorio *et al* reported that SNP rs1466785 located in the *NEIL2* gene was a breast cancer risk modifier for *BRCA2* mutation carriers (Osorio *et al*. 2014). Imputation using "1000 Genomes" data showed that there were several SNPs in strong linkage disequilibrium (LD) with rs1466785 (Osorio *et al*. 2014). Of these, we considered rs804271 to be the best candidate, given that it showed the most significant associations and that there were epidemiological and functional data supporting its putative role in cancer (Osorio *et al*. 2014), although the molecular mechanism underlying this association is unknown. This SNP is located at the promoter region of the *NEIL2* gene, within a previously described transcriptional regulatory region (Kinslow *et al*. 2010). Indeed, 18 proteins are predicted to interact with that region, and 3 motifs, which are binding regions for transcription factors (E2F, Sin3Ak-20 and YY1), are predicted to be altered in the presence of this polymorphism (http://archive.broadinstitute.org).

Previous characterization of the *NEIL2* gene promoter region showed that *NEIL2* transcription is influenced by certain SNPs located upstream of the transcription start site (Kinslow *et al*. 2008). The results presented in this report support these findings and suggest that rs804271 is associated with constitutive transcriptional activation of *NEIL2*.

First, we checked the effect of rs804271 on *NEIL2* mRNA levels in different tissues using the Gtex eQTL database (http://www.gtexportal. org), and we found a significant up-regulation associated with the presence of the SNP in several tissues including breast, ovary and blood ($p<0.0001$) (Supplementary Table S3).

Next, we validated these results in our FBOC series and we found significantly increased *NEIL2* mRNA levels in individuals harboring the SNP ($p=0.003$), suggesting that it is associated with transcriptional activation of the *NEIL2* gene (Supplementary Table S4).

Consistent with the fact that NEIL2 is an important enzyme of the BER pathway, it was recently reported to be the gene most frequently displaying loss of copy number (Chae YK *et al* 2016). In addition, it appears to be significantly down-regulated in several tumors (Hildrestrand *et al*. 2009). Taking these facts into consideration, it seems unlikely that *NEIL2* transcriptional activation is the causal explanation for the cancer modifier effect of this polymorphism in *BRCA2* mutation carriers.

As an alternative hypothesis, it is possible that this SNP reduces the activity of the NEIL2 enzyme, leading to an accumulation of oxidative lesions and to a *NEIL2* transcriptional activation by a positive feedback mechanism.

Since NEIL2 is involved in oxidative DNA damage repair at the telomeres (Zhou *et al*. 2015; Chakraborty *et al*. 2015) and since these regions are very susceptible to being oxidized, we evaluated telomere oxidation levels to assess the constitutive oxidative DNA repair capacity among the different FBOC genotypes. Strikingly, we found that *BRCA2* mutation carriers

presented significantly higher levels of oxidation at the telomeres ($p<0.0001$); those levels were mainly explained by the subgroup of patients harboring the *NEIL2* SNP (Figure 1a & Figure 1b), which suggests that oxidative DNA repair is compromised when the rs804271 is present together with a *BRCA2* mutation. These results were unrelated to oxidative stress susceptibility (Supplementary Table S7).

In support of a functional role of this polymorphism in the performance of the NEIL2 enzyme, it was previously reported in the literature that polymorphism rs804271 (previously ss74800505) was associated with significantly increased mutagen-induced genetic damage (Kinslow *et al*. 2008).

A functional effect on transcription was initially expected, since this SNP is in the promoter region of *NEIL2*. However, our results suggest that this polymorphism is also associated with a reduced enzymatic activity exclusively in *BRCA2* mutation carriers that leads to an accumulation of oxidative DNA damage, which can be detected at the telomere region. This scenario could be the molecular mechanism explaining the cancer modifier effect of this SNP in *BRCA2* mutation carriers.

Regarding the role of this SNP in *BRCA1* mutation carriers, we found it to be significantly associated with higher MDA levels in plasma (Supplementary Table 6). This result correlated with a higher telomere instability reflected by reduced TL (β=-0.54; p= 0.007), accumulation of short telomeres (β=0.45; p= 0.024) and lower telomerase activity levels (β=-0.57; p= 0.035) (Supplementary Table S8). In relation with these results, a large number of studies have demonstrated that the BRCA1 protein is also involved in the response to oxidative stress through its interaction with NFR2, a key player that regulates antioxidant signaling response and cell proliferation (Gorrini *et al*. 2013; Marks 2013). Since oxidative stress correlates with telomere shortening (Richter & Zglinicki 2007), it was not surprising to find this telomere phenotype in *BRCA1* mutation carriers, although the SNP is not associated with cancer risk for this group.

Altogether, our results suggest that rs804271, located in the promoter region of the gene *NEIL2*, has a functional effect on *NEIL2* mRNA transcriptional activation although it is unlikely to be related to the cancer risk modifier effect of the SNP in *BRCA2* mutation carriers. In addition, we found that the SNP is associated with short TL, accumulation of short telomeres and lower telomerase activity in *BRCA1* mutation carriers, likely due to a higher oxidative stress susceptibility for this group. Finally, we found that the SNP in *BRCA2* mutation carriers may reduce NEIL2 enzyme activity leading to a significant accumulation of oxidative DNA damage that can be detected at the telomere region. This suggests that the effect of this SNP on cancer risk for *BRCA2* mutation carriers could be driven by its effect on enzymatic activity.

BER DNA GLYCOSYLASES AS POTENTIAL TARGETS FOR TREATING *BRCA1*/ *BRCA2*-DERIVED TUMORS

Article 4

As was shown in articles 2 and 3, common genetic variations in *OGG1* and *NEIL2* can contribute to cancer risk for *BRCA1* and *BRCA2* mutation carriers, likely through a synthetic lethal interaction between both genetic events.

These results not only imply that DNA glycosylases play an important role in telomere maintenance and genome stability in *BRCA1* and *BRCA2* mutation carriers, but also that *OGG1* and *NEIL2* could be targets for the development of molecules inhibiting enzyme activity in *BRCA1*- and *BRCA2*-derived tumors, to promote synthetic lethality as an anticancer strategy against these types of tumors.

Following this hypothesis, we tested a set of novel molecules that effectively inhibit OGG1 enzyme activity "*in vitro*" (data not shown) in a breast cancer cell line (MDA-MB-231) with functional BRCA1 protein, and in the same cell line with *BRCA1* inactivated through shRNA constructs (MDA-MB-231sh*BRCA1*) (Supplementary Figure1).

We observed that in this specific model the entire set of molecules tested sensitized preferentially MDA-MB-231sh*BRCA1* after 5 days of treatment compared to MDA-MB-231 with functional BRCA1 protein (Figure1 and Table1). In addition, we confirmed this result in a commercial *BRCA1*-deficient breast cancer cell line (MDA-MB-436). In contrast, the pancreatic *BRCA2*-deficient cancer cell line PL45 was not sensitized at all by OGG1 inhibitors (figure2).
To explain the sensitization observed in *BRCA1*-deficient cells after pharmacological inhibition of OGG1, we evaluated oxidative DNA damage accumulation and its conversion into DSBs in both MDA-MB-231 and MDA-MB-231sh*BRCA1* cells.

To study the accumulation of oxidative DNA damage, we modified a previously described protocol to detect oxidative lesions (8-oxoG) at the telomere region (O'Callaghan *et al*. 2011). We used this method to quantify the effectiveness of the OGG1 inhibitor molecule TH5487 in cultured cells.

After 24 hours of exposure to TH5487, we observed higher levels of oxidative damage at the telomere in both MDA-MB-231 and MDA-MB-231sh*BRCA1* cells, suggesting that cells cannot effectively repair endogenous oxidative DNA damage generated during cell culture. As a result, we found a significant accumulation of these lesions at the telomere (Figure2).

Accumulation of oxidative lesions was significantly higher in MDA-MB-231sh*BRCA1* cells than in MDA-MB-231 breast cancer cells, which suggests a role for BRCA1 in the repair of oxidative lesions at the telomere region. In relation with this, BRCA1 contributes to the repair of the 8-oxoG oxidative damage in human cells (Le Page *et al*. 2000) protecting against oxidative

DNA damage being converted into double-strand breaks during DNA replication (Fridlich *et al*. 2015). Hence, it is likely that BRCA1 is involved in oxidative DNA damage repair at telomeres, since there is evidence that the BRCA1 protein interacts with the telomere (Acharya *et al*. 2014; Badie *et al*. 2015).

Finally, we could confirm by immunofluorescence (IF) that after 5 days of TH5487 exposure, MDA-MB-231 cells presented an induction of the γH2AX nuclear signal and foci formation (Figure 4). This may suggest that inhibition of OGG1 first leads to an accumulation of oxidative damage, which later is converted into DSBs, contributing to a higher genome instability.

Considering that DSBs are the most dangerous perturbation for DNA, and because BRCA1 is an essential protein in the HR DNA repair pathway for DSBs, we believe that this could be the mechanistic explanation of the effects observed on proliferation in MDA-MB-231sh*BRCA1* cells when exposed to the OGG1 inhibitor (TH5487).

In summary, in the present report we described how in cells with the same genetic background, inactivation of *BRCA1* makes cells very sensitive to OGG1 inhibitors. This effect on proliferation correlates with an accumulation of oxidative damage and nuclear γH2AX induction. This evidence, together with previous evidence (Osorio *et al*. 2014) points to a synthetic lethal interaction between *OGG1* and *BRCA1*.

TL MODIFICATION CAUSED BY OTHER GENETIC EVENTS

Defects in genes involved in telomere maintenance (shelterin complex or telomerase) result in a wide spectrum of overlapping symptoms (Kirwan & Dokal 2008), which converge in disruption of TL regulation and end protection, and finally in disease manifestation.

In article 5 and article 6, two examples of TL dysregulation caused by defects in genes from the shelterin or telomerase complex are shown. In these examples, disease manifestation is not exclusively associated with telomere shortening. TL equilibrium is maintained by both telomerase and the shelterin complex, and aberrant telomere elongation or shortening can converge in disease manifestation.

Article 5

We found a novel damaging missense variant (p.R117C) in the *POT1* gene in TP53-negative Li-Fraumeni-like families with cardiac angiosarcoma and other tumors. Mutations in POT1 were recently associated with familial melanoma (Shi *et al*. 2014; Robles-Espinoza *et al*. 2014), glioma (Bainbridge *et al*. 2015), and mutated POT1 was shown to be a driver for chronic lymphocytic leukemia (Ramsay *et al*. 2013). This suggests a new role of POT1 not only as telomere protector, but also as one of the main proteins responsible for the development of

different familial cancer types when mutated. *In silico* studies showed that the p.R117C substitution putatively disrupts the interaction between oligonucleotide/oligosaccharide-binding (OB) folds 1 and 2 (Figure 2d) and affects the site for binding to TPP1 (Supplementary Table 4), which might result in the loss of capability of the $POT1^{R117C}$ protein to interact with ssDNA and to be recruited to telomeres. POT1 has been shown to be important to prevent telomerase access to telomeres by sequestering the DNA terminus (Baumann & Price 2010; Loayza & De Lange 2003). Indeed, telomere lengthening was observed in mutation carriers likely due to unlimited telomerase recruitment and action on telomeres.

In addition, disruption of POT1 function was associated with increased DNA damage at telomeres and telomere fragility (Ramsay *et al*. 2013).

Therefore, it is tempting to speculate that telomere elongation induced by this mutation in POT1 may constitute the underlying molecular mechanism favoring tumor formation.

Article 6

Telomerase activation may be a good therapeutic strategy to treat those forms of aplastic anemia that are associated with short telomeres. Indeed, we previously developed a telomerase (Tert) gene therapy using adeno-associated virus (AAV) 9 vectors, which attenuated or reverted aging-associated telomere erosion in peripheral blood mononuclear cells (PBMCs; Bernardes de Jesus *et al*. 2012). To test the efficacy of this strategy for the treatment of aplastic anemia, we first used a mouse model of aplastic anemia generated by us in which we depleted the TRF1 shelterin protein specifically in the bone marrow, leading to a bone marrow phenotype that recapitulates the main pathological findings in human aplastic anemia patients, including extreme telomere shortening (Beier *et al*. 2012; Bär *et al*. 2015).

Administration of a high dose of AAV9-Tert particles led to robust Tert expression in whole bone marrow isolates 2 weeks after treatment. AAV9-Tert treatment of mice with aplastic anemia triggered by short telomeres rescued mortality concomitant with telomere re-elongation in blood and bone marrow cells.

These findings were confirmed in a second mouse model of aplastic anemia produced by short telomeres, in this case due to telomerase deficiency (Herrera *et al*. 1999a; Herrera *et al*. 1999b). In this case, Tert gene therapy of the Tert-deficient bone marrow mouse model also resulted in increased telomere length, improved blood counts and, albeit moderately, survival.

GENERAL DISCUSSION

Telomere association studies are subject to reverse causality, which refers to a direction of cause-and-effect contrary to a common presumption, especially in case-control and

retrospective studies. This is one of the reasons for the lack of consensus when TL is used as a predictor for cancer risk.

Hence, it is important to redefine TL association studies: large sample size, long follow-up with periodical TL measurements, homogeneous ethnicity of the studied population and identification and correction of exogenous factors that can modify and bias TL association studies, such as chemotherapy. All these improvements need to be implemented across laboratories to minimize reverse causality and to clarify which is the relation between TL and cancer/disease susceptibility.

Reverse causality and possible bias due to exogenous and endogenous factors that can modify TL may be avoided by using a Mendelian randomization approach. Because genotype–phenotype associations are not vulnerable to biases by the environment, Mendelian randomization is an attractive approach for estimating relationships between TL and cancer risk. It consists in testing the association between TL-associated SNPs and the relative risk for cancer/disease susceptibility.

Until now, not many TL-associated SNPs have been described. For this reason, it is important to identify new TL-associated genetic variants to improve this type studies. We believe genetic variants in DNA glycosylases could be TL-associated SNPs in a specific genetic context: for example, rs2304277 in *BRCA1* and *BRCA2* mutation carriers, and rs804271 in *BRCA1* mutation carriers are both associated with short TL.

Interestingly, rs2304277 also modifies cancer risk for *BRCA1* mutation carriers, and rs804271 modifies the risk for *BRCA2* mutation carriers. Again, telomere shortening is associated with cancer risk in the context of hereditary breast and ovarian cancer, although in this case this is true for a specific group of *BRCA1* and *BRCA2* mutation carriers, namely those who harbor a specific "cancer modifier" SNP in *OGG1* and *NEIL2*, respectively.

It is possible that these SNPs affect two or more seemingly unrelated traits, such as cancer risk or TL in an independent manner. However, it is also possible that their effect (telomere/genome instability) directly modifies cancer risk for *BRCA1* and *BRCA2* mutation carriers and TL in a specific genetic context (*BRCA1/BRCA2*).

Indeed, our results suggest the existence of a synthetic lethal interaction between *OGG1* and *BRCA1*, with oxidative DNA accumulation, especially at telomeres, as the potential driver of the anti-proliferative effect observed in *BRCA1*-deficient breast cancer cells after drug inhibition of OGG1. Hence, the combination of both genetic events (cancer-causing SNPs in DNA glycosylases and *BRCA1* and *BRCA2* mutations) may be related to both cancer risk and telomere shortening, since oxidative DNA damage is associated with telomere shortening.

The most recent results of TL association studies indicate a complex relationship between TL and cancer risk, rather than a simple linear relationship. Short telomeres may be associated with an increased risk for some cancer types (gastrointestinal tumor and head and neck cancer)

(Zhu *et al*. 2016) while longer telomeres confer risk for other types such as glioma, ovarian cancer, and lung adenocarcinoma (Haycock *et al* 2017). This variability across cancer types may reflect different carcinogenic mechanisms in specific cancer types (Zhu *et al*. 2016). As illustrated in this thesis (articles 5 and 6), telomere lengthening or shortening can converge in disease manifestation due to impairment of two different telomere-related genes affecting two different molecular mechanisms of telomere maintenance (shelterin and telomerase).

To conclude, further insights into telomere biology are needed. It seems likely that the sole focus on LTL, rather than on other features of telomere maintenance and stability, is overly simplistic. Similarly, the assumption that LTL is reflected in disease-relevant tissue needs further investigation, and consideration should be given to measuring LTL at more than one time point. It is important to take into consideration that TL in relation with cancer is not linear, but rather dynamic. Hence, we should break with the dogma in which telomere shortening and disease susceptibility are an unbreakable marriage. In addition, any diagnostic, prognostic, or therapeutic application based on TL should be regarded with caution.

CONCLUSIONS/CONCLUSIONES

1. Conventional chemotherapeutic agents included in breast cancer treatment exert a transient telomere shortening effect. One year after completion of cancer treatment TL is restored to normal values. Chemotherapy is a confounding factor in TL association studies, and must be corrected for to obtain reliable results.

2. We found that rs2304277, located at the 3´UTR of the *OGG1* DNA glycosylase gene from the BER pathway, is associated with a constitutive transcriptional downregulation of *OGG1* that leads to both genome and telomere instability in patients harboring deleterious mutations in the *BRCA1* or *BRCA2* genes. This could be the molecular mechanism by which rs2304277 contributes to cancer risk susceptibility for *BRCA1* mutation carriers.

3. We found that rs804271, located in the promoter region of the *NEIL2* gene from the BER pathway, may reduce NEIL2 enzyme activity leading to a significant accumulation of oxidative DNA damage at telomeres in *BRCA2* mutation carriers. This could be the molecular mechanism by which rs804271 contributes to cancer risk susceptibility for *BRCA2* mutation carriers. In addition, we found that the SNP is associated with short TL, accumulation of short telomeres and lower telomerase activity in *BRCA1* mutation carriers, likely due to a higher oxidative stress susceptibility for this group.

4. In cells with the same genetic background, inactivation of BRCA1 make cells very sensitive to OGG1 inhibitors. This effect on proliferation correlates with an accumulation of oxidative damage and nuclear γH2AX induction, suggesting the existence of a synthetic lethal interaction between *OGG1* from the BER pathway and *BRCA1* from the HR pathway.

5. Telomere length dysregulation caused by defects in genes from the shelterin or telomerase complex can converge in disease manifestation through (or in parallel with) telomere elongation or shortening. This fact underscores the complexity of TL maintenance, which appears to depend on several endogenous and exogenous factors.

1. El tratamiento con agentes quimioterapéuticos en el cáncer de mama tiene un efecto secundario relacionado con el acortamiento telomerico. Este acortamiento es transitorio, y la longitud telomerica se recupera pasado un año desde la finalización del último ciclo de la quimioterapia. La quimioterapia es un agente modificador de la longitud telomérica y, en aquellos estudios de asociación en los que la longitud telomérica se utiliza como un biomarcador para predecir el riesgo a desarrollar ciertas enfermedades, es importante que se identifique la quimioterapia como un factor de confusión que ha de ser corregido con el fin de obtener resultados fiables.

2. Hemos identificado que el polimorfismo rs2304277 localizado en la región 3´UTR del gen *OGG1*, el cual está involucrado en la vía de reparación del ADN por escisión de base (BER), está asociado a unos niveles más bajos de transcrito. Esto se correlaciona con unos mayores niveles de inestabilidad genética y telomérica para los pacientes portadores de mutaciones en los genes de alta susceptibilidad al desarrollo de cáncer de mama y ovario hereditarios *BRCA1* y *BRCA2.* Este podría ser el mecanismo por el cual este polimorfismo está asociado a un mayor riesgo de desarrollar cáncer en individuos portadores de mutación en *BRCA1*.

3. Hemos encontrado que el polimorfismo rs804271, situado en la región promotora del gen *NEIL2* de la vía de reparación del ADN por escisión de base (BER), puede reducir la actividad de la enzima NEIL2 conduciendo a una acumulación significativa de daño oxidativo del ADN en telómeros para los portadores de mutación *BRCA2*. Este podría ser el mecanismo molecular por el cual el rs804271 contribuiría a una mayor susceptibilidad al desarrollo de cáncer en portadores de mutaciones en *BRCA2*. Además, hemos encontrado que este SNP se asocia con una menor longitud telomérica, una acumulación de telómeros cortos y una menor actividad de la telomerasa para los portadores de mutación *BRCA1*, probablemente debido a una mayor susceptibilidad al estrés oxidativo para este grupo.

4. Un estudio preliminar en el que se ha inhibido farmacológicamente la enzima OGG1 en líneas tumorales de mama con inactivación en BRCA1*,* sugiere que podría existir una relación de letalidad sintética entre *OGG1*, de la vía de reparación del ADN por escisión de base (BER) y *BRCA1*, de la vía de la recombinación homóloga (HR).

5. La desregulación en la homeostasis de la longitud telomérica causada por defectos en los genes del complejo protector de las shelterinas o en la telomerasa pueden dar lugar a la manifestación de enfermedad/cáncer mediante la elongación o el acortamiento de los telómeros. Este hecho remarca la complejidad en la relación existente entre la longitud telomérica y el riesgo a desarrollar enfermedad/cáncer, el cual parece depender de varios factores endógenos y exógenos.

BIBLIOGRAPHY

Andrew, T. *et al*. Mapping genetic loci that determine leukocyte telomere length in a large sample of unselected female sibling pairs. American journal of human genetics, **78(3)**, pp.480–6. (2006)

Antoniou, A. *et al*. Average Risks of Breast and Ovarian Cancer Associated with BRCA1 or BRCA2 Mutations Detected in Case Series Unselected for Family History: A Combined Analysis of 22 Studies. The American Journal of Human Genetics, **72(5)**, pp.1117–1130. (2003)

Aubert, G. & Lansdorp, P.M. Telomeres and Aging. Physiological reviews, **88(2)**, pp.557-579. (2008)

Audeh, M.W. *et al*. Oral poly (ADP-ribose) polymerase inhibitor olaparib in patients with *BRCA1* or *BRCA2* mutations and recurrent ovarian cancer: A proof-of-concept trial. The Lancet, **376(9737)**, pp.245–251. (2010)

Aviv, A. *et al*. Impartial comparative analysis of measurement of leukocyte telomere length/DNA content by Southern blots and qPCR. Nucleic Acids Research, **39(20)**, e134. (2011)

Badie, S. *et al*. BRCA1 and CtIP promote alternative non- homologous end-joining at uncapped telomeres. The EMBO Journal, **34(3)**, pp.410–424. (2015)

Badie, S. *et al*., 2010. BRCA2 acts as a RAD51 loader to facilitate telomere replication and capping. Nature structural & molecular biology, **17(12)**, pp.1461–9. (2010)

Bainbridge, M.N. *et al*. Germline Mutations in Shelterin Complex Genes Are Associated With Familial Glioma. Journal of National Cancer Istitute, **107(1)**, pp.1–4. (2015)

Bär, C. *et al*. Therapeutic effect of androgen therapy in a mouse model of aplastic anemia produced by short telomeres. Haematologica, **100(10)**, pp.1267–1274. (2015)

Bartkova, J. *et al*. Oncogene-induced senescence is part of the tumorigenesis barrier imposed by DNA damage checkpoints. Nature, **444(7119)**, pp.633–637. (2006)

Basiak, J. *et al*. Inhibition of telomerase activity in endometrial cancer cells by selenium-cisplatin conjugate despite suppression of its DNA-damaging activity by sodium ascorbate. Teratogenesis Carcinogenesis and Mutagenesis, **22(1)**, pp.73–82. (2002)

Baumann, P. & Cech, T.R. Pot1, the putative telomere end-binding protein in fission yeast and humans. Science (New York, N.Y.), **292(5519)**, pp.1171-5. (2001)

Baumann, P. & Price, C. Pot1 and telomere maintenance. FEBS Letters, **584(17)**, pp.3779–3784. (2010)

Beier, F. *et al*. Conditional TRF1 knockout in the hematopoietic compartment leads to bone marrow failure and recapitulates clinical features of dyskeratosis congenita. Blood, **120(15)**, pp.2990–3000. (2012)

Benetos, A. *et al*. Sex difference in leukocyte telomere length is ablated in opposite-sex co-twins. International Journal of Epidemiology, **43(6)**, pp.1799–1805. (2014)

Benitez-Buelga, C. *et al*. Molecular insights into the OGG1 gene, a cancer risk modifier in BRCA1 and BRCA2 mutations carriers. Oncotarget. **7(18)**, pp. 25815-25. (2016)

Benz, C.C. & Yau, C. Ageing, oxidative stress and cancer: paradigms in parallax. Nature reviews. Cancer, **8(11)**, pp.875–9. (2008)

Berger, F. *et al*. The impact of single-nucleotide polymorphisms (SNPs) in OGG1 and XPC on the age at onset of Huntington disease. Mutation Research - Genetic Toxicology and Environmental Mutagenesis, **755(2)**, pp.115–119. (2013)

Bernardes de Jesus, B. *et al*. Telomerase gene therapy in adult and old mice delays aging and increases longevity without increasing cancer. EMBO Molecular Medicine, **4(8)**, pp.691–704. (2012)

Blasco, M.A. Telomeres and human disease: ageing, cancer and beyond. Nat Rev Genet, **6(8)**, pp.611–622. (2005)

Bojesen S.E. *et al*. Multiple independent variants at the TERT locus are associated with telomere length and risks of breast and ovarian cancer. Nature genetics, **45(4)**, pp.371–384. (2013)

Bolzán D.A. Effect of chemotherapeutic drugs on telomere length and telomerase activity. Telomere and telomerase. **3**: e1488. (2016)

Boonekamp, J.J. *et al*. Nestling telomere shortening, but not telomere length, reflects developmental stress and predicts survival in wild birds. Proceedings of the Royal Society B: Biological Sciences, **281(1785)**: 20133287. (2014)

Borodkina, A. *et al.* Interaction between ROS dependent DNA damage, mitochondria and p38 MAPK underlies senescence of human adult stem cells. Aging, **6(6)**, pp.481–495. (2014)

Brewster, B.L. *et al*. Identification of fifteen novel germline variants in the BRCA1 3UTR reveals a variant in a breast cancer case that introduces a functional miR-103 target site. Human Mutation, **33(12)**, pp.1665–1675. (2012)

Broer, L. *et al*., 2013. Meta-analysis of telomere length in 19 713 subjects reveals high heritability, stronger maternal inheritance and a paternal age effect. European Journal of Human Genetics, **21(10)**, pp.1163–1168. (2013)

Bryan, T.M. & Cech, T.R. Telomerase and the maintenance of chromosome ends. Current Opinion in Cell Biology, **11(3)**, pp.318–324. (1999)

Burger, A.M., Double, J.A. & Newell, D.R. Inhibition of telomerase activity by cisplatin in human testicular cancer cells. European Journal of Cancer, **33(4)**, pp.638–644. (1997)

Cabuy, E., Newton, C. & Slijepcevic, P. BRCA1 knock-down cause's telomere dysfunction in mammary epithelial cells. Cytogenetic and Genome Research, **122(3–4)**, pp.336–342. (2009)

Caldecott, K.W. Single-strand break repair and genetic disease. Nature reviews. Genetics, **9(8)**, pp.619–31. (2008)

Canela, A. *et al*. High-throughput telomere length quantification by FISH and its application to human population studies. Proceedings of the National Academy of Sciences of the United States of America, **104(13)**, pp.5300–5. (2007)

Cardin, R. *et al*. Oxidative DNA damage correlates with cell immortalization and mir-92 expression in hepatocellular carcinoma. BMC cancer, **12**, pp.177. (2012)

Cawthon, R. *et al*. Association between telomere length in blood and mortality in people aged 60 years or older. The Lancet, **361(9355)**, pp.393–395. (2003)

Cawthon, R.M. Telomere length measurement by a novel monochrome multiplex quantitative PCR method. Nucleic Acids Research, **37(3)** e21. **(**2009)

Cawthon R.M. Telomere measurement by quantitative PCR. Nucleic Acids Res. **30(10)**: e47. (2002)

Celli, G.B. & de Lange, T. DNA processing is not required for ATM-mediated telomere damage response after TRF2 deletion. Nature cell biology, **7(7)**, pp.712–8. (2005)

Cesare, A.J. *et al*. Spontaneous occurrence of telomeric DNA damage response in the absence of chromosome fusions. Nat Struct Mol Biol, **16(12)**, pp.1244–1251. (2009)

Chakraborty, A. *et al.* Neil2-null mice accumulate oxidized DNA bases in the transcriptionally active sequences of the genome and are susceptible to innate inflammation. Journal of Biological Chemistry, **290(41)**, pp.24636–24648. (2015)

Chen, L.-Y., Liu, D. & Songyang, Z. Telomere maintenance through spatial control of telomeric proteins. Molecular and cellular biology, **27(16)**, pp.5898–909. (2007)

Chen, S. *et al.* Short leukocyte telomere length is associated with obesity in American Indians: The strong heart family study. Aging, **6(5)**, pp.380–389. (2014)

Clop, A. *et al*. A mutation creating a potential illegitimate microRNA target site in the myostatin gene affects muscularity in sheep. Nat Genet, **38(7)**, pp.813–818. (2006)

Codd, V. *et al*. Common variants near TERC are associated with mean telomere length. Nature genetics, **42(3)**, pp.197–9. (2010)

Codd, V. *et al*. Identification of seven loci affecting mean telomere length and their association with disease. Nature Genetics, **45(4)**, p.422. (2013)

Cooke, M.S. *et al*. Oxidative DNA damage: mechanisms, mutation, and disease. Faseb J, **17(10),** pp.1195–214. (2003)

Counter, C.M. *et al*. Telomere shortening associated with chromosome instability is arrested in immortal cells which express telomerase activity. The EMBO Journal, **1(1)**, pp.921–1929. (1992)

Crabbe, L. *et al*., 2004. Defective telomere lagging strand synthesis in cells lacking WRN helicase activity. Science (New York, N.Y.), **306(5703)**, pp.1951–3. (2004)

Dagan, E. & Gershoni-Baruch, R. Hereditary breast/ovarian cancer--pitfalls in genetic counseling. Clinical genetics, **60(4)**, pp.310–3. (2001)

Dehbi, A.Z., Radstake, T.R.D.J. & Broen, J.C. a. Accelerated telomere shortening in rheumatic diseases: cause or consequence? Expert review of clinical immunology, **9(12)**, pp.1193–204. (2013)

Dianov, G. & Lindahl, T. Reconstitution of the DNA base excision-repair pathway. Current Biology, **4(12)**, pp.1069–1076. (1994)

Dianov, G.L. & Hübscher, U. Mammalian base excision repair: The forgotten archangel. Nucleic Acids Research, **41(6)**, pp.3483–3490. (2013)

Dilley, R.L. *et al*. Break-induced telomere synthesis underlies alternative telomere maintenance. Nature, **539(7627)**, pp.54–58. (2016)

Du, J. *et al*. Telomere length, genetic variants and gastric cancer risk in a Chinese population. Carcinogenesis, **36(9)**, pp.963–970. (2015)

Dziaman, T. *et al*. PARP-1 expression is increased in colon adenoma and carcinoma and correlates with OGG1. PLoS ONE, **9(12)**. e21. (2014)

Elmore, L.W. *et al*. Adriamycin-induced senescence in breast tumor cells involves functional p53 and telomere dysfunction. Journal of Biological Chemistry, **277(38)**, pp.35509–35515. (2002)

Finkel, T. *et al.* Oxidants, oxidative stress and the biology of ageing. Nature, **408(6809)**, pp.239–247. (2000)

Fouquerel, E. *et al.* Oxidative guanine base damage regulates human telomerase activity. Nature Structural & Molecular Biology, **23(12)**, pp.1092-1100. (2016)

Fridlich, R. *et al.* BRCA1 and BRCA2 protect against oxidative DNA damage converted into double-strand breaks during DNA replication. DNA Repair, **30**, pp.11–20. (2015)

Friedberg, E.C. DNA damage and repair. Nature, **421(6921)**, pp.436–40. (2003)

Fumagalli, M. *et al*. Telomeric DNA damage is irreparable and causes persistent DNA-damage-response activation. Nature cell biology, **14(4)**, pp.355–65. (2012)

Gavory, G., Farrow, M. & Balasubramanian, S. Minimum length requirement of the alignment domain of human telomerase RNA to sustain catalytic activity in vitro. Nucleic acids research, **30(20)**, pp.4470–80. (2002)

Gilson, E. & Géli, V. How telomeres are replicated. Nature reviews. Molecular cell biology, **8(10)**, pp.825–38. (2007)

Gorrini, C. *et al*. BRCA1 interacts with Nrf2 to regulate antioxidant signaling and cell survival. The Journal of experimental medicine, **210(8)**, pp.1529–44. (2013)

Graakjaer, J. *et al*. The relative lengths of individual telomeres are defined in the zygote and strictly maintained during life. Aging Cell**, 3(3)**, pp.97–102. (2004)

Greider, C.W. Telomeres do D-loop-T-loop. Cell, **97(4)**, pp.419–422. (1999)

Griffith, J., Michalowski, S. & Makhov, A.M. Electron microscopy of DNA-protein complexes and chromatin. Methods in Enzymology, **304**, pp.214–230. (1999)

Gu H. *et al* Deletion of a DNA polymerase beta gene segment in T cells using cell type-specific gene targeting. Science. Jul 1; **265 (5168)**, pp.103-6. (1994)

Guan, J.Z. *et al.* Patients with multiple sclerosis show increased oxidative stress markers and somatic telomere length shortening. Molecular and cellular biochemistry, **400(1–2)**, pp.183–7. (2015)

Harley, C.B., Futcher, A.B. & Greider, C.W. Telomeres shorten during ageing of human fibroblasts. Nature, **345(6274)**, pp.458–60. (1990)

Harley, C.B. Telomerase is not an oncogene. Oncogene, **21**, 494-502. (2002)

Haussmann, M.F. *et al*. Embryonic exposure to corticosterone modifies the juvenile stress response, oxidative stress and telomere length. Proceedings. Biological sciences / The Royal Society, **279(1732)**, pp.1447–56. (2012)

Heidenreich, B. *et al.* TERT promoter mutations in cancer development. Current Opinion in Genetics and Development, **24(1)**, pp.30–37. (2014)

Heidinger, B.J. *et al*. Telomere length in early life predicts lifespan. Proceedings of the National Academy of Sciences of the United States of America, **109(5)**, pp.1743–8. (2012)

Hemann, M.T. *et al*. The shortest telomere, not average telomere length, is critical for cell viability and chromosome stability. Cell, **107(1)**, pp.67–77. (2001)

Herborn, K. *et al*. Stress exposure in early post-natal life reduces telomere length: an experimental demonstration in a long-lived seabird. Proceedings. Biological sciences / The Royal Society, **281(1782)**, p.20133151. (2014)

Herrera, E. *et al*. Disease states associated with telomerase deficiency appear earlier in mice with short telomeres. EMBO Journal, **18(11)**, pp.2950–2960. (1999a)

Herrera, E., Samper, E. & Blasco, M.A. Telomere shortening in mTR-/- embryos is associated with failure to close the neural tube. Embo J, **18(5)**, pp.1172–1181. (1999b)

Hewitt, G. *et al*. Telomeres are favoured targets of a persistent DNA damage response in ageing and stree-induced senescence. Nature communications, **3**, p.708. (2012)

Hildrestrand, G. *et al*. Expression patterns of Neil3 during embryonic brain development and neoplasia. BMC neuroscience, **10**, p.45. (2009)

Hoffmeyer, K. *et al*. Wnt/β-catenin signaling regulates telomerase in stem cells and cancer cells. Science (New York, N.Y.), **336(6088)**, pp.1549–54. (2012)

Holohan, B., Wright, W.E. & Shay, J.W. Telomeropathies: An emerging spectrum disorder. Journal of Cell Biology, **205(3)**, pp.289–299. (2014)

Houben, J.M.J. *et al*. Telomere shortening in chronic obstructive pulmonary disease. Respiratory Medicine, **103(2)**, pp.230–236. (2009)

Houghtaling, B.R. *et al*. A dynamic molecular link between the telomere length regulator TRF1 and the chromosome end protector TRF2. Current Biology, **14(18)**, pp.1621–1631. (2004)

Hughes, M.M., Connor, T.J. & Harkin, A. Stress-Related Immune Markers in Depression: Implications for Treatment. International Journal of Neuropsychopharmacology, **19(6)**, pp.1–19. (2016)

Iles, M.M. *et al*. The effect on melanoma risk of genes previously associated with telomere length. Journal of the National Cancer Institute, **106(10)**. (2014)

Ishibashi, T. & Lippard, S.J. Telomere loss in cells treated with cisplatin. Proceedings of the National Academy of Sciences of the United States of America, **95(8)**, pp.4219–4223. (1998)

Jackowska, M. *et al*. Short Sleep Duration Is Associated with Shorter Telomere Length in Healthy Men: Findings from the Whitehall II Cohort Study. PLoS ONE, **7(10)**. (2012)

Johnston, J.S. *et al*. Synergy between 3′-azido-3′-deoxythymidine and paclitaxel in human pharynx FaDu cells. Pharmaceutical Research, **20(7)**, pp.957–961. (2003)

Kavli *et al*. B cells from hyper-IgM patients carrying UNG mutations lack ability to remove uracil from ssDNA and have elevated genomic uracil. J Exp Med, **201(12)**, pp.2011-21. (2005)

Killick, E. *et al*. Telomere length shows no association with BRCA1 and BRCA2 mutation status. PLoS ONE, **9(1)**: e86659. (2014)

Kim, N.W. *et al*. Specific association of human telomerase activity with immortal cells and cancer. Science (New York, N.Y.), **266(5193)**, pp.2011–5. (1994)

Kim, S.H. *et al*. TIN2, a new regulator of telomere length in human cells. Nature genetics, **23(4)**, pp.405–412. (1999).

Kim, S.H. *et al*. TIN2 mediates functions of TRF2 at human telomeres. Journal of Biological Chemistry, **279(42)**, pp.43799–43804. (2004)

Kimura, M. *et al*. Telomere length and mortality: A study of leukocytes in elderly danish twins. American Journal of Epidemiology, **167(7)**, pp.799–806. (2008)

Kinslow, C.J. *et al*. Regulatory regions responsive to oxidative stress in the promoter of the human DNA glycosylase gene NEIL2. Mutagenesis, **25(2)**, pp.171–177. (2010)

Kinslow, C.J. *et al*.Single nucleotide polymorphisms 5¨ Upstream the coding region of the NEIL2 gene influence gene transcription levels and alter levels of genetic damage. Genes Chromosomes and Cancer, **47(11)**, pp.923–932. (2008)

Kirwan, M. & Dokal, I. Dyskeratosis congenita: A genetic disorder of many faces. Clinical Genetics, **73(2)**, pp.103–112. (2008)

Kiyozuka, Y. *et al*. Correlation of chemosensitivity to anticancer drugs and telomere length, telomerase activity and telomerase RNA expression in human ovarian cancer cells. Anticancer Research, **20(1 A)**, pp.203–212. (2000)

Kordinas, V., Ioannidis, A. & Chatzipanagiotou, S. The telomere/telomerase system in chronic inflammatory diseases. Cause or effect? Genes, **7(9)**: e60. (2016)

Krupa, R. *et al*. DNA damage and repair in endometrial cancer in correlation with the hOGG1 and RAD51 genes polymorphism. Molecular Biology Reports, **38(2)**, pp.1163–1170. (2011)

Kubota, Y. *et al*. Reconstitution of DNA base excision-repair with purified human proteins: interaction between DNA polymerase beta and the XRCC1 protein. The EMBO journal, **15(23)**, pp.6662–70. (1996)

Kucherlapati M. *et al*. Haploinsufficiency of Flap endonuclease (Fen1) leads to rapid tumor progression. Proc Natl Acad Sci U S A. **99(15)**, pp.9924-9. (2002)

Kunifuji, Y. *et al*. Down-regulation of telomerase activity by anticancer drugs in human ovarian cancer cells. ANTI-CANCER DRUGS, **13(6)**, pp.595–598. (2002)

De Lange, T. How shelterin solves the telomere end-protection problem. Cold Spring Harbor Symposia on Quantitative Biology, **75**, pp.167–177. (2010)

De Lange, T. How telomeres solve the end-protection problem. Science 326(5955):948-52 (2009)

De Lange, T. Shelterin: The protein complex that shapes and safeguards human telomeres. Genes and Development, **19(18)**, pp.2100–2110. (2005)

Lazzerini D.E. Give me a break: How telomeres suppress the DNA damage response. **8(9)**:1118-26. (2009)

Lee, B.J. *et al*. Change of the expression of human telomerase reverse transcriptase mRNA and human telomerase RNA after cisplatin and 5-fluorouracil exposure in head and neck squamous cell carcinoma cell lines. J Korean Med Sci, **22 Suppl**, pp. S73-8. (2007)

Lei, M., Podell, E.R. & Cech, T.R. Structure of human POT1 bound to telomeric single-stranded DNA provides a model for chromosome end-protection. Nature Structural & Molecular Biology, **11(12)**, pp.1223–1229. (2004)

Levy, D. *et al*. Genome-wide association identifies OBFC1 as a locus involved in human leukocyte telomere biology. Proceedings of the National Academy of Sciences of the United States of America, **107(20)**, pp.9293–8. (2010)

Li, B., Oestreich, S. & de Lange, T. Identification of Human Rap1: Implications for Telomere Evolution. Cell, **101(5)**, pp.471–483. (2000)

Li, P. *et al*. Telomere dysfunction induced by chemotherapeutic agents and radiation in normal human cells. International Journal of Biochemistry and Cell Biology, **44(9)**, pp.1531–1540. (2012)

Liew, C.W., Holman, A. & Kulkarni, R. The roles of telomeres and telomerase in β-cell regeneration. Diabetes, Obesity and Metabolism, **11(SUPPL. 4)**, pp.21–29. (2009)

Lin, S.Y. & Elledge, S.J. Multiple tumor suppressor pathways negatively regulate telomerase. Cell, 113(7), pp.881–889. (2003)

Lindahl, T. DNA Glycosylases, Endonucleases for Apurinic/Apyrimidinic Sites, and Base Excision-Repair. Progress in Nucleic Acid Research and Molecular Biology, **22(C)**, pp.135–192. (1979)

Lindahl, T. Instability and decay of the primary structure of DNA. Nature, **362(6422)**, pp.709–715. (1993)

Lindahl, T. Repair of intrinsic DNA lesions. Mutation Research/Reviews in Genetic Toxicology, **238(3)**, pp.305–311. (1990)

Lindqvist, D. *et al*. Psychiatric disorders and leukocyte telomere length: Underlying mechanisms linking mental illness with cellular aging. Neuroscience and Biobehavioral Reviews, **55,** pp.333–364. (2015)

Lingner, J., Cooper, J.P. & Cech, T.R. Telomerase and DNA end replication: No longer a lagging strand problem? Science, **269(5230)**, pp.1533-4. (1995)

Liu, M. *et al*. The effects of chemotherapy with bleomycin, etoposide, and cis-platinum on telomeres in rat male germ cells. Andrology, **3(6)**, pp.1104–1112. (2015)

Liu, M., Hales, B.F. & Robaire, B. Effects of Four Chemotherapeutic Agents, Bleomycin, Etoposide, Cisplatin, and Cyclophosphamide, on DNA Damage and Telomeres in a Mouse Spermatogonial Cell Line. Biology of reproduction, **90(February)**, pp.1–10. (2014)

Loayza, D. & de Lange, T. POT1 as a terminal transducer of TRF1 telomere length control. Nature, **423(6943)**, pp.1013–1018. (2003)

Lombard, D.B. *et al*. DNA repair, genome stability, and aging. Cell, **120(4)**, pp.497–512. (2005)

Lu, J. & Liu, Y. Deletion of Ogg1 DNA glycosylase results in telomere base damage and length alteration in yeast. The EMBO journal, **29(2)**, pp.398–409. (2010)

Lu, Y. *et al*. Telomeric impact of conventional chemotherapy. Frontiers of Medicine in China, **7(4)**, pp.411–417. (2013)

Ma, H. *et al*. Shortened telomere length is associated with increased risk of cancer: a meta-analysis. PLoS One, **6(6)**, pp. e20466. (2011)

Mangino, M. *et al*. mA regulatory SNP of the BICD1 gene contributes to telomere length variation in humans. Human Molecular Genetics, **17(16)**, pp.2518–2523. (2008)

Marcon, L. *et al*. Effects of chemotherapeutic agents for testicular cancer on rat spermatogonial stem/progenitor cells. Journal of andrology, **32(4)**, pp.432–443. (2011)

Marks, J.R., Refining the role of BRCA1 in combating oxidative stress. Breast cancer research, **15(6)**, pp.320. (2013)

Martens, U.M. *et al*. Accumulation of short telomeres in human fibroblasts prior to replicative senescence. Experimental cell research, **256(1)**, pp.291–299. (2000)

Martinez-Delgado, B. *et al*. Genetic anticipation is associated with Telomere shortening in hereditary breast cancer. PLoS Genetics, **7(7)**: e1002182. (2011)

Masi, S. *et al.* Oxidative stress, chronic inflammation, and telomere length in patients with periodontitis. Free Radical Biology and Medicine, **50(6)**, pp.730–735. (2011)

Matsutani, N. *et al*. Expression of MRE11 complex (MRE11, RAD50, NBS1) and hRAP1 and its relation with telomere regulation, telomerase activity in human gastric carcinomas. Pathobiology, **69(4)**, pp.219–224. (2001)

McElligott, R. & Wellinger, R.J. The terminal DNA structure of mammalian chromosomes. EMBO Journal, **16(12)**, pp.3705–3714. (1997)

Meillère, A. *et al.* Traffic noise exposure affects telomere length in nestling house sparrows. Biology Letters, **11**, pp.2–5. (2015)

Mena, S., Ortega, A. & Estrela, J.M. Oxidative stress in environmental-induced carcinogenesis. Mutation Research - Genetic Toxicology and Environmental Mutagenesis, **674(1–2)**, pp.36–44. (2009)

Milne, R.L. *et al.* The average cumulative risks of breast and ovarian cancer for carriers of mutations in BRCA1 and BRCA2 attending genetic counseling units in Spain. Clinical Cancer Research, **14(9)**, pp.2861–2869. (2008)

Mitra, J. *et al*. New perspectives on oxidized genome damage and repair inhibition by pro-oxidant metals in neurological diseases. Biomolecules, **4(3)**, pp.678–703. (2014)

Mo, Y. *et al*. Simultaneous targeting of telomeres and telomerase as a cancer therapeutic approach. Cancer Research, **63(3)**, pp.579–585. (2003)

Moritz, E. *et al*. hOGG1-Cys326 variant cells are hypersensitive to DNA repair inhibition by nitric oxide. Carcinogenesis, **35(6)**, pp.1426–1433. (2014)

Multani, A.S. *et al*. Cell-killing by paclitaxel in a metastatic marine melanoma cell line is mediated by extensive telomere erosion with no decrease in telomerase activity. Oncology Reports, **6(1)**, pp.39–44. (1999a)

Multani, A.S. *et al*. Cell death in paclitaxel-dependent chinese hamster ovary cells is initiated by the loss of telomeric DNA repeats. Oncol Res, **11(10)**, pp.455–460. (1999b)

Noguera, J.C. *et al*. Sex-dependent effects of nutrition on telomere dynamics in zebra finches (Taeniopygia guttata). Biology letters, **11(2)**, p.20140938. (2015)

O'Callaghan, N. *et al*. A qPCR-based assay to quantify oxidized guanine and other FPG-sensitive base lesions within telomeric DNA. BioTechniques, **51(6)**, pp.403–412. (2011)

Oikawa, S. & Kawanishi, S. Site-specific DNA damage at GGG sequence by oxidative stress may accelerate telomere shortening. FEBS Letters, **453(3)**, pp.365–368. (1999)

Oliver M. *et al.* 2003.Multiple Colorectal Adenomas, Classic Adenomatous Polyposis, and Germ-Line Mutations in MYH. N Engl J Med, **348**, pp.791-799. (2003)

Opresko, P.L. *et al*. Oxidative damage in telomeric DNA disrupts recognition by TRF1 and TRF2. Nucleic Acids Research, **33(4)**, pp.1230–1239. (2005)

Opresko, P.L. & Shay, J.W. Telomere-Associated Aging Disorders. Ageing research reviews. **33**:52-66. (2016)

Osorio, A. *et al.* DNA Glycosylases Involved in Base Excision Repair May Be Associated with Cancer Risk in BRCA1 and BRCA2 Mutation Carriers. PLoS Genetics, **10(4)**: e1004256. 10(4). (2014)

Le Page, F. *et al.* BRCA1 and BRCA2 are necessary for the transcription-coupled repair of the oxidative 8-oxoguanine lesion in human cells. Cancer Research, **60(19)**, pp.5548–5552. (2000)

Palm, W. & de Lange, T. How Shelterin Protects Mammalian Telomeres. Annual Review of Genetics, **42(1)**, pp.301–334. (2008)

Park, K.H. *et al*. Telomerase activity and telomere lengths in various cell lines: Changes of telomerase activity can be another method for chemosensitivity evaluation. International Journal of Oncology, **13(3)**, pp.489–495. (1998)

Passos, J.F., Saretzki, G. & Von Zglinicki, T.DNA damage in telomeres and mitochondria during cellular senescence: Is there a connection? Nucleic Acids Research, **35(22)**, pp.7505–7513. (2007)

Pavanello, S. *et al*. Shortened telomeres in individuals with abuse in alcohol consumption. International Journal of Cancer, **129(4)**, pp.983–992. (2011)

Peixoto, A. *et al*., 2006. BRCA1 and BRCA2 germline mutational spectrum and evidence for genetic anticipation in Portuguese breast/ovarian cancer families. Familial Cancer, **5(4)**, pp.379–387. (2006)

Pooley, K.A. *et al.* Lymphocyte telomere length is long in BRCA1 and BRCA2 mutation carriers regardless of cancer-affected status. Cancer Epidemiology Biomarkers and Prevention, **23(6)**, pp.1018–1024. (2014)

Price, L.H. *et al*. Telomeres and early-life stress: An overview. Biological Psychiatry, **73(1)**, pp.15–23. (2013)

Puebla-Osorio N. *et al*. Early embryonic lethality due to targeted inactivation of DNA ligase III. Mol Cell Biol, **26(10)**:3935-41. (2006)

Rafie, N. *et al*. Dietary patterns, food groups and telomere length: a systematic review of current studies. European Journal of Clinical Nutrition. **71(2)**:151-158. (2016)

Ramsay, A.J. *et al*. POT1 mutations cause telomere dysfunction in chronic lymphocytic leukemia. Nature genetics. **45(5)**:526-30. (2013)

Raschenberger, J. *et al*. Influence of DNA extraction methods on relative telomere length measurements and its impact on epidemiological studies. Scientific Reports, **6(3)**, pp.25398. (2016)

Rhee, D.B. *et al*. Factors that influence telomeric oxidative base damage and repair by DNA glycosylase OGG1. DNA Repair, **10(1)**, pp.34–44. (2011)

Richter, T. & Zglinicki, T. von. A continuous correlation between oxidative stress and telomere shortening in fibroblasts. Experimental Gerontology, **42(11)**, pp.1039–1042. (2007)

Robles-Espinoza, C.D. *et al*. POT1 loss-of-function variants predispose to familial melanoma. Nat Genet, **46(5)**, pp.478–481. (2014)

Rode, L., Nordestgaard, B.G. & Bojesen, S.E. Peripheral blood leukocyte telomere length and mortality among 64,637 individuals from the general population. Journal of the National Cancer Institute, **107(6)**, p.074. (2015)

Romano, G.H. *et al.* Environmental Stresses Disrupt Telomere Length Homeostasis. PLoS Genetics, **9(9)**:e1003721. (2013)

Roy, R., Chun, J. & Powell, S.N., 2012. BRCA1 and BRCA2: different roles in a common pathway of genome protection. Nature reviews. Cancer, **12(1)**, pp.68–78. (2012)

Salihu H.M. *et al*. Impact of intrauterine tobacco exposure on fetal telomere length. Am J Obstet Gynecol. **212(2)**:205.e1-8. (2014)

Sexton, A.N. *et al*. Genetic and molecular identification of three human TPP1 functions in telomerase action: Recruitment, activation, and homeostasis set point regulation. Genes and Development, **28(17)**, pp.1885–1899. (2014)

Shaffer, J.A. *et al*. Depressive Symptoms Are Not Associated with Leukocyte Telomere Length: Findings from the Nova Scotia Health Survey (NSHS95), a Population-Based Study. **76(3)**:190-6. PLoS ONE, 7(10). (2012)

Shay, J.W. & Wright, W.E. Telomerase: A target for cancer therapeutics. Cancer Cell, **2(4)**, pp.257–265. (2002)

Shi, J. *et al*. Rare missense variants in POT1 predispose to familial cutaneous malignant melanoma. Nat Genet, **46(5)**, pp.482–486. (2014).

Slagboom, P.E., Droog, S. & Boomsma, D.I. Genetic determination of telomere size in humans: a twin study of three age groups. American journal of human genetics, **55(5)**, pp.876–82 (1994)

Smith, G.D. & Ebrahim, S. "Mendelian randomization": Can genetic epidemiology contribute to understanding environmental determinants of disease? International Journal of Epidemiology, **32(1)**, pp.1–22. (2003)

Tebbs R.S. *et al*. Requirement for the Xrcc1 DNA base excision repair gene during early mouse development. Dev Biol. **208(2)**:513-29. (1999)

Thorvaldsdottir *et al.* Telomere length is predictive of breast cancer risk in BRCA2 mutation carriers. Cancer Epidemiol Biomarkers Prev. **pii: cebp.0946. 2016.** (2017)

Uziel O. *et al*. BRCA1/2 mutations perturb telomere biology: characterization of structural and functional abnormalities in vitro and in vivo, **7(3)**: 2433–2454. (2016)

Van Steensel, B. & de Lange, T., Control of telomere length by the human telomeric protein TRF1. Nature, **385(6618)**, pp.740–3. (1997)

Van Steensel, B., Smogorzewska, A. & De Lange, T. TRF2 protects human telomeres from end-to-end fusions. Cell, **92(3)**, pp.401–413. (1998)

Stephens, J.W., Khanolkar, M.P. & Bain, S.C. The biological relevance and measurement of plasma markers of oxidative stress in diabetes and cardiovascular disease. Atherosclerosis, **202(2)**, pp.321–329. (2009)

Takubo, K. *et al*. Telomere lengths are characteristic in each human individual. Experimental Gerontology, **37(4)**, pp.523–531. (2002)

Vaksman, O. *et al*. miRNA profiling along tumour progression in ovarian carcinoma. Journal of Cellular and Molecular Medicine, **15(7)**, pp.1593–1602. (2011)

Vallabhaneni, H. *et al*. Defective repair of uracil causes telomere defects in mouse hematopoietic cells. Journal of Biological Chemistry, **290(9)**, pp.5502–5511. (2015)

Vasa-Nicotera, M. *et al.* Mapping of a major locus that determines telomere length in humans. American journal of human genetics, **76(1)**, pp.147–51. (2005)

Vorlícková, M. *et al*. 8-Oxoguanine in a quadruplex of the human telomere DNA sequence. FEBS Journal, **279(1)**, pp.29–39. (2012)

Wallace, S.S. Base excision repair: A critical player in many games. DNA Repair, **19**, pp.14–26. (2014)

Wang, Z. *et al*. Characterization of oxidative guanine damage and repair in mammalian telomeres. PLoS Genetics, **6(5)**, pp.28. (2010)

Webb, C.J., Wu, Y. & Zakian, V.A.DNA repair at telomeres: Keeping the ends intact. Cold Spring Harbor Perspectives in Biology, **5(6)**, pii: a012666. (2013)

Weischer, M. *et al.* Short telomere length, cancer survival, and cancer risk in 47102 individuals. Journal of the National Cancer Institute, **105(7)**, pp.459–468. (2013)

Wentzensen, I.M. *et al*. The association of telomere length and cancer: A meta-analysis. Cancer Epidemiology Biomarkers and Prevention, **20(6)**, pp.1238–1250. (2011)

Wright, W.E. *et al*. Telomerase activity in human germline and embryonic tissues and cells. Developmental Genetics, **18(2)**, pp.173–179. (1996)

Wu, C.H. *et al*. Premature telomere shortening in polymorphonuclear neutrophils from patients with systemic lupus erythematosus is related to the lupus disease activity. Lupus, **16(4)**, pp.265–272. (2007)

Wu, K.J. *et al.* Direct activation of TERT transcription by c-MYC. Nature genetics, **21(2)**, pp.220–224(1999)

Wu, X. *et al*. Telomere dysfunction: a potential cancer predisposition factor. Journal of the National Cancer Institute, **95(16)**, pp.1211–1218. (2003)

Xanthoudakis S. *et al*. The redox/DNA repair protein, Ref-1, is essential for early embryonic development in mice. Proc Natl Acad Sci U S A, **93 (17)**:8919-23. (1996)

Ye, J.Z.S. *et al.* TIN2 binds TRF1 and TRF2 simultaneously and stabilizes the TRF2 complex on telomeres. Journal of Biological Chemistry, **279(45)**, pp.47264–47271. (2004)

Yuan, T. *et al*. Polymorphisms of base-excision repair genes hOGG1 326cys and XRCC1 280His increase hepatocellular carcinoma risk. Digestive Diseases and Sciences, **57(9)**, pp.2451–2457. (2012)

Von Zglinicki, T. Oxidative stress shortens telomeres. Trends in Biochemical Sciences, **27(7)**, pp.339–344. (2002)

Zhang, C. *et al*. Genetic determinants of telomere length and risk of common cancers: a <DRIVE, ELLIPSE, FOCI, and TRICL. Human Molecular Genetics, **24(18)**, pp.5356–5366. (2015)

Zhang, R.G. *et al.* Telomerase inhibition and telomere loss in BEL-7404 human hepatoma cells treated with doxorubicin. World Journal of Gastroenterology, **8(5)**, pp.827–831. (2002)

Zhou, J. *et al.* The NEIL glycosylases remove oxidized guanine lesions from telomeric and promoter quadruplex DNA structures. Nucleic Acids Research, **43(8)**, pp.4039–4054. (2015)

Zhu, X. *et al*. The association between telomere length and cancer risk in population studies. Scientific reports, **6**, p.22243. (2016)

Zou, Y. *et al*. Does a sentinel or a subset of short telomeres determine replicative senescence? Molecular biology of the cell, **15(8)**, pp.3709–18. (2004)